Regulation of Cardiac Gap Junctional Communication: Metabolic regulation of Cx40 and Cx43 via phosphorylation

by

Jason Bradley Iden

A thesis submitted in partial fulfillment of the requirements for the degree of

Doctor of Philosophy

Department of Medicine
University of Alberta

Abstract

Alterations in myocardial metabolism and cardiac electrophysiology associated with structural heart disease generate lethal arrhythmias. Differential levels of energy (ATP) supply and demand are generated with structural heart disease that is expected to activate 5'-amp activated protein kinase (AMPK) and other pathways that may contribute to an arrhythmogenic substrate in the human heart. Cardiac gap junctions (GJ) determine the level of electrical and 'macroscopic/metabolic' communication between heart cells. This level of conductance is one factor responsible for generating an arrhythmogenic substrate in humans and experimental animal models. Regulation of cardiac connexins by phosphorylation has been demonstrated and the cardiac GJ proteins Cx40, Cx43, and Cx45 contain putative AMPK phosphorylation sites.

Initially we tested the hypothesis that rapid pacing (which also simulates atrial ventricular tachycardia) would activate AMPK and result in reduced GJ conductance and arrhythmia. These effects were readily apparent in a porcine model treated with rapid (200bpm) pacing for 3h. AMPK activity levels were increased, as were levels of (activated) phospho-AMPK. These animals exhibited atrial and ventricular arrhythmia after pacing not found in control animals. Expression levels of Cx43 (LV), and Cx40 (LA) were not significantly decreased despite the reduction in LV GJ conductance. We also show that Cx43 may be phosphorylated *in vitro* by AMPK but the residues affected were not identified.

Due to complicating factors, we attempted to monitor Cx conductance in a variety of 'simpler' models so as to allow us to use viral and pharmacological methods to activate or inhibit AMPK. The models included isolated Langendorf perfused rat hearts (epicardial electrical mapping, tissue resistivity, optical mapping), in isolated neonatal cardiac myocytes (dye injections, scrape loading of dye, and growth on multi-electrode arrays), and in communication deficient cell lines transfected with Cx40 and Cx43 (dual cell patch clamp, dye injection/

transfer, and fluorescence recovery after photo-bleaching GapFRAP). These techniques have been used in the GJ literature. Of the available techniques we chose to focus on the GapFRAP method as it was cost effective, most amenable to our manipulations, and had a high rate of success.

Using the GapFRAP system, we examined the effects of pharmacological AMPK activation (using AICAR, phenformin, and infection with either constitutively active or dominant negative AMPK adenovirus) on the rate of dye transfer 'macroscopic conductance' between pairs of Hek293 cells. We were able to show that viral infection alone caused a significant decrease in junctional conductance, and that phenformin significantly reduced Cx40 and Cx43 conductance, which was associated with a decrease in plasmalemmal Cx protein expression. AICAR had no effect on conductance indicating that this decrease was likely independent of direct phosphorylation on Cx43 or Cx40. AICAR did appear to alter the distribution of Cx40 at the membrane including some evidence for a shift in the overall phosphorylation level, and internalization associated with increased AMPK activity.

To follow up, we generated stable cell lines expressing mutated Cx40, to mimic or prevent phosphorylation by converting four putative Cx40 phosphorylation sites to alanine (a) or aspartic acid (d). Based on these data we show that phospho-mimetic mutation of Cx40 in the cytoplasmic loop (CL) significantly altered Cx40 permeability. These effects were opposite in the two nearby residues (120,122), and were associated with altered expression, and in the modeled 3D structure including surface charge distribution in the pore forming regions. The data indicates that phosphorylation at one site s122 was essential for normal function, and that phosphorylation of s120 was not likely responsible for previously observed conductance increase due to cAMP activation. We also show that mutation of a highly conserved n-terminal residue t19 significantly reduces its conductance and expression at the plasma membrane.

In all, we have shown that atrial or ventricular tachycardia can degenerate quite rapidly into a highly arrhythmogenic substrate. That Cx40 and Cx43 can be affected by altered metabolic states which activate AMPK and other stress response pathways, that phosphorylation of Cx43 by AMPK may occur, and we have identified three novel Cx40 phosphorylation sites, including two in the CL that can affect its function and expression. These combined results highlight the current lack of knowledge related to Cx40 modulation by phosphorylation, and the importance of expanding that knowledge with respect to the generation of arrhythmogenic substrates in the heart.

Preface

This thesis is an original work by Jason Bradley Iden. A portion of chapter 3 was previously published in abstract form. Portions of chapter 6 were submitted for publication in *The Journal of Biological Chemistry* (under review). The chapter 6 manuscript was prepared by Jason Iden under the supervision and editorial guidance of co-authors Dr. Henry Duff, Dr. Paul Lampe (post defense) and Dr. Katherine Kavanagh. Some GapFRAP experiments in chapter 5,6 were performed by David Dilworth under the supervision of Jason Iden. Experimental design, procedures, data analysis, and interpretation of these experiments were done by Jason Iden.

Acknowledgements

I would like to thank first and foremost my supervisor Dr. Katherine Kavanagh for her unwavering support in so many aspects of this research. She provided me with more patience than I rightly deserve, and allowed me the freedom to pursue this project despite its foray away from our labs normal focus. She accepted me into her home and family in Calgary, and brought me through so much more than any supervisor could ever be expected to. For all of that and more I will always be grateful.

To Gary Lopaschuk for agreeing to act as my University of Alberta supervisor, and assist to push me over the finish line – I would not be here now without your help.

To the rest of my supervisory/examining committee both original, and those that have joined me nearest the end, Dr.'s Gary Lopaschuk, Henry Duff, Dick Jones, Jason Dyck, Gavin Oudit, Steve Archer, Sandy Clanachan, and Peter Light, you provided me with timely guidance, scientific discourse, and challenged me to be a better scientist.

To Deb and Grant, Finlay and Esme, They say you don't get to choose your family, but I cannot picture anyone more amazing to have than you. You have always been there for me; you are my inspiration, and my closest friends. I will never forget how much you mean to me - even if I have to fight you now and then. Remember the timeless wisdom of the monkey that ate a Pickle Melt - *Theoretically – it's all bs*.

To my parents – without your incessant abilities to love, support, and annoy… I would not be the man I am today. Thank you. One day I may even get the job I've been telling you about for so long.

To all my friends and colleagues at the U of A and U of C, you were an amazing group of people to work with, and I would not be here today if not for you. I would like to especially recognize those that began as colleagues and have now become the closest of friends - Jay Jaswal, Ernst Hoppenbrouwers, Rohit Moudgil, Grant Masson, and Euwin Allan. To my friends near and far, my Canucks, fellow Dudesmas celebrators, those that both designed, and survived the devastator, and that brought out the best, and worst parts of me – '*Endeavors*'. May the adventures continue and may the stories never… end. Craig you get a special mention as the man responsible for bailing me out of jail the night before my grad school interview… for helping to get me there in the first place, and for helping me get here in the end.

To Ange – you have joined this ride near the very end, but that in no way diminishes your ability to captivate, motivate, and inspire me to succeed. Thank you for always believing in me, and for being just around the corner.

Lastly, thanks to the Department of Medicine, Sharon Campbell, Aileen Leskow, Karen Madsen, and the agencies that funded my salary and this research: the Canadian Institutes of Health Research (operating grant to Dr. Katherine Kavanagh, and studentship to Jason Iden), and the Heart and Stroke Research Fund (operating grant to Dr. Katherine Kavanagh).

Table of Contents

List of Tables

List of Figures

Symbols and Abbreviations

Abbreviation	Definition
%	percent
°	degrees celsius
µ	micro
^{32}P	radioactive phosphate 32
^{32}P	radiolabeled 32-phosphate
α	alpha
Å	angstrom (1.0 × 10-10 meters)
AAP	anti-arrhythmic peptide
ACC	acetyl-coA-carboxylase
ADM	adenosine diphosphate
AF	atrial fibrillation
AMP	adenosine monophosphate
AMPK	5'-AMP-activated protein kinase
$AMPK_{CA}$	constitutively active AMPK adenovirus
$AMPK_{DN}$	dominant negative AMPK adenovirus
AMPKK	AMPK kinase
ANOVA	analysis of variance
ATP	adenosine triphosphate
β	beta
BB	bundle branch
BDM	butanedione monoxime
bpm	beats per minute
BSA	bovine serum albumin
CaMKβ	calmodulin kinase beta
cAMP	cyclic adenosine mono-phosphate
CK1	casein kinase 1
CoA	coenzyme A
CPT-1	carnitine:palmitoyl-transferase 1
cSRC	proto-oncogene tyrosine-protein kinase Src
CT	c-terminal Cx sub-domain
CV	conduction velocity
Cx	connexin
Cx40	connexin 40
Cx43	connexin 43
Cx50	connexin 50
Da	dalton (1 atomic mass unit)
DAD's	delayed after-depolarization's

DMEM	Dulbecco's Modified Eagle Medium
DMEM/F-12	Dulbecco's Modified Eagle Medium: Nutrient Mixture F-12
DMSO	Dimethyl sulfoxide
dV/dt	delta Voltage/delta time
E1-2	extracellular loop 1-2
EAD's	early after-depolarization's
ECG	electro-cardiogram
EDTA	Ethylenediaminetetraacetic acid
eEF-2	eukaryotic elongation factor 2
FA	fatty acids
FAO	fatty acid oxidation
FBS	fetal bovine serum
FoxO1,3	forkhead box proteins 1,3
FRT	Flp recombinase integration site
ga	gauge (needle, wire)
GFP	green fluorescent protein
gj	electrical junctional conductance
GJ	gap junction
GLUT4	glucose transporter 4
Gmax	maximum conductance state
Gmin	minimum conductance state
H^+	hydrogen ion
heteromeric	gap junction consisting of more than one type of Cx
heterotypic	gap junction consisting of more than one type of homomeric connexon hemi-channel (e.g. Cx40, Cx43)
homomeric	gap junction consisting of one type of Cx
HRP	horse radish peroxidase
HS	horse serum
HuR	cytoplasmic HuR mRNA-binding proteins
I_{m25}	inward membrane currents at 25% of its maximum value
IP	immuno-precipitation
I_{TO}	transient outward potassium current
JNK	c-Jun activated protein kinase
k	kilo (1000)
KCL	potassium chloride
KD	knock-down
KI	knock-in
K_{IR}	inward rectifying potassium current
KO	knock-out
λ	lambda

λ	space constant, tau (lambda)
LA	left atrial
LAD	left anterior descending coronary artery
LKB1	liver kinase B1 (human tumour suppressor LKB1)
LV	left ventricle
LY	lucifer yellow dye
M1-4	membrane spanning/transmembrane segment 1-4
MAPK	mitogen activated protein kinase
MCD	malonyl Co-A decarboxylase
MEA	multi-electrode array
mM	millimolar, millimole/liter
moi	multiplicity of infection (# viral particles/target cell)
mTOR	mammalian target of rapamycin
mTORC1	mTOR-1 complex
N2A	neuronal 2 a neuroblastoma cells
NBD-TMA	cationic dye [2-(4-nitro-2,1,3-benzoxadiazol-7-yl)aminoethyl]trimethylammonium
NP40	Nonidet P40 detergent
NT	n-terminal Cx sub-domain
NTS	non-triton soluble
P0, P1, P2	isoforms of Cx proteins P0 ('non' phosphorylated), P2 ('fully' phosphorylated)
PBS	phosphate buffered saline
PBS-T	phosphate buffered saline with 0.1% Tween-20 detergent
PCR	Polymerase chain reaction
PDH	pyruvate dehydrogenase
PDK4	pyruvate dehydrogenase kinase 4
PFK2	phospho-fructokinase 2
pfu	plaque forming units (viral concentration)
Pj	junctional permeability of a particular permeant (Pj-permeant)
PKA	protein kinase A
PKC_{ζ}	protein kinase C epsilon
pS	pico-Siemens (conductance)
RA	right atrial
RV	right ventricle
s120	serine 120
s122	serine 122
s349	serine 349
SA node	sino atrial node
SDS-Page	sodium dodecyl sulphate poly acrylamide gel electrophoresis

SKHep1	human hepatoma cell line
t19	threonoine-19 residue
TG	triacyl glygerol
TIF-IA	RNA polymerase I (Pol I)-associated transcription factor
TS	triton-soluble
TSC1/2	tuberous sclerosis (TSC)1/2 complex
TSC2	tuberous sclerosis complex tumor suppressor protein
ULK1	unc-51-like kinase
vSRC	Rous sarcoma virus tyrosine kinase
VT	ventricular tachycardia
ZO1	zona occludens 1 (scaffolding protein)
Ω	ohm (resistance)

Chapter 1 General Introduction: Regulation of cardiac gap junction conductance.

This thesis is an original work by Jason Bradley Iden.

No part of this chapter has been previously published.

Figures that have been adapted are reproduced without permission.

1.1 Overall Introduction

1.1a Clinical problem

Cardiac tachyarrhythmias are a public health issue of epidemic proportion. Ventricular tachyarrhythmias are responsible for more than 300,000 sudden cardiac deaths in North America on an annual basis [1-7]. Eighty percent of these victims are between 35-64 years of age [1-3, 8]. Atrial fibrillation is the most common sustained cardiac arrhythmia seen in clinical practice. It affects more than 2 million North Americans and is associated with increased mortality, more frequent hospitalizations, decreased quality of life and significant health care expenditures [9, 10]. Long term therapeutic options for patients with these tachyarrhythmias are expensive, often ineffective and poorly tolerated. Preventative therapy is not even an option [3, 11-16]. It is therefore imperative that we increase our understanding of arrhythmogenic substrates and the factors that modulate them. In this thesis, I focus on the potential interactions between arrhythmia formation and the control of junctional conductance by regulators of cardiac metabolism. In the following sections, I will outline the basic process of cardiac electrical activity, arrhythmogenesis, regulation of energy metabolism, and the potential link between them.

1.1 Myocardial electrophysiology substrate

The unique, normal, anisotropic, conduction of a cardiac impulse, which enables an orderly sequence of electrical and mechanical activity, is dependent on both active and passive myocardial membrane properties [17-22]. The active properties depend on various ion channels, exchangers, and pumps (Figure 1-1).

1.1a Ion channels and active properties of cardiac electrophysiology

In brief, the activation of cardiac tissue depends on an automatic cycle of changing membrane potential (the voltage gradient between the inside and outside of the cell) known as an action potential [23-25]. Membrane voltage potential is maintained at a polarized ~-80-90mV “resting membrane potential”

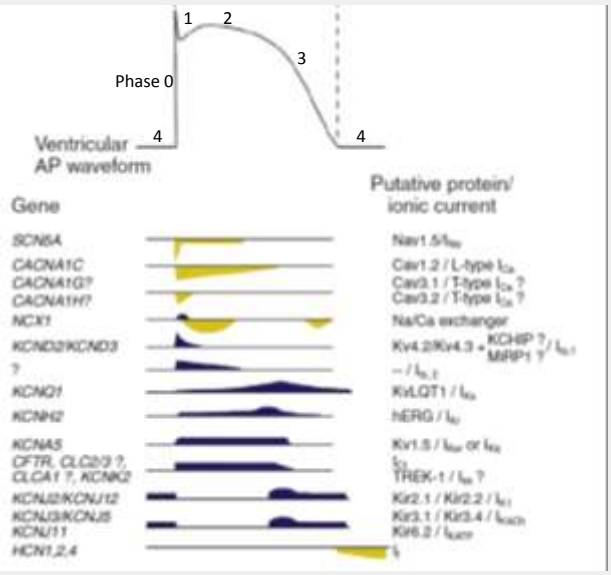

Figure 1-1 Cardiac ion channels and the cardiac action potential.
The different ionic currents that contribute to action potential generation and the putative encoding genes are shown. Depolarizing currents are shown in yellow, repolarizing currents in dark blue. INa sodium current; ICa,L L-type calcium current; Ito transient outward current; IKur ultra rapidly activating delayed rectifier current; IKr and IKs rapidly and slowly activating delayed rectifier current; IK1 inward rectifier current; IK,ACh acetylcholine-activated potassium current. Phase 0, rapid depolarization; phase 1, rapid early repolarization phase; phase 2, slow repolarization phase ('plateau' phase); phase 3, rapid late repolarization phase; phase 4, resting membrane potential (from Issa *et al.* (2012), "*CLINICAL ARRHYTHMOLOGY AND ELECTROPHYSIOLOGY*, Ch. 1,p2" .

by I_{k1}, and Na/K+ ATPase activity which actively maintain a gradient of potassium ions (more inside the cell) and sodium ions (more outside the cell) combined with the inherent concentration of negatively charged proteins inside the cell. Activation of the membrane is begun by a generic act of increasing (depolarizing) the membrane potential to ~-60 mV. At -60mV (the activation threshold) voltage gated sodium channels open, allowing sodium to enter the cell (down its concentration gradient), further depolarizing the membrane to ~+20mV (phase 0). This change in local membrane potential is propagated because it induces an electrotonic (not due to altered membrane ion channel conductance) depolarization of the surrounding membrane. Assuming that the activation threshold is reached, this process continues outward from a central point (normally the sinus node in the high right atria). The rate of propagation is known as conduction velocity (CV) and will be discussed throughout this thesis.

Concurrent to membrane depolarization, activation of voltage dependent calcium channels (I_{CaL}) and the sodium-calcium exchanger (NCX) allow calcium ions to enter the cell stimulating the further release of calcium stored in the sarcoplasmic reticulum. This increased calcium inside the cell causes actin-myosin interaction (muscle contraction). Upon initial depolarization, activation of voltage dependent potassium channels also causes the release of potassium (again down its concentration gradient). This loss of K^+ and the loss of positive charge from inside the cell causes the membrane potential to initially decline rapidly due to transient K channels (I_{TO}) (phase 1). Then, due to a balance between activation of inward rectifying K channels (K_{IR}) and the still active Ca++ influx, a plateau is formed (phase 2). Eventually, this balance favors the K channels and membrane potential decreases (phase 3) towards the resting state at ~-80mV (phase 4).

1.1b Refractory periods

Following an action potential, the membrane becomes unresponsive to new depolarizing stimuli based on the voltage dependent inactivation of sodium channels, and the time, voltage and calcium dependent inactivation of L-type calcium channels [24, 25]. This period is known as the effective refractory period (no further AP can be generated by conducted activation, vs. 'absolute refractory period' where no stimulus of any origin (ie pacing) will induce activation). Over time, as the cell is re-polarized, and intracellular calcium decreases, a greater proportion of I_{CaL} channels are reset (able to be re-activated) and the cell enters what is referred to as the relative refractory period. At this point a depolarizing stimulus of sufficient strength to reach the action potential threshold will evoke another action potential. However, normally by this time the membrane potential is rapidly re-polarized, there will be no further stimulus, and the channels remain inactive in the resting state.

1.1c Passive properties of cardiac electrophysiology

As stated previously, the propagation of an action potential is dependent on the local electrotonic depolarization of the membrane. From any one point, this electrotonic source dissipates exponentially in space. The rate of activation of surrounding membrane depends on sodium channel activity, as a faster influx creates a stronger 'source' current, charging the capacitance of the surrounding membrane. Propagation is also dependent on the geometry of the cell, as increased membrane area requires exponentially more current. In fact, if there is not enough current in the 'source', the surrounding membrane will not reach the threshold potential and propagation will slow down or fail. Increased cell diameter is equivalent to decreased resistance as there is a greater area of low resistance conductive internal solution relative to the amount of membrane to be charged. In theory, propagation can proceed indefinitely down the length of the cell at a rate dependent on the cells internal diameter and sodium channel activity. With finite cell length, a propagating stimulus eventually encounters an infinitely small "diameter" which would inhibit propagation to the next cell if the membrane was inert.

The end of the cell is however also an area densely packed with both sodium channels, and the junctional plaque. This plaque is an aggregate of anchoring structural proteins and transmembrane channels. The resistance to propagation then becomes dependent on the resistance of the junctional plaque. Because this resistance is greater than that of the internal solutions, propagation will proceed faster when there are fewer cell-cell interfaces or greater junctional coupling (as is the case at the longitudinal border). As such, propagation in the longitudinal direction of the cell is generally much faster than propagation in the transverse direction (a smaller number of the same transmembrane channels are present between the cells), thus leading to anisotropic conduction [26, 27].

1.2 Junctional activity/inhibition and arrhythmias.

The transmembrane channels in the junctional plaque that facilitate myocyte–to-myocyte communication (including small molecules such as: cAMP, IP3, 5-HT, siRNA and small peptides)[28-31] and electrical coupling are called gap junctions (GJs) [32]. The protein components of the GJs are connexins (Cx) and they are named for their respective predicted molecular weight in kDa, often with a prefix indicating the species (e.g. human hCx43 is 43kDa, hCx45 is 45kDa). The expression and distribution of these Cx proteins are important for proper electrical conduction [33-35], and alterations in their function or expression have been linked to arrhythmia predisposition [36-61], some of which are described in the following observations.

Cx43 knockout mice exhibit arrhythmias both pre- and post-birth, with altered electrical conduction properties and 100% mortality due to sudden cardiac death by ~2 months of age [37, 38, 50, 58, 62-64]. Similarly, Cx40 knockout mice are susceptible to atrial arrhythmias following burst pacing that did not occur in wild-type controls [40, 41, 57, 59, 60, 65]. Furthermore, exchange of Cx43 for Cx45 was not able to functionally replace and prevent these arrhythmias [66, 67]. In an experimental canine model, redistribution to the longitudinal myocyte border in the border zone of a healing myocardial infarct is associated with the formation of reentrant arrhythmias in the same region [42]. Loss of Cx43 is also associated with the formation of reentrant arrhythmias and sudden cardiac death in a transgenic mouse model of cardiac myocyte ablation, even in cases of only minor myocyte loss and fibrosis [39]. Preventing dephosphorylation of Cx43 at three sites prevented arrhythmia susceptibility, whereas mutation to prevent phosphorylation increased it [68]. Inhibition of junctional conductance with generic pharmacological gap junction uncouplers results in arrhythmia in isolated perfused hearts [69]. Finally, increased expression of Cx40 is associated with the formation of AF in patients following cardiac surgery [36]. Further, improving Cx mediated conduction has led to the prevention of arrhythmia in a

number of models [68, 70-79]. Although the precise mechanisms leading to these arrhythmias are largely unknown, in combination, it is apparent that any alteration (up or down) in the expression, distribution, or activity of myocardial connexin proteins can play a profound role in altering the arrhythmogenicity of the heart.

1.3 Cardiac connexin physiology

There are three major connexins expressed in the heart that have been studied most extensively (see Figure 1-2). Cx43 is expressed throughout the myocardium (non-specialized tissues) as well as in the His-Purkinje system (although restricted to the distal sections in mouse and rat species)[80-91]. In adults of many species including humans, Cx40 is expressed in atrial myocardium (although not in rat hearts), as well as extensively in the specialized conductive pathways (sinoatrial node, atrioventricular node, bundles of His, and Purkinje fibres) [83-90, 92-95]. Cx45 expression is restricted to the specialized conducting pathways except early in embryogenesis [83-89, 96, 97]. Although it is not found in human cardiac tissue [98] Cx31.9, has been found in the nodal tissues of some murine species: slowing conduction within these structures [99-106].

Connexin expression and junctional communication between contractile myocytes, and non-contractile cells of the heart, predominantly fibroblasts, has been demonstrated *in vitro* repeatedly (review [107]). Fibroblast co-culture can maintain conduction across myocyte gaps up to 300µm [107-109]. Although junctional connections between fully differentiated cardiac myocytes, and fully differentiated fibroblasts have been difficult to locate *in vivo*, they have been observed and fibroblasts themselves can be well coupled to each other [107]. As shown in Figure 1-2B, there is evidence that these junctional connections involve both Cx43, and Cx40, and other studies have also indicated Cx45 [108, 110]. It is also clear and that connection to the fibroblast can modulate myocardial conduction in areas where fibroblast density is high (eg. the AV node)[107].

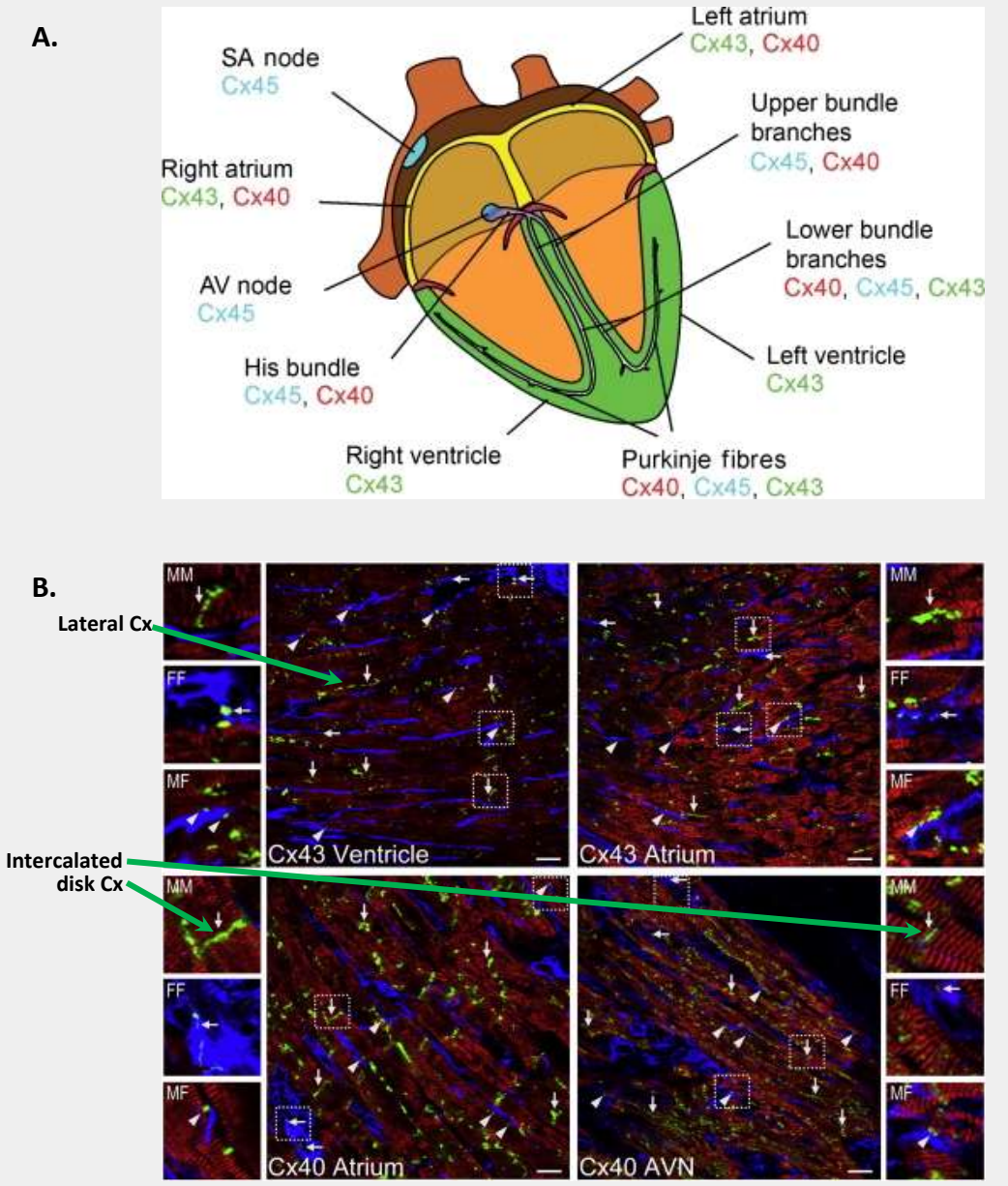

Figure 1-2 Connexin Expression patterns in atrial and ventricular myocardium.
A. Three principal connexins are expressed in cardiac myocytes, connexin43 (Cx43), Cx40, and Cx45. Cx43 is expressed in the atrial, and ventricular myocardium, as well as in the specialized conductive pathways. Cx40 in the atrial myocardium, and His-Purkinje system. Cx45 is exclusive to the conductive pathways (from Severs et al. 2008. *Cardiovasc Res*. 2008; 80(1): 9–19). **B.** In these pictures myocytes are stained red, fibroblasts are stained blue, and Cx expression is shown in green. Cx40 and Cx43 are primarily located at the intercalated disk joining two myocytes, perpendicular to the myocyte axis ("MM"), although they are also visible on the lateral borders of the myocytes (parallel to the myocyte axis). Cx40 staining is stronger in the atrial myocardium, and AV node (AVN). Expression of both Cx40 and Cx43 is apparent in cardiac fibroblasts, joining them to another fibroblast ("FF"), or to myocyte(s) ("MF") (from Kohl, Gourdie, 2014. *JMCC*, V70:37- 46).

1.3a Connexin life cycle

The connexin life cycle is fairly well established [111-115]. Connexins are expressed in the rough endoplasmic reticulum then (as with most integral membrane proteins) they are transferred to the cis-, then to the trans Golgi apparatus, where they oligomerize to form a circular hexamer known as a connexon, and undergo post-translational modifications, including phosphorylation. A single connexon (or hemi-channel) can be made up of one (homomeric) or many (heteromeric) Cx subtypes (although certain subtypes are less/not capable of interacting). The formation of a functional gap junction involves the trafficking of a connexon from the Golgi Apparatus to the lateral cell membrane then to the cell-cell interface where it interacts with a connexon from another cell allowing the formation of the transmembrane pore (Figure

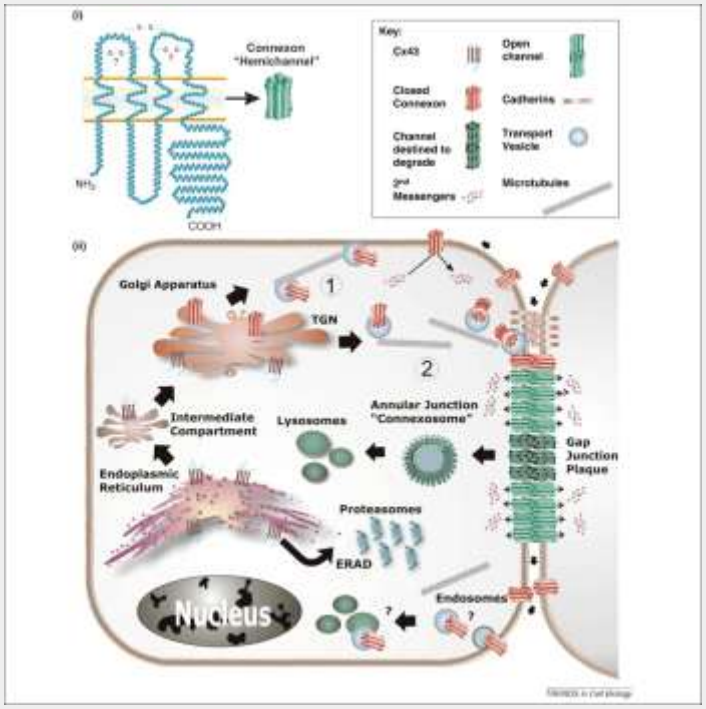

Figure 1-3 Gap Junction Life Cycle.
GJ are formed in the rough Endoplasmic Reticulum near the Nucleus, transferred to the Golgi Apparatus, then on to the lateral cell membrane. From the lateral membrane connexons are mobilized to the cell-cell border region where they join with a connexon from the other cell. These junctions merge by accretion to the lateral edge of an existing plaque. They are later internalized from the center of the plaque into an annular junction for degradation via lysosomal or proteosomal pathways (from Laird (2010), *Trends in Cell Biology*. 20(2):92-101).

1-3)[116]. Individual connexins/connexons have a relatively short half-life (~1-3 hours for Cx43 vs. 17-100h for some integral membrane proteins)[117-122]. Gap Junctional plaques are continuously being formed, peripherally enlarged, partially recycled (central/oldest first), internalized, and degraded by both the lysosomal and proteosomal pathways [123-126] resulting in dynamic junctional coupling.

1.3b Connexin structure and morphology

All connexin proteins have a similar structural organization [127-133]: four α-helical transmembrane domains (M1-4), two extracellular loops (E1, E2), a cytoplasmic loop (CL) and N- and C- termini (NT, CT) also facing the cytosol (see Figure 1-4A). The extracellular loops, which are important for docking, are highly conserved. In contrast, the greatest isoform specific variation occurs in the three intracellular regulatory domains. These domains are structurally flexible, can interact with other proteins or domains within the connexon, and are thought to adjust their conformation affecting conductance parameters (eg. channel diameter, open probability, and membrane stability) [133]. The N-terminal (NT) domain is important for voltage sensitivity, and permeability: forming a pore funnel and ring (Asp3, Trp4, Phe6) when open and a plug like domain when closed [131-136]. The cytoplasmic loop (CL) domain is thought to interact with the C-terminal (CT) domain in a “particle-receptor” model important for gating of the channel [129, 132, 137-140]. The CT also contains many sites known to facilitate interaction with nearby proteins. These associated proteins can be grouped into (1) other Cx, (2) scaffolding/structural proteins eg. actin, ZO1, tubulin, (3) post-translational modifiers eg. kinases, phosphatases, (4) trafficking regulators, and (5) growth regulators etc. [116].

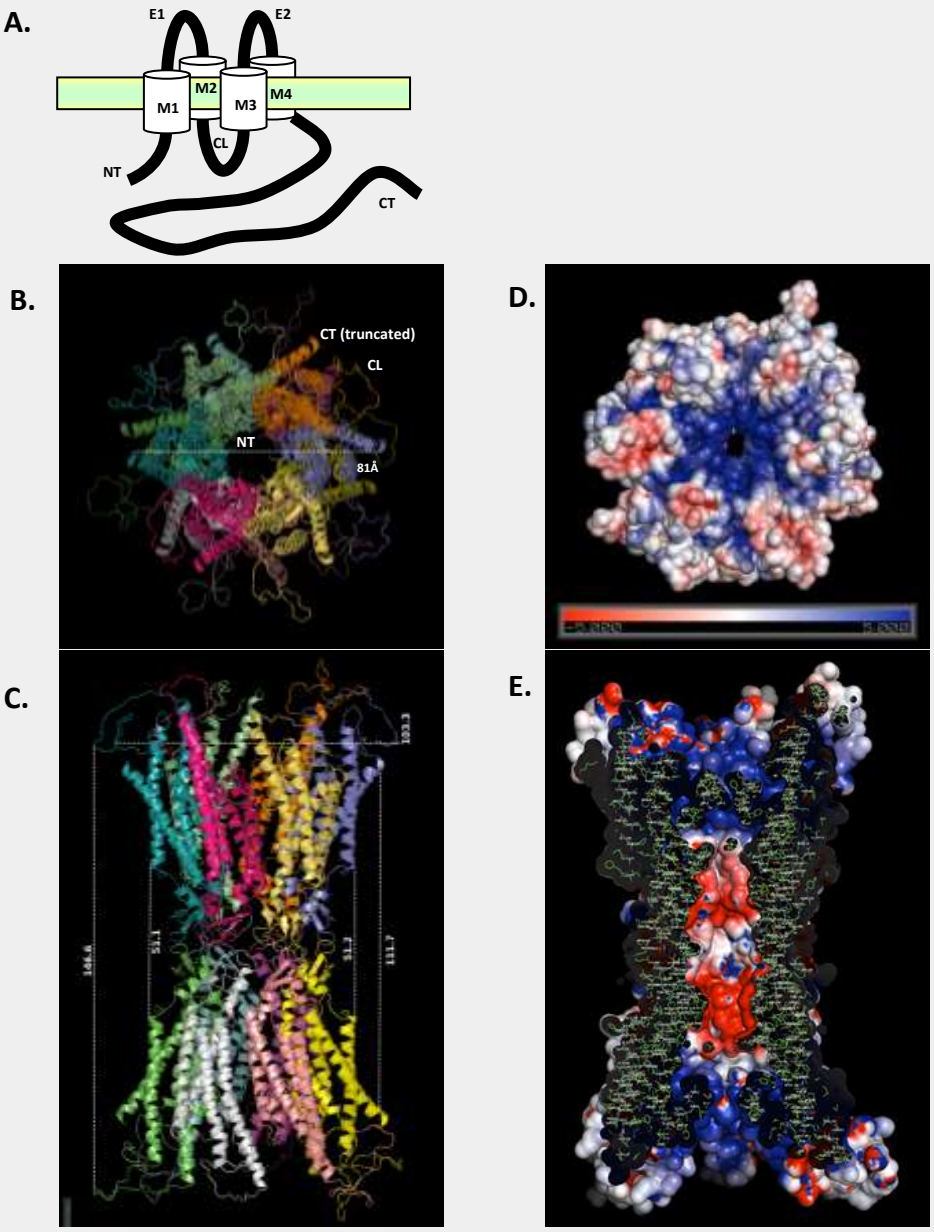

Figure 1-4 General structure of a gap junction Cx hexamer.
A. Generalized Cx subunit topology: each Cx has four transmembrane domains (M1-M4), an n-terminal (NT), cytoplasmic loop (CL), and c-terminal (CT) cytoplasmic domain as shown. **B-C.** Cartoon representation of 3.5 Å homology domain modelled Cx43 3D structure (Swiss-Model Server, see Chapter 6 for methodology). **B.** Cytoplasmic end on view showing hexamer of Cx subunits in cross section. Distance between residues shown with white dotted lines (Å). Individual Cx subunits are colored. The central pore contains the NT tail, and the CL is visible. The CT has been truncated as it was not modeled (due to its labile nature). **D-E.** Solvent accessible surface charge based on 3.5Å model. Regions of positive (blue), neutral (white) and negative(red) are visible. D. End on view as in C. E. Longitudinal cross-section showing pore lining surface charge.

1.3c Connexin conductance and selectivity

In terms of relative *electrical conductance* (K^+, Na^+, Cl^- etc. mediated, measured by dual cell patch clamping), the cardiac connexins are only mildly affected by the ion charge, and ranked Cx40>Cx43>Cx45, with single channel 'fully open' conductance measured at ~175pS, 100pS, and 35pS respectively [28]. The permeability or conductance of the channel is dependent on the pore shape, and surface charge, both of which can be modified by regulatory events [140].

1.3d Connexin voltage sensitivity and gating

Gap junctions are (in general) voltage sensitive such that, with increasing trans-junctional voltage, macroscopic conductance is reduced within milliseconds to seconds over a physiological range of voltage potential [141-144]. This can be important during conduction across the heart as the cardiac connexins are all sensitive to trans-junctional voltage in the action potential range, such that Cx43 conductance can be reduced by 60% within 10-20ms [145].

The decline in macroscopic conductance (g_j) with voltage is sigmoidal from a peak around 0mV across the junctional pore (g_{max}) with a minimum non-voltage sensitive conductance (g_{min}) (see Figure 1-5A). The relationship is normally fitted to a modified Boltzmann equation for comparison of various parameters (see Figure 1-5A-C).

At the single channel level, voltage sensitivity is seen as a transition from the 'fully open' conductance state to a range of lower conductance 'sub-states' (leading to g_{min}). This voltage sensitivity is subtype specific. Thus, the relationship is homogenous when the junctional channels are made up of the same Cx subtype (since they have an identical but oppositely oriented voltage sensor). However, they can be asymmetric (see Figure 1-5C) when the hemichannels are made up of different Cx subtypes. Heteromeric mixing of Cx subtypes can also reduce the overall voltage sensitivity as mixing Cx45 and Cx43 reduced overall sensitivity versus either homomeric channel [146, 147].

There are subtype differences in voltage sensitivity. Cx40 closes with depolarization: positive charge inside, and Cx43 and Cx45 close with hyper-polarization: negative charge inside. Mechanistically, this polarity appeared to be dependent on the charge of a few specific residues (2, 41, and 42) on the n-

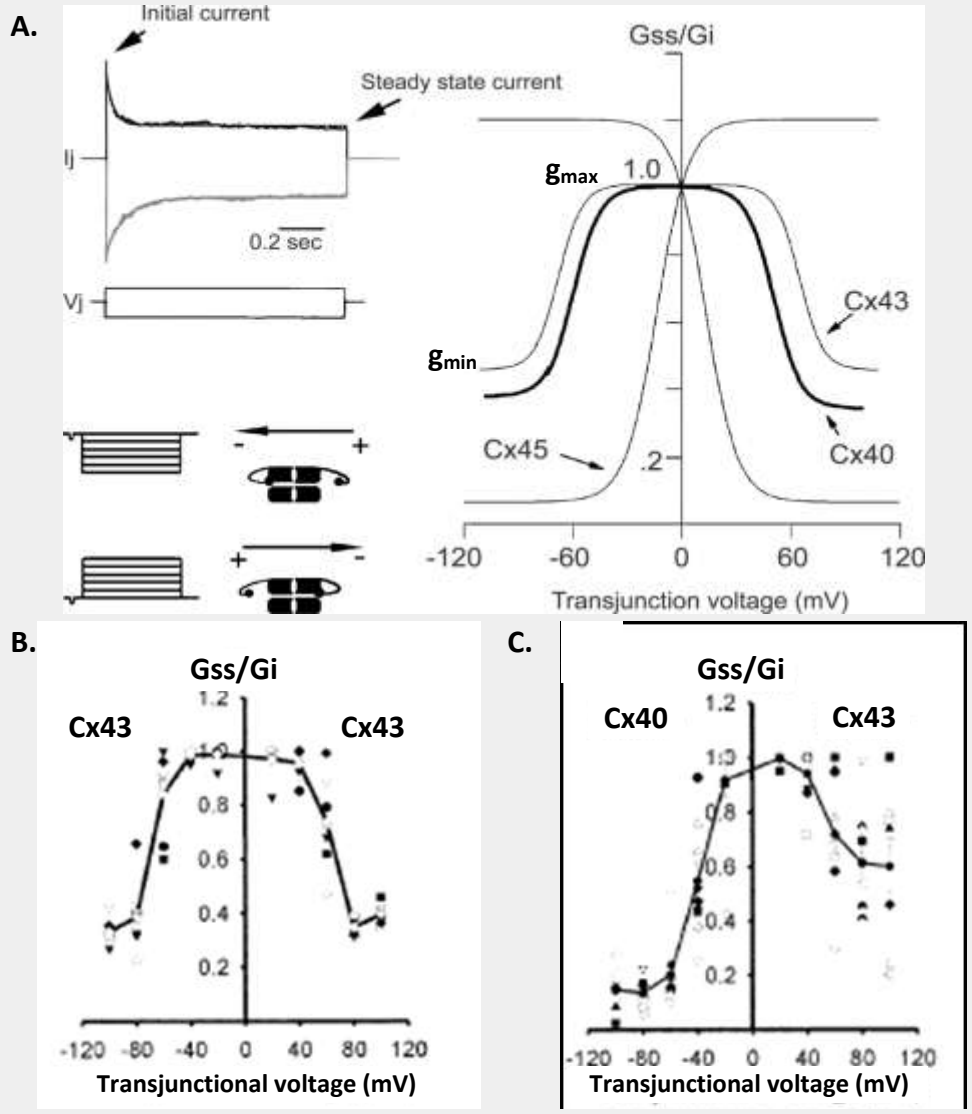

Figure 1-5. Voltage sensitivity of cardiac gap junctions.
A. Conductance (g_j) of junctional channels is maximal at transjunctional gradient of 0mV, and decays sigmoidally as you increase the junctional voltage gradient (100mV curve shown) to a g_{min} value. Typical sensitivity of the cardiac Cx is shown in the right panel (from Moreno *et al. Cardiovasc Res.* 2004, 62(2):276-86). **B.** Voltage sensitivity of homomeric Cx43 channels have symmetrical voltage sensitive decay. **B.** Whereas Cx40 and Cx43 heteromeric channels (Cx40 on one cell, and Cx43 on the other) show that Cx40 is more sensitive to voltage with a smaller g_{min} compared to Cx43 (from Cottrell *et al. Cell Commun Adhes*. 2001;8:193-7.)

terminal (NT) domain of many connexins studied [148]. Therefore, indicating that closure may follow a model where the membrane voltage moves the NT into the pore occluding it. This view is also supported by recent 3.5Å visualizations of Cx26 which indicate that the NT domain was found in the central pore region forming what could be a plug [132]. However, it is likely that other residues/interactions are involved since Cx43 and Cx45 have opposite charge (2- vs. 2+ respectively) and both close with negative polarity. This view was further complicated by the observation that the c-terminal domain is also important for voltage sensitivity, such that addition of a GFP tag removed voltage sensitivity [149]. Truncation of the CT also removed the voltage sensitive component, and subconductance state, in both Cx40 and Cx43 [150, 151]. This sensitivity was restored upon re-expression of the CT as a free peptide for both truncated Cx43 and Cx40 (using the Cx43 CT peptide), indicating that the CT may bind in a ball and chain type interaction [150]. This mechanism was also found to be important for other gating events including: sensitivity to low pH, cSRC interactions, and chemical gating in general, which all involve some type of interaction with the cytoplasmic loop domain [152-158]. It is quite likely that some or all of these various interactions are important at different times, due to different stimuli, in subtype specific ways.

Although the mechanism that generates these sub-states is not fully understood, it should be noted that they involve multiple domains in the Cx protein, and that probability of each sub-state can be affected by phosphorylation and other regulatory events [140, 159-162]. They can also have surprising effects on large molecule conductance. As might be expected some sub-states can block the passage of certain molecules while maintaining electrical connectivity; others become more permeable than the 'fully open' state to certain molecules [140, 163, 164]. It is the aggregate number of channels in a specific location, in a specific conductance state, that combine to determine the overall rate of electrical conductance (g_j) and the junctional permeability (P_j) between two cells.

1.3e Molecular conductance

As stated, based on electrical conductance alone the relative g_j rank would be **Cx40>Cx43>Cx45** [28]. However, the degree of electrical coupling is not correlated to the degree of 'molecular coupling'; i.e. permeability to second messengers or other larger molecules often measured by dye conductance [140]. With respect to larger molecules cardiac Cx conductance is typically ranked **Cx43>>Cx45>Cx40** [28, 140, 165, 166]. These studies tended to use negatively charged tracers (eg. calcein green, Lucifer yellow, AlexaFluor 594). Cx43 is also ~10x more permeable than Cx40 to cAMP [167]. However, permeability to small positively charged dye (NBD-TMA) showed similar conductance in all three cardiac Cx [168]. In this study negatively charged AlexaFluor 350 (AF350) permeability was similar in Cx43 and Cx45 and somewhat proportional to their electrical conductance. Cx40 permeability to AF350 was 1/3 that of NBD despite their similar small size. Overall, Cx43 and Cx45 are minimally charge selective whereas Cx40 is cation selective [169]. This selectivity is reduced with smaller permeants, and exacerbated with larger molecules approaching the 12-14 Å pore diameter [140, 168]. Measurement of Cx40 and Cx45 permeability must be optimized by using smaller, and neutral or positively charged dyes like calcein blue, NBD-TMA, or dapi [170, 171], whereas measurement of Cx43 permeability is more flexible.

1.3f Factors which Affect Cx Permeability

In most cases Cx permeability to larger molecules appears to depend on the size of the permeant relative to the pore, and in some cases the charge of the permeant in relation to the surface charges lining the pore. As shown above, anything which modulates either the structural conformation of the Cx altering the pore size, or alters the charge on specific residues (phosphorylation, methylation etc.) will alter the permeability of the GJ.

Mixing of Cx subtypes tends to reduce their permeability to a level below that of either homomeric channel [170, 171]. Co-expression of Cx45 with Cx43 leads to decreased pore size and more cation selective junctions [172].

Increasing concentrations of highly mobile anions tends to reduce Cx40 conductance [173]. Thus it was proposed that, as with other larger pore size channels, anion-cation complexes form in the open Cx pore and interact with fixed anionic charges on the pore surface leading to a charge screening effect [173].

1.3g Pharmacological regulation of junctional conductance

In general, there is a lack of chemical ligands that increase or decrease junctional conductance specifically. In fact, the most commonly used substances are generic organic molecules like heptanol, octanol, oleic acid, and anesthetics like halothane that reduce junctional conductance non-specifically. They have been used to study single channel Cx gating events, and have been integral to showing that specific events, like dye movements, are gap junction mediated [69, 174-184]. The main drawback to these pharmacological manipulations is that it is not possible to specifically block one particular type of junction or Cx subtype.

This limitation has been partially addressed, as Cx mimetic peptides resembling the extracellular E1 or E2 domains have been shown to more specifically inhibit junctional conductance [185-188]. In addition, the peptide Rotigaptide/ZP123 (Zealand Pharmaceuticals), a much more stable (>140x) analog of the naturally occurring 'Anti-Arrhythmic peptide (AAP)'[189-194], has been shown to increase Cx43 conductance [76, 78, 195-198]. This new class of AAP ligand allows more specific modulation of Cx function in patients. It also implies proof of principle that junctional regulation can be altered clinically. These studies also show that increasing junctional conductance can prevent arrhythmias (onset of VF with ouabain)[199], and further underline the importance of Cx regulation on arrhythmogenesis and cardiac function in general.

1.4 Cardiac electrophysiology is energy dependent

The maintenance of normal electrical activity in the myocardium is an adenosine triphosphate (ATP), or energy-dependent process [200-202]. This is more obviously important for the regulation of resting membrane potential, and the function of the various 'active' ion channel mediated processes. However, it is also increasingly thought to alter the passive properties of cardiac electrophysiology.

In fact, although mitochondrial inhibition is known to open unopposed connexons [201, 203-205], during ischemia, GJ conductance between cells normally decreases [206, 207]. In addition, the development of such cardiac abnormalities as heart failure [208] and ischemia [209] are commonly associated with (among other changes) alterations in the expression, conductance, and distribution of GJs that are associated with cardiac tachyarrhythmias [210]. Heart failure and ischemia are also associated with an imbalance between ATP supply and demand causing a decrease in the ATP:AMP ratio and activation of the 5'-AMP-activated protein kinase (AMPK) cascade [209, 211].

Based on the fact that increased arrhythmogenesis, alterations in junctional conductance, and altered ATP supply and demand leading to AMPK activation occur concurrently, it may be possible that they are related. As a primer, the metabolic pathways regulated by AMPK and their potential linkage to cardiac electrophysiology will be discussed in the following sections.

1.5 Metabolism and regulation by AMPK

1.5a AMPK as an energy sensor

In living cells energy is provided by the charged adenine nucleotide: adenosine triphosphate (ATP), with it's dephosphorylated forms: adenosine monophosphate (AMP), and adenosine di-phosphate (ADP. The concentration ratio of the adenine nucleotides is driven by adenylate kinase which converts

$2ADP \leftrightarrow AMP + ATP$, such that $[ATP]:[ADP]:[AMP]^2$. The relative concentration of each nucleotide is indicative of the energy status of the cell, and Atkinson [212] defined the charge parameter as AEC, ranging from 0 (100% AMP), to 1 (100% ATP). He also postulated that flux through all metabolic pathways is controlled allosterically by the relative concentrations of ATP, ADP and AMP. For at least ten years it has been thought that 5'- AMP activated protein kinase (AMPK) acts as a master sensor of these ratios. Until recently AMP (or the ratio of AMP:ATP) was thought to control AMPK activity [213-215]. It is now clear that many pathways contribute.

AMPK activity is affected by four main pathways [215-217]: (1) The most potent involves phosphorylation of Thr-172, which causes 100 fold increase in activity, and its dephosphorylation/inactivation by protein phosphatases. (2) Allosteric stimulation by AMP (1.5-5 fold activity vs. Thr-172 phosphorylation alone), and inhibition by ATP. (3) Inhibition by intracellular carbohydrate (glycogen). (4) Phosphorylation in other areas (eg. by Akt, PI3K, or glycogen synthase kinase). Pathways (1), and (2) are mediated as follows:

AMPK is a heterotrimer (Figure 1-6A-B) containing an α-subunit with an n-terminal kinase domain (KD), a c-terminal auto-inhibitory domain (AID), serine threonine rich loop (ST loop) and the β-subunit interaction domain. The β subunit contains a carbohydrate/ glycogen binding module (CBM), an n-terminal myristoylation site (G2), and a c-terminal α/γ-subunit binding domain. The γ-subunit contains four adenine nucleotide binding sites (CBS domains) [216, 218] of which two (sites 1, and 3) can bind AMP, ADP, or ATP with differential μM affinities (both appear to favor AMP>ATP>ADP [215] although other studies have reported differences under varying conditions e.g that CBS1 AMP=ATP[217]). Site 4 appears more specific to AMP, which is tightly bound and not exchangeable in solution leading to proposals that it plays a role in adenine nucleotide discrimination, and allosteric activation of AMPK [216, 219]. Site 2 is normally

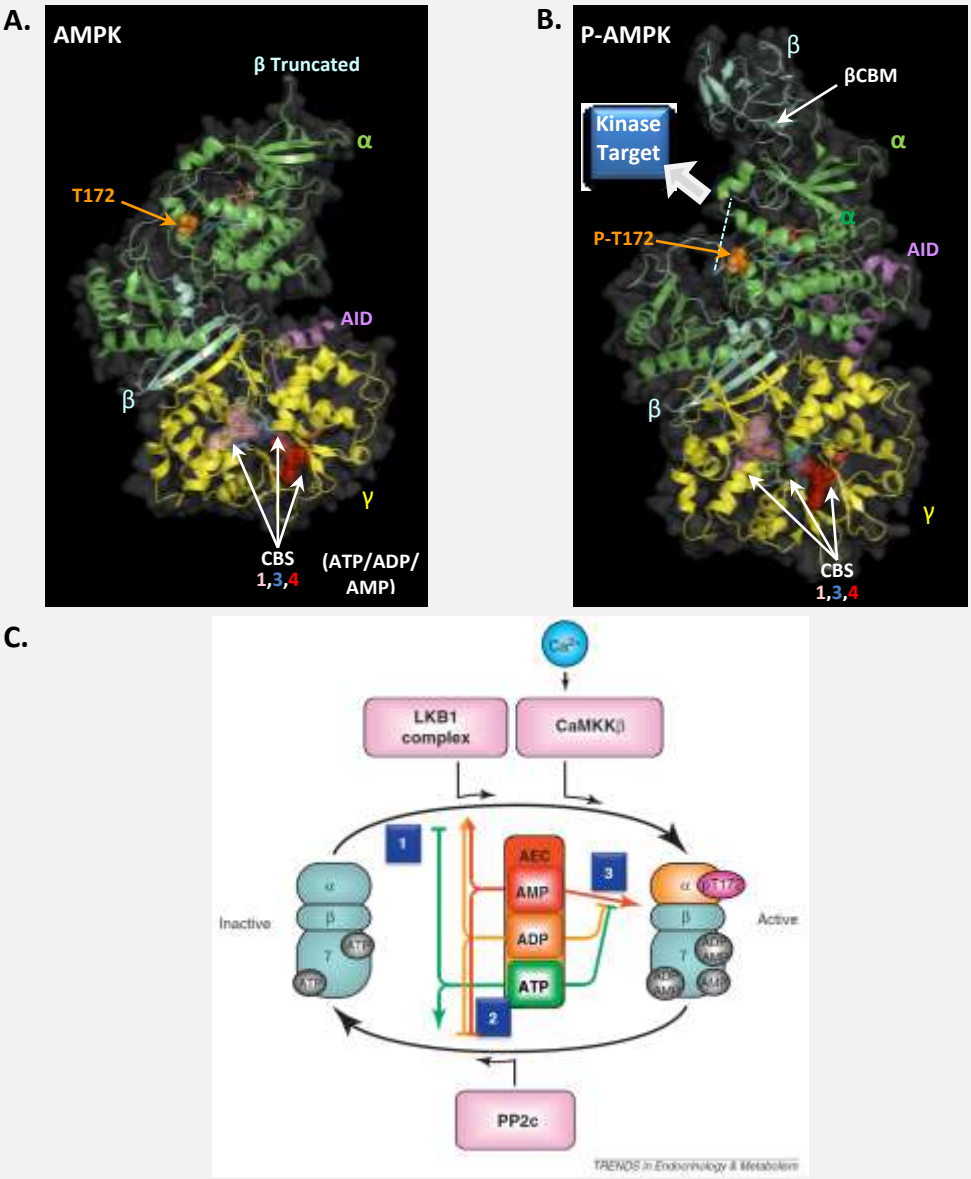

Figure 1-6. AMPK Regulation by ADP/AMP, and AMPKK's .
A. Cartoon representation of 4Å non-phosphorylated human AMPK trimer (PDB-4REW). The α1-subunit (green), scaffolding β2-subunit (cyan), and regulatory γ1-subunit (yellow) are shown. ATP/ADP/AMP binding site (CBS domains) are shown as sticks with colored spheres (1salmon/3blue/4red). The α-auto-inhibitory domain (AID) is visible (pink). The β-subunit is missing the n-terminal 78 residues, including the myristoylation site and CBM domain. **B.** Phosphorylated active AMPK as in A. (PDB-4RER). A significant conformational shift has occurred. The kinase domain has been exposed, the α-subunit p-T172 activation loop/kinase domain is now protected. The AID inhibition of the KD is now associated with the γ-CBS2 domain. The scaffolding β-subunit which links the γ and α subunits is shown in B with its glycogen binding module (CBM). Based on PDB structures from Li *et al. Cell Research* (2015),25:50–66). **D.** Sequential regulation of AMPK by ADP/AMP binding to CBS 4,1,3 (pointed, blunt arrows indicate activation, or inhibition of activity respectively). AMP/ADP binding exposes the Thr-172 phosphorylation sites, which is followed by phosphorylation of Thr-172 by upstream kinases (AMPKK's e.g. LKB1, CaMKKβ), leading to 100 fold activation (from Oakhill *et al. Trends Endocrinol Metab.* (2012),23(3):125-32).

unbound in mammalian cells, and although it can bind ADP in *E. coli*, binding does not appear to affect α-subunit kinase activity) [215].

Oakhill *et al.* have proposed that sequential binding of AMP/ADP on sites 1, which then promotes binding of AMP/ADP to site 3 (based on differential binding affinity for AMP/ADP), induces a conformational change that reveals some portion of the threonine (t172) activation site [215, 220]. This site is subsequently phosphorylated by upstream kinase(s) (AMPKK's) leading to 100 fold AMPK activation (Figure 1-6C). This has been confirmed by x-ray crystallography data that identified an α-subunit AMP sensor structure (known as α-hook/αRIM) in the CBS3 binding domain [216, 217]. Binding of AMP/ADP to CBS3 and the αRIM3 mediates a conformational shift in the α-subunit auto-inhibitory domain (AID). The AID normally interacts with the kinase domain (KD) preventing phosphorylation of T-172 (the AID is truncated in Figure 1-6A). In the presence of AMP, the AID shifts and binds to the AMPK core in the αRIM2/αRIM3 region (Figure 1-6A vs. B)[217]. AMP/ADP dependent stimulation of Thr-172 phosphorylation is dependent on β-subunit myristoylation [221], and binding of ATP in CBS3 site competitively blocks the conformational change [217]. In addition, ATP binding also destabilizes the interaction between the AID and αRIM independent of ATP binding to CBS3 [217]. The concentration of AMP required to induce the change is almost 3 orders of magnitude lower (μM) vs than that of ATP(mM) [219]. It has also been shown that AMP or ADP binding also directly activates Thr-172 phosphorylation by stimulating interaction between AMPKK (LKB1) and AMPK via the scaffolding protein axin [220, 222]).

CBS3 binding to AMP (and more weakly ADP) has the opposite effect on Thr-172 dephosphorylation (the principle means of deactivating AMPK) by intracellular phosphatases including PP2A, and PP2C [223-225]. This is based on an interaction between the activation loop (containing pThr-172) and the AMPK regulatory core, stabilized by the association between the αRIM and γ-CBS3

region [216, 217]. This pTHR-172 protection/association may be destabilized by ATP binding to CBS3 leading to AMPK deactivation. This effect is dependent on the carbohydrate binding module (CBM) in the β subunit but not on β-subunit myristoylation [215, 217, 219-221].

Allosteric activation of AMPK is also not dependent on β-subunit myristoylation, and binding of AMP to the phosphorylated AMPK further increases its activity by 1.5-5 fold. Mutation of CBS4 blocked 100% of allosteric stimulation by 200μM AMP, and mutation of sites 3, and 1 blocked it by 85% and 50% respectively [220]. This allosteric activation is antagonized by both ADP and free-ATP.

The levels of ADP and AMP have been measured in a variety of systems both at rest and stressed by metabolic inhibition, ischemia, muscle contraction etc. (summarized in [215]). Under these conditions typical concentrations of free-AMP (not protein bound) range from 0.2μM-46μM, whereas free ADP ranges from 36-212μM. With K_d binding constants of ~1-2.5μM at CBS1, versus 50-80μM at CBS3, this would indicate that the effects of ADP may out compete AMP [215]. This is countered by observations that ADP appears to only weakly prevent dephosphorylation at Thr-172 [216, 226, 227], and that it has no effect on direct activation of kinase activity [216, 217, 227].

Although less well understood, we must also take into account: (1) secondary inhibition of AMPK by glycogen binding to the β-subunit (which appears to impair an association between the CBM and the KD domains), and potential acetylation of α-subunits[228]. (2) Regulation of activity due to phosphorylation in other areas (e.g AMPK inhibition due phosphorylation of s491 by AKT/PKA [229, 230] [231, 232], α-s173 phosphorylation by PKA [233], and β subunit phosphorylation at s24, s28) which will modulate the overall effect on AMPK activity *in vivo*. (3) Modulation of upstream kinase activity independent of any change in metabolic status (e.g calcium induced activation of CaMKKβ [234-237], in response to DNA damage via ATM [238], increased activity due to hormone

signaling via adiponectin/leptin [239], and/or increased activity due to oxidative stress etc. [240]).

Although there are non-energy related activators of AMPK, and new targets are being identified continuously [241] the activity of AMPK is still highly linked to the energy status of a cell and the organism in general. Once activated, downstream AMPK signaling is now known to affect many targets including (but not limited to), exercise induced conditioning in skeletal muscle [214], hypothalamic driven food intake and energy expenditure [242-246], autophagy/mitophagy and lysosomal protein degradation in the heart and other tissues [247], and gene transcription [248, 249] including mitochondrial biogenesis (stimulated by long term AMPK activation via PGC1α leading to upregulation of mitochondrial DNA and increased long term energy production)[250-254]. Based on these mechanisms AMPK acts as an energy sensor: typically stimulating catabolic ATP production (via glycolysis, glucose oxidation and fatty acid oxidation)[242, 255] and reducing anabolic energy consumption via various pathways (see Figure 1-7) primarily due to phosphorylation of multiple downstream targets [216, 221].

1.5b Stimulation of fatty acid oxidation by AMPK

Cardiac tissues do not produce or contain high levels of fatty acids (FA) normally, as such its ability to process fatty acid is dependent on their uptake into the cell, and into the mitochondria [256]. Lipoprotein lipase on the endothelial cell membrane is activated by AMPK increasing FA transport into the cardiomyocyte [257-259]. Fatty acid transporters (FABP-PM, FATP, and CD36) are found on the sarcolemma, and AMPK can activate their translocation [260-262]. Once inside the cell these FA are converted to acetyl-CoA bound forms awaiting transport into the mitochondria (Figure 1-8).

One of the original AMPK phosphorylation targets is the enzyme acetyl-coA-carboxylase (ACC2) [263, 264]. It was shown to be phosphorylated and

inactivated by AMPK, leading to a decrease in production of malonyl-CoA (from acetyl-CoA). This in turn leads to decreased inhibition of carnitine:palmitoyl-transferase 1 (CPT-1) on the outer mitochondrial membrane, increasing fatty acid uptake into the mitochondria, and hence increased fatty acid oxidation (FAO) [211, 265-268]. This effect can be potentiated by activation of malonyl Co-A decarboxylase (MCD), leading to increased degradation of malonyl Co-A to acetyl-CoA [269, 270]. Although this cascade is well documented, evidence from genetic knockout mice indicate that there are other pathways involved in the regulation of ACC and fatty acid oxidation in response to AMPK activation [271,

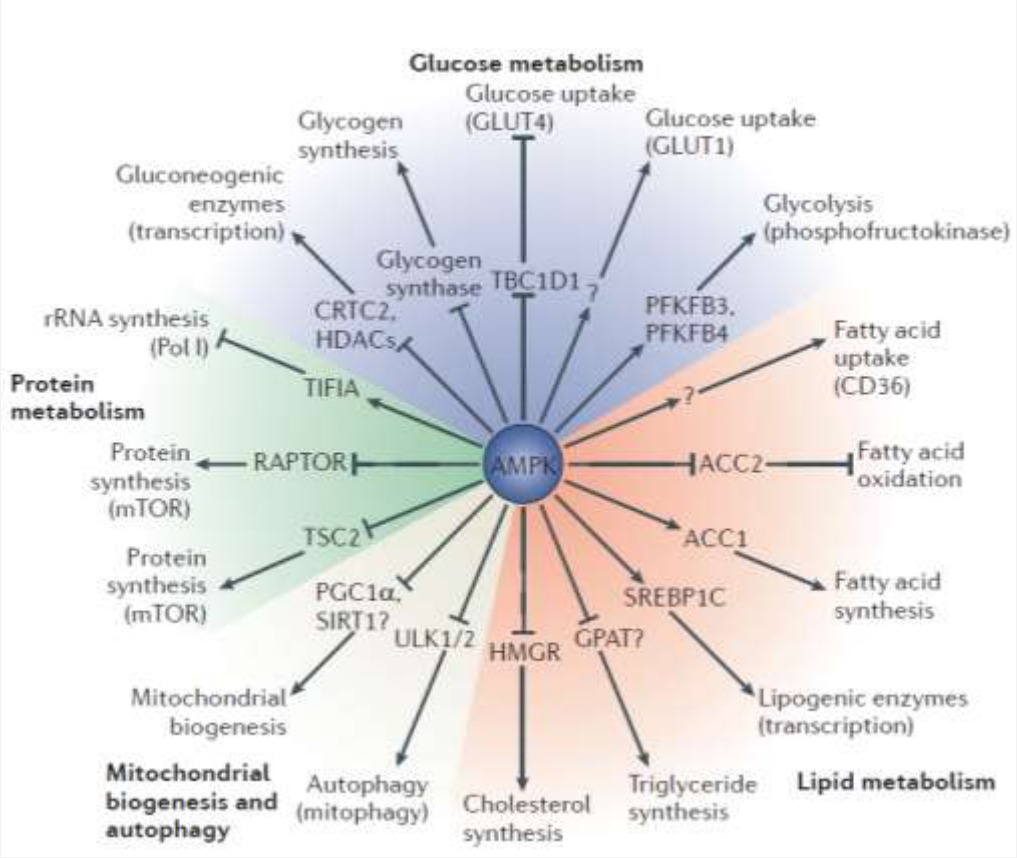

Figure 1-7. Downstream AMPK phosphorylation targets in cellular metabolism. Catabolic pathways that produce energy are enhanced: glucose uptake via glucose transporter type 4 (GLUT4) and GLUT1, glycolysis, fatty acid uptake via CD36, fatty acid oxidation, mitochondrial biogenesis and autophagy. Anabolic pathways which consume energy are inhibited: fatty acid synthesis, transcription of lipogenic enzymes, triglyceride synthesis, cholesterol synthesis, transcription of gluconeogenic enzymes, glycogen synthesis, protein synthesis, and ribosomal RNA (rRNA) synthesis (from Hardie *et al. Nat Rev Mol Cell Biol*. 2012 Mar 22;13(4):251-62).

272]. Possibly by activating CD36 found on the mitochondrial membrane where it transports FA into the mitochondria via CPT1 independent means [273].

Despite these mechanistic controversies, when AMPK is stimulated more FA is available, less is stored, and the released FA is transported into mitochondria producing more ATP.

1.5c AMPK stimulates glucose uptake and glycogen breakdown

When glycogen stores are depleted [274] activation of AMPK leads to increased uptake of glucose by stimulating glucose transporter 1 (GLUT 1)[261, 275-277], and by inducing translocation of GLUT4 to the sarcolemma via both insulin independent pathways [278-284], and via (typically insulin mediated) Akt/AS160 dependent pathways [285-287] (Figure 1-8). Although cellular glycogen content can be increased with prolonged pharmacological AMPK activation, AMPK mediated phosphorylation of glycogen synthase reduces its activity acutely [288-291], and glycogen breakdown appears to be stimulated by AMPK mediated activation of glycogen phosphorylase [292, 293]. In combination, AMPK activation typically leads to increased glucose availability in the cell.

1.5d AMPK stimulates glycolysis

AMPK activation also leads to phosphorylation of phospho-fructokinase 2 (PFK2) leading to formation of fructose 2,6 bisphosphate (from glucose via glucose-6-phosphate), which stimulates the rate limiting step of glycolysis [294, 295] (Figure 1-8). Thus, with increased glucose available in the cell, and faster flux through the glycolytic pathway, there is a significant increase in ATP supplied by glycolysis, with a concomitant increase in glycolytic pyruvate. This pyruvate is typically converted to lactate/used for glucose oxidation when possible.

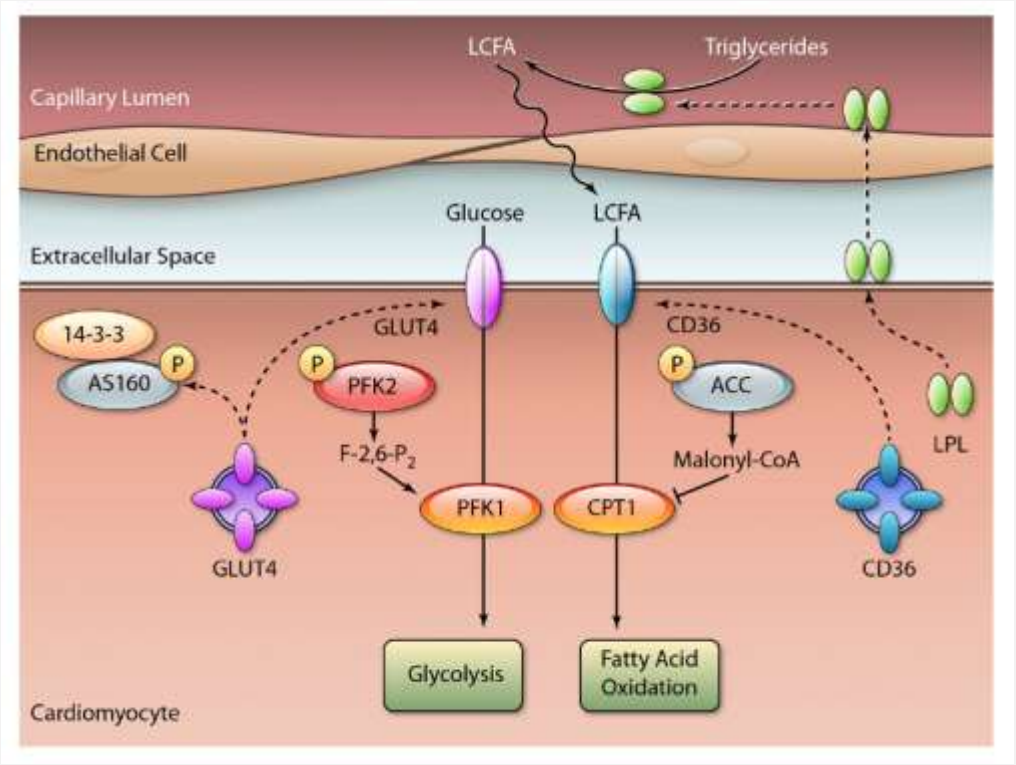

Figure 1-8. AMPK regulation of cardiac energy metabolism.
AMPK regulates substrate transporters and the concentrations of allosteric regulators of glycolysis and fatty acid oxidation. *Glucose uptake/glycolysis*: AMPK phosphorylates AS160, induces GLUT4 translocation to the sarcolemma. AMPK phosphorylates PFK2, leading to the synthesis of fructose-2,6-bisphosphate, an allosteric activator of PFK1 and glycolysis. *Fatty Acid Uptake*: AMPK promotes LPL translocation from the myocyte to capillary endothelial cells, where it catalyzes the release of long-chain fatty acids (LCFA) from FA-containing lipoproteins. Activated AMPK also stimulates CD36 translocation to the sarcolemma, increasing cardiomyocyte free fatty acid uptake. Fatty acid oxidation (FAO): AMPK phosphorylates and inactivates ACC, decreasing the concentration of FAO inhibitor malonyl-CoA. Molecules that are phosphorylated by AMPK are designated by the symbol "P". Proteins directly activated by AMPK are highlighted in red and proteins inactivated by AMPK are in gray (from Zaha *et al. Circ Res.* 2012;111: 800-814).

1.5e The balance between fatty acid oxidation, and glucose oxidation

The Randall cycle dictates that increased fatty acid oxidation rates tend to reduce glucose oxidation rates. In part this is due to end product inhibition of Krebs cycle, meaning that as pyruvate builds up, Krebs cycle is inhibited. Thus, increased supply of pyruvate from either pathway means the other will naturally decrease. In other words, maximal fatty acid oxidation will competitively inhibit glucose oxidation, and vice versa. Thus when fatty acid oxidation is high (when AMPK is activated), if there is a ready supply of fat, then oxidation of glucose is

inhibited. If there is no fatty acid to use, then glucose oxidation will be stimulated by the increase in pyruvate supplied by glycolysis.

1.5f Uncoupling of glycolysis and glucose oxidation induced by AMPK

There is a potential problem with this system, especially in certain situations with a ready supply of fatty acid (as in the heart, especially after ischemia). In such a state, AMPK activation and increased fatty acid oxidation (with reduced glucose oxidation) and increased glycolytic flux, can cause an imbalance between glycolysis and oxidation of glucose via Krebs's cycle, leading to buildup of lactate and H^+ [296, 297]. This proton accumulation decreases local pH and leads to increased activity of the sodium hydrogen exchanger. As sodium accumulates, it leads eventually to a reversal in the sodium calcium exchanger, further leading to calcium uptake and either impaired contraction/function, or in extreme cases, hyper-contracture and eventual cell death, or abnormal electrical activity. This pathway is the focus of attempts to increase glucose oxidation and restore contractile function following myocardial infarction, while also improving cardiac efficiency [296, 298-304].

1.5g Regulation of Nuclear Transcription by AMPK

As mentioned previously, AMPK activation typically leads to a decrease in energy consuming pathways. This is somewhat limited in scope as AMPK activation actually leads to an increase in gene transcription of certain proteins related to metabolic pathways (including medium chain acyl-CoA dehydrogenase, carnitine palmitoyltransferase-1, cytochrome C, and uncoupling protein-3 – proteins which mediate an increase in metabolic throughput, via the transcription factor estrogen-related receptor-α) [305]. In addition, transcription of genes related to mitochondrial biogenesis (via phosphorylating and activating peroxisome proliferator activated receptor-coactivator (PGC)-1α) [239, 250-254, 306]. This would lead to the longer term increase in energy production by new mitochondria.

1.5h Regulation of Protein synthesis by AMPK

As stated, AMPK activation also reduces energy consuming pathways. One way that it does this is by inhibiting protein translation by reducing cytoplasmic HuR mRNA-binding proteins and thus decreasing the stability of many mRNA species [307]. It also inhibits the formation of new mRNA species by phosphorylating the RNA polymerase I (Pol I)-associated transcription factor (TIF-IA) at a single serine residue (Ser-635) [308]. Phosphorylation by AMPK impairs the interaction of TIF-IA with the TBP-containing promoter selectivity factor SL1, thereby precluding the assembly of functional transcription initiation complexes in response to low energy levels.

AMPK also phosphorylates several key modulators of protein translation thus blocking the activation of protein synthesis by growth hormone/insulin/Akt signaling [229, 232, 309, 310]. This is accomplished by inhibiting the mTOR-1 complex (mTORC1) via two pathways. (1) AMPK phosphorylates and activates the tuberous sclerosis complex tumor suppressor protein 2 (TSC2) [311], which converts RHEB-GTP to *inactive* RHEB-GDP and inhibits the RHEB-GTP activation of mTORC1. AMPK also phosphorylates and inactivates the Raptor subunit protein of mTORC1 [312, 313]. By doing so, AMPK blocks the mTORC1 mediated activation of ribosomal protein S6 kinase 1 (S6K1), its stimulation of ribosomal RNA and translation of ribosomal proteins, and its phosphorylation of eIF4E binding protein 1 (4EBP1) relieving 4EBP1 inhibition of protein translation [310]. Via another pathway, AMPK also activates eukaryotic elongation factor 2 (eEF-2) kinase which results in the phosphorylation and inactivation of eEF-2 [314, 315], and inhibition of heart protein synthesis [316, 317].

Protein translation is an energy-consuming process, thus AMPK mediated down-regulation of bulk protein synthesis may function to conserve energy during stressful times. However, by reducing energy consumed, it may profoundly

affect shorter half-life proteins like the cardiac connexins (1-5 hours) potentially leading to altered Cx expression and increased arrhythmogenesis.

1.5i Regulation of Autophagy by AMPK

Recent evidence indicates that the control of autophagy is partially mediated by Akt and AMPK signaling in the heart [247, 318]. Autophagy is the intentional engulfing and lysosomal degradation of persistent macromolecular complexes (proteins, mitochondria, and other organelles including internalized gap junctions [319]): an intracellular recycling program to maintain homeostasis. The lysosomal products are released back into the cytosol as amino acids and other building blocks. These pathways have been linked to the proper healthy function of the heart, occur continuously under baseline conditions, and are impaired

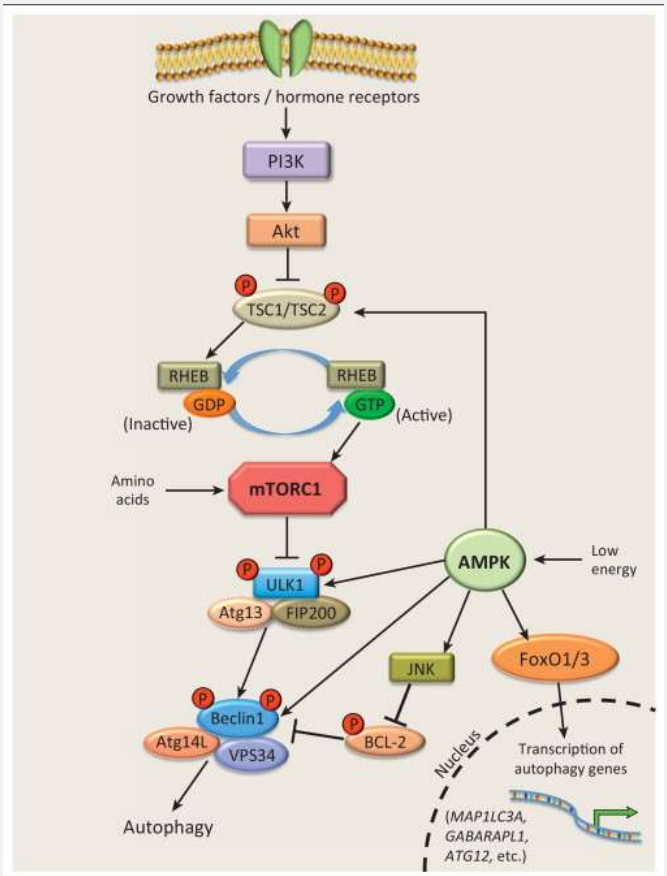

Figure 1-9. Activation of Autophagy by AMPK.
Insulin/growth hormone signaling (inhibition of autophagy) is countered by AMPK activation. Pointed arrows indicate activation, whereas blunt arrows indicate inhibition. (from Kubli DA, Gustafsson AB. Trends in endocrinology and metabolism: TEM. 2014;25:156-64).

with aging and other diseases (diabetes, metabolic syndrome, heart failure etc.). Experimental impairment of autophagy results in rapid accumulation of protein aggregates and dysfunctional organelles, leading to heart failure [247]. Inactivity has also been linked to the formation of post-operative cardiac arrhythmias (AF) where cellular debris accumulate and lead to fibrosis, lipofuscin deposits (undigested waste material), vacuolization, and an arrhythmogenic substrate not seen in patients without impaired autophagy [320]. Stimulation of autophagy (for example by caloric restriction) is associated with increased longevity, and improved function in many organs including the heart. However, unregulated/chronically activated autophagy can have a detrimental effect – for example it has been linked to the switch from stable cardiac hypertrophy to decompensated (dilated) heart failure [321]. In a canine model where AF was stimulated by rapid pacing, autophagy, and AMPK activity markers were both elevated within one day, with similar time dependent responses over 6 weeks [322]. These were correlated with LA tissue samples from patients with and without pre-op AF. Those with pre-op AF showed signs of increased autophagy, and their results would indicate that formation of an arrhythmogenic substrate may be developed over a short time due to excessive autophagy [322]. It is clear that a proper balance must be maintained to maintain homeostasis and normal heart function.

The overall pathway proposed for AMPK regulation of autophagy (from Kubli and Gustafsson [247]) is shown in Figure 1-9. AMPK affects at least five pathways, (1) via activation of JNK (removing inhibition by BCL2), (2) by activation of FoxO1,3 (leading to transcription of autophagy genes), (3) by phosphorylating and activating ULK1 (leading to activation of Beclin1), (4) by phosphorylating TSC1/2, and (5) by directly phosphorylating Beclin1 [247]. Based on its role in recycling internalized gap junctional proteins [319], and its regulation by AMPK we must consider this to be one potential mechanism for AMPK mediated effects on junctional physiology.

1.5j Pharmacological activation of AMPK

The study of AMPK is of keen interest to the scientific community, and its scope is becoming increasingly broad as we learn more about the many and diverse systems that it affects. As with all research, as time goes on, the number of tools available to activate or inhibit AMPK activity has also grown (recently reviewed [323]). Our study of AMPK initially required a clear understanding of its potential pharmacological regulation.

Since AMPK is activated when energy levels are low, the initial approach to activate AMK was to block the metabolic production of energy, for example by treating with cyanide or oligomycin, leading to accumulation of AMP. However, this leads to a decline in energy affecting almost all physiological functions, making specific interpretation of AMPK dependent effects most difficult. To bypass this limitation, most AMPK studies also use the adenosine analog AICAR to stimulate AMPK. This compound forms ZMP inside the cell which is sufficiently similar in size and structure to mimic AMP, and maintains a reasonably long half-life (versus other AMP analogs) allowing sustained activation of AMPK. This activation is independent of energy status within the cell and it is possibly the most commonly used AMPK activator for this reason.

The most well-known clinical (used to treat diabetes) AMPK activating drug is metformin with over 100 million patients being prescribed it each year. Phenformin is a related drug, previously used to treat diabetes, but was withdrawn due to complications including lactic acidosis. In some cases there has been a debate that metformin/phenformin do not alter the ATP:AMP ratio. This debate will probably continue, but their ability to activate AMPK was shown to be dependent on inhibition of the cytochrome-C pathways involved in the electron transport chain [324, 325]. Taking into account the observed biological concentration that occurs with metformin and phenformin in the mitochondria,

these studies correlate inhibition of the electron transport chain with physiological concentrations of metformin/phenformin [324]. As with cyanide, this inhibition effectively reduces the production of ATP by mitochondrial oxidative metabolism. However, perfusion of hearts with phenformin and metformin caused accumulation of cytosolic AMP without altering the total AMP, or total AMP:ATP ratios [326]. These observations would argue that at least some of their effects are mediated by this inhibition even if AMP:ATP ratios are not detectibly different in some models.

Although not available when this thesis work was completed, the small molecule AMPK activators "A-769662", and compound "991" are now known to bind to the β-subunit in a location between the β-CBM, and the α-subunit [219, 327, 328]. These molecules are quite specific, require the β-CBM to be effective, prevent dephosphorylation of Thr-172, and allosterically activate Thr-172 phosphorylated recombinant AMPK. Compound 991 was able to allosterically activate all subtype combinations to various degrees (lowest α1β2γ1 (2.4 fold, vs α2β1γ1 12.2 fold, with half maximal activation (A0.5) of 0.09±0.02 mM. However, A-769662 was effective in allosterically activating only β1 containing recombinant subunits (α2β1γ1 A0.5= 0.39±0.03 mM)[219]. Both activated endogenous AMPK in HEK-293 cells [219]. PT1, and its more potent form C24 is another small molecule that has been shown to interact with the α-subunit near the AID activating AMPK by inhibiting autoinhibition [329, 330]. Lastly, in 2010 it was also shown that salicylate activates AMPK, requiring the β-CBM domain, indicating that it too may act via a similar A769662/991 mechanism [219, 331].

1.5k Pharmacological inhibition of AMPK

Although there are a number of viable AMPK activators, there are presently only two commercially available pharmacological inhibitors of AMPK. One, known as 'Compound C' or 'Dorsomorphin' in the literature [332-334], was originally developed by Merck, and was not commercially available for some time as it was

being screened for potential value as a clinical agent. As this research program became less active over time, its availability for use in research has gradually increased. It has been used as an AMPK inhibitor but has been shown to be promiscuous affecting many protein kinases (including BMP receptor kinase, c-Src, EphA2, Flt1, Flt3, KDR, Lck, Mnk1, and Rsk1 with various affinities [335]. Based on Compound C, a series of small molecule inhibitors have been tested, all were susceptible to promiscuity although with different cross-reactivity profiles [335]. Another small molecule inhibitor, developed as a tyrosine kinase inhibitor known as Sunitinib has been shown to be cardiotoxic with off target inhibition of AMPK activity in cell free and isolated cell assays [336, 337]. These were not available to us for these thesis studies, and are mentioned for the sake of completeness, and for future use if necessary.

1.5l Upstream kinase regulation of AMPK

As mentioned previously, activation of AMPK is dependent on phosphorylation of threonine 172 on the α subunit, and is enhanced by AMP/ADP. There are two main upstream AMPK kinases (AMPKK's): liver kinase beta 1 (LKB1), and CaMKβ, with various reports that PKCζ , and a TGF-β- activated kinase (TAK-1) can also phosphorylate Thr-172 or regulate its LKB1 mediated phosphorylation [235, 236, 338-347]. In some cases, activation by LKB1 versus CAMKKβ is essential i.e. deletion of LKB1 in a mouse model has blocked some AMPK dependent effects, but others are maintained. This implies that residual AMPKK activity is sufficient in some cases, that AMPK is a meeting point for many stress activated protein kinases, and that signaling by a number of different factors can lead to activation of AMPK independent of changes in energy metabolism (AMP/ADP:ATP ratio). In general, upstream activation of AMPK results in downstream phosphorylation events and physiological changes by a vast array of possible mediators/AMPK targets.

1.6 Phosphorylation mediated regulation of Cx proteins

Almost every part of the Cx lifecycle is affected in some way by the balance between kinase dependent phosphorylation and phosphatase dependent dephosphorylation: expression, trafficking, activity, gating, and internalization/degradation. These effects have been reviewed a number of times [80, 117, 347-356], but the majority of our knowledge is focused on Cx43. Phospho-regulation of the other main cardiac connexins (Cx40 and Cx45) is, with a few exceptions, relatively unknown. The following sections will briefly outline the known phosphorylation sites, kinases/phosphatases responsible, and effects on Cx function where known.

1.6a Regulation of Cx43 by phosphorylation

Cx43 is by far the most studied connexin, possibly in all respects, but certainly in regard to phosphoregulation. It can be phosphorylated on primarily serine, but also threonine, and tyrosine residues by a wide variety of protein kinases [350, 357]. Pulse chase experiments (transiently treating cells with radiolabeled ^{32}P), show that Cx43 becomes a phosphoprotein within 15 minutes of synthesis within the ER and Golgi apparatus [358, 359].

Cx43 is found in many post-translational electrophoretic isoforms, including three abundant sizes, a larger P2, medium P1, and smaller P0. All of these isoforms are converted to the P0 form when treated with alkaline phosphatase to remove phosphate groups [360, 361]. Thus it is assumed that these isoforms shifts are due to phosphorylation. However, the P0 band does contain some phosphorylated residues [362], and the addition of even multiple phosphate groups (at 80 Da per residue), is not consistent with the magnitude of the shift (2-4 kDa), thus indicating that the phosphorylation event also induces a lasting conformational change that is detectable in SDS-PAGE mobility. Based on phospho-site specific antibody data, there can be multiple phospho-variants of

each isoform (different phosphorylation status at any one site), which can co-migrate during SDS-PAGE separation with the P1, P2, or P0 forms [363].

These isoforms begin to appear in separate intracellular pools almost immediately [160, 362]. Both the P1 and P2 isoforms are found at the plasma membrane [159], but the largest P2 isoform is far less soluble in 1% triton detergent solution [364], indicating that formation of the P2 form may be related to stabilizing it inside the junctional plaque. The smaller isoforms are much more readily solubilized and are (generally) found in the intracellular fraction in membranes of the ER and Golgi [359].

Phosphorylation targets have been identified in Cx43 that are phosphorylated by specific protein kinases (see) with varying degrees of functional effect. The affected residues are primarily located in the c-terminal intracellular tail region of Cx43, although in other Cx proteins they have been located in the cytoplasmic

Table 1-1. Known Cx43 phosphoregulation sites.

Kinase Involved or activated	**Cx43 Residue(s) phosphorylated**	**Reference**
Akt	s373, s369	[122, 363, 365]
CK1	s325, s328, s330	[366]
MAPK	s255, s279, s282	[366-372]
PKC	s368, s262?	[161, 179, 373-377]
p34cdc2/cyclin B kinase	262	[378-380]
PKA	s364, s365	[381-387]
Src	y247,y265	[357, 388-391]
CAMKII	S244, s255, s257,s296,s297, s306, s314,s325, s328, s330, s364, s365, s369, s372, s373	[392]
unknown	s5, s262, s296, s297, s306, y312, y313, s314, s369, s372	[117, 377, 386, 393-395]

loop region as well (eg. Cx56). Until recently there were no known phosphorylation sites in the n-terminal region, however, large scale mass spectrometry analysis of brain samples which included Cx43 indicates that at least one residue is phosphorylated *in vivo* (serine 5) [350, 393]. We have identified multiple putative phosphorylation sites for AMPK in Cx43 as well as the other cardiac connexins, but at this time I will focus on the known/confirmed sites with functional data.

Assembly of Cx43 into gap junctions is regulated by phosphorylation. Cx43 translocation from the Golgi to the plasma membrane is stimulated by cAMP and PKA activation [373, 381, 383, 384, 387, 394, 396, 397], and likely involves phosphorylation of s365 [160, 398]. Consistent with this, phosphorylation of s365 is necessary for the shift to the P1 isoform [160]. Recruitment of Cx43 into GJ plaques from the plasma membrane , and a shift to the P2 isoform, has been linked to casein kinase CK1 dependent phosphorylation of s325/s328/s330 [159, 366], and activation of PKC (via phorbol ester) can block the assembly of new junctions [376].

Hypoxia, wound healing, or activation of PKC (phorbol ester), leads to phosphorylation of s368 and downregulation of Cx43 [163, 362, 399, 400]. Phosphorylation of s365 partially prevents the phosphorylation of s368 leading to protection of Cx43 conductance [160]. Lampe's group has observed that internalization of Cx43 in response to injury/wound healing is typically preceded by an acute accumulation of Cx43 in the junctional plaque with s373 (Akt) phosphorylation increased (within 5-15 min), followed by phosphorylation of s279 and s282 via MAPK activity (15-30 min), which is further followed by phosphorylation of y247 by Src tyrosine kinases (at 30+ min) leading to internalization and lysosomal degradation (Figure 1-10)[117]. Whether this sequence is active in response to other stimuli remains to be determined.

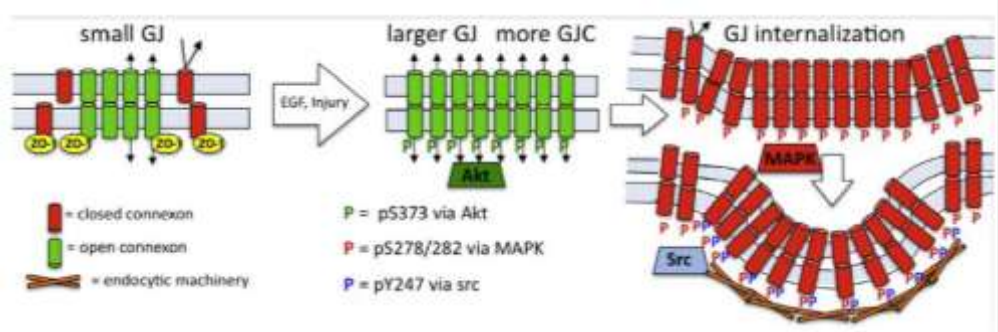

Figure 1-10. A model for regulation of gap junction size by phosphorylation. Phosphorylation of Cx43 by AKT on site s373 leads to incorporation of Cx43 into larger gap junctions with increased permeability. Phosphorylation at s279/s282 closes the gap junction and then phosphorylation at y247 leads to binding of GJ internalization machinery due to epidermal growth factor (EGF) (MAPK) or phorbol ester (TPA) induced PKC activity.(from Solan, Lampe *FEBS Lett*. 2014 Apr 17;588(8):1423-9).

Phosphorylation of s373 by Akt has been shown to induce GJ growth, and increase Cx43 stability, effects which were inhibited by Akt inhibition/ knockdown [122, 365]. This is postulated to occur by inhibiting the interaction between Cx43 and the scaffolding protein ZO-1, preventing Cx43 internalization [122, 401]. Mutation of the Akt site to alanine (s373a) prevented the association with ZO-1 increasing GJ size, whereas mutation to aspartic acid (s373d) increased the association with ZO-1 and formed small GJ [122, 363]. It was also shown that s373a mutation also blocked the response to Akt activation, and s373d mimics it with larger GJ and increased permeability to calcein dye [363].

As noted above, phosphorylation of s255, can be driven by p34cdc2 [379], leading to cell-cycle dependent downregulation of Cx43 (inhibition during mitosis), but it was also reported that s255 is also phosphorylated by big MAPK1/ extracellular regulated protein kinase 5 (ERK5) [372]. Similarly, phosphorylation of s325/328/330 by CK1 has also been reported due to CAMKII mediated phosphorylation [392]. These results emphasize that fact that phosphorylation of the same residue by different protein kinases is possible, or related in some upstream kinase manner.

Using site specific antibodies and mutagenesis studies, it was found that Src (a tyrosine kinase) dependent downregulation of Cx43 conductance was dependent on direct Src mediated phosphorylation of y247, and y265 [357, 388-391]. Unfortunately, it was also shown that Src activation also leads to phosphorylation of ERK, and decreased phosphorylation of Akt [117] leading to subsequent phosphorylation of MAPK sites s262, s279, s282 [369, 402]) and a decrease in phosphorylation of s373 [117]. Thus the active mediator of these effects is likely a combination.

1.6b Cx40 regulation by phosphatases

Since the identification of the first protein kinases, the role of protein phosphatases in biology, including early Cx biology, was unfortunately assumed to be a continuous passive removal of phospho-groups by general non-specific protein phosphatases [403]. This view has expanded significantly, and the complexity of Cx regulation by phosphorylation has been suitably revised to include the active, specific dephosphorylation of residues when possible. The role of phosphatases in Cx biology was reviewed by Herve *et al.* in 2006 [80] and much like the study of Cx phosphorylation in general, it focuses almost exclusively on Cx43.

Protein phosphatases can be grouped into 2 main areas with differential requirements for various co-factors (eg. Mg^{++}, Ca^{++}, metals, subunit proteins): (1) Phosphoserine / phosphothreonine protein phosphatases (**PS/PTPP**) including PP1, PP2A, PP2B (calcineurin), and PP2C - isoforms encoded by the PPP and PPM gene families. (2) Phosphotyrosine (**PTyPP**) and dual specificity protein phosphatases. These include the receptor type (transmembrane) PTyPPs, low molecular weight, and dual specificity subtypes (including the MAPK deactivators MKP-1/CL100). The membrane bound ecto-enzyme (active on outside of the cell) alkaline phosphatases are also included in this group although due to this location they are not expected to interact with Cx channels *in vivo* [80]. The

PS/PTPP phosphatases are typically heteromeric protein complexes ‘holoenzymes’ (much like AMPK) with an active catalytic domain (eg. PP1), and one or more regulatory scaffolding subunits (for PP1 these contain a conserved RVxF motif). These subunits associate with target proteins, endogenous inhibitor proteins etc. thus dictating the subcellular localization and activity of the holoenzyme (eg. PP1, with MYPT1 subunit associates with myosin forming “myosin light chain phosphatase”, versus PP1 with ‘subunit G’ associates with glycogen forming “phosphorylase phosphatase”)[403].

The following are specific phosphatases that have been associated with Cx proteins in different cell lines and tissues: PP1/PP2A [404], PP2B/CN [162, 367, 405], PP1 [406-408], vascular protein tyrosine phosphatase 1[409], receptor protein tyrosine phosphatase PTyPPμ [410]. Cx43 co-precipitates with PP1, and PP2A in cardiac tissue preparations, and the associated PP2A increased 2.5 fold when Cx43 was isolated from human heart failure samples [404]. It was shown in rat astrocytes, that calcineurin (PP2B or CN) activity leads to Cx43 dephosphorylation under chemical hypoxia, which was inhibited by cyclosporinA, and FK506 (CN inhibitors)[411]. CN inhibition had no effect on Cx43 phosphorylation in another cell line under resting conditions [412].

Cx activity is dependent on ATP, and removal of ATP from patch clamp electrode solutions, or the decline in cellular ATP in cardiac tissues due to hypoxia etc. is linked to Cx dephosphorylation and reduced Cx activity [406, 408]. This inhibition can be prevented by the addition of free-ATP to the patch electrode, or in some cases by inhibition of phosphatase activity. For example by broad spectrum inhibitors like okadaic acid (PP2A>PP1>PP2B)/calyculinA (PP1=PP2A), or more specific inhibitors such as heparin/I2 (PP1), or fostriecin (PP2A inhibitor). Using these, with a neonatal cardiac myocyte model it was shown that PP1 (vs PP2a) was responsible for this decline [408]. In other cases, despite increasing the abundance of the larger MW (P2) form of Cx43 (which would indicate that

overall phosphorylation levels were increased), long term hypoxia (6h) caused a decline in “phospho-Cx43” that was not prevented by these PP1/PP2A inhibitors [413]. In this case, agents which stimulated various protein kinases (including MAPK, JNK, PKCe, or AMPK) failed to prevent the decline during hypoxia, but PMA activation of PKC did eliminate the ‘dephosphorylated Cx43’ signal at rest. In this case they used a specific Cx43 antibody now known to recognize the non-phosphorylated Cx43 PKC site s368, yet their interpretation was that overall dephosphorylation was not prevented. This study in particular highlights the complex nature of the system, and the need to examine the full range of Cx43 phosphorylation sites available before making any conclusion as to the mechanism of any one treatment effect.

In short, these studies indicate that Cx phosphoregulation is a very complex phenomenon, with interacting kinase pathways, a balance between phosphorylation and dephosphorylation on specific targets, and functional effects. It was recently postulated, in a 3D space filled model, that many of these interacting phosphorylation targets tend to be clustered with protein binding sites (eg. SH3, SH2 which are Src binding regions, or the PDZ region which binds the scaffolding protein ZO1) [352]. Thus indicating that phosphorylation, mutation, or interaction with different proteins can all affect one another in cardiac myocytes as demonstrated experimentally in a number of different models [156, 412, 414]. In order to understand the regulation of any Cx in this light it is thus imperative that we learn as much as possible about these events in a simple system, and then proceed to the more complex interactions.

1.6c Cx40 regulation by phosphorylation

At this point, in comparison to Cx43, Cx40 phosphoregulation is relatively understudied and thus less understood. However, it has been demonstrated by the incorporation of ^{32}P in vivo, and the immuno-reactivity to phospho-serine and phospho-threonine antibodies that Cx40 is regulated by phosphorylation as

well [415]. However to date there is scant evidence directly linking various phosphorylating conditions with Cx40 phosphorylation and changes in function, that which we do know is summarized as follows:

Cx40 was shown to be a phospho-protein by western blot [415, 416] and that treatment with PKC (TPA) and PKA (8-Br cAMP) activators increased the incorporation of ^{32}ATP in HeLa cells transfected with mCx40 without altering the size of the peptide [415]. In later studies – treatment of SKHep1 cells (human hepatoma) transfected with human Cx40 with PKA activator 8-Br cAMP increased electrical conductance (dual cell patch) as well as permeability to Lucifer yellow dye. The molecular weight of this Cx40 shifted from 40 to 42 kDa with PKA activation (Alpha Diagnostics goat anti-Cx40) indicating that it had been phosphorylated [416]. In addition, "phosphorylation" appears to alter the single channel conductance pattern of Cx40. This is based on frequency histograms of single channel events which indicate that the Cx40 in this system displayed conductance events of ~117, 82 and 30pS. However, upon treatment with 8-Br cAMP for 10 min there was a shift in frequency from the subconductance state at 82pS to events at 122pS indicating that single channel conductance was increased. Potential phosphorylation sites were proposed based on the putative PKA recognition sequence as either s120 or s345 however they were not identified conclusively by mutagenesis. Although Cx40 also seems to exhibit an altered gating state, as with Cx43, stimulation of Cx40 maturation seems to be driven, at least in part, by PKA activation [417]. These similarities are encouraging, but by no means indicative, as often the effects of one treatment can have very different effects on other subtypes [418, 419].

1.6d Cx45 regulation by phosphorylation

Phosphorylation of Cx45 was demonstrated first in 1994 [420, 421] then again in HeLa cells by Hertlein *et. al.* in 1998, who found as with Cx43, and Cx40, that Cx45 contained primarily phosphorylated serine residues, as well as fewer but

some phospho-threonine, and phospho-tyrosine residues that were not detected in the earlier studies [422]. It was noted in the earlier studies that treatment with cAMP, or cGMP did not alter the phosphorylation density of Cx45, whereas phorbol ester (PKC activation) did increase it significantly. This does not preclude the possibility that multiple additions or subtractions may occur during metabolic labeling [420]. However, in the later studies, ^{32}P incorporation was reduced by 90% when the nine c-terminal residues were removed or exchanged, indicating that phosphorylation occurs primarily on these residues. In addition, the truncated Cx45 molecules were trapped in perinuclear organelles whereas they behaved normally when the same residues were exchanged. The half-life of Cx45 was decreased by 50% when either s381 and s382 or s384 and s385 were replaced by other amino acids, indicating that phosphorylation of these residues, alone or in combination increased the stability of the molecule [422].

Functional regulation was confirmed later in dual cell patch clamp experiments where PKC activation was shown to increase Cx45 conductance, and PKA activation decreased it. cGMP activation had no effect, but inhibition of tyrosine phosphatase decreased conductance, indicating that phosphorylation of tyrosine is beneficial to Cx45 conductance whereas it is inhibitive to Cx43 [97].

In the end, we are left with distinct probability that Cx40, 43, and 45 are all regulated by phosphorylation, and that this regulation is not the same among all Cx studied. It is also clear, that we must study these complex phenomena from many angles to have even a rudimentary understanding of their physiological importance.

1.6e Potential phosphorylation of Cx43, 40, and 45 by AMPK

Based on consensus sequences identified from known AMPK phosphorylation sites [240, 312, 423, 424], we identified potential serine/threonine AMPK (α2) phosphorylation sites in all three main cardiac GJ subunits: at residue **t118** in the cytoplasmic loop region of Cx43. On **t18**, and **t36** within the N-terminal region of

Cx45, a region that has only recently been shown to be phosphorylated in Cx43[350], yet a region that is very important in other forms of regulation (including pH sensitivity). **t19** in the N-terminal region, **s122** in the cytoplasmic loop region, and **s349** in the C-terminal region were all identified as possible AMPK targets in Cx40. Despite their varied locations, it is clear that identification of phosphorylation at any of these sites may have important consequences on the regulation of cardiac gap junctions, and their influence on cardiac electrophysiology and arrhythmogenesis.

1.7 Mechanisms of arrhythmia formation.

There are two main forms of cardiac arrhythmia, brady-arrhythmia- slower than normal heart rates, and tachyarrhythmia – faster than normal heart rates. These can further be divided into atrial or ventricular arrhythmias based on their site of origin, and subdivided based on the underlying mechanism at the cellular or tissue level [109, 425-428].

1.7a Arrhythmias and Automaticity

At the most basic level, there are normal forms of automaticity, due to the regular depolarization/re-polarization of small pacemaker regions in the SA node which are propagated out into the atria then to the rest of the heart- resulting in the 'normal sinus heart rate/rhythm' (NSR). These rates can be modulated by sympathetic nervous regulation leading to sinus-tachycardia or sinus-bradycardia (eg. by affecting the rate via I_f activation, calcium cycling, I_{CaL}, I_{ks}, and Na-K+ ATPase I_{NaK}) [23, 25, 426]. At a sufficiently slow rate of sinus activity the heart has a backup mechanism, where regular automaticity in other cells of the heart will drive the heart rate (an 'escape rhythm' with rates in the SA node>AV node>Purkinje>LV myocardium). The slowest of which – the ventricular escape rhythm, is often too slow to support all but the lowest of human activity levels (often requiring an external pacemaker).

1.7b Bradycardia -Heart Block

There are many potential mechanisms leading to bradycardia at the tissue, and cellular levels (eg. reduced automaticity in the SA node, altered adrenergic signaling, sinoatrial exit block). One of the primary causes is a functional (vs. physically damaged) blockage in conduction within the SA node (SAN), the AV node (AVN) or the left and right His-Purkinje bundles (LBB/RBB). These are known as SA block, AV block, or infra-hisian/bundle branch block (LBBB/RBBB) respectively, and they are graded based on their increasing degree of severity and type (eg. 2nd° type I AVB). Increasing degrees of fibrosis, as well as modified cell-cell conduction in the SAN and AVN node can lead to these functional blockages [109, 425, 429].

Sustained normal propagation (fast or slow depending on the region) of SAN, AVN, and His depolarization depends on activation (or automaticity), and also on proper isolation from the surrounding atrial tissues. As introduced in section 1.1c the propagation of depolarization depends on a sufficiently large current 'source' - depolarizing an appropriately sized region of 'sink' tissue. When the source (nodal cell region) is small (in both physical size and low Na channel density), and the sink (surrounding atria) is large: electrical expansion is needed, and propagation can fail. This can be prevented by partially isolating the source from the surrounding atrial tissues increasing the source/sink ratio. This isolation is based on fibrosis, superficial adipose tissue, and the degree of cell-cell coupling (including unidirectional GJ voltage sensitivity as discussed in section 1.3d)[429, 430]. These factors necessitate defined pathways of conduction from the SAN to atria (Figure 1-11), and atria to AVN to bundles of HIS and Purkinje fibres [109, 430]. The SAN complex is shown in Figure 1-11. Here we see that the SAN has three pathways for activating the atria successfully.

The AVN pathway is shown in Figure 1-12)[430]. Within the AVN there is a fast pathway (inhibited at very high atrial rates), and a slow pathway (normally

A. SAN Pacemaker Complex

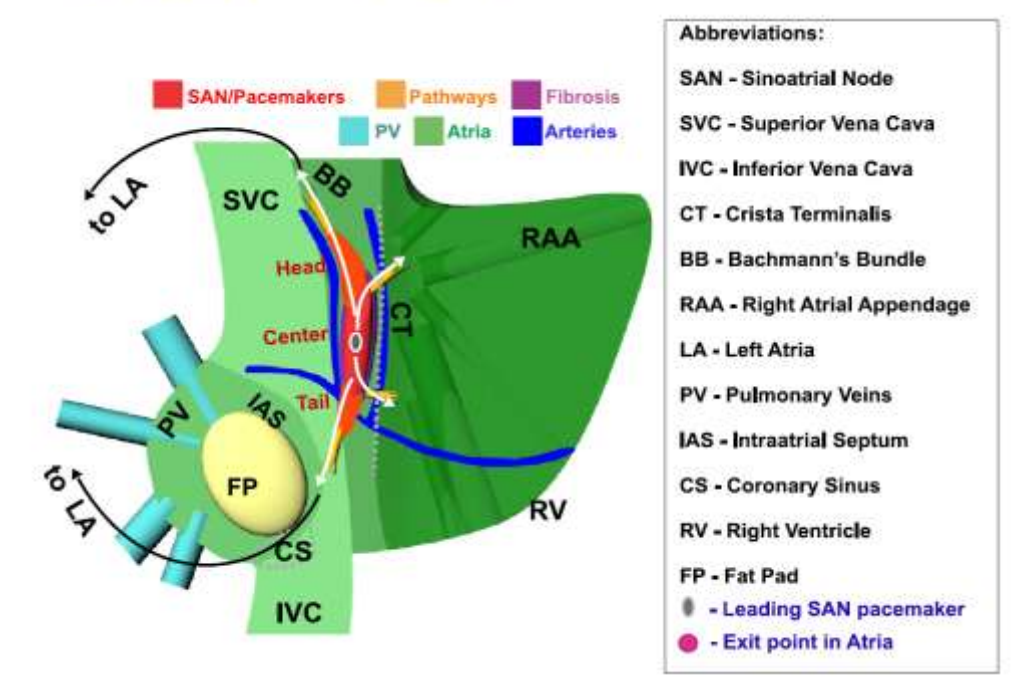

B. SAN Conduction Pathways, Cx Expression

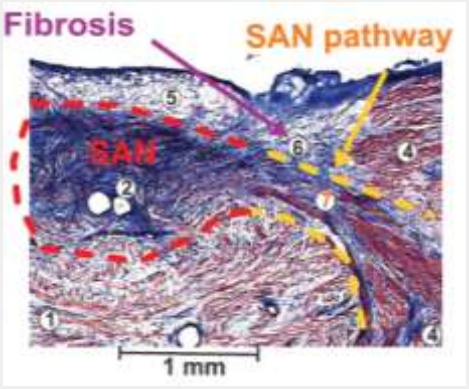

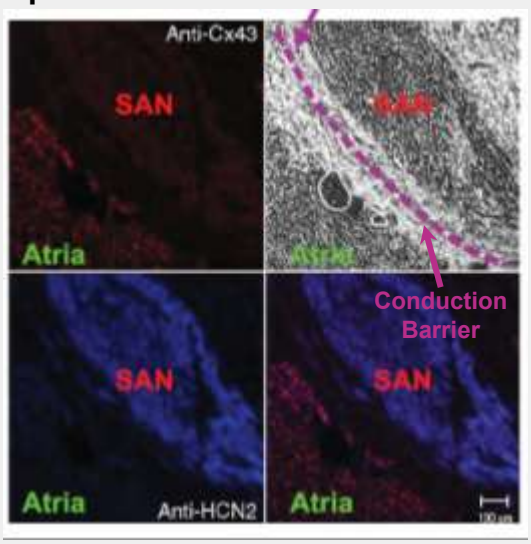

Figure 1-11. Conduction pathways in the Sino Atrial Node (SAN) and atrioventricular node (AVN).

A. Anatomy of the SAN. There are three main pathways of conductance out of the SAN. The rest is isolated from the atrial tissue by adipose tissue (FP), fibrosis, blood vessels (arteries), and a lack of Cx43 expression). **B.** Histological staining of canine SAN. **Left:** Masson Trichrome staining of human SAN showing fibrosis (blue) surrounding the SAN. **Right:** Canine SAN (stained blue via HCN2 antibody) is isolated from the atria via reduced Cx. (modified from Fedorov *et al.* (2012) *Am J Physiol Heart Circ Physiol* 302: H1773–H1783).

bypassed at slower atrial rates). Each pathway has a distinctive cellular structure, Cx expression profile, refractory rate, and sodium channel abundance. Alterations these properties including (for our purposes) Cx lateralization, conductance, phosphorylation status, or subunit distribution will affect the degree of coupling. For example: Cx40 homozygous knockout mice have impaired conduction through the AV node, and His-Purkinje pathways [431]. As both Cx45 and Cx40 (with variable levels of Cx43) are extensively expressed in the specialized conduction pathways, it is quite possible that specific alterations in their activity can lead to or pre-dispose for arrhythmias of this nature.

A. Human AVN Conduction Pathways, Cx Expression

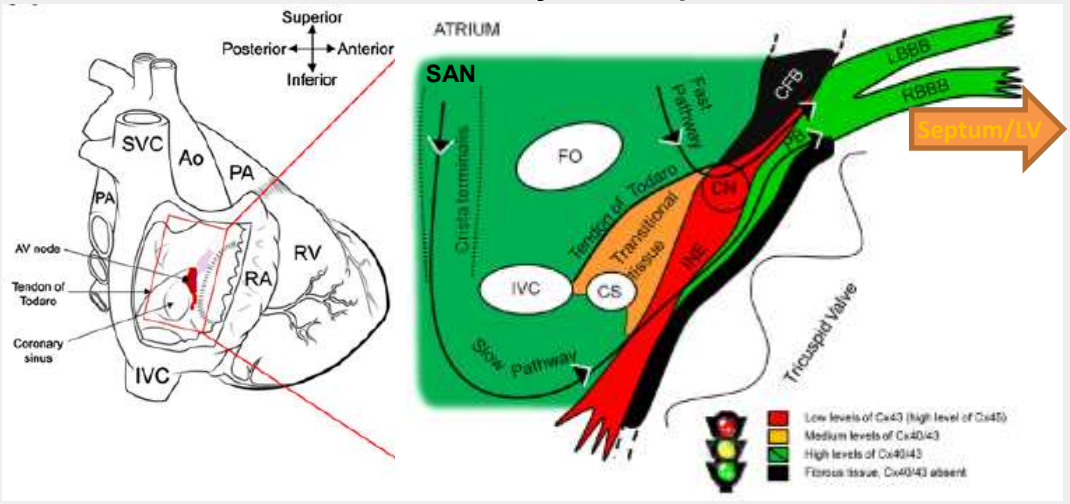

B. Human Cx mRNA Abundance

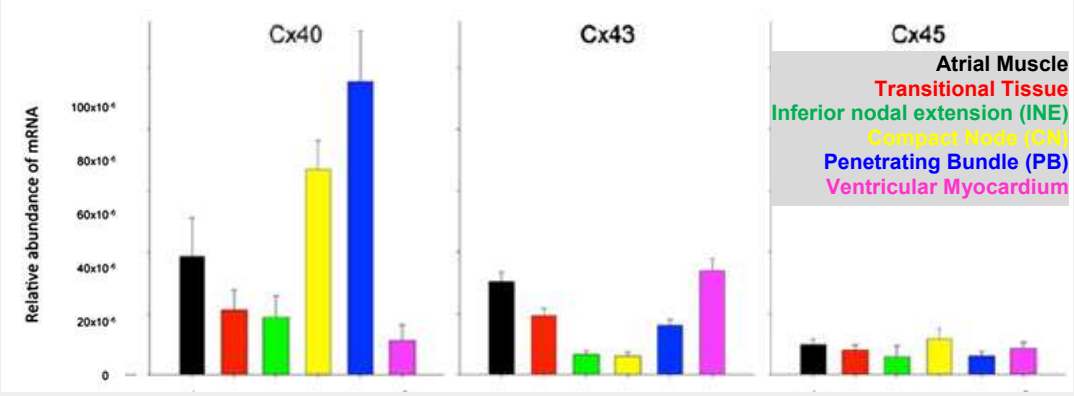

Figure 1-12. Conduction pathways and Cx expression in the atrioventricular node (AVN). **A.** Anatomy of the AV node. Left: Heart viewed from behind with window cut in the right atrium to expose the AV node (shown in red). **Right:** Exploded view of boxed region on the left showing slow path, and fast entry path (arrows). Relative expression of Cx43/Cx40 in stop light colors - Red: low Cx43 high Cx45, Orange: medium Cx40/43, Green: high Cx40/43. **B.** Relative abundance of mRNA for connexin isoforms in different regions of the AV junction of the human heart. Means ±SEM values are shown (n =6). Ao: aorta, CN: compact node, CS: coronary sinus, FO: fossa ovalis, IVC inferior vena cava, LBBB left bundle branch, PA pulmonary artery, PB penetrating bundle, RA right atrium, RBBB right bundle branch, RV right ventricle, SVC superior vena cava (modified from Temple *et al. Heart Rhythm.* (2013), 10(2): 297–304).

1.7c Abnormal Automaticity- Tachycardia

There are three main causes of tachyarrhythmia in humans. Early after-depolarization's (EAD's), delayed after-depolarization's (DAD's), and reentrant circuits. The first two types are related to the spontaneous generation of spatiotemporally isolated abnormal automaticity (an ectopic focus), which can then propagate to other regions of the heart.

The cellular basis for EAD's is the generation of a prolonged action potential, and the eventual re-activation of L-type calcium channels causing small membrane depolarizations on this plateau [24, 25, 426, 432]. When these fluctuations occur following the absolute refractory period another action potential is developed. The prolongation of action potential duration can be due to pathological states (eg. heart failure), or due to genetic factors (eg. long QT syndrome) and is often due to downregulation of potassium channels, or sustained Na channel activity which contribute to the action potential plateau (as summarized in section 1.1a) [426]. The ryanodine receptor RyR is responsible for action potential/calcium induced calcium release from the myocyte sarcoplasmic reticulum leading to muscle contracture. It has been shown in a rabbit long QT model, that EAD's can also (vs. I_{CaL} reactivation) be due to calcium waves related to hyperactivity and hyper-phosphorylation of RyR in response to β-adrenergic stimulation [432].

DAD's occur once the cell is fully re-polarized, and are generally caused by calcium accumulation and overload, resulting in ryanodine receptor mediated spontaneous Ca^{2+} waves (also called store overload–induced Ca^{2+} release or "SOICR")[433], and a transient inward current which causes depolarization (of debatable origin)[426]. Calcium overload, and calcium waves can be induced by RyR mutations [433], excessive Na^{+}/Ca^{2+} exchanger (NCX) activity, and β-adrenergic stimulation [426]. As with all point source activations, well coupled cells tend to inhibit the propagation of EAD's or DAD's, and extremely low levels of coupling prevent propagation entirely [426].

1.7d AMPK and Spontaneous Activity

The formation of EAD's is generally attributed to the prolongation of action potential duration in the plateau phase. AMPK activation has now been shown to affect a number of ion channels, either directly or indirectly, which can affect (among other properties) action potential duration (APD) [434]. AMPK activation via constitutively active ($AMPK_{CA}$) adenovirus, has been shown to affect voltage gated sodium channels causing prolonged action potential duration, slowed voltage dependent inactivation, made them more likely to activate at lower membrane potentials, and caused the formation of EAD's in adult rat LV myocytes [435]. This was presumed to be due to activation of AMPK. However, the particular sites affected have not yet been confirmed.

Action potential duration is also affected by chloride channels. The CFTR Cl^- channel has both inward and outward currents with an equilibrium potential of ~-65 to -40mV, as such it can have both depolarizing (at lower potentials) and re-polarizing effects (at higher potentials). The magnitude of these effects depends on the Cl^- transmembrane concentration gradient, and the relative background conductance due to other channel activity. In the heart, CFTR activation results in shortened action potentials, whereas inhibition results in prolonged action potentials and EAD formation [436].

CFTR actively opens following PKA binding, and additive PKA mediated phosphorylation at up to 15 different sites in the regulatory R domain increased its activation (10 mutations were needed to remove PKA sensitivity, and no one site was essential) [437-440]. AMPK mediated inhibition of PKA activated CFTR and *in vitro* phosphorylation of s768 was demonstrated [441-443]. It was also shown that background AMPK activity inhibited CFTR conductance, and that this inhibition was blocked when AMPK was inhibited [444, 445]. Following these observations it was later shown that AMPK mediated CFTR inhibition required AMPK binding to the (R) domain, in the presence of NDPK-A (Nucleoside

Diphosphate Kinase A), which appears to mediate the impaired conductance [446]. This interaction and inhibition was blocked by competitive AMPK binding CFTR peptide fragments highlighting the need for AMPK to bind to CFTR prior to phosphorylation.

The Kv2.1 channel (I_{Kr}) is directly phosphorylated by AMPK, at s440, and this resulted in hyperpolarizing shifts in channel activation/inactivation in neuronal and Hek-293 cells [447]. The K_{ATP} channel Kir6.2 is phosphorylated by AMPK on s385 resulting in decreased current amplitude [448, 449]. Activation of AMPK has also been shown to cause the internalization of membrane ion channels (including Kv2.1, Kv7.1, and ENaC) by phosphorylating and activating NEDD4-2, a protein that marks them for internalization and degradation via ubiquitination [25, 434]. These studies would indicate that AMPK can mediate prolonged action potential duration via sodium, potassium, and chloride channel currents (in complex combination) leading to potential spontaneous activity.

1.7e Macro-Reentry – Atrio-Ventricular-Septum Bypass Circuits (WPW)

At the whole heart level, reentry involves the formation of an activation circle where action potentials propagate to a new region (which is not refractory), then follow a path back to the original area, continuing until they are interrupted. One prime example of this type of arrhythmia is known as Wolff-Parkinson-White (WPW) Syndrome. The atria are normally well insulated from the ventricle by a region of fibrotic non-conductive tissue (the AV septum), forcing the atrial activation wave to enter the ventricle via the AVN. In WPW cases, this insulation is bypassed by the formation of a cellular isthmus/bridge to the other side during embryonic development. This was found to be caused by a mutation in the AMPK γ2 subunit (gene PRKAG2), and a mouse model expressing the same mutation was generated [450-452]. The model, as well as the human subjects affected showed excessive glycogen deposition in myocardial tissues and the bypass tract [450-453]. In the model, it was also shown that early in

development, AMPK activity was increased, but that activity in hearts from adult mice were not (likely due to glycogen mediated inhibition of AMPK as noted in section 1.5a). Based on three identified γ2 mutants that caused the WPW phenotype, the common theme was excessive myocyte glycogen accumulation during embryonic development, and this is presumed to cause the disruption of the fibrotic AV septum. In the mouse model, normal activation of the atria was typically propagated to the ventricle via anterograde conduction through the AVN. Subsequent retrograde conduction and pre-mature activation of the atria proceeded via the bypass pathway [454]. Reentrant arrhythmia formation is particularly relevant to this thesis, and structural changes in the myocardium (eg, scar formation, fibrosis, or impaired GJ), can lead to areas of slow conduction and the formation of a reentry circuit via a similar reentry mechanism as follows:

1.7f Mechanisms of arrhythmia formation – reentry.

Reentry can occur (as in WPW) around anatomical, structural, or physical obstructions: so called “anatomical defined reentry” (including pathways around pulmonary veins, cardiac valves, chordae tendinae, trebeculae, scar tissue etc.). In these cases and in WPW especially, the key factor leading to reentry is the long pathway that is taken. This physical distance travelled allows the atria time to repolarize and become non-refractory: ready for the next wavefront from the ventricle to activate it. In smaller areas and typical conduction velocity, the path around an obstacle does not allow enough time for repolarization, and the original area is still refractory when the wave gets back to it. This stops the reentry cycle and ends the potential tachyarrhythmia. On a much smaller scale, another example which we have discussed above is conduction through the AV node. Based on their properties the slow and fast pathways in the AV node are a perfect example of a two pronged region with differential conduction.

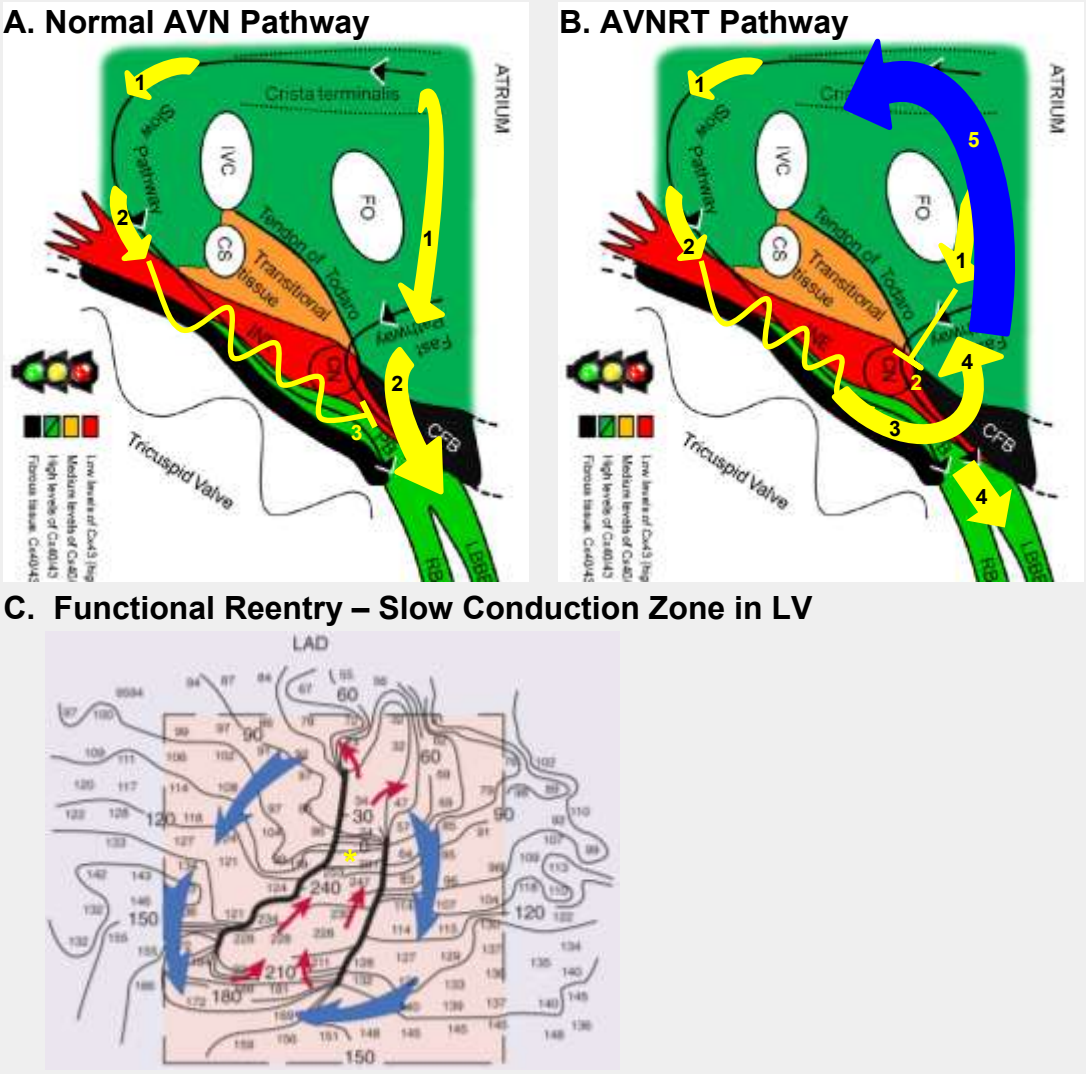

Figure 1-13. Re-Entrant Circuits.

A. AV nodal reentry. (1) A typical SAN activation occurs, (2) anterograde propagation occurs down the fast pathway, the atrial impulse also enters the slow pathway and (3) is blocked when it reaches the entrance to the fast path which is now refractory. **B.** With premature atrial excitation: (1) The previous beat has depolarized the fast pathway which is still refractory. (2) The activation wave enters the slow pathway and is blocked from entering the fast path. (3) When the slow impulse reaches the fast pathway it propagates into the His bundle and retrograde up into the atria (4). (5) Presuming the atria has since repolarized – a reentrant circuit is formed. (modified from Temple et al. Heart Rhythm. (2013), 10(2): 297–304).

C. Activation of a region in the LV with heterogenous cell-cell coupling, and areas of slow conduction. An ectopic focus (EAD/DAD – yellow star). Propagation travels outward from the initial activation, an area of slow conduction is found in a region of the LV with areas of functional block (the dark lines). Isochronal lines show time (in ms) since first activation (crowding indicates slow conduction). The normally propagating wave (blue arrows) encounters a region with slow conduction (*), enter the slow region (red arrows). As the red arrows propagate backwards, they can encounter non-refractory tissue and complete the circuit. If these circuits are maintained – ventricular tachycardia is observed. (Image from Braunwald Heart Disease, 8th Edition).

As shown in Figure 1-13, a pre-mature atrial activation can lead to “AV nodal reentrant tachycardia” (AVRT). Reentry does not occur with a typical atrial activation, because propagation into the AVN occurs via anterograde propagation down the fast pathway and into the bundle of His. As the waveform enters the slow pathway at the same (or similar) time, by the time this wave reaches the fast pathway it is blocked by its refractory tissue. However, in the case of a rapid atrial rate, or a pre-mature atrial activation (for example due to DAD formation near the pulmonary veins), the previous beat has depolarized the fast pathway which is still refractory and propagation is blocked. The activation wave enters the slow pathway (where conduction is often maintained at a slow but steady rate by I_{CaL} dependent action potential activation waves). When the slow impulse reaches the fast pathway which (due to the previous fast activation, it has recovered and is no longer refractory), the slow path wavefront propagates backwards (retrograde) up the fast pathway re-exciting the atrial myocardial tissue. If atrial propagation is slow enough and this wave reaches the top of the slow pathway after it partially repolarizes, the circuit will continue [426, 430].

Of particular importance is the fact that junctional conductance is reduced in these regions. In the nodal pathways it is based on differential expression of the various Cx subunits, and their intrinsic properties, in addition to the expression of different ion channels. A similar difference underlies the interface between fast conducting electrical pathways of the Purkinje fibers, and the slower conducting myocardial tissue, or in the border zone of a myocardial infarction, which can form areas with slower conduction and impaired cell-cell coupling in the absence of any physical blockage. These situations all involve a degree of heterogeneity in cell-cell coupling which is a key factor in developing an arrhythmogenic substrate [426, 427]. In the working myocardium, which is typically (in the absence of ischemia, structural heart disease, heart failure etc.) quite homogenous, these factors play a much smaller role, and hence there is a

much smaller likelihood of forming a reentrant circuit. In this case, even if cell-cell coupling and conduction slows down in larger areas, the intrinsic safety factor due to the refractory period is maintained (as conduction velocity is proportional to action potential duration and proportional to refractory period). This relationship generally prevents conduction from propagating in the reverse direction. However, there are limits, and if an initial wave of excitation is sufficiently slowed, it can eventually form a reentrant circuit (in a miniscule area), by turning back in on itself (forming a spiral wave around a stable central core) [426].

Overall, any change in junctional coupling can lead to heterogeneity in the electrical cardiac substrate, and lead to alterations in the normal propagation of electrical wave fronts. This is the reason that so many of the alterations in junctional conductance or expression we discussed in section 1.3 lead to arrhythmia formation, because when junctional activity is not ideal it forms a substrate that is far more arrhythmogenic.

1.8 Hypothesis and Objectives

The heart is ultra-sensitive to abnormal energy supply and demand, leading to a situation where acute alterations in energy supply alter AMPK phosphorylating activity. This affects many of its downstream targets, including reductions in protein synthesis. As gap junctions are sensitive to phosphorylation and have a short half-life there is a very significant possibility that junctional conductance will be impacted.

AMPK appears to be evolutionarily designed in all organisms studied, to maintain energy delivery, and this would be expected to result in a system which favors survival over life threatening arrhythmia. However, in our evolutionary past: facing perceived metabolic starvation, there may have been a greater evolutionary benefit to activating AMPK, and down regulating communication

between cells (even though it appears to lead to arrhythmia). This is supported by the observation that (although our understanding may be limited), we now know that AMPK activation can lead to arrhythmia via sodium, and potassium channel dys(regulation). Again we must assume that this is evolutionarily less risky than the perceived metabolic consequences.

Based on this premise, our overarching hypothesis is that AMPK activation will lead to an arrhythmogenic substrate, and this will include detrimental impairment of junctional conductance. This thesis has been designed to explore this interaction, and we will demonstrate to some extent that AMPK activation, and phosphorylation of the lesser known cardiac connexins is at the same time, remarkably complex, and profoundly important for cardiac electrophysiology.

1.9 Literature Cited

[1] Bayes de Luna A, Coumel P, Leclercq JF. Ambulatory sudden cardiac death: mechanisms of production of fatal arrhythmia on the basis of data from 157 cases. American Heart Journal. 1989;117:151-9.

[2] Gillum RF. Sudden coronary death in the United States: 1980-1985. Circulation. 1989;79:756-65.

[3] Kavanagh KM, Wyse DG. Ventricular arrhythmias. CMAJ. 1988;138:903-13.

[4] Innerfield RJ. Metformin-associated mortality in U.S. studies. The New England journal of medicine. 1996;334:1611-2; author reply 2-3.

[5] The Cardiac Arrhythmia Suppression Trial I. Special Report, preliminary report: effect of encainide and flecainide on mortality in a randomized trial of arrhythmia suppression after myocardial infarction. New England Journal of Medicine. 1989;321:406-12.

[6] Deo R, Albert CM. Epidemiology and genetics of sudden cardiac death. Circulation. 2012;125:620-37.

[7] Betensky BP, Dixit S. Sudden cardiac death in patients with nonischemic cardiomyopathy. Indian heart journal. 2014;66s1:S35-s45.

[8] Nikolic G, Bishop RL, Singh JB. Sudden death recorded during Holter monitoring. Circulation. 1982;66:218-25.

[9] Maisel WH, Stevenson LW. Atrial fibrillation in heart failure: epidemiology, pathophysiology, and rationale for therapy. Am J Cardiol. 2003;91:2D-8D.

[10] Khazanie P, Liang L, Qualls LG, Curtis LH, Fonarow GC, Hammill BG, et al. Outcomes of medicare beneficiaries with heart failure and atrial fibrillation. JACC Heart failure. 2014;2:41-8.

[11] Echt DS, Armstrong K, Schmidt P, Oyer PE, Stinson EB, Winkle RA. Clinical experience, complications, and survival in 70 patients with the automatic implantable cardioverter/defibrillator. Circulation. 1985;71:289-96.

[12] Mirowski M. The automatic implantable cardioverter-defibrillator: An overview. Journal of the American College of Cardiology. 1985;6:461-6.

[13] Tchou PJ, Kadri N, Anderson J, Caceres JA, Jazayeri M, Akhtar M. Automatic implantable cardioverter defibrillators and survival of patients with left ventricular dysfunction and malignant ventricular arrhythmias. Annals of Internal Medicine. 1988;109:529-34.

[14] Wyse DG, Waldo AL, DiMarco JP, Domanski MJ, Rosenberg Y, Schron EB, et al. A comparison of rate control and rhythm control in patients with atrial fibrillation. NEnglJMed. 2002;347:1825-33.

[15] Wyse DG. Rhythm versus Rate Control Trials in Atrial Fibrillation. JCardiovascElectrophysiol. 2003;14 Suppl 9:S35-S9.

[16] Wyse DG. Rhythm management in atrial fibrillation: less is more. JAmCollCardiol. 2003;41:1703-6.

[17] Hoyt RH, Cohen ML, Saffitz JE. Distribution and three-dimensional structure of intercellular junctions in canine myocardium. CircRes. 1989;64:563-74.

[18] Kieval RS, Spear JF, Moore EN. Gap junctional conductance in ventricular myocyte pairs isolated from postischemic rabbit myocardium. Circulation research. 1992;71:127-36.

[19] Luke RA, Saffitz JE. Remodeling of ventricular conduction pathways in healed canine infarct border zones. The Journal of clinical investigation. 1991;87:1594-602.

[20] Odegarden S. Organization of connexons and gap junctions in human heart cells. Acta Physiology Scandanavia. 1991;S599:61-70.

[21] Saffitz JE, Corr PB, Sobel BE. Arrhythmogenesis and ventricular dysfunction after myocardial infarction. Is anomalous cellular coupling the elusive link? Circulation. 1993;87:1742-5.

[22] Roth BJ. Influence of a perfusing bath on the foot of the cardiac action potential. CircRes. 2000;86:E19-E22.

[23] Yaniv Y, Lakatta EG, Maltsev VA. From two competing oscillators to one coupled-clock pacemaker cell system. Frontiers in physiology. 2015;6:28.

[24] Catterall WA. Voltage-gated calcium channels. Cold Spring Harbor perspectives in biology. 2011;3:a003947.

[25] Schmitt N, Grunnet M, Olesen SP. Cardiac potassium channel subtypes: new roles in repolarization and arrhythmia. Physiological reviews. 2014;94:609-53.

[26] Saffitz JE, Davis LM, Darrow BJ, Kanter HL, Laing JG, Beyer EC. The molecular basis of anisotropy: role of gap junctions. Journal of cardiovascular electrophysiology. 1995;6:498-510.

[27] Valderrabano M. Influence of anisotropic conduction properties in the propagation of the cardiac action potential. Progress in biophysics and molecular biology. 2007;94:144-68.

[28] Harris AL. Emerging issues of connexin channels: biophysics fills the gap. Quarterly reviews of biophysics. 2001;34:325-472.

[29] Bedner P, Niessen H, Odermatt B, Kretz M, Willecke K, Harz H. Selective permeability of different connexin channels to the second messenger cyclic AMP. J Biol Chem. 2006;281:6673-81.

[30] Valiunas V, Polosina YY, Miller H, Potapova IA, Valiuniene L, Doronin S, et al. Connexin-specific cell-to-cell transfer of short interfering RNA by gap junctions. The Journal of physiology. 2005;568:459-68.

[31] Neijssen J, Herberts C, Drijfhout JW, Reits E, Janssen L, Neefjes J. Cross-presentation by intercellular peptide transfer through gap junctions. Nature. 2005;434:83-8.

[32] Jalife J, Morley GE, Vaidya D. Connexins and impulse propagation in the mouse heart. Journal of cardiovascular electrophysiology. 1999;10:1649-63.

[33] Beyer EC, Davis LM, Saffitz JE, Veenstra RD. Cardiac intercellular communication: consequences of connexin distribution and diversity. Braz J Med Biol Res. 1995;28:415-25.

[34] Kanter HL, Beyer EC, Saffitz JE. Structural and molecular determinants of intercellular coupling in cardiac myocytes. Microsc Res Tech. 1995;31:357-63.

[35] Kleber AG, Rudy Y. Basic mechanisms of cardiac impulse propagation and associated arrhythmias. Physiological reviews. 2004;84:431-88.

[36] Dupont E, Ko Y, Rothery S, Coppen SR, Baghai M, Haw M, et al. The gap-junctional protein connexin40 is elevated in patients susceptible to postoperative atrial fibrillation. Circulation. 2001;103:842-9.

[37] Gutstein DE, Morley GE, Tamaddon H, Vaidya D, Schneider MD, Chen J, et al. Conduction slowing and sudden arrhythmic death in mice with cardiac-restricted inactivation of connexin43. Circulation research. 2001;88:333-9.

[38] Vaidya D, Tamaddon HS, Lo CW, Taffet SM, Delmar M, Morley GE, et al. Null mutation of connexin43 causes slow propagation of ventricular activation in the late stages of mouse embryonic development. Circulation research. 2001;88:1196-202.

[39] Lee P, Morley G, Huang Q, Fischer A, Seiler S, Horner JW, et al. Conditional lineage ablation to model human diseases. Proceedings of the National Academy of Sciences of the United States of America. 1998;95:11371-6.

[40] Hagendorff A, Schumacher B, Kirchhoff S, Luderitz B, Willecke K. Conduction disturbances and increased atrial vulnerability in Connexin40-deficient mice analyzed by transesophageal stimulation. Circulation. 1999;99:1508-15.

[41] Verheule S, van Kempen MJ, Postma S, Rook MB, Jongsma HJ. Gap junctions in the rabbit sinoatrial node. American journal of physiology. 2001;280:H2103-15.

[42] Qin D, Zhang ZH, Caref EB, Boutjdir M, Jain P, el Sherif N. Cellular and ionic basis of arrhythmias in postinfarction remodeled ventricular myocardium. CircRes. 1996;79:461-73.

[43] Dhillon PS, Chowdhury RA, Patel PM, Jabr R, Momin AU, Vecht J, et al. The Relationship between Connexin Expression and Gap Junction Resistivity in Human Atrial Myocardium. Circ Arrhythm Electrophysiol. 2014.

[44] Yan J, Kong W, Zhang Q, Beyer EC, Walcott G, Fast VG, et al. c-Jun N-terminal kinase activation contributes to reduced connexin43 and development of atrial arrhythmias. Cardiovascular research. 2013;97:589-97.

[45] Paul M, Wichter T, Gerss J, Arps V, Schulze-Bahr E, Robenek H, et al. Connexin expression patterns in arrhythmogenic right ventricular cardiomyopathy. Am J Cardiol. 2013;111:1488-95.

[46] Lubkemeier I, Requardt RP, Lin X, Sasse P, Andrie R, Schrickel JW, et al. Deletion of the last five C-terminal amino acid residues of connexin43 leads to lethal ventricular arrhythmias in mice without affecting coupling via gap junction channels. Basic research in cardiology. 2013;108:348.

[47] Lubkemeier I, Andrie R, Lickfett L, Bosen F, Stockigt F, Dobrowolski R, et al. The Connexin40A96S mutation from a patient with atrial fibrillation causes decreased atrial conduction velocities and sustained episodes of induced atrial fibrillation in mice. J Mol Cell Cardiol. 2013;65:19-32.

[48] Wu W, Li Y, Lu Z, Hu X. Increased susceptibility to ischemia-induced ventricular tachyarrhythmias in depressed rats: Involvement of reduction of connexin 43. Experimental and therapeutic medicine. 2012;3:192-4.

[49] Makita N, Seki A, Sumitomo N, Chkourko H, Fukuhara S, Watanabe H, et al. A connexin40 mutation associated with a malignant variant of progressive familial heart block type I. Circ Arrhythm Electrophysiol. 2012;5:163-72.

[50] Jansen JA, Noorman M, Musa H, Stein M, de Jong S, van der Nagel R, et al. Reduced heterogeneous expression of Cx43 results in decreased Nav1.5 expression and reduced sodium current that accounts for arrhythmia vulnerability in conditional Cx43 knockout mice. Heart Rhythm. 2012;9:600-7.

[51] Delmar M, Makita N. Cardiac connexins, mutations and arrhythmias. Current opinion in cardiology. 2012;27:236-41.

[52] Wirka RC, Gore S, Van Wagoner DR, Arking DE, Lubitz SA, Lunetta KL, et al. A common connexin-40 gene promoter variant affects connexin-40 expression in human atria and is associated with atrial fibrillation. Circ Arrhythm Electrophysiol. 2011;4:87-93.

[53] Strom M, Wan X, Poelzing S, Ficker E, Rosenbaum DS. Gap junction heterogeneity as mechanism for electrophysiologically distinct properties across the ventricular wall. American journal of physiology. 2010;298:H787-94.

[54] Soltysinska E, Olesen SP, Christ T, Wettwer E, Varro A, Grunnet M, et al. Transmural expression of ion channels and transporters in human nondiseased and end-stage failing hearts. Pflugers Arch. 2009;459:11-23.

[55] Chaldoupi SM, Loh P, Hauer RN, de Bakker JM, van Rijen HV. The role of connexin40 in atrial fibrillation. Cardiovascular research. 2009;84:15-23.

[56] Sato T, Ohkusa T, Honjo H, Suzuki S, Yoshida MA, Ishiguro YS, et al. Altered expression of connexin43 contributes to the arrhythmogenic substrate during the development of heart failure in cardiomyopathic hamster. American journal of physiology. 2008;294:H1164-73.

[57] Leaf DE, Feig JE, Vasquez C, Riva PL, Yu C, Lader JM, et al. Connexin40 imparts conduction heterogeneity to atrial tissue. Circulation research. 2008;103:1001-8.

[58] Danik SB, Liu F, Zhang J, Suk HJ, Morley GE, Fishman GI, et al. Modulation of cardiac gap junction expression and arrhythmic susceptibility. Circulation research. 2004;95:1035-41.

[59] VanderBrink BA, Sellitto C, Saba S, Link MS, Zhu W, Homoud MK, et al. Connexin40-deficient mice exhibit atrioventricular nodal and infra-Hisian conduction abnormalities. Journal of cardiovascular electrophysiology. 2000;11:1270-6.

[60] Bevilacqua LM, Simon AM, Maguire CT, Gehrmann J, Wakimoto H, Paul DL, et al. A targeted disruption in connexin40 leads to distinct atrioventricular conduction defects. J Interv Card Electrophysiol. 2000;4:459-67.

[61] Verheule S, van Batenburg CA, Coenjaerts FE, Kirchhoff S, Willecke K, Jongsma HJ. Cardiac conduction abnormalities in mice lacking the gap junction protein connexin40. Journal of cardiovascular electrophysiology. 1999;10:1380-9.

[62] Danik SB, Rosner G, Lader J, Gutstein DE, Fishman GI, Morley GE. Electrical remodeling contributes to complex tachyarrhythmias in connexin43-deficient mouse hearts. Faseb J. 2008;22:1204-12.

[63] van Rijen HV, Eckardt D, Degen J, Theis M, Ott T, Willecke K, et al. Slow conduction and enhanced anisotropy increase the propensity for ventricular tachyarrhythmias in adult mice with induced deletion of connexin43. Circulation. 2004;109:1048-55.

[64] Yao JA, Gutstein DE, Liu F, Fishman GI, Wit AL. Cell coupling between ventricular myocyte pairs from connexin43-deficient murine hearts. Circulation research. 2003;93:736-43.

[65] Bagwe S, Berenfeld O, Vaidya D, Morley GE, Jalife J. Altered right atrial excitation and propagation in connexin40 knockout mice. Circulation. 2005;112:2245-53.

[66] Alcolea S, Jarry-Guichard T, de Bakker J, Gonzalez D, Lamers W, Coppen S, et al. Replacement of connexin40 by connexin45 in the mouse: impact on cardiac electrical conduction. Circulation research. 2004;94:100-9.

[67] Wolfle SE, Schmidt VJ, Hoepfl B, Gebert A, Alcolea S, Gros D, et al. Connexin45 cannot replace the function of connexin40 in conducting endothelium-dependent dilations along arterioles. Circulation research. 2007;101:1292-9.

[68] Remo BF, Qu J, Volpicelli FM, Giovannone S, Shin D, Lader J, et al. Phosphatase-resistant gap junctions inhibit pathological remodeling and prevent arrhythmias. Circulation research. 2011;108:1459-66.

[69] Keevil VL, Huang CL, Chau PL, Sayeed RA, Vandenberg JI. The effect of heptanol on the electrical and contractile function of the isolated, perfused rabbit heart. Pflugers Arch. 2000;440:275-82.

[70] O'Quinn MP, Palatinus JA, Harris BS, Hewett KW, Gourdie RG. A peptide mimetic of the connexin43 carboxyl terminus reduces gap junction remodeling and induced arrhythmia following ventricular injury. Circulation research. 2011;108:704-15.

[71] Bikou O, Thomas D, Trappe K, Lugenbiel P, Kelemen K, Koch M, et al. Connexin 43 gene therapy prevents persistent atrial fibrillation in a porcine model. Cardiovascular research. 2011;92:218-25.

[72] Zhang QY, Wang W, Shi QX, Li YL, Huang JH, Yao Y, et al. Antiarrhythmic effect mediated by kappa-opioid receptor is associated with Cx43 stabilization. Crit Care Med. 2010;38:2365-76.

[73] Unuma K, Shintani-Ishida K, Tsushima K, Shimosawa T, Ueyama T, Kuwahara M, et al. Connexin-43 redistribution and gap junction activation during forced restraint protects against sudden arrhythmic death in rats. Circ J. 2010;74:1087-95.

[74] Quan XQ, Bai R, Lu JG, Patel C, Liu N, Ruan Y, et al. Pharmacological Enhancement of Cardiac Gap Junction Coupling Prevents Arrhythmias in Canine LQT2 Model. Cell Commun Adhes. 2009:1-10.

[75] Roell W, Lewalter T, Sasse P, Tallini YN, Choi BR, Breitbach M, et al. Engraftment of connexin 43-expressing cells prevents post-infarct arrhythmia. Nature. 2007;450:819-24.

[76] Stahlhut M, Petersen JS, Hennan JK, Ramirez MT. The antiarrhythmic peptide rotigaptide (ZP123) increases connexin 43 protein expression in neonatal rat ventricular cardiomyocytes. Cell Commun Adhes. 2006;13:21-7.

[77] Haugan K, Miyamoto T, Takeishi Y, Kubota I, Nakayama J, Shimojo H, et al. Rotigaptide (ZP123) improves atrial conduction slowing in chronic volume overload-induced dilated atria. Basic & clinical pharmacology & toxicology. 2006;99:71-9.

[78] Dhein S, Larsen BD, Petersen JS, Mohr FW. Effects of the new antiarrhythmic peptide ZP123 on epicardial activation and repolarization pattern. Cell Commun Adhes. 2003;10:371-8.

[79] Weng S, Lauven M, Schaefer T, Polontchouk L, Grover R, Dhein S. Pharmacological modification of gap junction coupling by an antiarrhythmic peptide via protein kinase C activation. Faseb J. 2002;16:1114-6.

[80] Herve JC, Sarrouilhe D. Protein phosphatase modulation of the intercellular junctional communication: importance in cardiac myocytes. Progress in biophysics and molecular biology. 2006;90:225-48.

[81] Veenstra RD. Developmental changes in regulation of embryonic chick heart gap junctions. J Membr Biol. 1991;119:253-65.

[82] van Kempen MJ, Fromaget C, Gros D, Moorman AF, Lamers WH. Spatial distribution of connexin43, the major cardiac gap junction protein, in the developing and adult rat heart. Circulation research. 1991;68:1638-51.

[83] Gourdie RG, Green CR, Severs NJ, Thompson RP. Immunolabelling patterns of gap junction connexins in the developing and mature rat heart. Anatomy and embryology. 1992;185:363-78.

[84] Kanter HL, Laing JG, Beau SL, Beyer EC, Saffitz JE. Distinct patterns of connexin expression in canine Purkinje fibers and ventricular muscle. Circulation research. 1993;72:1124-31.

[85] Oosthoek PW, Viragh S, Mayen AE, van Kempen MJ, Lamers WH, Moorman AF. Immunohistochemical delineation of the conduction system. I: The sinoatrial node. Circulation research. 1993;73:473-81.

[86] Oosthoek PW, Viragh S, Lamers WH, Moorman AF. Immunohistochemical delineation of the conduction system. II: The atrioventricular node and Purkinje fibers. Circulation research. 1993;73:482-91.

[87] Davis LM, Kanter HL, Beyer EC, Saffitz JE. Distinct gap junction protein phenotypes in cardiac tissues with disparate conduction properties. J Am Coll Cardiol. 1994;24:1124-32.

[88] Gros DB, Jongsma HJ. Connexins in mammalian heart function. Bioessays. 1996;18:719-30.

[89] Davis LM, Rodefeld ME, Green K, Beyer EC, Saffitz JE. Gap junction protein phenotypes of the human heart and conduction system. Journal of cardiovascular electrophysiology. 1995;6:813-22.

[90] Van Kempen MJ, Vermeulen JL, Moorman AF, Gros D, Paul DL, Lamers WH. Developmental changes of connexin40 and connexin43 mRNA distribution patterns in the rat heart. Cardiovascular research. 1996;32:886-900.

[91] Severs NJ, Bruce AF, Dupont E, Rothery S. Remodelling of gap junctions and connexin expression in diseased myocardium. Cardiovascular research. 2008;80:9-19.

[92] Bastide B, Neyses L, Ganten D, Paul M, Willecke K, Traub O. Gap junction protein connexin40 is preferentially expressed in vascular endothelium and conductive bundles of rat myocardium and is increased under hypertensive conditions. Circulation research. 1993;73:1138-49.

[93] De Maziere A, Analbers L, Jongsma HJ, Gros D. Immunoelectron microscopic visualization of the gap junction protein connexin 40 in the mammalian heart. European journal of morphology. 1993;31:51-4.

[94] Gros D, Jarry-Guichard T, Ten Velde I, de Maziere A, van Kempen MJ, Davoust J, et al. Restricted distribution of connexin40, a gap junctional protein, in mammalian heart. Circulation research. 1994;74:839-51.

[95] Delorme B, Dahl E, Jarry-Guichard T, Marics I, Briand JP, Willecke K, et al. Developmental regulation of connexin 40 gene expression in mouse heart correlates with the differentiation of the conduction system. Dev Dyn. 1995;204:358-71.

[96] Coppen SR, Dupont E, Rothery S, Severs NJ. Connexin45 expression is preferentially associated with the ventricular conduction system in mouse and rat heart. Circulation research. 1998;82:232-43.

[97] van Veen TA, van Rijen HV, Jongsma HJ. Electrical conductance of mouse connexin45 gap junction channels is modulated by phosphorylation. Cardiovascular research. 2000;46:496-510.

[98] Kreuzberg MM, Liebermann M, Segschneider S, Dobrowolski R, Dobrzynski H, Kaba R, et al. Human connexin31.9, unlike its orthologous protein connexin30.2 in the mouse, is not detectable in the human cardiac conduction system. Journal of Molecular and Cellular Cardiology. 2009;46:553-9.

[99] Bukauskas FF, Kreuzberg MM, Rackauskas M, Bukauskiene A, Bennett MV, Verselis VK, et al. Properties of mouse connexin 30.2 and human connexin 31.9 hemichannels: implications for atrioventricular conduction in the heart. Proceedings of the National Academy of Sciences of the United States of America. 2006;103:9726-31.

[100] Nielsen PA, Kumar NM. Differences in expression patterns between mouse connexin-30.2 (Cx30.2) and its putative human orthologue, connexin-31.9. FEBS Lett. 2003;540:151-6.

[101] Sohl G, Nielsen PA, Eiberger J, Willecke K. Expression profiles of the novel human connexin genes hCx30.2, hCx40.1, and hCx62 differ from their putative mouse orthologues. Cell Commun Adhes. 2003;10:27-36.

[102] Nielsen PA, Beahm DL, Giepmans BN, Baruch A, Hall JE, Kumar NM. Molecular cloning, functional expression, and tissue distribution of a novel human gap junction-forming protein, connexin-31.9. Interaction with zona occludens protein-1. J Biol Chem. 2002;277:38272-83.

[103] White TW, Srinivas M, Ripps H, Trovato-Salinaro A, Condorelli DF, Bruzzone R. Virtual cloning, functional expression, and gating analysis of human connexin31.9. Am J Physiol Cell Physiol. 2002;283:C960-70.

[104] Belluardo N, White TW, Srinivas M, Trovato-Salinaro A, Ripps H, Mudo G, et al. Identification and functional expression of HCx31.9, a novel gap junction gene. Cell Commun Adhes. 2001;8:173-8.

[105] Kreuzberg MM, Schrickel JW, Ghanem A, Kim JS, Degen J, Janssen-Bienhold U, et al. Connexin30.2 containing gap junction channels decelerate impulse propagation through the atrioventricular node. Proceedings of the National Academy of Sciences of the United States of America. 2006;103:5959-64.

[106] Kreuzberg MM, Willecke K, Bukauskas FF. Connexin-mediated cardiac impulse propagation: connexin 30.2 slows atrioventricular conduction in mouse heart. Trends in cardiovascular medicine. 2006;16:266-72.

[107] Kohl P, Gourdie RG. Fibroblast–myocyte electrotonic coupling: Does it occur in native cardiac tissue?(). Journal of Molecular and Cellular Cardiology. 2014;70:37-46.

[108] Gaudesius G, Miragoli M, Thomas SP, Rohr S. Coupling of cardiac electrical activity over extended distances by fibroblasts of cardiac origin. Circulation research. 2003;93:421-8.

[109] Dhein S, Seidel T, Salameh A, Jozwiak J, Hagen A, Kostelka M, et al. Remodeling of cardiac passive electrical properties and susceptibility to ventricular and atrial arrhythmias. Frontiers in physiology. 2014;5:424.

[110] Miragoli M, Gaudesius G, Rohr S. Electrotonic modulation of cardiac impulse conduction by myofibroblasts. Circulation research. 2006;98:801-10.

[111] Lopez P, Balicki D, Buehler LK, Falk MM, Chen SC. Distribution and dynamics of gap junction channels revealed in living cells. Cell Commun Adhes. 2001;8:237-42.

[112] Falk MM, Lauf U. High resolution, fluorescence deconvolution microscopy and tagging with the autofluorescent tracers CFP, GFP, and YFP to study the structural composition of gap junctions in living cells. Microsc Res Tech. 2001;52:251-62.

[113] Segretain D, Falk MM. Regulation of connexin biosynthesis, assembly, gap junction formation, and removal. Biochim Biophys Acta. 2004;1662:3-21.

[114] Flores CE, Nannapaneni S, Davidson KG, Yasumura T, Bennett MV, Rash JE, et al. Trafficking of gap junction channels at a vertebrate electrical synapse in vivo. Proceedings of the National Academy of Sciences of the United States of America. 2012;109:E573-82.

[115] Zhang SS, Shaw RM. Trafficking highways to the intercalated disc: new insights unlocking the specificity of connexin 43 localization. Cell Commun Adhes. 2014;21:43-54.

[116] Laird DW. The gap junction proteome and its relationship to disease. Trends in cell biology. 2010;20:92-101.

[117] Solan JL, Lampe PD. Specific Cx43 phosphorylation events regulate gap junction turnover in vivo. FEBS Lett. 2014.

[118] Laird DW, Puranam KL, Revel JP. Turnover and phosphorylation dynamics of connexin43 gap junction protein in cultured cardiac myocytes. Biochem J. 1991;273(Pt 1):67-72.

[119] Beardslee MA, Laing JG, Beyer EC, Saffitz JE. Rapid turnover of connexin43 in the adult rat heart. Circulation research. 1998;83:629-35.

[120] Li X, Su V, Kurata WE, Jin C, Lau AF. A novel connexin43-interacting protein, CIP75, which belongs to the UbL-UBA protein family, regulates the turnover of connexin43. J Biol Chem. 2008;283:5748-59.

[121] Traub O, Look J, Paul D, Willecke K. Cyclic adenosine monophosphate stimulates biosynthesis and phosphorylation of the 26 kDa gap junction protein in cultured mouse hepatocytes. Eur J Cell Biol. 1987;43:48-54.

[122] Dunn CA, Su V, Lau AF, Lampe PD. Activation of Akt, not connexin 43 protein ubiquitination, regulates gap junction stability. J Biol Chem. 2012;287:2600-7.

[123] Laing JG, Beyer EC. The gap junction protein connexin43 is degraded via the ubiquitin proteasome pathway. J Biol Chem. 1995;270:26399-403.

[124] Laing JG, Tadros PN, Westphale EM, Beyer EC. Degradation of connexin43 gap junctions involves both the proteasome and the lysosome. Exp Cell Res. 1997;236:482-92.

[125] Laing JG, Tadros PN, Green K, Saffitz JE, Beyer EC. Proteolysis of connexin43-containing gap junctions in normal and heat-stressed cardiac myocytes. Cardiovascular research. 1998;38:711-8.

[126] Gaietta G, Deerinck TJ, Adams SR, Bouwer J, Tour O, Laird DW, et al. Multicolor and electron microscopic imaging of connexin trafficking. Science. 2002;296:503-7.

[127] Unger VM, Kumar NM, Gilula NB, Yeager M. Projection structure of a gap junction membrane channel at 7 A resolution. Nature structural biology. 1997;4:39-43.

[128] Yeager M, Unger VM, Falk MM. Synthesis, assembly and structure of gap junction intercellular channels. Current opinion in structural biology. 1998;8:517-24.

[129] Unger VM, Kumar NM, Gilula NB, Yeager M. Three-dimensional structure of a recombinant gap junction membrane channel. Science. 1999;283:1176-80.

[130] Kronengold J, Trexler EB, Bukauskas FF, Bargiello TA, Verselis VK. Single-channel SCAM identifies pore-lining residues in the first extracellular loop and first transmembrane domains of Cx46 hemichannels. J Gen Physiol. 2003;122:389-405.

[131] Maeda S, Tsukihara T. Structure of the gap junction channel and its implications for its biological functions. Cell Mol Life Sci. 2011;68:1115-29.

[132] Maeda S, Nakagawa S, Suga M, Yamashita E, Oshima A, Fujiyoshi Y, et al. Structure of the connexin 26 gap junction channel at 3.5 A resolution. Nature. 2009;458:597-602.

[133] Oshima A. Structure and closure of connexin gap junction channels. FEBS Lett. 2014.

[134] Beyer EC, Lipkind GM, Kyle JW, Berthoud VM. Structural organization of intercellular channels II. Amino terminal domain of the connexins: sequence, functional roles, and structure. Biochim Biophys Acta. 2012;1818:1823-30.

[135] Oh S, Rubin JB, Bennett MV, Verselis VK, Bargiello TA. Molecular determinants of electrical rectification of single channel conductance in gap junctions formed by connexins 26 and 32. J Gen Physiol. 1999;114:339-64.

[136] Purnick PE, Oh S, Abrams CK, Verselis VK, Bargiello TA. Reversal of the gating polarity of gap junctions by negative charge substitutions in the N-terminus of connexin 32. Biophys J. 2000;79:2403-15.

[137] Stergiopoulos K, Alvarado JL, Mastroianni M, Ek-Vitorin JF, Taffet SM, Delmar M. Hetero-domain interactions as a mechanism for the regulation of connexin channels. Circulation research. 1999;84:1144-55.

[138] Zhou L, Kasperek EM, Nicholson BJ. Dissection of the molecular basis of pp60(v-src) induced gating of connexin 43 gap junction channels. The Journal of cell biology. 1999;144:1033-45.

[139] Morley GE, Taffet SM, Delmar M. Intramolecular interactions mediate pH regulation of connexin43 channels. Biophys J. 1996;70:1294-302.

[140] Ek-Vitorin JF, Burt JM. Structural basis for the selective permeability of channels made of communicating junction proteins. Biochim Biophys Acta. 2013;1828:51-68.

[141] Spray DC, White RL, Mazet F, Bennett MV. Regulation of gap junctional conductance. The American journal of physiology. 1985;248:H753-64.

[142] Rubin JB, Verselis VK, Bennett MV, Bargiello TA. Molecular analysis of voltage dependence of heterotypic gap junctions formed by connexins 26 and 32. Biophys J. 1992;62:183-93; discussion 93-5.

[143] White TW, Bruzzone R, Paul DL. The connexin family of intercellular channel forming proteins. Kidney Int. 1995;48:1148-57.

[144] Spray DC, Harris AL, Bennett MV. Equilibrium properties of a voltage-dependent junctional conductance. J Gen Physiol. 1981;77:77-93.

[145] Lin X, Crye M, Veenstra RD. Regulation of connexin43 gap junctional conductance by ventricular action potentials. Circulation research. 2003;93:e63-73.

[146] Bukauskas FF, Angele AB, Verselis VK, Bennett MV. Coupling asymmetry of heterotypic connexin 45/ connexin 43-EGFP gap junctions: properties of fast and slow gating mechanisms. Proceedings of the National Academy of Sciences of the United States of America. 2002;99:7113-8.

[147] Moreno AP. Biophysical properties of homomeric and heteromultimeric channels formed by cardiac connexins. Cardiovascular research. 2004;62:276-86.

[148] Verselis VK, Ginter CS, Bargiello TA. Opposite voltage gating polarities of two closely related connexins. Nature. 1994;368:348-51.

[149] Bukauskas FF, Bukauskiene A, Bennett MV, Verselis VK. Gating properties of gap junction channels assembled from connexin43 and connexin43 fused with green fluorescent protein. Biophys J. 2001;81:137-52.

[150] Anumonwo JM, Taffet SM, Gu H, Chanson M, Moreno AP, Delmar M. The carboxyl terminal domain regulates the unitary conductance and voltage dependence of connexin40 gap junction channels. Circulation research. 2001;88:666-73.

[151] Moreno AP, Chanson M, Elenes S, Anumonwo J, Scerri I, Gu H, et al. Role of the carboxyl terminal of connexin43 in transjunctional fast voltage gating. Circulation research. 2002;90:450-7.

[152] Duffy HS, Delmar M, Coombs W, Tafftet SM, Hertzberg EL, Spray DC. Functional demonstration of connexin-protein binding using surface plasmon resonance. Cell Commun Adhes. 2001;8:225-9.

[153] Duffy HS, Sorgen PL, Girvin ME, O'Donnell P, Coombs W, Taffet SM, et al. pH-dependent intramolecular binding and structure involving Cx43 cytoplasmic domains. J Biol Chem. 2002;277:36706-14.

[154] Sorgen PL, Duffy HS, Cahill SM, Coombs W, Spray DC, Delmar M, et al. Sequence-specific resonance assignment of the carboxyl terminal domain of Connexin43. Journal of biomolecular NMR. 2002;23:245-6.

[155] Delmar M, Coombs W, Sorgen P, Duffy HS, Taffet SM. Structural bases for the chemical regulation of Connexin43 channels. Cardiovascular research. 2004;62:268-75.

[156] Duffy HS, Ashton AW, O'Donnell P, Coombs W, Taffet SM, Delmar M, et al. Regulation of connexin43 protein complexes by intracellular acidification. Circulation research. 2004;94:215-22.

[157] Sorgen PL, Duffy HS, Sahoo P, Coombs W, Delmar M, Spray DC. Structural changes in the carboxyl terminus of the gap junction protein connexin43 indicates signaling between binding domains for c-Src and zonula occludens-1. J Biol Chem. 2004;279:54695-701.

[158] Sorgen PL, Duffy HS, Spray DC, Delmar M. pH-dependent dimerization of the carboxyl terminal domain of Cx43. Biophys J. 2004;87:574-81.

[159] Lampe PD, Cooper CD, King TJ, Burt JM. Analysis of Connexin43 phosphorylated at S325, S328 and S330 in normoxic and ischemic heart. Journal of cell science. 2006;119:3435-42.

[160] Solan JL, Marquez-Rosado L, Sorgen PL, Thornton PJ, Gafken PR, Lampe PD. Phosphorylation at S365 is a gatekeeper event that changes the structure of Cx43 and prevents down-regulation by PKC. The Journal of cell biology. 2007;179:1301-9.

[161] Lampe PD, TenBroek EM, Burt JM, Kurata WE, Johnson RG, Lau AF. Phosphorylation of connexin43 on serine368 by protein kinase C regulates gap junctional communication. The Journal of cell biology. 2000;149:1503-12.

[162] Moreno AP, Saez JC, Fishman GI, Spray DC. Human connexin43 gap junction channels. Regulation of unitary conductances by phosphorylation. Circulation research. 1994;74:1050-7.

[163] Ek-Vitorin JF, King TJ, Heyman NS, Lampe PD, Burt JM. Selectivity of connexin 43 channels is regulated through protein kinase C-dependent phosphorylation. Circulation research. 2006;98:1498-505.

[164] Eckert R. Gap-junctional single-channel permeability for fluorescent tracers in mammalian cell cultures. Biophys J. 2006;91:565-79.

[165] Elfgang C, Eckert R, Lichtenberg-Frate H, Butterweck A, Traub O, Klein RA, et al. Specific permeability and selective formation of gap junction channels in connexin-transfected HeLa cells. The Journal of cell biology. 1995;129:805-17.

[166] Veenstra RD, Wang HZ, Beblo DA, Chilton MG, Harris AL, Beyer EC, et al. Selectivity of connexin-specific gap junctions does not correlate with channel conductance. Circulation research. 1995;77:1156-65.

[167] Kanaporis G, Mese G, Valiuniene L, White TW, Brink PR, Valiunas V. Gap junction channels exhibit connexin-specific permeability to cyclic nucleotides. J Gen Physiol. 2008;131:293-305.

[168] Kanaporis G, Brink PR, Valiunas V. Gap junction permeability: selectivity for anionic and cationic probes. Am J Physiol Cell Physiol. 2011;300:C600-9.

[169] Heyman NS, Kurjiaka DT, Ek Vitorin JF, Burt JM. Regulation of gap junctional charge selectivity in cells coexpressing connexin 40 and connexin 43. American journal of physiology. 2009;297:H450-9.

[170] Weber PA, Chang HC, Spaeth KE, Nitsche JM, Nicholson BJ. The permeability of gap junction channels to probes of different size is dependent on connexin composition and permeant-pore affinities. Biophys J. 2004;87:958-73.

[171] Rackauskas M, Verselis VK, Bukauskas FF. Permeability of homotypic and heterotypic gap junction channels formed of cardiac connexins mCx30.2, Cx40, Cx43, and Cx45. American journal of physiology. 2007;293:H1729-36.

[172] Koval M, Geist ST, Westphale EM, Kemendy AE, Civitelli R, Beyer EC, et al. Transfected connexin45 alters gap junction permeability in cells expressing endogenous connexin43. The Journal of cell biology. 1995;130:987-95.

[173] Beblo DA, Veenstra RD. Monovalent cation permeation through the connexin40 gap junction channel. Cs, Rb, K, Na, Li, TEA, TMA, TBA, and effects of anions Br, Cl, F, acetate, aspartate, glutamate, and NO3. J Gen Physiol. 1997;109:509-22.

[174] Moore LK, Beyer EC, Burt JM. Characterization of gap junction channels in A7r5 vascular smooth muscle cells. The American journal of physiology. 1991;260:C975-81.

[175] He DS, Burt JM. Mechanism and selectivity of the effects of halothane on gap junction channel function. Circulation research. 2000;86:E104-9.

[176] Rozental R, Srinivas M, Spray DC. How to close a gap junction channel. Efficacies and potencies of uncoupling agents. Methods in molecular biology (Clifton, NJ. 2001;154:447-76.

[177] Moreno AP, Eghbali B, Spray DC. Connexin32 gap junction channels in stably transfected cells: unitary conductance. Biophys J. 1991;60:1254-66.

[178] Campos-de-Carvalho AC, Eiras LA, Waltzman M, Hertzberg EL, Spray DC. Properties of channels from rat liver gap junction membrane fractions incorporated into planar lipid bilayers. Braz J Med Biol Res. 1992;25:81-92.

[179] Reynhout JK, Lampe PD, Johnson RG. An activator of protein kinase C inhibits gap junction communication between cultured bovine lens cells. Exp Cell Res. 1992;198:337-42.

[180] Rami A, Volkmann T, Winckler J. Effective reduction of neuronal death by inhibiting gap junctional intercellular communication in a rodent model of global transient cerebral ischemia. Experimental neurology. 2001;170:297-304.

[181] Hirschi KK, Minnich BN, Moore LK, Burt JM. Oleic acid differentially affects gap junction-mediated communication in heart and vascular smooth muscle cells. The American journal of physiology. 1993;265:C1517-26.

[182] Huang YS, Tseng YZ, Wu JC, Wang SM. Mechanism of oleic acid-induced gap junctional disassembly in rat cardiomyocytes. J Mol Cell Cardiol. 2004;37:755-66.

[183] Moreno AP, Rook MB, Fishman GI, Spray DC. Gap junction channels: distinct voltage-sensitive and -insensitive conductance states. Biophys J. 1994;67:113-9.

[184] Turner LA, Vodanovic S, Bosnjak ZJ. Interaction of anesthetics and catecholamines on conduction in the canine His-Purkinje system. Adv Pharmacol. 1994;31:167-84.

[185] O'Carroll SJ, Alkadhi M, Nicholson LF, Green CR. Connexin 43 mimetic peptides reduce swelling, astrogliosis, and neuronal cell death after spinal cord injury. Cell Commun Adhes. 2008;15:27-42.

[186] Chaytor AT, Bakker LM, Edwards DH, Griffith TM. Connexin-mimetic peptides dissociate electrotonic EDHF-type signalling via myoendothelial and smooth muscle gap junctions in the rabbit iliac artery. British journal of pharmacology. 2005;144:108-14.

[187] Kwak BR, Jongsma HJ. Selective inhibition of gap junction channel activity by synthetic peptides. The Journal of physiology. 1999;516 (Pt 3):679-85.

[188] Chaytor AT, Evans WH, Griffith TM. Peptides homologous to extracellular loop motifs of connexin 43 reversibly abolish rhythmic contractile activity in rabbit arteries. The Journal of physiology. 1997;503 (Pt 1):99-110.

[189] Aonuma S, Kohama Y, Akai K, Iwasaki S. Studies on heart. II. Further effects of bovine ventricle protein (BVP) and antiarrhythmic peptide (AAP) on myocardial cells in culture. Chem Pharm Bull (Tokyo). 1980;28:3340-6.

[190] Aonuma S, Kohama Y, Makino T, Hattori K. [Studies on the heart (22). Inhibitory effect of an atrial peptide (AAP) on drug-induced arrhythmia]. Yakugaku Zasshi. 1983;103:662-6.

[191] Aonuma S, Kohama Y, Makino T, Fujisawa Y. Studies of heart. XXI. Amino acid sequence of antiarrhythmic peptide (AAP) isolated from atria. J Pharmacobiodyn. 1982;5:40-8.

[192] Muller A, Gottwald M, Tudyka T, Linke W, Klaus W, Dhein S. Increase in gap junction conductance by an antiarrhythmic peptide. European journal of pharmacology. 1997;327:65-72.

[193] Dhein S, Tudyka T. Therapeutic potential of antiarrhythmic peptides. Cellular coupling as a new antiarrhythmic target. Drugs. 1995;49:851-5.

[194] Dhein S, Manicone N, Muller A, Gerwin R, Ziskoven U, Irankhahi A, et al. A new synthetic antiarrhythmic peptide reduces dispersion of epicardial activation recovery interval and

diminishes alterations of epicardial activation patterns induced by regional ischemia. A mapping study. Naunyn Schmiedebergs ArchPharmacol. 1994;350:174-84.

[195] Xing D, Kjolbye AL, Nielsen MS, Petersen JS, Harlow KW, Holstein-Rathlou NH, et al. ZP123 increases gap junctional conductance and prevents reentrant ventricular tachycardia during myocardial ischemia in open chest dogs. Journal of cardiovascular electrophysiology. 2003;14:510-20.

[196] Boitano S, Evans WH. Connexin mimetic peptides reversibly inhibit Ca(2+) signaling through gap junctions in airway cells. American journal of physiology Lung cellular and molecular physiology. 2000;279:L623-30.

[197] Spray DC, Rozental R, Srinivas M. Prospects for rational development of pharmacological gap junction channel blockers. Curr Drug Targets. 2002;3:455-64.

[198] De Vriese AS, Van dV, Lameire NH. Effects of connexin-mimetic peptides on nitric oxide synthase- and cyclooxygenase-independent renal vasodilation. Kidney Int. 2002;61:177-85.

[199] Kjolbye AL, Knudsen CB, Jepsen T, Larsen BD, Petersen JS. Pharmacological characterization of the new stable antiarrhythmic peptide analog Ac-D-Tyr-D-Pro-D-Hyp-Gly-D-Ala-Gly-NH2 (ZP123): in vivo and in vitro studies. J Pharmacol Exp Ther. 2003;306:1191-9.

[200] Erichsen JE. Oxygen Lack: Ischemia and Angina. In: Opie LH, editor. Philadelphia: Lippincott - Raven; 1998. p. 515-41.

[201] Contreras JE, Sanchez HA, Eugenin EA, Speidel D, Theis M, Willecke K, et al. Metabolic inhibition induces opening of unapposed connexin 43 gap junction hemichannels and reduces gap junctional communication in cortical astrocytes in culture. Proceedings of the National Academy of Sciences of the United States of America. 2002;99:495-500.

[202] Weiss JN, Lamp ST. Glycolysis preferentially inhibits ATP-sensitive K+ channels in isolated guinea pig cardiac myocytes. Science. 1987;238:67-9.

[203] Beyer EC, Steinberg TH. Evidence that the gap junction protein connexin-43 is the ATP-induced pore of mouse macrophages. J Biol Chem. 1991;266:7971-4.

[204] Clarke TC, Williams OJ, Martin PE, Evans WH. ATP release by cardiac myocytes in a simulated ischaemia model Inhibition by a connexin mimetic and enhancement by an antiarrhythmic peptide. European journal of pharmacology. 2008.

[205] Faigle M, Seessle J, Zug S, El Kasmi KC, Eltzschig HK. ATP release from vascular endothelia occurs across Cx43 hemichannels and is attenuated during hypoxia. PLoS ONE. 2008;3:e2801.

[206] Hendrickson SC, St.Louis JD, Lowe JE, Abdel-Aleem S. Free fatty acid metabolism during myocardial ischemia and reperfusion. MolCell Biochem. 1997;166:85-94.

[207] Yamada KA, McHowat J, Yan GX, Donahue K, Peirick J, Kleber AG, et al. Cellular uncoupling induced by accumulation of long-chain acylcarnitine during ischemia. Circulation research. 1994;74:83-95.

[208] Barger PM, Kelly DP. Fatty acid utilization in the hypertrophied and failing heart: molecular regulatory mechanisms. AmJMedSci. 1999;318:36-42.

[209] Tian R, Musi N, D'Agostino J, Hirshman MF, Goodyear LJ. Increased adenosine monophosphate-activated protein kinase activity in rat hearts with pressure-overload hypertrophy. Circulation. 2001;104:1664-9.

[210] Pogwizd SM, Corr PB. Biochemical and electrophysiological alterations underlying ventricular arrhythmias in the failing heart. EurHeart J. 1994;15 Suppl D:145-54.

[211] Kudo N, Gillespie JG, Kung L, Witters LA, Schulz R, Clanachan AS, et al. Characterization of 5'AMP-activated protein kinase activity in the heart and its role in inhibiting acetyl-CoA carboxylase during reperfusion following ischemia. Biochim Biophys Acta. 1996;1301:67-75.

[212] Atkinson DE. The energy charge of the adenylate pool as a regulatory parameter. Interaction with feedback modifiers. Biochemistry. 1968;7:4030-4.

[213] Hardie DG, Carling D. The AMP-activated protein kinase--fuel gauge of the mammalian cell? European journal of biochemistry / FEBS. 1997;246:259-73.

[214] O'Neill HM, Holloway GP, Steinberg GR. AMPK regulation of fatty acid metabolism and mitochondrial biogenesis: implications for obesity. Mol Cell Endocrinol. 2013;366:135-51.

[215] Oakhill JS, Scott JW, Kemp BE. AMPK functions as an adenylate charge-regulated protein kinase. Trends in endocrinology and metabolism: TEM. 2012;23:125-32.

[216] Xiao B, Sanders MJ, Underwood E, Heath R, Mayer FV, Carmena D, et al. Structure of mammalian AMPK and its regulation by ADP. Nature. 2011;472:230-3.

[217] Li X, Wang L, Zhou XE, Ke J, de Waal PW, Gu X, et al. Structural basis of AMPK regulation by adenine nucleotides and glycogen. Cell Res. 2015;25:398.

[218] Li X, Wang L, Zhou XE, Ke J, de Waal PW, Gu X, et al. Structural basis of AMPK regulation by adenine nucleotides and glycogen. Cell Res. 2015;25:50-66.

[219] Xiao B, Sanders MJ, Carmena D, Bright NJ, Haire LF, Underwood E, et al. Structural basis of AMPK regulation by small molecule activators. Nature communications. 2013;4:3017.

[220] Oakhill JS, Chen ZP, Scott JW, Steel R, Castelli LA, Ling N, et al. beta-Subunit myristoylation is the gatekeeper for initiating metabolic stress sensing by AMP-activated protein kinase (AMPK). Proceedings of the National Academy of Sciences of the United States of America. 2010;107:19237-41.

[221] Oakhill JS, Steel R, Chen ZP, Scott JW, Ling N, Tam S, et al. AMPK is a direct adenylate charge-regulated protein kinase. Science. 2011;332:1433-5.

[222] Zhang YL, Guo H, Zhang CS, Lin SY, Yin Z, Peng Y, et al. AMP as a low-energy charge signal autonomously initiates assembly of AXIN-AMPK-LKB1 complex for AMPK activation. Cell Metab. 2013;18:546-55.

[223] Wu Y, Song P, Xu J, Zhang M, Zou MH. Activation of protein phosphatase 2A by palmitate inhibits AMP-activated protein kinase. J Biol Chem. 2007;282:9777-88.

[224] Sanders MJ, Grondin PO, Hegarty BD, Snowden MA, Carling D. Investigating the mechanism for AMP activation of the AMP-activated protein kinase cascade. Biochem J. 2007;403:139-48.

[225] Wang MY, Unger RH. Role of PP2C in cardiac lipid accumulation in obese rodents and its prevention by troglitazone. Am J Physiol Endocrinol Metab. 2005;288:E216-21.

[226] Gowans GJ, Hardie DG. AMPK: a cellular energy sensor primarily regulated by AMP. Biochem Soc Trans. 2014;42:71-5.

[227] Gowans GJ, Hawley SA, Ross FA, Hardie DG. AMP is a true physiological regulator of AMP-activated protein kinase by both allosteric activation and enhancing net phosphorylation. Cell Metab. 2013;18:556-66.

[228] Lin YY, Kiihl S, Suhail Y, Liu SY, Chou YH, Kuang Z, et al. Functional dissection of lysine deacetylases reveals that HDAC1 and p300 regulate AMPK. Nature. 2012;482:251-5.

[229] Kovacic S, Soltys CL, Barr AJ, Shiojima I, Walsh K, Dyck JR. Akt activity negatively regulates phosphorylation of AMP-activated protein kinase in the heart. J Biol Chem. 2003;278:39422-7.

[230] Pulinilkunnil T, He H, Kong D, Asakura K, Peroni OD, Lee A, et al. Adrenergic regulation of AMP-activated protein kinase in brown adipose tissue in vivo. J Biol Chem. 2011;286:8798-809.

[231] Hawley SA, Ross FA, Gowans GJ, Tibarewal P, Leslie NR, Hardie DG. Phosphorylation by Akt within the ST loop of AMPK-alpha1 down-regulates its activation in tumour cells. Biochem J. 2014;459:275-87.

[232] Soltys CL, Kovacic S, Dyck JR. Activation of cardiac AMP-activated protein kinase by LKB1 expression or chemical hypoxia is blunted by increased Akt activity. American journal of physiology. 2006;290:H2472-9.

[233] Djouder N, Tuerk RD, Suter M, Salvioni P, Thali RF, Scholz R, et al. PKA phosphorylates and inactivates AMPKalpha to promote efficient lipolysis. EMBO J. 2010;29:469-81.

[234] Fogarty S, Hawley SA, Green KA, Saner N, Mustard KJ, Hardie DG. Calmodulin-dependent protein kinase kinase-beta activates AMPK without forming a stable complex: synergistic effects of Ca2+ and AMP. Biochem J. 2010;426:109-18.

[235] Anderson KA, Ribar TJ, Lin F, Noeldner PK, Green MF, Muehlbauer MJ, et al. Hypothalamic CaMKK2 contributes to the regulation of energy balance. Cell Metab. 2008;7:377-88.

[236] Hurley RL, Anderson KA, Franzone JM, Kemp BE, Means AR, Witters LA. The Ca2+/calmodulin-dependent protein kinase kinases are AMP-activated protein kinase kinases. J Biol Chem. 2005;280:29060-6.

[237] Woods A, Dickerson K, Heath R, Hong SP, Momcilovic M, Johnstone SR, et al. Ca2+/calmodulin-dependent protein kinase kinase-beta acts upstream of AMP-activated protein kinase in mammalian cells. Cell Metab. 2005;2:21-33.

[238] Sanli T, Steinberg GR, Singh G, Tsakiridis T. AMP-activated protein kinase (AMPK) beyond metabolism: A novel genomic stress sensor participating in the DNA damage response pathway. Cancer biology & therapy. 2014;15:156-69.

[239] Zaha VG, Young LH. AMP-activated protein kinase regulation and biological actions in the heart. Circulation research. 2012;111:800-14.

[240] Hardie DG, Ross FA, Hawley SA. AMPK: a nutrient and energy sensor that maintains energy homeostasis. Nat Rev Mol Cell Biol. 2012;13:251-62.

[241] Ducommun S, Deak M, Sumpton D, Ford RJ, Nunez Galindo A, Kussmann M, et al. Motif affinity and mass spectrometry proteomic approach for the discovery of cellular AMPK targets: Identification of mitochondrial fission factor as a new AMPK substrate. Cell Signal. 2015.

[242] Ruderman NB, Saha AK, Kraegen EW. Minireview: malonyl CoA, AMP-activated protein kinase, and adiposity. Endocrinology. 2003;144:5166-71.

[243] Unger RH. The hyperleptinemia of obesity-regulator of caloric surpluses. Cell. 2004;117:145-6.

[244] Folmes CD, Lopaschuk GD. Role of malonyl-CoA in heart disease and the hypothalamic control of obesity. Cardiovascular research. 2007;73:278-87.

[245] Lane MD, Wolfgang M, Cha SH, Dai Y. Regulation of food intake and energy expenditure by hypothalamic malonyl-CoA. Int J Obes (Lond). 2008;32 Suppl 4:S49-54.

[246] Minokoshi Y, Shiuchi T, Lee S, Suzuki A, Okamoto S. Role of hypothalamic AMP-kinase in food intake regulation. Nutrition (Burbank, Los Angeles County, Calif. 2008;24:786-90.

[247] Kubli DA, Gustafsson AB. Cardiomyocyte health: adapting to metabolic changes through autophagy. Trends in endocrinology and metabolism: TEM. 2014;25:156-64.

[248] Ju TC, Chen HM, Lin JT, Chang CP, Chang WC, Kang JJ, et al. Nuclear translocation of AMPK-alpha1 potentiates striatal neurodegeneration in Huntington's disease. The Journal of cell biology. 2011;194:209-27.

[249] McGee SL, Hargreaves M. AMPK-mediated regulation of transcription in skeletal muscle. Clin Sci (Lond). 2010;118:507-18.

[250] Marcinko K, Steinberg GR. The role of AMPK in controlling metabolism and mitochondrial biogenesis during exercise. Exp Physiol. 2014;99:1581-5.

[251] Funk JA, Odejinmi S, Schnellmann RG. SRT1720 induces mitochondrial biogenesis and rescues mitochondrial function after oxidant injury in renal proximal tubule cells. J Pharmacol Exp Ther. 2010;333:593-601.

[252] Jornayvaz FR, Shulman GI. Regulation of mitochondrial biogenesis. Essays in biochemistry. 2010;47:69-84.

[253] Li L, Pan R, Li R, Niemann B, Aurich AC, Chen Y, et al. Mitochondrial biogenesis and peroxisome proliferator-activated receptor-gamma coactivator-1alpha (PGC-1alpha) deacetylation by physical activity: intact adipocytokine signaling is required. Diabetes. 2011;60:157-67.

[254] Li L, Muhlfeld C, Niemann B, Pan R, Li R, Hilfiker-Kleiner D, et al. Mitochondrial biogenesis and PGC-1alpha deacetylation by chronic treadmill exercise: differential response in cardiac and skeletal muscle. Basic research in cardiology. 2011;106:1221-34.

[255] Marsin AS, Bouzin C, Bertrand L, Hue L. The stimulation of glycolysis by hypoxia in activated monocytes is mediated by AMP-activated protein kinase and inducible 6-phosphofructo-2-kinase. J Biol Chem. 2002;277:30778-83.

[256] Nagendran J, Waller TJ, Dyck JR. AMPK signalling and the control of substrate use in the heart. Mol Cell Endocrinol. 2013;366:180-93.

[257] Solskov L, Lofgren B, Kristiansen SB, Jessen N, Pold R, Nielsen TT, et al. Metformin induces cardioprotection against ischaemia/reperfusion injury in the rat heart 24 hours after administration. Basic & clinical pharmacology & toxicology. 2008;103:82-7.

[258] Hauton D. Does long-term metformin treatment increase cardiac lipoprotein lipase? Metabolism. 2011;60:32-42.

[259] Pulinilkunnil T, Puthanveetil P, Kim MS, Wang F, Schmitt V, Rodrigues B. Ischemia-reperfusion alters cardiac lipoprotein lipase. Biochim Biophys Acta. 2010;1801:171-5.

[260] Chabowski A, Coort SL, Calles-Escandon J, Tandon NN, Glatz JF, Luiken JJ, et al. The subcellular compartmentation of fatty acid transporters is regulated differently by insulin and by AICAR. FEBS Lett. 2005;579:2428-32.

[261] Luiken JJ, Coort SL, Koonen DP, Bonen A, Glatz JF. Signalling components involved in contraction-inducible substrate uptake into cardiac myocytes. The Proceedings of the Nutrition Society. 2004;63:251-8.

[262] Habets DD, Coumans WA, El Hasnaoui M, Zarrinpashneh E, Bertrand L, Viollet B, et al. Crucial role for LKB1 to AMPKalpha2 axis in the regulation of CD36-mediated long-chain fatty acid uptake into cardiomyocytes. Biochim Biophys Acta. 2009;1791:212-9.

[263] Munday MR, Campbell DG, Carling D, Hardie DG. Identification by amino acid sequencing of three major regulatory phosphorylation sites on rat acetyl-CoA carboxylase. European journal of biochemistry / FEBS. 1988;175:331-8.

[264] Munday MR, Carling D, Hardie DG. Negative interactions between phosphorylation of acetyl-CoA carboxylase by the cyclic AMP-dependent and AMP-activated protein kinases. FEBS Lett. 1988;235:144-8.

[265] McGarry JD, Leatherman GF, Foster DW. Carnitine palmitoyltransferase I. The site of inhibition of hepatic fatty acid oxidation by malonyl-CoA. J Biol Chem. 1978;253:4128-36.

[266] McGarry JD, Brown NF. The mitochondrial carnitine palmitoyltransferase system. From concept to molecular analysis. European journal of biochemistry / FEBS. 1997;244:1-14.

[267] Dyck JR, Kudo N, Barr AJ, Davies SP, Hardie DG, Lopaschuk GD. Phosphorylation control of cardiac acetyl-CoA carboxylase by cAMP-dependent protein kinase and 5'-AMP activated protein kinase. European journal of biochemistry / FEBS. 1999;262:184-90.

[268] Olson DP, Pulinilkunnil T, Cline GW, Shulman GI, Lowell BB. Gene knockout of Acc2 has little effect on body weight, fat mass, or food intake. Proceedings of the National Academy of Sciences of the United States of America. 2010;107:7598-603.

[269] Dyck JR, Barr AJ, Barr RL, Kolattukudy PE, Lopaschuk GD. Characterization of cardiac malonyl-CoA decarboxylase and its putative role in regulating fatty acid oxidation. The American journal of physiology. 1998;275:H2122-9.

[270] Saha AK, Schwarsin AJ, Roduit R, Masse F, Kaushik V, Tornheim K, et al. Activation of malonyl-CoA decarboxylase in rat skeletal muscle by contraction and the AMP-activated protein kinase activator 5-aminoimidazole-4-carboxamide-1-beta -D-ribofuranoside. J Biol Chem. 2000;275:24279-83.

[271] Thomson DM, Brown JD, Fillmore N, Condon BM, Kim HJ, Barrow JR, et al. LKB1 and the regulation of malonyl-CoA and fatty acid oxidation in muscle. Am J Physiol Endocrinol Metab. 2007;293:E1572-9.

[272] Dzamko NL, Schertzer JD, Ryall J, Steel R, Macaulay SL, Wee S, et al. AMPK independent pathways regulate skeletal muscle fatty acid oxidation. The Journal of physiology. 2008.

[273] Smith BK, Jain SS, Rimbaud S, Dam A, Quadrilatero J, Ventura-Clapier R, et al. FAT/CD36 is located on the outer mitochondrial membrane, upstream of long-chain acyl-CoA synthetase, and regulates palmitate oxidation. Biochem J. 2011;437:125-34.

[274] Omar MA, Fraser H, Clanachan AS. Ischemia-induced activation of AMPK does not increase glucose uptake in glycogen-replete isolated working rat hearts. American journal of physiology. 2008;294:H1266-73.

[275] Jing M, Cheruvu VK, Ismail-Beigi F. Stimulation of glucose transport in response to activation of distinct AMPK signaling pathways. Am J Physiol Cell Physiol. 2008;295:C1071-82.

[276] Barnes K, Ingram JC, Porras OH, Barros LF, Hudson ER, Fryer LG, et al. Activation of GLUT1 by metabolic and osmotic stress: potential involvement of AMP-activated protein kinase (AMPK). Journal of cell science. 2002;115:2433-42.

[277] O'Neill HM, Maarbjerg SJ, Crane JD, Jeppesen J, Jorgensen SB, Schertzer JD, et al. AMP-activated protein kinase (AMPK) beta1beta2 muscle null mice reveal an essential role for AMPK in maintaining mitochondrial content and glucose uptake during exercise. Proceedings of the National Academy of Sciences of the United States of America. 2011;108:16092-7.

[278] Russell RR, 3rd, Li J, Coven DL, Pypaert M, Zechner C, Palmeri M, et al. AMP-activated protein kinase mediates ischemic glucose uptake and prevents postischemic cardiac dysfunction, apoptosis, and injury. The Journal of clinical investigation. 2004;114:495-503.

[279] Russell RR, 3rd, Bergeron R, Shulman GI, Young LH. Translocation of myocardial GLUT-4 and increased glucose uptake through activation of AMPK by AICAR. The American journal of physiology. 1999;277:H643-9.

[280] Corton JM, Gillespie JG, Hawley SA, Hardie DG. 5-aminoimidazole-4-carboxamide ribonucleoside. A specific method for activating AMP-activated protein kinase in intact cells? European journal of biochemistry / FEBS. 1995;229:558-65.

[281] Coven DL, Hu X, Cong L, Bergeron R, Shulman GI, Hardie DG, et al. Physiological role of AMP-activated protein kinase in the heart: graded activation during exercise. Am J Physiol Endocrinol Metab. 2003;285:E629-36.

[282] Till M, Ouwens DM, Kessler A, Eckel J. Molecular mechanisms of contraction-regulated cardiac glucose transport. Biochem J. 2000;346 Pt 3:841-7.

[283] Ducommun S, Wang HY, Sakamoto K, MacKintosh C, Chen S. Thr649Ala-AS160 knock-in mutation does not impair contraction/AICAR-induced glucose transport in mouse muscle. Am J Physiol Endocrinol Metab. 2012;302:E1036-43.

[284] Chen S, Wasserman DH, MacKintosh C, Sakamoto K. Mice with AS160/TBC1D4-Thr649Ala knockin mutation are glucose intolerant with reduced insulin sensitivity and altered GLUT4 trafficking. Cell Metab. 2011;13:68-79.

[285] Sakamoto K, Holman GD. Emerging role for AS160/TBC1D4 and TBC1D1 in the regulation of GLUT4 traffic. Am J Physiol Endocrinol Metab. 2008;295:E29-37.

[286] Gaidhu MP, Perry RL, Noor F, Ceddia RB. Disruption of AMPKalpha1 signaling prevents AICAR-induced inhibition of AS160/TBC1D4 phosphorylation and glucose uptake in primary rat adipocytes. Mol Endocrinol. 2010;24:1434-40.

[287] Treebak JT, Glund S, Deshmukh A, Klein DK, Long YC, Jensen TE, et al. AMPK-mediated AS160 phosphorylation in skeletal muscle is dependent on AMPK catalytic and regulatory subunits. Diabetes. 2006;55:2051-8.

[288] Hunter RW, Treebak JT, Wojtaszewski JF, Sakamoto K. Molecular mechanism by which AMP-activated protein kinase activation promotes glycogen accumulation in muscle. Diabetes. 2011;60:766-74.

[289] Bouskila M, Hunter RW, Ibrahim AF, Delattre L, Peggie M, van Diepen JA, et al. Allosteric regulation of glycogen synthase controls glycogen synthesis in muscle. Cell Metab. 2010;12:456-66.

[290] Carling D, Hardie DG. The substrate and sequence specificity of the AMP-activated protein kinase. Phosphorylation of glycogen synthase and phosphorylase kinase. Biochim Biophys Acta. 1989;1012:81-6.

[291] Jorgensen SB, Nielsen JN, Birk JB, Olsen GS, Viollet B, Andreelli F, et al. The alpha2-5'AMP-activated protein kinase is a site 2 glycogen synthase kinase in skeletal muscle and is responsive to glucose loading. Diabetes. 2004;53:3074-81.

[292] Longnus SL, Wambolt RB, Parsons HL, Brownsey RW, Allard MF. 5-Aminoimidazole-4-carboxamide 1-beta -D-ribofuranoside (AICAR) stimulates myocardial glycogenolysis by allosteric mechanisms. Am J Physiol Regul Integr Comp Physiol. 2003;284:R936-44.

[293] Ercan-Fang N, Gannon MC, Rath VL, Treadway JL, Taylor MR, Nuttall FQ. Integrated effects of multiple modulators on human liver glycogen phosphorylase a. Am J Physiol Endocrinol Metab. 2002;283:E29-37.

[294] Marsin AS, Bertrand L, Rider MH, Deprez J, Beauloye C, Vincent MF, et al. Phosphorylation and activation of heart PFK-2 by AMPK has a role in the stimulation of glycolysis during ischaemia. CurrBiol. 2000;10:1247-55.

[295] Hue L, Beauloye C, Marsin AS, Bertrand L, Horman S, Rider MH. Insulin and ischemia stimulate glycolysis by acting on the same targets through different and opposing signaling pathways. J Mol Cell Cardiol. 2002;34:1091-7.

[296] Liu Q, Docherty JC, Rendell JC, Clanachan AS, Lopaschuk GD. High levels of fatty acids delay the recovery of intracellular pH and cardiac efficiency in post-ischemic hearts by inhibiting glucose oxidation. J Am Coll Cardiol. 2002;39:718-25.

[297] Itoi T, Huang L, Lopaschuk GD. Glucose use in neonatal rabbit hearts reperfused after global ischemia. The American journal of physiology. 1993;265:H427-33.

[298] Lopaschuk GD. AMP-activated protein kinase control of energy metabolism in the ischemic heart. Int J Obes (Lond). 2008;32 Suppl 4:S29-35.

[299] Lopaschuk GD, Stanley WC. Malonyl-CoA decarboxylase inhibition as a novel approach to treat ischemic heart disease. Cardiovascular drugs and therapy / sponsored by the International Society of Cardiovascular Pharmacotherapy. 2006;20:433-9.

[300] Lopaschuk GD, Barr R, Thomas PD, Dyck JR. Beneficial effects of trimetazidine in ex vivo working ischemic hearts are due to a stimulation of glucose oxidation secondary to inhibition of long-chain 3-ketoacyl coenzyme a thiolase. Circulation research. 2003;93:e33-7.

[301] Hopkins TA, Dyck JR, Lopaschuk GD. AMP-activated protein kinase regulation of fatty acid oxidation in the ischaemic heart. Biochem Soc Trans. 2003;31:207-12.

[302] Dyck JR, Lopaschuk GD. Malonyl CoA control of fatty acid oxidation in the ischemic heart. J Mol Cell Cardiol. 2002;34:1099-109.

[303] Kantor PF, Dyck JR, Lopaschuk GD. Fatty acid oxidation in the reperfused ischemic heart. The American journal of the medical sciences. 1999;318:3-14.

[304] Liu B, Clanachan AS, Schulz R, Lopaschuk GD. Cardiac efficiency is improved after ischemia by altering both the source and fate of protons. Circulation research. 1996;79:940-8.

[305] Hu X, Xu X, Lu Z, Zhang P, Fassett J, Zhang Y, et al. AMP activated protein kinase-alpha2 regulates expression of estrogen-related receptor-alpha, a metabolic transcription factor related to heart failure development. Hypertension. 2011;58:696-703.

[306] Zhu L, Wang Q, Zhang L, Fang Z, Zhao F, Lv Z, et al. Hypoxia induces PGC-1alpha expression and mitochondrial biogenesis in the myocardium of TOF patients. Cell Res. 2010;20:676-87.

[307] Wang W, Fan J, Yang X, Furer-Galban S, Lopez de Silanes I, von Kobbe C, et al. AMP-activated kinase regulates cytoplasmic HuR. Mol Cell Biol. 2002;22:3425-36.

[308] Hoppe S, Bierhoff H, Cado I, Weber A, Tiebe M, Grummt I, et al. AMP-activated protein kinase adapts rRNA synthesis to cellular energy supply. Proceedings of the National Academy of Sciences of the United States of America. 2009;106:17781-6.

[309] Cheng SW, Fryer LG, Carling D, Shepherd PR. Thr2446 is a novel mammalian target of rapamycin (mTOR) phosphorylation site regulated by nutrient status. J Biol Chem. 2004;279:15719-22.

[310] Hardie DG, Ashford ML. AMPK: regulating energy balance at the cellular and whole body levels. Physiology (Bethesda, Md. 2014;29:99-107.

[311] Inoki K, Li Y, Zhu T, Wu J, Guan KL. TSC2 is phosphorylated and inhibited by Akt and suppresses mTOR signalling. Nature cell biology. 2002;4:648-57.

[312] Gwinn DM, Shackelford DB, Egan DF, Mihaylova MM, Mery A, Vasquez DS, et al. AMPK phosphorylation of raptor mediates a metabolic checkpoint. Mol Cell. 2008;30:214-26.

[313] Hardie DG. AMPK and Raptor: matching cell growth to energy supply. Mol Cell. 2008;30:263-5.

[314] Horman S, Browne G, Krause U, Patel J, Vertommen D, Bertrand L, et al. Activation of AMP-activated protein kinase leads to the phosphorylation of elongation factor 2 and an inhibition of protein synthesis. Curr Biol. 2002;12:1419-23.

[315] Browne GJ, Finn SG, Proud CG. Stimulation of the AMP-activated protein kinase leads to activation of eukaryotic elongation factor 2 kinase and to its phosphorylation at a novel site, serine 398. J Biol Chem. 2004;279:12220-31.

[316] Inoki K, Zhu T, Guan KL. TSC2 mediates cellular energy response to control cell growth and survival. Cell. 2003;115:577-90.

[317] Horman S, Beauloye C, Vertommen D, Vanoverschelde JL, Hue L, Rider MH. Myocardial ischemia and increased heart work modulate the phosphorylation state of eukaryotic elongation factor-2. J Biol Chem. 2003;278:41970-6.

[318] Nakai A, Yamaguchi O, Takeda T, Higuchi Y, Hikoso S, Taniike M, et al. The role of autophagy in cardiomyocytes in the basal state and in response to hemodynamic stress. Nature medicine. 2007;13:619-24.

[319] Fong JT, Kells RM, Gumpert AM, Marzillier JY, Davidson MW, Falk MM. Internalized gap junctions are degraded by autophagy. Autophagy. 2012;8:794-811.

[320] Garcia L, Verdejo HE, Kuzmicic J, Zalaquett R, Gonzalez S, Lavandero S, et al. Impaired cardiac autophagy in patients developing postoperative atrial fibrillation. J Thorac Cardiovasc Surg. 2012;143:451-9.

[321] Yan L, Vatner DE, Kim SJ, Ge H, Masurekar M, Massover WH, et al. Autophagy in chronically ischemic myocardium. Proceedings of the National Academy of Sciences of the United States of America. 2005;102:13807-12.

[322] Yuan Y, Zhao J, Yan S, Wang D, Zhang S, Yun F, et al. Autophagy: A potential novel mechanistic contributor to atrial fibrillation. International journal of cardiology. 2014;172:492-4.

[323] Sinnett SE, Brenman JE. Past strategies and future directions for identifying AMP-activated protein kinase (AMPK) modulators. Pharmacology & therapeutics. 2014.

[324] Hinke SA, Martens GA, Cai Y, Finsi J, Heimberg H, Pipeleers D, et al. Methyl succinate antagonises biguanide-induced AMPK-activation and death of pancreatic beta-cells through restoration of mitochondrial electron transfer. British journal of pharmacology. 2007;150:1031-43.

[325] Sakamoto K, Goransson O, Hardie DG, Alessi DR. Activity of LKB1 and AMPK-related kinases in skeletal muscle: effects of contraction, phenformin, and AICAR. Am J Physiol Endocrinol Metab. 2004;287:E310-7.

[326] Zhang L, He H, Balschi JA. Metformin and phenformin activate AMP-activated protein kinase in the heart by increasing cytosolic AMP concentration. American journal of physiology. 2007;293:H457-66.

[327] Cool B, Zinker B, Chiou W, Kifle L, Cao N, Perham M, et al. Identification and characterization of a small molecule AMPK activator that treats key components of type 2 diabetes and the metabolic syndrome. Cell Metab. 2006;3:403-16.

[328] Goransson O, McBride A, Hawley SA, Ross FA, Shpiro N, Foretz M, et al. Mechanism of action of A-769662, a valuable tool for activation of AMP-activated protein kinase. J Biol Chem. 2007.

[329] Pang T, Zhang ZS, Gu M, Qiu BY, Yu LF, Cao PR, et al. Small molecule antagonizes autoinhibition and activates AMP-activated protein kinase in cells. J Biol Chem. 2008;283:16051-60.

[330] Li YY, Yu LF, Zhang LN, Qiu BY, Su MB, Wu F, et al. Novel small-molecule AMPK activator orally exerts beneficial effects on diabetic db/db mice. Toxicology and applied pharmacology. 2013;273:325-34.

[331] Hawley SA, Fullerton MD, Ross FA, Schertzer JD, Chevtzoff C, Walker KJ, et al. The ancient drug salicylate directly activates AMP-activated protein kinase. Science. 2012;336:918-22.

[332] Kim EK, Miller I, Aja S, Landree LE, Pinn M, McFadden J, et al. C75, a fatty acid synthase inhibitor, reduces food intake via hypothalamic AMP-activated protein kinase. J Biol Chem. 2004;279:19970-6.

[333] McCullough LD, Zeng Z, Li H, Landree LE, McFadden J, Ronnett GV. Pharmacological inhibition of AMP-activated protein kinase provides neuroprotection in stroke. J Biol Chem. 2005;280:20493-502.

[334] Zhou G, Myers R, Li Y, Chen Y, Shen X, Fenyk-Melody J, et al. Role of AMP-activated protein kinase in mechanism of metformin action. The Journal of clinical investigation. 2001;108:1167-74.

[335] Machrouhi F, Ouhamou N, Laderoute K, Calaoagan J, Bukhtiyarova M, Ehrlich PJ, et al. The rational design of a novel potent analogue of the 5'-AMP-activated protein kinase inhibitor compound C with improved selectivity and cellular activity. Bioorganic & medicinal chemistry letters. 2010;20:6394-9.

[336] Chu TF, Rupnick MA, Kerkela R, Dallabrida SM, Zurakowski D, Nguyen L, et al. Cardiotoxicity associated with tyrosine kinase inhibitor sunitinib. Lancet. 2007;370:2011-9.

[337] Kerkela R, Woulfe KC, Durand JB, Vagnozzi R, Kramer D, Chu TF, et al. Sunitinib-induced cardiotoxicity is mediated by off-target inhibition of AMP-activated protein kinase. Clinical and translational science. 2009;2:15-25.

[338] Altarejos JY, Taniguchi M, Clanachan AS, Lopaschuk GD. Myocardial ischemia differentially regulates LKB1 and an alternate 5'-AMP-activated protein kinase kinase. J Biol Chem. 2005;280:183-90.

[339] Hawley SA, Boudeau J, Reid JL, Mustard KJ, Udd L, Makela TP, et al. Complexes between the LKB1 tumor suppressor, STRAD alpha/beta and MO25 alpha/beta are upstream kinases in the AMP-activated protein kinase cascade. Journal of biology. 2003;2:28.

[340] Hawley SA, Selbert MA, Goldstein EG, Edelman AM, Carling D, Hardie DG. 5'-AMP activates the AMP-activated protein kinase cascade, and Ca2+/calmodulin activates the calmodulin-dependent protein kinase I cascade, via three independent mechanisms. J Biol Chem. 1995;270:27186-91.

[341] Shaw RJ, Kosmatka M, Bardeesy N, Hurley RL, Witters LA, DePinho RA, et al. The tumor suppressor LKB1 kinase directly activates AMP-activated kinase and regulates apoptosis in response to energy stress. Proceedings of the National Academy of Sciences of the United States of America. 2004;101:3329-35.

[342] Suzuki A, Kusakai G, Kishimoto A, Shimojo Y, Ogura T, Lavin MF, et al. IGF-1 phosphorylates AMPK-alpha subunit in ATM-dependent and LKB1-independent manner. Biochem Biophys Res Commun. 2004;324:986-92.

[343] Ussher JR, Jaswal JS, Wagg CS, Armstrong HE, Lopaschuk DG, Keung W, et al. Role of the atypical protein kinase Czeta in regulation of 5'-AMP-activated protein kinase in cardiac and skeletal muscle. Am J Physiol Endocrinol Metab. 2009;297:E349-57.

[344] Xie M, Zhang D, Dyck JR, Li Y, Zhang H, Morishima M, et al. A pivotal role for endogenous TGF-beta-activated kinase-1 in the LKB1/AMP-activated protein kinase energy-sensor pathway. Proceedings of the National Academy of Sciences of the United States of America. 2006;103:17378-83.

[345] Xie Z, Dong Y, Zhang M, Cui MZ, Cohen RA, Riek U, et al. Activation of protein kinase C zeta by peroxynitrite regulates LKB1-dependent AMP-activated protein kinase in cultured endothelial cells. J Biol Chem. 2006;281:6366-75.

[346] Hurley RL, Barre LK, Wood SD, Anderson KA, Kemp BE, Means AR, et al. Regulation of AMP-activated protein kinase by multisite phosphorylation in response to agents that elevate cellular cAMP. J Biol Chem. 2006;281:36662-72.

[347] Saez JC, Martinez AD, Branes MC, Gonzalez HE. Regulation of gap junctions by protein phosphorylation. Braz J Med Biol Res. 1998;31:593-600.

[348] Lowenstein WR. Regulation of cell-to-cell communication by phosphorylation. Biochemical Society symposium. 1985;50:43-58.

[349] Thevenin AF, Kowal TJ, Fong JT, Kells RM, Fisher CG, Falk MM. Proteins and mechanisms regulating gap-junction assembly, internalization, and degradation. Physiology (Bethesda, Md. 2013;28:93-116.

[350] Chen VC, Gouw JW, Naus CC, Foster LJ. Connexin multi-site phosphorylation: mass spectrometry-based proteomics fills the gap. Biochim Biophys Acta. 2013;1828:23-34.

[351] Marquez-Rosado L, Solan JL, Dunn CA, Norris RP, Lampe PD. Connexin43 phosphorylation in brain, cardiac, endothelial and epithelial tissues. Biochim Biophys Acta. 2012;1818:1985-92.

[352] Solan JL, Lampe PD. Connexin43 phosphorylation: structural changes and biological effects. Biochem J. 2009;419:261-72.

[353] Lampe PD, Lau AF. The effects of connexin phosphorylation on gap junctional communication. The international journal of biochemistry & cell biology. 2004;36:1171-86.

[354] Cooper CD, Solan JL, Dolejsi MK, Lampe PD. Analysis of connexin phosphorylation sites. Methods. 2000;20:196-204.

[355] Lampe PD, Lau AF. Regulation of gap junctions by phosphorylation of connexins. Archives of biochemistry and biophysics. 2000;384:205-15.

[356] Solan JL, Lampe PD. Key Connexin 43 Phosphorylation Events Regulate the Gap Junction Life Cycle. J Membr Biol. 2007.

[357] Swenson KI, Piwnica-Worms H, McNamee H, Paul DL. Tyrosine phosphorylation of the gap junction protein connexin43 is required for the pp60v-src-induced inhibition of communication. Cell regulation. 1990;1:989-1002.

[358] Crow DS, Beyer EC, Paul DL, Kobe SS, Lau AF. Phosphorylation of connexin43 gap junction protein in uninfected and Rous sarcoma virus-transformed mammalian fibroblasts. Mol Cell Biol. 1990;10:1754-63.

[359] Laird DW, Castillo M, Kasprzak L. Gap junction turnover, intracellular trafficking, and phosphorylation of connexin43 in brefeldin A-treated rat mammary tumor cells. The Journal of cell biology. 1995;131:1193-203.

[360] Musil LS, Cunningham BA, Edelman GM, Goodenough DA. Differential phosphorylation of the gap junction protein connexin43 in junctional communication-competent and -deficient cell lines. The Journal of cell biology. 1990;111:2077-88.

[361] Kadle R, Zhang JT, Nicholson BJ. Tissue-specific distribution of differentially phosphorylated forms of Cx43. Mol Cell Biol. 1991;11:363-9.

[362] Solan JL, Fry MD, TenBroek EM, Lampe PD. Connexin43 phosphorylation at S368 is acute during S and G2/M and in response to protein kinase C activation. Journal of cell science. 2003;116:2203-11.

[363] Dunn CA, Lampe PD. Injury-triggered Akt phosphorylation of Cx43: a ZO-1-driven molecular switch that regulates gap junction size. Journal of cell science. 2014;127:455-64.

[364] Musil LS, Goodenough DA. Biochemical analysis of connexin43 intracellular transport, phosphorylation, and assembly into gap junctional plaques. The Journal of cell biology. 1991;115:1357-74.

[365] Park DJ, Wallick CJ, Martyn KD, Lau AF, Jin C, Warn-Cramer BJ. Akt phosphorylates Connexin43 on Ser373, a "mode-1" binding site for 14-3-3. Cell Commun Adhes. 2007;14:211-26.

[366] Cooper CD, Lampe PD. Casein kinase 1 regulates connexin-43 gap junction assembly. J Biol Chem. 2002;277:44962-8.

[367] Lau AF, Kanemitsu MY, Kurata WE, Danesh S, Boynton AL. Epidermal growth factor disrupts gap-junctional communication and induces phosphorylation of connexin43 on serine. Molecular biology of the cell. 1992;3:865-74.

[368] Kanemitsu MY, Lau AF. Epidermal growth factor stimulates the disruption of gap junctional communication and connexin43 phosphorylation independent of 12-0-tetradecanoylphorbol 13-acetate-sensitive protein kinase C: the possible involvement of mitogen-activated protein kinase. Molecular biology of the cell. 1993;4:837-48.

[369] Warn-Cramer BJ, Cottrell GT, Burt JM, Lau AF. Regulation of connexin-43 gap junctional intercellular communication by mitogen-activated protein kinase. J Biol Chem. 1998;273:9188-96.

[370] Polontchouk L, Ebelt B, Jackels M, Dhein S. Chronic effects of endothelin 1 and angiotensin II on gap junctions and intercellular communication in cardiac cells. Faseb J. 2002;16:87-9.

[371] Petrich BG, Gong X, Lerner DL, Wang X, Brown JH, Saffitz JE, et al. c-Jun N-terminal kinase activation mediates downregulation of connexin43 in cardiomyocytes. Circulation research. 2002;91:640-7.

[372] Cameron SJ, Malik S, Akaike M, Lerner-Marmarosh N, Yan C, Lee JD, et al. Regulation of epidermal growth factor-induced connexin 43 gap junction communication by big mitogen-activated protein kinase1/ERK5 but not ERK1/2 kinase activation. J Biol Chem. 2003;278:18682-8.

[373] Brissette JL, Kumar NM, Gilula NB, Dotto GP. The tumor promoter 12-O-tetradecanoylphorbol-13-acetate and the ras oncogene modulate expression and phosphorylation of gap junction proteins. Mol Cell Biol. 1991;11:5364-71.

[374] Berthoud VM, Rook MB, Traub O, Hertzberg EL, Saez JC. On the mechanisms of cell uncoupling induced by a tumor promoter phorbol ester in clone 9 cells, a rat liver epithelial cell line. Eur J Cell Biol. 1993;62:384-96.

[375] Berthoud VM, Ledbetter ML, Hertzberg EL, Saez JC. Connexin43 in MDCK cells: regulation by a tumor-promoting phorbol ester and Ca2+. Eur J Cell Biol. 1992;57:40-50.

[376] Lampe PD. Analyzing phorbol ester effects on gap junctional communication: a dramatic inhibition of assembly. The Journal of cell biology. 1994;127:1895-905.

[377] Saez JC, Nairn AC, Czernik AJ, Fishman GI, Spray DC, Hertzberg EL. Phosphorylation of connexin43 and the regulation of neonatal rat cardiac myocyte gap junctions. J Mol Cell Cardiol. 1997;29:2131-45.

[378] Kanemitsu MY, Jiang W, Eckhart W. Cdc2-mediated phosphorylation of the gap junction protein, connexin43, during mitosis. Cell Growth Differ. 1998;9:13-21.

[379] Lampe PD, Kurata WE, Warn-Cramer BJ, Lau AF. Formation of a distinct connexin43 phosphoisoform in mitotic cells is dependent upon p34cdc2 kinase. Journal of cell science. 1998;111 (Pt 6):833-41.

[380] Xie H, Laird DW, Chang TH, Hu VW. A mitosis-specific phosphorylation of the gap junction protein connexin43 in human vascular cells: biochemical characterization and localization. The Journal of cell biology. 1997;137:203-10.

[381] Atkinson MM, Lampe PD, Lin HH, Kollander R, Li XR, Kiang DT. Cyclic AMP modifies the cellular distribution of connexin43 and induces a persistent increase in the junctional permeability of mouse mammary tumor cells. Journal of cell science. 1995;108 (Pt 9):3079-90.

[382] Burghardt RC, Barhoumi R, Sewall TC, Bowen JA. Cyclic AMP induces rapid increases in gap junction permeability and changes in the cellular distribution of connexin43. J Membr Biol. 1995;148:243-53.

[383] Paulson AF, Lampe PD, Meyer RA, TenBroek E, Atkinson MM, Walseth TF, et al. Cyclic AMP and LDL trigger a rapid enhancement in gap junction assembly through a stimulation of connexin trafficking. Journal of cell science. 2000;113 (Pt 17):3037-49.

[384] Yogo K, Ogawa T, Akiyama M, Ishida-Kitagawa N, Sasada H, Sato E, et al. PKA implicated in the phosphorylation of Cx43 induced by stimulation with FSH in rat granulosa cells. J Reprod Dev. 2006;52:321-8.

[385] Shah MM, Martinez AM, Fletcher WH. The connexin43 gap junction protein is phosphorylated by protein kinase A and protein kinase C: in vivo and in vitro studies. Mol Cell Biochem. 2002;238:57-68.

[386] Axelsen LN, Stahlhut M, Mohammed S, Larsen BD, Nielsen MS, Holstein-Rathlou NH, et al. Identification of ischemia-regulated phosphorylation sites in connexin43: A possible target for the antiarrhythmic peptide analogue rotigaptide (ZP123). J Mol Cell Cardiol. 2006;40:790-8.

[387] TenBroek EM, Lampe PD, Solan JL, Reynhout JK, Johnson RG. Ser364 of connexin43 and the upregulation of gap junction assembly by cAMP. The Journal of cell biology. 2001;155:1307-18.

[388] Solan JL, Lampe PD. Connexin 43 in LA-25 cells with active v-src is phosphorylated on Y247, Y265, S262, S279/282, and S368 via multiple signaling pathways. Cell Commun Adhes. 2008;15:75-84.

[389] Kanemitsu MY, Loo LW, Simon S, Lau AF, Eckhart W. Tyrosine phosphorylation of connexin 43 by v-Src is mediated by SH2 and SH3 domain interactions. J Biol Chem. 1997;272:22824-31.

[390] Lin R, Warn-Cramer BJ, Kurata WE, Lau AF. v-Src phosphorylation of connexin 43 on Tyr247 and Tyr265 disrupts gap junctional communication. The Journal of cell biology. 2001;154:815-27.

[391] Lin R, Martyn KD, Guyette CV, Lau AF, Warn-Cramer BJ. v-Src tyrosine phosphorylation of connexin43: regulation of gap junction communication and effects on cell transformation. Cell Commun Adhes. 2006;13:199-216.

[392] Huang RY, Laing JG, Kanter EM, Berthoud VM, Bao M, Rohrs HW, et al. Identification of CaMKII phosphorylation sites in Connexin43 by high-resolution mass spectrometry. Journal of proteome research. 2011;10:1098-109.

[393] Wisniewski JR, Nagaraj N, Zougman A, Gnad F, Mann M. Brain phosphoproteome obtained by a FASP-based method reveals plasma membrane protein topology. Journal of proteome research. 2010;9:3280-9.

[394] Yogo K, Ogawa T, Akiyama M, Ishida N, Takeya T. Identification and functional analysis of novel phosphorylation sites in Cx43 in rat primary granulosa cells. FEBS Lett. 2002;531:132-6.

[395] Bonnette PC, Robinson BS, Silva JC, Stokes MP, Brosius AD, Baumann A, et al. Phosphoproteomic characterization of PYK2 signaling pathways involved in osteogenesis. Journal of proteomics. 2010;73:1306-20.

[396] Li H, Liu TF, Lazrak A, Peracchia C, Goldberg GS, Lampe PD, et al. Properties and regulation of gap junctional hemichannels in the plasma membranes of cultured cells. The Journal of cell biology. 1996;134:1019-30.

[397] Lampe PD, Qiu Q, Meyer RA, TenBroek EM, Walseth TF, Starich TA, et al. Gap junction assembly: PTX-sensitive G proteins regulate the distribution of connexin43 within cells. Am J Physiol Cell Physiol. 2001;281:C1211-22.

[398] Sosinsky GE, Solan JL, Gaietta GM, Ngan L, Lee GJ, Mackey MR, et al. The C-terminus of connexin43 adopts different conformations in the Golgi and gap junction as detected with structure-specific antibodies. Biochem J. 2007;408:375-85.

[399] Richards TS, Dunn CA, Carter WG, Usui ML, Olerud JE, Lampe PD. Protein kinase C spatially and temporally regulates gap junctional communication during human wound repair via phosphorylation of connexin43 on serine368. The Journal of cell biology. 2004;167:555-62.

[400] Hund TJ, Lerner DL, Yamada KA, Schuessler RB, Saffitz JE. Protein kinase Cepsilon mediates salutary effects on electrical coupling induced by ischemic preconditioning. Heart Rhythm. 2007;4:1183-93.

[401] Hunter AW, Barker RJ, Zhu C, Gourdie RG. Zonula occludens-1 alters connexin43 gap junction size and organization by influencing channel accretion. Molecular biology of the cell. 2005;16:5686-98.

[402] Cottrell GT, Lin R, Warn-Cramer BJ, Lau AF, Burt JM. Mechanism of v-Src- and mitogen-activated protein kinase-induced reduction of gap junction communication. Am J Physiol Cell Physiol. 2003;284:C511-20.

[403] Brautigan DL. Protein Ser/Thr phosphatases--the ugly ducklings of cell signalling. The FEBS journal. 2013;280:324-45.

[404] Ai X, Pogwizd SM. Connexin 43 downregulation and dephosphorylation in nonischemic heart failure is associated with enhanced colocalized protein phosphatase type 2A. Circulation research. 2005;96:54-63.

[405] Moreno AP, Fishman GI, Spray DC. Phosphorylation shifts unitary conductance and modifies voltage dependent kinetics of human connexin43 gap junction channels. Biophys J. 1992;62:51-3.

[406] Duthe F, Plaisance I, Sarrouilhe D, Herve JC. Endogenous protein phosphatase 1 runs down gap junctional communication of rat ventricular myocytes. Am J Physiol Cell Physiol. 2001;281:C1648-56.

[407] Duthe F, Dupont E, Verrecchia F, Plaisance I, Severs NJ, Sarrouilhe D, et al. Dephosphorylation agents depress gap junctional communication between rat cardiac cells without modifying the Connexin43 phosphorylation degree. General physiology and biophysics. 2000;19:441-9.

[408] Jeyaraman M, Tanguy S, Fandrich RR, Lukas A, Kardami E. Ischemia-induced dephosphorylation of cardiomyocyte connexin-43 is reduced by okadaic acid and calyculin A but not fostriecin. Mol Cell Biochem. 2003;242:129-34.

[409] Singh D, Lampe PD. Identification of connexin-43 interacting proteins. Cell Commun Adhes. 2003;10:215-20.

[410] Giepmans BN, Feiken E, Gebbink MF, Moolenaar WH. Association of connexin43 with a receptor protein tyrosine phosphatase. Cell Commun Adhes. 2003;10:201-5.

[411] Morioka M, Hamada J, Ushio Y, Miyamoto E. Potential role of calcineurin for brain ischemia and traumatic injury. Progress in neurobiology. 1999;58:1-30.

[412] Li WE, Nagy JI. Connexin43 phosphorylation state and intercellular communication in cultured astrocytes following hypoxia and protein phosphatase inhibition. Eur J Neurosci. 2000;12:2644-50.

[413] Turner MS, Haywood GA, Andreka P, You L, Martin PE, Evans WH, et al. Reversible connexin 43 dephosphorylation during hypoxia and reoxygenation is linked to cellular ATP levels. Circulation research. 2004;95:726-33.

[414] Toyofuku T, Akamatsu Y, Zhang H, Kuzuya T, Tada M, Hori M. c-Src regulates the interaction between connexin-43 and ZO-1 in cardiac myocytes. J Biol Chem. 2001;276:1780-8.

[415] Traub O, Eckert R, Lichtenberg-Frate H, Elfgang C, Bastide B, Scheidtmann KH, et al. Immunochemical and electrophysiological characterization of murine connexin40 and -43 in mouse tissues and transfected human cells. Eur J Cell Biol. 1994;64:101-12.

[416] van Rijen HV, van Veen TA, Hermans MM, Jongsma HJ. Human connexin40 gap junction channels are modulated by cAMP. Cardiovascular research. 2000;45:941-51.

[417] Hoffmann A, Gloe T, Pohl U, Zahler S. Nitric oxide enhances de novo formation of endothelial gap junctions. Cardiovascular research. 2003;60:421-30.

[418] Dhein S, Polontchouk L, Salameh A, Haefliger JA. Pharmacological modulation and differential regulation of the cardiac gap junction proteins connexin 43 and connexin 40. Biology of the cell / under the auspices of the European Cell Biology Organization. 2002;94:409-22.

[419] Haussig S, Schubert A, Mohr FW, Dhein S. Sub-chronic nicotine exposure induces intercellular communication failure and differential down-regulation of connexins in cultured human endothelial cells. Atherosclerosis. 2007.

[420] Butterweck A, Gergs U, Elfgang C, Willecke K, Traub O. Immunochemical characterization of the gap junction protein connexin45 in mouse kidney and transfected human HeLa cells. J Membr Biol. 1994;141:247-56.

[421] Darrow BJ, Laing JG, Lampe PD, Saffitz JE, Beyer EC. Expression of multiple connexins in cultured neonatal rat ventricular myocytes. Circulation research. 1995;76:381-7.

[422] Hertlein B, Butterweck A, Haubrich S, Willecke K, Traub O. Phosphorylated carboxy terminal serine residues stabilize the mouse gap junction protein connexin45 against degradation. J Membr Biol. 1998;162:247-57.

[423] Hardie DG, Carling D, Carlson M. The AMP-activated/SNF1 protein kinase subfamily: metabolic sensors of the eukaryotic cell? Annual review of biochemistry. 1998;67:821-55.

[424] Scott JW, Norman DG, Hawley SA, Kontogiannis L, Hardie DG. Protein kinase substrate recognition studied using the recombinant catalytic domain of AMP-activated protein kinase and a model substrate. Journal of molecular biology. 2002;317:309-23.

[425] Csepe TA, Kalyanasundaram A, Hansen BJ, Zhao J, Fedorov VV. Fibrosis: a structural modulator of sinoatrial node physiology and dysfunction. Frontiers in physiology. 2015;6:37.

[426] Anumonwo JM, Pandit SV. Ionic mechanisms of arrhythmogenesis. Trends in cardiovascular medicine. 2015.

[427] Jalife J, Kaur K. Atrial remodeling, fibrosis, and atrial fibrillation. Trends in cardiovascular medicine. 2014.

[428] Hong K, Xiong Q. Genetic basis of atrial fibrillation. Current opinion in cardiology. 2014.

[429] Fedorov VV, Glukhov AV, Chang R. Conduction barriers and pathways of the sinoatrial pacemaker complex: their role in normal rhythm and atrial arrhythmias. American journal of physiology. 2012;302:H1773-83.

[430] Temple IP, Inada S, Dobrzynski H, Boyett MR. Connexins and the atrioventricular node. Heart Rhythm. 2013;10:297-304.

[431] Jansen JA, van Veen TA, de Bakker JM, van Rijen HV. Cardiac connexins and impulse propagation. J Mol Cell Cardiol. 2010;48:76-82.

[432] Terentyev D, Rees CM, Li W, Cooper LL, Jindal HK, Peng X, et al. Hyperphosphorylation of RyRs underlies triggered activity in transgenic rabbit model of LQT2 syndrome. Circulation research. 2014;115:919-28.

[433] Zhou Q, Xiao J, Jiang D, Wang R, Vembaiyan K, Wang A, et al. Carvedilol and its new analogs suppress arrhythmogenic store overload-induced Ca2+ release. Nature medicine. 2011;17:1003-9.

[434] Andersen MN, Rasmussen HB. AMPK: A regulator of ion channels. Commun Integr Biol. 2012;5:480-4.

[435] Light PE, Wallace CH, Dyck JR. Constitutively active adenosine monophosphate-activated protein kinase regulates voltage-gated sodium channels in ventricular myocytes. Circulation. 2003;107:1962-5.

[436] Duan D. Phenomics of cardiac chloride channels: the systematic study of chloride channel function in the heart. The Journal of physiology. 2009;587:2163-77.

[437] Hegedus T, Aleksandrov A, Mengos A, Cui L, Jensen TJ, Riordan JR. Role of individual R domain phosphorylation sites in CFTR regulation by protein kinase A. Biochim Biophys Acta. 2009;1788:1341-9.

[438] Hwang TC, Kirk KL. The CFTR ion channel: gating, regulation, and anion permeation. Cold Spring Harbor perspectives in medicine. 2013;3:a009498.

[439] Alzamora R, King JD, Jr., Hallows KR. CFTR regulation by phosphorylation. Methods in molecular biology (Clifton, NJ. 2011;741:471-88.

[440] Siwiak M, Edelman A, Zielenkiewicz P. Structural models of CFTR-AMPK and CFTR-PKA interactions: R-domain flexibility is a key factor in CFTR regulation. Journal of molecular modeling. 2012;18:83-90.

[441] Hallows KR, Raghuram V, Kemp BE, Witters LA, Foskett JK. Inhibition of cystic fibrosis transmembrane conductance regulator by novel interaction with the metabolic sensor AMP-activated protein kinase. The Journal of clinical investigation. 2000;105:1711-21.

[442] Hallows KR, McCane JE, Kemp BE, Witters LA, Foskett JK. Regulation of channel gating by AMP-activated protein kinase modulates cystic fibrosis transmembrane conductance regulator activity in lung submucosal cells. J Biol Chem. 2003;278:998-1004.

[443] Hallows KR. Emerging role of AMP-activated protein kinase in coupling membrane transport to cellular metabolism. Current opinion in nephrology and hypertension. 2005;14:464-71.

[444] King JD, Jr., Fitch AC, Lee JK, McCane JE, Mak DO, Foskett JK, et al. AMP-activated protein kinase phosphorylation of the R domain inhibits PKA stimulation of CFTR. Am J Physiol Cell Physiol. 2009;297:C94-101.

[445] Kongsuphol P, Cassidy D, Hieke B, Treharne KJ, Schreiber R, Mehta A, et al. Mechanistic insight into control of CFTR by AMPK. J Biol Chem. 2009;284:5645-53.

[446] King JD, Jr., Lee J, Riemen CE, Neumann D, Xiong S, Foskett JK, et al. Role of binding and nucleoside diphosphate kinase A in the regulation of the cystic fibrosis transmembrane conductance regulator by AMP-activated protein kinase. J Biol Chem. 2012;287:33389-400.

[447] Ikematsu N, Dallas ML, Ross FA, Lewis RW, Rafferty JN, David JA, et al. Phosphorylation of the voltage-gated potassium channel Kv2.1 by AMP-activated protein kinase regulates membrane excitability. Proceedings of the National Academy of Sciences of the United States of America. 2011;108:18132-7.

[448] Wang CZ, Wang Y, Di A, Magnuson MA, Ye H, Roe MW, et al. 5-amino-imidazole carboxamide riboside acutely potentiates glucose-stimulated insulin secretion from mouse pancreatic islets by KATP channel-dependent and -independent pathways. Biochem Biophys Res Commun. 2005;330:1073-9.

[449] Chang TJ, Chen WP, Yang C, Lu PH, Liang YC, Su MJ, et al. Serine-385 phosphorylation of inwardly rectifying K+ channel subunit (Kir6.2) by AMP-dependent protein kinase plays a key role in rosiglitazone-induced closure of the K(ATP) channel and insulin secretion in rats. Diabetologia. 2009;52:1112-21.

[450] Gollob MH. Glycogen storage disease as a unifying mechanism of disease in the PRKAG2 cardiac syndrome. Biochem Soc Trans. 2003;31:228-31.

[451] Gollob MH, Green MS, Tang AS, Gollob T, Karibe A, Hassan AS, et al. Identification of a gene responsible for familial Wolff-Parkinson-White syndrome. NEnglJMed. 2001;344:1823-31.

[452] Gollob MH, Seger JJ, Gollob TN, Tapscott T, Gonzales O, Bachinski L, et al. Novel PRKAG2 mutation responsible for the genetic syndrome of ventricular preexcitation and conduction system disease with childhood onset and absence of cardiac hypertrophy. Circulation. 2001;104:3030-3.

[453] Folmes KD, Chan AY, Koonen DP, Pulinilkunnil TC, Baczko I, Hunter BE, et al. Distinct early signaling events resulting from the expression of the PRKAG2 R302Q mutant of AMPK contribute to increased myocardial glycogen. Circulation Cardiovascular genetics. 2009;2:457-66.

[454] Gollob MH, Seger JJ, Gollob TN, Tapscott T, Gonzales O, Bachinski L, et al. Novel PRKAG2 mutation responsible for the genetic syndrome of ventricular preexcitation and conduction system disease with childhood onset and absence of cardiac hypertrophy. Circulation. 2001;104:3030-3.

Chapter 2 Detailed Materials and Methods

This thesis chapter is an original work by Jason Iden.

2.1 General Chemicals and Supplies

Standard chemicals were supplied by Sigma Aldrich (Oakville, ON, CAN), and Invitrogen (Burlington ON, CAN).

2.2 Animal Usage and Ethics Approvals

All animal studies were conducted in accordance with the Canadian Council on Animal Care Guidelines and Policies with approval from the Animal Care and Use Committee: Health Sciences for the University of Alberta, and the Care and Use of Laboratory Animals published by the US National Institutes of Health (Publication No. 85-23, revised 1996). Prior to animal use training in the care and use of the relevant species was completed and certificates granted to all personnel.

2.3 Cell Lines and Cell Culture

A detailed discussion of which cell lines were chosen, and why is included in section 5.3a (page 196).

2.3a Neonatal cardiac myocyte isolation and culture

Culture of neonatal cardiac myocytes has been documented previously [229, 435]. In brief, heart cells are isolated from 1-3 day old neonatal rat pups. Rat pups were sacrificed by administration of carbon dioxide anesthesia followed by decapitation with sharp scissors. The heart was quickly excised, the atria removed, and ventricular cells were dissociated mechanically and chemically via repeated (3x) (0.025%) DNase (w/v), (0.10%) collagenase (w/v), and (0.05%) trypsin (w/v) digestion. Each digestion was quenched with 20% FBS DMEM/F-12 media. Finally the isolated cells were differentially pre-plated (1h) to remove non-myocyte cells such as fibroblasts and then cultured at ~ 70-80% confluence (~1-2x10^6 cells/35mm dish) on primeria (BD Falcon) treated culture dishes at 37°C with 5% CO_2 in DMEM/F-12 plating media supplemented with 10% horse

serum (HS), 5% Fetal bovine serum (FBS), 50μg/ml gentamycin, 1% L-glutamine, and cytosine β-D-arabinofuranoside (to further minimize division of fibroblasts).

2.3b Neuronal N2A cell culture

Neuronal 2A cells (N2A) which are frequently used to study Cx biology due to their low expression of wildtype Cx proteins, shape, and ease of use were obtained from the American Type Culture Collection (ATCC). They were grown and maintained at 37°C in a 5% CO_2 incubator and cultured in Eagle Minimum Essential Medium with Earle's salts, non-essential amino acids and sodium bicarbonate (M-5650, Sigma Aldrich), supplemented with 1% glutamine, 1% penicillin-streptomycin (pen/strep), 1% sodium pyruvate, and 10% fetal bovine serum (FBS). Cells were maintained at ~30-70% confluence and split into subcultures as needed using 0.25% (w/v) Trypsin - 0.53 mM EDTA solution. Cells were frozen using standard media supplemented with 5% DMSO, and stored in liquid nitrogen vapor phase or -80°C freezer.

2.3c Hek293 Cell Culture Methodology

The Hek293 Flpin T-rex core kit was selected (Invitrogen, Burlington, ON, CAN) to allow the site specific integration of Cx40 and its mutants into a single genomic Flp recombinase (S.cerviseae) integration site (FRT) under the control of a tetracycline inducible promoter. Cells were graciously provided by Dr. Wayne Chen in collaboration with our laboratory. Cells were maintained in DMEM supplemented with 10% FBS, 1% pen/strep, and 1% non-essential amino acids. Zeocin (400μg/ml) was added to parental Hek293 cells prior to stable transfection and Hygromycin B (200μg/ml) was used for selection of stable colonies and maintenance of the same. A 24 hour pre-treatment with 1μg/mL tetracycline or doxycycline was used to induce expression prior to experimentation unless otherwise noted. Cells were maintained at ~30-90% confluence and split into subcultures as needed using 0.25% (w/v) Trypsin - 0.53 mM EDTA solution. Cells were frozen using 30% conditioned media with 60%

fresh standard media and 10% DMSO, and stored in liquid nitrogen vapor phase or -80°C freezer.

2.4 Cell and Tissue Collection and Preparation

Fresh tissue samples were collected by cutting small sections of tissue from the intact beating heart (LA appendage, LV apex and free wall). Remaining areas were clamped and/or sutured as needed, rinsed and the remainder stored in 2% formalin. The samples were snap frozen using a tissue clamp pre-chilled to the temperature of liquid nitrogen, and stored as needed at -80°C. Langendorf perfused hearts were freeze clamped whole as above while being perfused. When ready for processing - frozen tissue was powdered in a mortar and pestle pre-cooled to the temperature of liquid N_2, the powder was weighed and stored in sealed pre-chilled micro-centrifuge tubes – either under liquid N_2 (for immediate biochemical analysis) or at -80°C for longer term storage.

Cultured cells were rinsed with cold PBS (x2), then scraped in PBS (~250µL/10cm dish, or ~100µl/3cm dish), spun at ~16 000 x g (14,000 rpm) for 1 minute then snap frozen in liquid N_2 and stored at -80°C as necessary.

2.5 Sample Homogenization and Triton Soluble/Insoluble Fractionation.

Homogenates were generated by grinding tissue or cell pellet 2-3 times over 30 minutes in a glass Duall homogenizer on ice, with cell lysis buffer (modified AMPK cell lysis buffer) consisting of 20mM Tris HCl (pH 7.4), 50 NaCl, 50 NaF, 5 NaPyrophosphate and 250 Sucrose. This general lysis buffer was supplemented with 1% Triton X-100 detergent, or 1% Nonidet P40 detergent (NP40), as well as sigma mammalian protease inhibitor cocktail (1/1000), sigma phosphatase inhibitor cocktail I, and II (1/100), and di-thiothreitol (DTT) 1mM (from a frozen 1M stock). The resulting homogenate was subsequently centrifuged at ~16 000 x g for either 10 min (whole cell lysate) or 30 min for fraction separation. Total

triton soluble protein concentration was measured in the resulting supernatant by Bradford protein assay (Biorad, Hercules CA, USA).

The non-triton soluble (NTS) fraction pellet, containing plasma membrane bound gap junctional plaques, was re-suspended in a volume equal to that of the original supernatant containing the cytosolic fraction then either snap-frozen in liquid nitrogen or used for immunoprecipitation/western blotting as needed.

2.6 AMPK Activity.

The AMPK activity of 1µg total ventricular homogenate protein was determined by the *in vitro* incorporation of ^{32}P into the AMARA peptide for 5 minutes at 30°C as described previously [455]. Briefly, triton soluble whole cell homogenates (see section 2.4) were suspended in lysis buffer with 1% Triton X-100 or Nonidet-P40 (NP40) detergent (w/v) at 0.5µg/µl. 2µl of total cell homogenate was added to a reaction mixture (final volume, 25µl) composed of HEPES-NaOH (40mM) pH 7.0, NaCl (80mM), glycerol (8%, wt/vol), EDTA (0.8mM), AMARAASAAALARRR (AMARA) peptide (200µmol/l), dithiothreitol (0.8mM), [γ-^{32}P]ATP (200µmol/l), $MgCl_2$ (5mM), ±200µmol/l AMP, and 0.1% Triton X-100 or NP-40. This mixture was incubated for 5 min at 30°C. From this incubation mixture, 15µl were spotted on 1-cm^2 phosphocellulose paper. The paper was then washed four times for 10 min each with 150mM phosphoric acid, followed by a 5-min acetone wash. Papers were then dried and counted for radioactivity. AMPK activity was expressed as picomoles^{32}P incorporated in the AMARA peptide per minute per milligram protein.

2.7 Connexin immuno-precipitation and in vitro phosphorylation.

Cytosolic connexin and associated proteins were immuno-precipitated from fresh and/or frozen pig and rat left ventricle as per previous studies [118]. Briefly, whole cell homogenates were obtained (see section 2.4) by homogenizing ground and frozen tissue powder in modified AMPK lysis buffer

with 1% Nonidet-P40 (NP40) detergent. Triton soluble lysates were clarified by centrifugation at 10 000 x g for 10 minutes, whereas NT fractions were sonicated and re-suspended in an equal volume of lysis buffer, then pre-cleared with 20μl protein-A/G agarose (Santa Cruz) with 5μg normal goat IgG for 2h to overnight at 4°C. Immuno-precipitation of Cx protein was achieved by repeating the IP incubation using 5μg anti-Cx antibody (either Chemicon mouse anti-Cx 43, Zymed rabbit anti-Cx43, Chemicon rabbit anti-Cx40, Santa Cruz goat anti-Cx40) for 2h to overnight at 4°C.

2.8 Autoradiography.

IP samples were extensively washed (mixed by inversion) with high salt IP wash buffer (150mM NaCl) containing 1% NP-40 followed by 3 washes with PBS. IP beads were collected by gentle centrifugation at 1000 rpm for 1 minute following each wash. The washed IP samples were divided into 3 parts for western blot, and *in vitro* incubation with purified AMPK (Upstate Cell Signaling, rat liver AMPK). 4μg IP samples (in 2x assay buffer) were incubated in the presence and absence of 1μL purified AMPK with AMP at 30°C for 30 minutes (per the AMPK assay procedure in section 2.6). The incorporation reactions were stopped by adding 3x SDS sample loading buffer and boiled for 5 minutes. Samples were then separated by SDS- PAGE (10% gels). Coomassie blue stained gels were dried under vacuum 2h at 70°C in cellulose membrane and exposed to Kodak Biomax (MR) film with intensifying screen for 24-48 hours at -80°C.

2.9 **Western Blotting.**

As per the standard Laemelli SDS-Page technique [456] cell homogenates were combined with 5x sample loading buffer, when required NTS pellets were sonicated for 5 sec at an amplitude of 100% with a duty cycle of 1 using a UP50H sonicator (Hielscher - Ultrasound Technology) boiled for 5-10 minutes, cooled and spun to collect samples. Proteins were separated by 10% SDS-PAGE, gels were loaded with 30μg (unless otherwise noted) of protein per lane normalized

to the triton soluble protein concentration for each sample. Biorad precision plus dual color, and Invitrogen Magic Mark XP, molecular weight markers were used to assess the MW of identified bands and transfer efficiency. Separated proteins were transferred to nitrocellulose membrane (Biorad) by wet transfer usually overnight at 45V constant. The membranes were stained with Ponceau-S to qualitatively ensure equal protein loading and washed in 0.1% PBS-Tween20 (wash buffer). Membranes were blocked with 5% non-fat skim milk powder or 1% bovine serum albumin (BSA) (1 hour RT) and washed. Primary antibodies were diluted in PBS-T with 1% BSA and 0.01% sodium azide. 10mL of this solution was added to a 50mL centrifuge tube and membranes were incubated 2h at RT or overnight at 4°C on a rotator and then washed three times 5min PBS-T. Protein expression was measured using appropriate primary anti-bodies. Secondary antibodies were diluted in 1% milk PBS-T at 1:2000 dilution and incubated for 45min at RT. Membranes were further washed three times in PBS-T and once with PBS.

HRP conjugated secondary antibodies were visualized with ECL-plus (Amersham Biosciences, Piscataway, NJ, USA) and exposed to Kodak Biomax MR film (Fischer Scientific, Ottawa, ON, CAN). Fluorescence antibodies were imaged using a Licor Odyssey infrared scanner (LI-COR Biosciences, Lincoln, NB, USA). When required, membranes were stripped with 100mM 2-mercaptoethanol, 2% sodium dodecyl sulphate, 62.5mM Tris-HCl pH 6.7 for 30min at 50°C with occasional agitation (as per the Amersham protocol) for re-probing e.g. with rabbit anti-pan Actin (Sigma), mouse anti-Tubulin, mouse anti-golgin97 (Molecular Probes/Invitrogen) or mouse anti-αActin (Sigma) for loading comparisons as required. In some cases, total protein density was used as a loading control, as per Sheen et al. it is lonearly correlated with β-actin conventration between 10-40μg total protein [457, 458]. Densitometry was performed on scanned exposed films with the National Institutes of Health

ImageJ software suite (http://rsb.info.nih.gov/ij/), or via Licor Odyssey fluorescence imaging software where applicable.

2.10 Molecular Biology

2.10a Cloning and Expression of Cx40.

The human Cx40 gene was purchased from the American Type Culture Collection (ATCC) (genbank accession number BC013313) in the pOTB7 vector and isolated by PCR using:

Forward 5'-GGTACCACCATGGGCGATTGCAGC-3'
Reverse 5'- CTTAAGTCAGGCTTCTGGCCATAA -3'

PCR amplification was done using a Perkin Elmer DNA cycler (Waltham, MA, USA) with Platinum Pfx (Invitrogen) as per the manufacturer's instructions with 1 cycle at 95°C for 1min, followed by 29 cycles of 1 min 95°c, 1min 56°c, 2.4min 68°C. A portion of each PCR product was run on a 1% agarose (EtBr) gel to check for specific amplification. The resulting PCR product was incorporated into the pZeroBlunt vector using the pZeroBlunt TOPO cloning kit (Invitrogen) and sequenced (University of Calgary DNA Core Facility) to ensure that no mutations were incorporated into the coding sequence. The Cx40 sequence was cut out with EcoRI and NotI and directionally sub-cloned into the pTRACER vector (Invitrogen) for transient co-expression with GFP and initial screening studies. For stable transfection the Cx40 gene was then excised from the pTRACER vector using KpnI and NotI restriction sites and sub-cloned into the T-Rex pcDNA5/Frt/TO vector.

2.10b Cloning and Expression of Cx43.

Cx43 was also purchased from the ATCC (MGC-26323) (genbank accession number BC026329) in the pBluscript vector. The gene was isolated as with Cx40 by PCR using:

Forward 5'-GATATCACCATGGGTGACTGGAGCGCC-3'

Reverse 5'- GCGGCCGCCTAGATCTCCAGGTCATC -3'

These primers were designed to incorporate an EcoRV site at the 3'end of the gene and a NotI site at the 5' end of the gene for sub-cloning. As described for Cx40 the resulting PCR product was incorporated into the pZeroBlunt TOPO cloning vector. Due to earlier difficulties using the PCR product digested with EcoRV, and NotI, the Cx43 gene was incorporated into a TOPO vector by PCR cloning kit, then cut out with KpnI and NotI sites of the TOPO vector and directionally sub-cloned into the pTRACER vector (Invitrogen) for transient co-expression with GFP and initial screening studies. For stable transfection the Cx40 gene was then excised from the pTRACER vector using KpnI and NotI restriction sites and sub-cloned into the T-Rex pcDNA5/Frt/TO vector.

2.10c Transient Transfection of Cx Proteins.

Neuronal 2A cells (N2A) were cultured as described (see section 2.3) then transiently transfected for 24 hours with the pTRACER vector using Fugene 6 (Roche Diagnostics) as per the included protocols using 3:2 ratio (Fugene 6 µl: plasmid DNA µg) per 35mm dish. Transfection efficiency of up to 60% was measured visually based on co-expression of GFP. Expression of Cx40 and Cx43 were measured by western blot and functional activity was confirmed in a few limited cases by microinjection of membrane impermeable Alexa594 dye into one cell of a pair expressing GFP.

2.10d Generation of stable Cx40 and Cx43 Hek293 cells.

The Hek293 Flpin T-rex core kit was selected from Invitrogen (Burlington, ON, CAN) to allow the site specific integration of Cx40 or Cx43 into a single genomic Flp recombinase (S.cerviseae) integration site (FRT) under the control of a tetracycline inducible promoter. This cell line is the only commercially available with this system, and attempts were made to incorporate these modifications into N2A cells. These studies were unsuccessful and would have required a huge amount of resources, selection time, and verification to complete. Although Hek293 cells are reported to be 'communication deficient' they have been reported to express low endogenous levels of either Cx43 or Cx45 with some variability [372, 420, 459-461]. However, the relative influence of these endogenous Cx proteins was assumed to be very low when compared to the over expressed Cx40/43.

Cells were maintained as described in section 2.3, Zeocin (400μg/ml) was added to parental Hek-293 cells prior to stable transfection to ensure they contained the FRT integration site. A single sequenced plasmid clone of Cx40 or Cx43 was selected and transfected into Flpin T-Rex Hek-293 cells as per the Invitrogen instructions. Briefly ~0.5-1μg of plasmid DNA containing Cx40 or Cx43 was combined with 2-4μg of pOG44 DNA (expressing the Flp recombinase enzyme), diluted in serum free Opti-MEM media (Invitrogen) and transfected with Fugene 6 (Roche Diagnostics) into a 35mm dish containing Hek293 Flpin-Trex cells at ~40-60% confluence with normal growth media. 48 hours later the cells were trypsinized, and plated at lower density in a 10cm dish with media containing 200μg/ml Hygromycin B (the concentration previously determined to kill non-transfected Flpin T-Rex Hek293) and allowed to grow with media changes every 3-5 days until distinct colonies were identified and isolated by cloning cylinders or discs (Bel Art. Products, Sigma Aldrich). Cell clones were tested to be beta galactosidase negative (β-gal Staining Kit – Invitrogen) and they expressed Cx40 or Cx43 when induced with tetracycline/doxycycline (1μg/ml media).

2.10e Site directed mutagenesis of Cx40 Phosphorylation Sites.

The human hCx40 sequence, hereafter referred to as Cx40, was scanned for putative phosphorylation sites using the neural net program NetPhos2.0 [462] and NetPhosK [463] with a sensitivity of 100% and specificity of 40% for known PKA sites [464]. Cx40 mutations were made using the Quickchange II Site Directed Mutagenesis Kit (Stratagene Inc., La Jolla, CA, USA), using gel purified primers (Operon Biotechnologies Inc., Huntsville, AL, USA) per the manufacturer's instructions. Each mutant was sequenced to confirm the point mutation and ensure that there were no unwanted alterations in the Cx40 sequence.

2.11 Immuno-fluorescence.

Cells were plated on 0.1% gelatin, 12.5 μg/mL fibronectin coated 18x18mm coverslips (in a 6 well plate). Individual coverslips were rinsed in 37°C sterile PBS twice, followed by incubation with 4% fresh para-formaldehyde PBS for 30 minutes and rinsed twice in room temperature sterile PBS. Cells were permeabilized for 1 min (0.05% Triton X-100, 0.05% BSA in 1xPBS), then blocked with 5% FBS in PBS for 20 minutes. The cells were again rinsed with PBS, and the coverslip inverted onto a 200μL drop of primary antibody solution (on parafilm) for 2 hours at room temp. The coverslip was then returned to the 6 well plate for washing in PBS prior to another primary antibody or secondary antibody staining by the same technique. Cx antibodies were used at 0.2 μg/mL, Golgi organelles were stained with mouse anti-golgin97 primary antibody at 1:200.

Fluorescent conjugated secondary antibodies (Molecular Probes/Invitrogen) were used at 1:400 as required for dual or triple staining. The most common combinations were to use Alexa488 (green) conjugated antibodies to detect Cx proteins, Alexa594 (orange/red) conjugated anti-bodies to detect Golgi organelles. Following antibody staining the coverslip was again washed with PBS containing 0.5μM Hoechst 3342 (to stain nuclei blue) and then mounted on glass

slides using 1-2 drops of Prolong Gold anti fade solution (Molecular Probes/Invitrogen) and placed flat in the dark overnight for curing.

Slides were cleaned with Windex and visualized on a one of two microscopes. An LSM 510 confocal microscope (Carl Zeiss Inc. Peabody, MA, USA) equipped with a 488nm Argon laser (green), and 543nm HeNe laser (orange/red). Images were obtained at 63x magnification with an oil immersion lens (630x total magnification). Optical slices were obtained with spatial resolution of 0.14 x 0.14 x 1 μm (x, y, z) unless otherwise indicated.

As this microscope was not equipped to visualize nuclear staining, we also utilized a Leica DMRXA2 upright fluorescence microscope equipped with an Andor iXon+ DU-855k camera, and appropriate filters for Hoechst (DAPI), GFP (Alexa488) and Cy3 (Alexa594) fluorescence. Images were obtained at 1000x total magnification with an oil immersion lens (0.1 x 0.1 x 1μm resolution). For maximum resolution image stacks were obtained and processed using AutoDeblur Nearest Neighbor Deconvolution, and composite images were generated with IMARIS (Bitplane Scientific Software, South Windsor, CT, USA), and analyzed with ImageJ (for co- localization of image fluorescence).

2.12 Experimental Protocols – In vivo and Ex vivo Models

2.12a In vivo epicardial electrical mapping.

Surgical procedures were conducted in accordance with the regulations outlined in section 2.2, and have been described previously [465]. Briefly 10-week-old pigs (Landrace Yorkshire Cross) were anaesthetized. A temporary endocardial pacing catheter was inserted into the right atrium via the jugular vein. Arterial blood pressure, body temperature, and a five lead ECG were monitored throughout each experiment. Rapid pacing at 2 to 3 times the normal sinus rate of ~120 bpm for 3 hours (a rate sufficient to cause heart failure if maintained chronically [466, 467]) was used to mimic acute atrial fibrillation/ tachyarrhythmia presumably increasing ATP demand and stimulating AMPK as

observed in exercising skeletal muscle [468]. The time period was chosen because of the short (1-5 hours) half-lives of myocardial connexin proteins [118, 119, 123, 469, 470]. Immediately following the pacing protocol a median sternotomy was used to expose the surface of the heart for mapping studies.

Using a patented 'clock face' epicardial electrode mapping array developed in our lab - we were able to pace and record (16 kHz/channel) from any of 76 electrodes in an area ~0.5cm^2 with an inter-electrode distance of 210μm (see Figure 3-1). Electrograms were recorded during twice diastolic threshold pacing at an S1S1 interval of 260ms from the center electrode to determine activation times (peak dV/dt) and calculate longitudinal and transverse conduction velocity. The active properties of the myocardium were assessed during sinus rhythm by measuring the activation duration of inward membrane currents at 25% of its maximum value (I_{m25}) – a measurement of inward sodium channel activity that has been described previously [471, 472].

To assess the passive properties of conduction we measured the pacing threshold at various stimulus durations. The space constant (λ) was also calculated by the sub-threshold stimulus method outlined by Levine and Bonke [473] [474]. Briefly, sub-threshold rectangular depolarizing current pulses were delivered by a constant current source. The amplitude potential of the delivered pulse was measured sequentially by recording electrodes that are positioned every 420 μm up to a distance of 3990 μm. During the space constant determinations the heart was paced at a cycle length of 250-300ms (200-240 bpm) x10 beats (in order to avoid spontaneous activity and normalize the rate between animals), and the sub-threshold pulse was delivered late in diastole. The amplitude of the electrotonic potential is largest near the stimulating electrode, and declines exponentially with distance depending on the junctional coupling of the cells (tissue resistivity). The distance (λ) at which the amplitude is

decreased by 63.21% (1/e) was calculated by fitting each curve to an exponential equation [473].

2.12b Langendorf heart electrical mapping.

Hearts were isolated from adult Sprague Dawley rats under sodium pentobarbital anesthesia. The abdominal cavity was exposed and an ice-cold perfusion buffer was injected through the diaphragm to briefly arrest the heart. A median sternotomy was then performed to expose the heart for rapid excision. Following removal of the heart the aortic arch was cannulated and the heart was transferred to the Langendorf perfusion apparatus. The heart was perfused at a constant pressure of 75-80 mmHg from the aorta through the coronary circulation and out the coronary sinus. The temperature of the perfusate was continuously monitored and maintained at 37±0.5°C with the surrounding bath at ~36-37°C. Coronary flow-rates were monitored with Doppler flow probes (Transonic Systems, Ithaca, NY) and were approximately 7-15 ml/min with 60 mmHg constant pressure. Epicardial electrical mapping was achieved by placing the anterior surface of the left and right ventricles, or the posterior LV free wall on the mapping array.

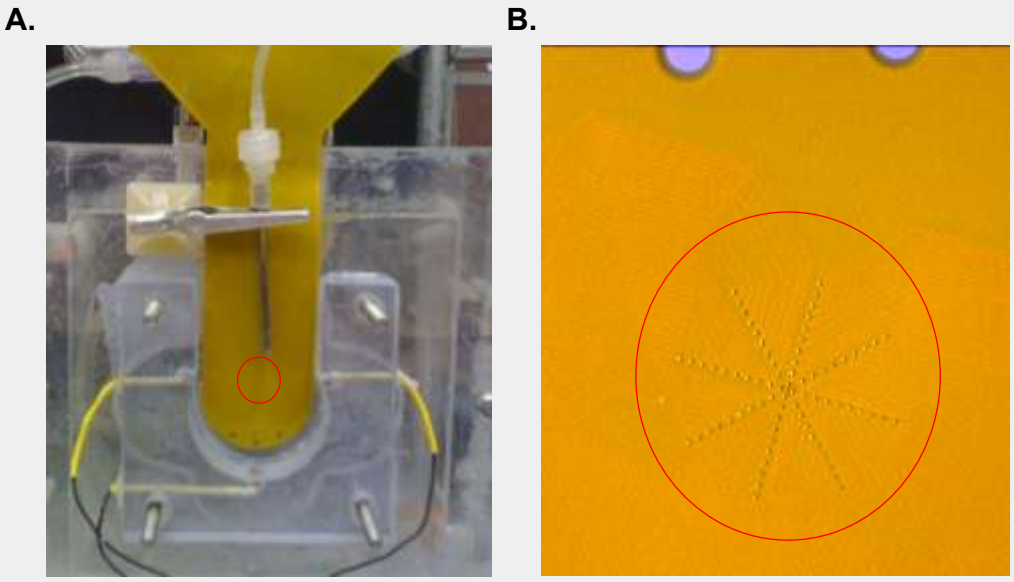

Figure 2-1. Custom built rat Langendorf perfusion apparatus.
A. Custom built Langendorf perfusion apparatus allowing recording of a volume conducted ECG, and situation of the heart on top of the electrical mapping array (red circle). **B.** Close up view of the mapping array used.

2.12c Four electrode technique.

The four electrode technique has been described previously [475-477]. In brief, 4 small plunge electrodes were placed in the LV free wall at ~1mm intervals. The exterior two electrodes were paced, and we measured the potential difference between the inner two electrodes - a measure of tissue impedance before, during and after treatment with the electrical uncoupler heptanol (5µM). The electrodes were built in our laboratory using 75µm Teflon coated platinum wire that had the ends exposed. The wires were mounted on a 200µm interval mesh support and set in place by epoxy. The resulting electrode array was then situated on the LV free wall, and the wires inserted into the muscle tissue to a depth of ~1-2mm. Electrical signals were recorded using the epicardial mapping array amplifier (as described in section 2.12a and b).

2.12d Optical mapping of Langendorf perfused rat hearts.

In vivo adenoviral gene transfer

In preparation for optical mapping of adenoviral infected rat hearts, we modified a technique for delivering adenovirus to the LV myocardium by direct myocardial injection [478, 479]. Surgery was completed under aseptic conditions in a class II laminar flow hood to prevent the spread of replication deficient adenovirus. Rats were anaesthetized using sodium pentobarbital (50 mg/kg i.p.) and intubated for ventilation. The chest cavity was entered using the left third intercostal space using a left lateral thoracotomy. The pericardium was opened and using a sterile 27ga needle with attached step syringe (to control the amount of fluid injected) ~20μL of tittered (~1-6 x10^{10} pfu/ml) adenovirus encoding GFP alone (negative control) or constitutively active $AMPK_{CA}$ was injected into a single location on the left ventricle. Any blood/air was removed from the chest cavity and a small chest tube was used to vent the chest during closure. The chest was sutured closed and the animal was extubated and returned to an observation cage for recovery. Total recovery/treatment time was 72 hours, during which time the animals were closely monitored. Post-surgery pain management was treated initially, and as needed, using buprenorphine analgesic. At the end of the recovery phase the animals were re-anaesthetized and the heart was excised as in the previous section for *in vitro* Langendorf mode perfusion and optical mapping.

Optical Mapping

Optical mapping procedures have been described previously [480-482]. Hearts were removed (as described in the previous section) and cannulated via the aorta in retrograde Langendorf perfusion. The area of infection was identified by using a GFP optical filter set (450-500nm bandpass excitation, 510-540nm bandpass emission), then a 75μm Teflon coated gold wire was inserted into the area (and at various locations in the field of view) for pacing. Hearts were perfused with voltage sensitive di-4ANNEPS (Molecular Probes/ Invitrogen) at 1/10 total coronary flow rate (10mL of 10x stock solution ~1μM final

concentration) to stain the epicardial membrane. Dye concentrations in excess of 1μM generally resulted in arrhythmia or poor function as described previously [483]. Following this infusion, the fungal toxin cytochalasin-D (which cleaves filamentous actin), was infused at a final concentration of 20μM to block contraction of the ventricle during electrical stimulation. This step is necessary to minimize motion artifacts in the optical signal. In certain experiments, the much less expensive electromechanical un-coupler butanedione monoxime (BDM) was used as a substitute.

Once properly stained, the area was paced with the subthreshold mapping train as in the previous electrical mapping studies (here we used a train of 5 S1 pacing stimuli, then one or two subthreshold stimuli 10-20ms duration, followed by a pause of 2 seconds).

Optical signals were analyzed using a custom software suite developed in MatLab v6.5 (Mathworks) as described in section 4.4. Conduction velocity [484], and the space constant of electrotonic coupling (λ) were calculated from measured parameters as previously described for the electrical mapping protocols.

2.13 Experimental Protocols – In vitro Cell Culture Models

2.13a Single Cell Dye Microinjection

Neonatal cardiac myocytes were isolated per section 2.3 and plated on 35mm glass bottomed microscopy dishes (Mattek, Ashland, MA, USA) pre-coated (0.1% gelatin, 12.5 μg/mL fibronectin to promote cell attachment. Cells were plated at 50-60% confluence 1-2x10^6 cells/dish, and allowed to grow for 2 days during which they were either untreated, or infected with 10moi adenovirus containing GFP, or $AMPK_{CA}$ as needed. Treatment with 2-deoxyglucose (5mM) plus oligomycin (5μM) was used to uncouple junctional conductance (presumably by inducing ATP depletion)[413]. During microinjection cells were placed in Tyrode solution containing (in mM) 140 NaCl, 5.4 KCl, 1 MgCl, 10 HEPES, 10 glucose, 1.8 $CaCl_2$, pH 7.4 (adjusted with 1M NaOH ~250μl/50ml). They were briefly treated with 5μM Hoechst 33342 for 5 minutes to stain the nuclei thus facilitating cell counting in the tightly confluent monolayers used.

Small bore (5-6 MΩ resistance) micropipettes were fashioned using an electrode puller. Settings were optimized for the production of long thin pointed injection pipettes ideal for piercing the myocyte plasma membrane. Injection was achieved using an Eppendorf Microinjection system equipped with micromanipulators for positioning of the electrode just above the cell to be injected. The system was also equipped with an automatically timed injection system that briefly plunged the electrode into the cell to be injected and simultaneously increased the pressure inside the microelectrode above the 32psi compensation pressure (preventing buffer uptake into the dye due to capillary action) for 30s to 1min. Injection time and pressures were optimized daily to minimize morphological changes in the injected cell and prevent cell rupture due to overloading. Following injection a diffusion time of 1-5 minutes allowed dye to pass through gap junction channels from the initial cell into its neighbors. Bright field, GFP, Dapi (Hoechst 33342), and CY3 (AlexaFluor 594) channel photographs were acquired in sequence to document the cell injected, whether it was

infected with virus, and how many cells were co-expressing Hoechst and AlexaFluor594).

2.13b Scrape Loading

Cells, including neonatal cardiac myocytes, were prepared as described in section 2.3. Cells were plated at $1x10^6$ cells/35mm dish and allowed to reach confluency for at least 24hours. Immediately prior to scraping, the media was replaced with 35°C CMF PBS (calcium and magnesium free PBS) containing membrane permeable Hoechst 33342 (5μM) to allow identification of cell numbers. Then rinsed and replaced with scrape loading media containing 10μL/ml AlexaFluor 594 (GJ permeable), and 0.5% FITC dextran (non-GJ-permeable). Cell monolayers were then scored in 3 parallel lines with a scalpel blade, and dye allowed to permeate the damaged cells for 2 minutes. The cells were then rinsed with warm CMF-PBS and fixed with 10% formalin for 30 minutes for subsequent imaging on a fluorescent microscope.

2.13c Dual Cell Patch Clamp

It is almost impossible to patch two cells at the same time when they are contractile, and connected together (although techniques such as actin filament cleavage via cytochalasin-d, or removal of intracellular calcium can be effective). To bypass this limitation, and for ease of use and culture, we elected to use non-contractile mammalian cell lines. N2A and Hek293 T-Rex cells were cultured as per section 2.3.

The MultiClamp system was purchased from Axon Instruments (Molecular Devices, LLC), and setup on a Zeiss Axiovert 200M microscope (Carl Zeiss Canada Ltd.) equipped with epifluorescent illumination for green fluorescent protein. Borosilicate glass microelectrodes at 3-5MΩ resistance were fabricated with a Sutter Instruments micropipette puller. Internal solutions were in mM KAsp 100, KCL 10, MgCl 5, NaATP 5, EGTA 10, HEPES 5, $CaCl_2$ 1 mM at pH 7.2.

Cells were maintained per section 2.3. Prior to experimentation, cells were trypsinized until pairs of cells were visible, then re-seeded at low density on glass coverslips pre-treated with 0.1% gelatin, 12.5 μg/mL fibronectin and allowed to re-attach and equilibrate for 4-12 hours prior to experimentation.

A gigaohm seal was attempted on the first of a cell pair. Upon successful seal, the second cell was approached, sealed, at which point both membranes would be ruptured. Numerous correction factors would be applied to these measurements to reduce series resistance artifacts etc. [485].

2.13d GapFRAP Dye Transfer.

Another method of measuring kinetics of dye transfer can be assessed by the GapFRAP technique with some modifications to the protocol described previously for Cx43 containing cells [372].

Hek293 cells were trypsinized and plated on pre-coated (0.1% gelatin, 12.5 μg/mL fibronectin) glass bottom dishes (MatTek). Cell density was optimized for the selection of cell pairs (~100 000 cells/ 35 mm dish). Immediately prior to imaging the cells were rinsed in Tyrode solution containing (in mM) 140 NaCl, 5.4 KCl, 1 MgCl, 10 HEPES, 10 glucose, 1.8 CaCl2, pH 7.4 (adjusted with 1M NaOH ~250μl/50ml). Cells were then exposed to 5 μM Cell Trace Calcein Blue AM (Molecular Probes/Invitrogen) for 5 min at RT. Used because it is a relatively small, neutrally charged dye, which is suitable for measuring both Cx40 or Cx43 conductance. Cells were rinsed in fresh Tyrode buffer and allowed to equilibrate for 3-5 minutes then transferred to the stage of a Zeiss NLO510 Multi-Photon Microscope (Carl Zeiss Canada Ltd.) system equipped with a Coherent Mira 900 femto-second Titanium Sapphire laser pumped with a 5W Verdi laser (Coherent Inc.) tuned to 740nm for optimal two photon excitation of the blue dye. Cells were visualized by using the 40x oil immersion lens and scanned at 0.2μs/pixel 1000x1000 pixels (0.1 x 0.1μm), with a standard frame time of ~900ms. The

pinhole of the detector was always maximally opened to allow us to record a large slice of the cell's cytoplasmic compartment with each scan.

Using the LSM Meta software - one cell of a pair was outlined and selected to be bleached. A pre-bleach scan was recorded using 3-5% transmittance of the 740nm laser line. The selected cell was bleached to ~30-50% of the initial fluorescence by repeatedly scanning the selected cell with 30 iterations at 100% laser transmittance. 20 subsequent scans were recorded at either 5s (Cx43) or 10s (Cx40) intervals to measure the rate of fluorescence recovery in the bleached cell.

In addition to GFP staining (indicating viral infection) cell pairs were chosen based on three main criteria wherever possible – 1. Non-symmetrical orientation (dividing cells are generally symmetrical). 2. Similar degree of joined membrane surface ~50% of the length of the cell. 3. Similar size and shape to each other. Equilibration gradient recovery curves were generated by calculating the ratio of the fluorescence in the bleached cell to the fluorescence in the recipient cell to correct for variations in the lighting, or amount of dye available to be transferred to the recipient cell. Ideally speaking with two cells of equal size, upon photo bleaching of the recipient cell, the fluorescence equilibrates to 40-50% of the original intensity. Exclusion criteria were set to remove any curves that exhibited (1) greater than 10% decline in fluorescence during the recovery phase (2) those that exceeded two standard deviations from the group mean at 30 seconds of recovery, and (3) curves that by artifact exceeded a ratio of more than 120%. Those that did were excluded from the analysis.

2.14 Modulation of AMPK Activity.

Modification of AMPK activity was achieved by adenoviral mediated expression of either a constitutively active ($AMPK_{CA}$) or dominant negative ($AMPK_{DN}$) adenovirus as described previously [435, 486] at a standard dosage of 1-5 moi

and compared to adenovirus containing GFP alone. AMPK activation was also achieved pharmacologically by treating cells for 2h with 1mM AICAR (forming a stable AMP analogue ZMP within the cell), or with 10mM phenformin as described previously [325, 326, 487].

2.15 Statistical Analysis.

Standard statistical analysis was performed using the SigmaStat 3.5, and SigmaPlot (version 9 and 12.5) software packages (Systat Software Inc., San Jose, CA).

For simple comparison of two group data the standard 'students two tailed t-test' with critical p-values <0.05 were used (e.g. to compare pacing versus control measurements of heart rate, conduction velocity, AMPK activity etc.).

Unless otherwise stated a two way repeated measures analysis of variance (ANOVA) with a post-hoc Holm-Sidak test for specific comparisons was used to test for statistically significant differences in repeated measurement data sets (e.g. pacing thresholds, sub-threshold decay curves, GapFRAP fluorescence recovery curves).

A one way analysis of variance (ANOVA) on ranks with post-hoc Dunn's analysis was used to quantify differences parameters which did not meet requirements for group normality (e.g. in quantification of immunofluorescence parameters).

2.16 Literature Cited

[118] Laird DW, Puranam KL, Revel JP. Turnover and phosphorylation dynamics of connexin43 gap junction protein in cultured cardiac myocytes. Biochem J. 1991;273(Pt 1):67-72.

[119] Beardslee MA, Laing JG, Beyer EC, Saffitz JE. Rapid turnover of connexin43 in the adult rat heart. Circulation research. 1998;83:629-35.

[123] Laing JG, Beyer EC. The gap junction protein connexin43 is degraded via the ubiquitin proteasome pathway. J Biol Chem. 1995;270:26399-403.

[229] Kovacic S, Soltys CL, Barr AJ, Shiojima I, Walsh K, Dyck JR. Akt activity negatively regulates phosphorylation of AMP-activated protein kinase in the heart. J Biol Chem. 2003;278:39422-7.

[325] Sakamoto K, Goransson O, Hardie DG, Alessi DR. Activity of LKB1 and AMPK-related kinases in skeletal muscle: effects of contraction, phenformin, and AICAR. Am J Physiol Endocrinol Metab. 2004;287:E310-7.

[326] Zhang L, He H, Balschi JA. Metformin and phenformin activate AMP-activated protein kinase in the heart by increasing cytosolic AMP concentration. American journal of physiology. 2007;293:H457-66.

[372] Cameron SJ, Malik S, Akaike M, Lerner-Marmarosh N, Yan C, Lee JD, et al. Regulation of epidermal growth factor-induced connexin 43 gap junction communication by big mitogen-activated protein kinase1/ERK5 but not ERK1/2 kinase activation. J Biol Chem. 2003;278:18682-8.

[413] Turner MS, Haywood GA, Andreka P, You L, Martin PE, Evans WH, et al. Reversible connexin 43 dephosphorylation during hypoxia and reoxygenation is linked to cellular ATP levels. Circulation research. 2004;95:726-33.

[420] Butterweck A, Gergs U, Elfgang C, Willecke K, Traub O. Immunochemical characterization of the gap junction protein connexin45 in mouse kidney and transfected human HeLa cells. J Membr Biol. 1994;141:247-56.

[435] Light PE, Wallace CH, Dyck JR. Constitutively active adenosine monophosphate-activated protein kinase regulates voltage-gated sodium channels in ventricular myocytes. Circulation. 2003;107:1962-5.

[455] Sakamoto J, Barr RL, Kavanagh KM, Lopaschuk GD. Contribution of malonyl-CoA decarboxylase to the high fatty acid oxidation rates seen in the diabetic heart. American journal of physiology. 2000;278:H1196-204.

[456] Laemmli UK. Cleavage of structural proteins during the assembly of the head of bacteriophage T4. Nature. 1970;227:680-5.

[457] Li R, Shen Y. An old method facing a new challenge: re-visiting housekeeping proteins as internal reference control for neuroscience research. Life sciences. 2013;92:747-51.

[458] Romero-Calvo I, Ocon B, Martinez-Moya P, Suarez MD, Zarzuelo A, Martinez-Augustin O, et al. Reversible Ponceau staining as a loading control alternative to actin in Western blots. Analytical biochemistry. 2010;401:318-20.

[459] Dang X, Jeyaraman M, Kardami E. Regulation of connexin-43-mediated growth inhibition by a phosphorylatable amino-acid is independent of gap junction-forming ability. Mol Cell Biochem. 2006;289:201-7.

[460] Gemel J, Lin X, Veenstra RD, Beyer EC. N-terminal residues in Cx43 and Cx40 determine physiological properties of gap junction channels, but do not influence heteromeric assembly with each other or with Cx26. Journal of cell science. 2006;119:2258-68.

[461] Lin X, Gemel J, Beyer EC, Veenstra RD. Dynamic model for ventricular junctional conductance during the cardiac action potential. American journal of physiology. 2005;288:H1113-23.

[462] Blom N, Gammeltoft S, Brunak S. Sequence and structure-based prediction of eukaryotic protein phosphorylation sites. Journal of molecular biology. 1999;294:1351-62.

[463] Blom N, Sicheritz-Ponten T, Gupta R, Gammeltoft S, Brunak S. Prediction of post-translational glycosylation and phosphorylation of proteins from the amino acid sequence. Proteomics. 2004;4:1633-49.

[464] Huang HD, Lee TY, Tzeng SW, Horng JT. KinasePhos: a web tool for identifying protein kinase-specific phosphorylation sites. Nucleic acids research. 2005;33:W226-9.

[465] Kavanagh KM, Guerrero PA, Jugdutt BI, Witkowski FX, Saffitz JE. Electrophysiologic properties and ventricular fibrillation in normal and myopathic hearts. Canadian journal of physiology and pharmacology. 1999;77:510-9.

[466] Balaji S, Hewett KW, Krombach RS, Clair MJ, Ye X, Spinale FG. Inducible lethal ventricular arrhythmias in swine with pacing-induced heart failure. Basic Res Cardiol. 1999;94:496-503.

[467] McElmurray JH, Mukherjee R, Patterson TM, Goldberg A, King MK, Hendrick JW, et al. Comparison of amlodipine or nifedipine treatment with developing congestive heart failure: effects on myocyte contractility. JCard Fail. 2001;7:158-64.

[468] Stephens TJ, Chen ZP, Canny BJ, Michell BJ, Kemp BE, McConell GK. Progressive increase in human skeletal muscle AMPKalpha2 activity and ACC phosphorylation during exercise. Am J Physiol Endocrinol Metab. 2002;282:E688-94.

[469] Saffitz JE, Laing JG, Yamada KA. Connexin expression and turnover : implications for cardiac excitability. Circulation research. 2000;86:723-8.

[470] Salameh A. Life cycle of connexins: regulation of connexin synthesis and degradation. Advances in cardiology. 2006;42:57-70.

[471] Witkowski FX, Kavanagh KM, Penkoske PA, Plonsey R. In vivo estimation of cardiac transmembrane current. CircRes. 1993;72:424-39.

[472] Witkowski FX, Plonsey R, Penkoske PA, Kavanagh KM. Significance of inwardly directed transmembrane current in determination of local myocardial electrical activation during ventricular fibrillation. CircRes. 1994;74:507-24.

[473] Levine JH, Moore EN, Weisman HF, Kadish AH, Becker LC, Spear JF. Depression of action potential characteristics and a decreased space constant are present in postischemic, reperfused myocardium. JClin Invest. 1987;79:107-16.

[474] Bonke FI. Passive electrical properties of atrial fibers of the rabbit heart. Pflugers Arch. 1973;339:1-15.

[475] Steendijk P, Mur G, van der Velde ET, Baan J. The four-electrode resistivity technique in anisotropic media: theoretical analysis and application on myocardial tissue in vivo. IEEE TransBiomedEng. 1993;40:1138-48.

[476] Padilla F, Garcia-Dorado D, Rodriguez-Sinovas A, Ruiz-Meana M, Inserte J, Soler-Soler J. Protection afforded by ischemic preconditioning is not mediated by effects on cell-to-cell electrical coupling during myocardial ischemia-reperfusion. American journal of physiology. 2003;285:H1909-16.

[477] Baynham TC, Knisley SB. Effective epicardial resistance of rabbit ventricles. AnnBiomedEng. 1999;27:96-102.

[478] Guzman RJ, Lemarchand P, Crystal RG, Epstein SE, Finkel T. Efficient gene transfer into myocardium by direct injection of adenovirus vectors. Circulation research. 1993;73:1202-7.

[479] Hajjar RJ, Schmidt U, Matsui T, Guerrero JL, Lee KH, Gwathmey JK, et al. Modulation of ventricular function through gene transfer in vivo. Proceedings of the National Academy of Sciences of the United States of America. 1998;95:5251-6.

[480] Nygren A, Clark RB, Belke DD, Kondo C, Giles WR, Witkowski FX. Voltage-sensitive dye mapping of activation and conduction in adult mouse hearts. AnnBiomedEng. 2000;28:958-67.

[481] Witkowski FX, Leon LJ, Penkoske PA, Giles WR, Spano ML, Ditto WL, et al. Spatiotemporal evolution of ventricular fibrillation. Nature. 1998;392:78-82.

[482] Witkowski FX, Clark RB, Larsen TS, Melnikov A, Giles WR. Voltage-sensitive dye recordings of electrophysiological activation in a Langendorff-perfused mouse heart. CanJCardiol. 1997;13:1077-82.

[483] Nygren A, Kondo C, Clark RB, Giles WR. Voltage-sensitive dye mapping in Langendorff-perfused rat hearts. American journal of physiology. 2003;284:H892-902.

[484] Guo Q, Mandal MK, Liu G, Kavanagh KM. Cardiac video analysis using Hodge-Helmholtz field decomposition. Computers in biology and medicine. 2006;36:1-20.

[485] Xin L, Gong XQ, Bai D. The role of amino terminus of mouse Cx50 in determining transjunctional voltage-dependent gating and unitary conductance. Biophys J. 2010;99:2077-86.

[486] Woods A, Azzout-Marniche D, Foretz M, Stein SC, Lemarchand P, Ferre P, et al. Characterization of the role of AMP-activated protein kinase in the regulation of glucose-activated gene expression using constitutively active and dominant negative forms of the kinase. Mol Cell Biol. 2000;20:6704-11.

[487] Woollhead AM, Scott JW, Hardie DG, Baines DL. Phenformin and 5-aminoimidazole-4-carboxamide-1-beta-D-ribofuranoside (AICAR) activation of AMP-activated protein kinase inhibits transepithelial Na+ transport across H441 lung cells. The Journal of physiology. 2005;566:781-92.

Chapter 3 Alterations in cardiac gap junctional communication by rapid pacing: activation of AMPK, arrhythmia induction and altered electrophysiological substrate - implications for stress activated arrhythmia formation.

This thesis chapter is an original work by Jason Iden.
Portions of this chapter have been previously published in abstract form.

***Iden, JB.**, Liu, G., Kovithavongs, K., Kavanagh, KM. Phosphorylation of Connexin 43 by AMP Activated Protein Kinase (AMPK): Implications for Stress Activated Arrhythmia Formation. Circulation 108(17) Supplement IV-240. 2003.*

***Iden, JB.**, Liu, G., Kavanagh, KM. AMPK and the passive properties of myocardial conduction. Canadian Journal of Cardiology 18: Supplement 197B. 2002.*

Surgical procedures were carried out by Jason Iden with assistance from Dr. Gang Liu.

3.1 Introduction

Although much is known about the regulation of myocardial metabolism, and its importance in ischemic heart disease and heart failure with respect to increasing energy supply and reducing energy demand, at this point there is little known about how these same pathways are linked to the regulation of cardiac electrophysiology. Thus our goal is to examine the importance of energy sensing and its potential role in generating an arrhythmogenic substrate using acute supraventricular tachycardia as a model of increased energy demand in the absence of structural heart disease.

3.1a Energy Sensing and the Regulation of Cardiac Metabolism.

AMP-activated protein kinase (AMPK) is a rapidly activated energy sensor stimulating adenosine tri-phosphate (ATP) production in response to the accumulation of ADP and AMP (from the use of ATP and the conversion of 2(ADP) $\leftrightarrow$ ATP + AMP). This is accomplished via phospho-regulation of glycolysis, glucose uptake, and fatty acid oxidation rates [255, 423]. AMPK has also been shown to reduce energy consumption by multiple pathways including phospho-inhibition of the mTOR (mammalian target of rapamycin) pathway inhibiting protein synthesis, activation of autophagy pathways, inhibition of fatty acid biosynthesis, and phosphorylation of various other downstream targets [239, 310, 488-491]. Thus, due to the influence of the AMPK cascade, the proteins and systems underlying normal cardiac electrophysiology can be affected by both relatively rapid transcriptional (hours) and very rapid (seconds) phosphorylation mediated regulation. The following sections will outline the potential regulation of electrophysiology by situations that activate AMPK.

3.1b AMPK activity in Cardiomyopathies

To various extents ischemic heart disease and heart failure are associated with an imbalance between ATP supply and demand causing a decrease in the ATP:AMP/ADP ratio and activation of the AMPK cascade [209, 211, 303]. In some

cases reduced coronary flow limits the supply of oxygen and metabolic substrates relative to myocardial demand in localized regions, with mild angina and myocardial infarction representing a range of the possible scenarios. In these regions, myocardial metabolism is impaired, and in most cases the electrophysiological substrate in the ischemic area is affected by altered expression, density, conductance, and distribution of gap junctions and ion channels leading to an arrhythmogenic substrate [206-208, 210, 492-497]. This can often trigger cardiac tachyarrhythmias either by forming reentrant circuits, or by the generation of spontaneous automatic activity within this region. However, the non-uniformity of the region of ischemia/infarction makes each case unique. It also leads to alterations in numerous other pathways that can significantly complicate the interpretation of changes to junctional coupling (eg. low flow means greater accumulation of lactate/low pH). As such, a much simpler model is desirable.

Tachyarrhythmias can be defined by their site of origin as being either supra-ventricular (atrial tachycardia, atrial fibrillation) or ventricular in nature (ventricular tachycardia, ventricular fibrillation). But in general they result in faster than normal ventricular rates (even when atrial in origin ventricular rates of >200 bpm are not uncommon). In these cases, the metabolic demands of the entire heart increase significantly. This increased demand is combined with a reduced duration of diastole which in turn reduces coronary blood flow and thus nutrient/oxygen supply to the heart, potentially exacerbating the problem. Mimicry of this phenomenon by rapid pacing allows us to minimize the potential for non-uniform ischemia driven changes, and focus on the more global and homogeneous increase in metabolic demand and decrease in relative oxygen/nutrient supply that increase AMPK activity in the same way as a de novo tachyarrhythmia would.

It is well documented that the persistence of these tachyarrhythmias can contribute to structural remodeling of both the atria and ventricle and the formation of cardiomyopathies over extended time periods [3, 498-501]. Structural remodeling can include fibrosis, hypertrophy, and dilatation resulting in congestive heart failure which is often associated with lethal ventricular arrhythmias estimated to kill 30 000 Canadians annually [1-5]. However, the persistence, and re-occurrence of these arrhythmias are thought to be dependent on rapid electrical remodeling induced by the tachyarrhythmia itself. It is this early phase of electrical remodeling that is the focus of these studies.

3.1c Short term electrical remodeling: tachyarrhythmias beget tachyarrhythmias.
Atrial fibrillation (AF) is the most common clinical arrhythmia. As mentioned previously, this tachyarrhythmia exhibits longer term electrical and structural remodeling, however the short term effects on electrophysiology are not well understood. What is known is that, in animal models, within a very short time (1 day), once AF is induced the duration is strongly correlated with the likelihood and duration of re-occurrence, and negatively associated with successful cardioversion [502]. Clinically this is confirmed as longer durations of AF lead to increased likelihood of re-occurrence despite treatment. Since metabolic demand presumably increases rapidly with tachyarrhythmia, and AMPK is a rapidly activated energy sensor that can phosphorylate many downstream targets, and/or rapidly reduce protein expression to save energy; it follows that this pathway may be a common factor that can induce the electrical remodeling observed with tachyarrhythmia. The numerous possible targets of this remodeling include ion channels and the gap junctional channels that connect myocardial cells electrically.

3.1d Atrial Tachyarrhythmias reduce the Wavelength of Activation.
Tachyarrhythmia dependent electrical remodeling appears to reduce the wavelength of activation. Where wavelength is normally defined as a coefficient

of refractory period multiplied by conduction velocity – i.e. shorter refractory periods with slower conduction velocity = shorter wavelength.

This means that when an activation wave propagates it moves more slowly, and there is a shorter margin of safety (less time between the end of the refractory period and the wave front) preventing re-activation. Ultimately there is a greater chance that a wave can form a reentrant circuit arrhythmia (the most common mechanism of tachyarrhythmia).

There is already some evidence that electrical remodeling during longer term atrial fibrillation reduces the refractory period of atrial tissue in a heterogeneous manner [499, 502]. However, if combined with a reduction in junctional conductance or reduced sodium channel activity (which can also reduce conduction velocity) the arrhythmic potential will be amplified. In support of this relationship, it has been shown that some gap junctional proteins are reduced or re-distributed with prolonged AF [503-506], and mutations in junctional genes have also been implicated in the formation of idiopathic AF [507]. Since any change in the expression or distribution of gap junctions have already been shown to increase arrhythmogenic potential (for example with hypertrophy, and ischemic heart disease)[508-515], in combination, these observations imply that gap junctions may be a prime target in tachycardia induced electrical remodeling leading to an arrhythmogenic substrate. The following sections will outline gap junctional physiology and their potential modes of regulation.

3.1e Cardiac Gap Junctions.

For detailed summary see Chapter 1, section 1.3. Gap junctions are formed by connexin (Cx) proteins including Cx43, 40, 45 each of which are expressed in a specific pattern in the human heart. These Cx proteins have an extremely short half-life (relative to other integral membrane proteins) estimated at 1-5 hours [118, 119, 123, 469, 470]. Their activity is dependent on both their characteristic conductance (which can be regulated acutely by phosphorylation/protein

interaction/pH etc.), as well as by their expression at the cell-cell border which is determined by an equilibrium between rates of expression/transport, and rates of protein internalization and degradation [111, 113, 128, 470, 516]. As mentioned previously, different cardiac tissues have specific connexins expressed resulting in their characteristic electrophysiological properties. The relative conductance of the cardiac connexin proteins are ranked Cx43 >> Cx40 > Cx45 [28].

In general it has been shown that increasing expression of Cx40 relative to Cx43 results in slower conduction velocity indicating that as might be expected the relative expression of each type of subunit will determine the overall speed of conduction and degree of junctional coupling [517]. As such it is not surprising that Cx40 and Cx45 are expressed in the specialized conducting pathways including the sinoatrial node and atrioventricular node that are characterized by slow conduction [106, 430]. Cx43 is expressed throughout the ventricular and atrial myocardium, as well as in the purkinje fibers. In these areas it is responsible for the rapid propagation of a conduction wavefront. This coupling is reduced in the atria due to increased overall Cx40 expression throughout the tissue.

The proper function, expression and distribution of these specific Cx proteins is important for proper electrical conduction in the heart, and alterations in either their function or expression is again commonly associated with cardiac arrhythmias or a pre-disposition for them [36-42].

3.1f Potential Phosphorylation of Connexins by AMPK.

Cardiac GJ function is profoundly affected by phosphorylation resulting in altered expression, trafficking, conductance, and stability/degradation [117, 347, 348]. We identified putative AMPK (α1,2) phosphorylation sites [423] in three cardiac GJ subunits: at residue t118 in the cytoplasmic loop region of Cx43, at t18, and t36 within the N-terminal region of Cx45, and at t19 in the N-terminal region,

s122 in the cytoplasmic loop region, and at s349 in the C-terminal region of Cx40. This implies that all the commonly recognized junctional proteins may be affected by AMPK phosphorylation.

Here we test the hypothesis that acute (3 hour) atrial pacing will increase the metabolic load on the heart, stimulate AMPK activity and rapidly induce alterations in the gap junction mediated properties of cardiac electrophysiology leading to an arrhythmogenic substrate (prior to the structural re-modeling induced by long term rapid pacing that has been previously described).

3.2 Materials and Methods

3.2a Rapid Pacing Model.

Surgical procedures have been described previously [465]. See section 2.2, and 2.12a for detailed methods. Briefly 10-week-old pigs were anaesthetized. A temporary endocardial pacing catheter was inserted into the right atrium via the jugular vein. Rapid pacing at 2 to 3 times the normal sinus rate of ~120 bpm for 3 hours (a rate sufficient to cause heart failure if maintained chronically [466, 467]) was used to mimic acute atrial fibrillation/tachyarrhythmia presumably increasing ATP demand and stimulating AMPK as observed in exercising skeletal muscle [468]. The time period was chosen because of the short (1-5 hours) half-lives of myocardial connexin proteins [118, 119, 123, 469, 470]. Immediately following the pacing protocol a median sternotomy was used to expose the surface of the heart for mapping studies.

3.2b Epicardial Mapping.

Using a patented 'clock face' epicardial electrode mapping array and the methods described in section 2.12a, we measured activation times, calculated longitudinal and transverse conduction velocity, measured I_{m25} to assess sodium channel activity. We also calculated pacing thresholds, and the space constant (λ) to assess the passive properties of the LV. Per section 2.12a, the amplitude of the electrotonic potential is largest near the stimulating electrode, and declines exponentially with distance depending on the junctional coupling of the cells (tissue resistivity). The distance (λ) at which the amplitude is decreased by 63.21% (1/e) was calculated by fitting each curve to an exponential equation [473].

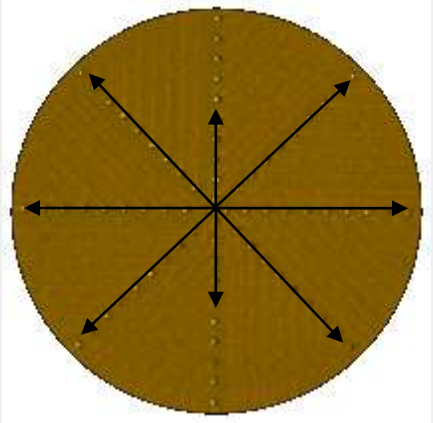

Figure 3-1. Epicardial mapping array with 210μm inter-electrode

3.2c AMPK Activity.

The AMPK activity of 1μg total ventricular homogenate protein was determined by the *in vitro* incorporation of ^{32}P into the AMARA peptide for 5 minutes at 30°C as described previously in section 2.6 [455].

3.2d Triton Soluble/Insoluble Fractionation.

Myocardial tissue samples were isolated as described in section 2.4 and separated for triton soluble (TS) vs. non-triton soluble (NTS) fractions, and total triton soluble protein concentration was measured by Bradford protein assay (Biorad, Hercules CA, USA).

3.2e Immuno-precipitation and in vitro phosphorylation.

Cytosolic Cx43 and its associated proteins were immuno-precipitated from fresh and/or frozen pig and rat left ventricle homogenate per section 2.7 in modified AMPK lysis buffers with sigma mammalian protease inhibitor cocktail, and 1% Nonidet-P40 detergent. Immuno-precipitation of Cx43 was achieved using 5μg anti-Cx43 antibody (Chemicon mouse anti-Cx 43, or Zymed rabbit anti-Cx43).

3.2f Autoradiography.

Per section 2.8, IP samples were extensively washed with high salt IP wash buffer (150mM NaCl) containing 1% NP-40 followed by 3 washes with PBS. IP beads were collected and divided into 3 parts for western blot, and *in vitro* incubation with purified AMPK (Upstate Cell Signaling). IP samples were incubated in the presence and absence of 1μL purified AMPK at 30°C for 30 minutes. The incorporation reactions were stopped by addition of SDS sample loading buffer, boiling, then separated by SDS- PAGE (10% gels). Coomassie blue stained gels were dried under vacuum and exposed to Kodak Biomax (MR) film with intensifying screen for 24-48 hours at -80°C.

3.2g Western Blotting.

Following the techniques outlined in section 2.9, and using commercial antibodies from Cell Signaling Technologies (New York, USA) cytosolic phospho-AMPK at threonine 172 (product #2531) versus total AMPK (product #2532) was measured to further examine AMPK activation by rapid pacing. Connexin expression was assessed in both triton soluble and insoluble fractions using antibodies for ventricular connexin 43 (Chemicon MAB3067, Temecula CA, USA and Zymed/Invitrogen 71-0700, Carlsbad, CA, USA)) and connexin 40 (Santa Cruz Biotechnology SC-20466, Santa Cruz, CA) for left ventricular and left atrial expression respectively. Expression of α-tubulin (Cell Signaling #2125S) was used to normalize for slight differences in loading.

3.2h Statistical Analysis.

Standard students two tailed t-test with critical p-values <0.05 were used to compare pacing versus control measurements of heart rate, conduction velocity, AMPK activity, and western blot quantifications (Sigma Stat 3.5). A two way repeated measures analysis of variance (ANOVA) with a post-hoc Holm-Sidak test for specific comparisons was used to test for statistically significant differences in pacing thresholds and sub-threshold decay curves.

3.3 Results

Heart rates for the non-paced animals were 116.1 ± 7.6 (mean ± SEM) versus 286.4 ± 5.8 bpm for the duration of pacing (animals were paced close to 300 bpm depending on AV conduction properties and the rate at which 1:1 conduction failed). Following rapid atrial pacing for 3 hours we mapped the LV epicardial surface to assess its active and passive electrophysiological properties.

3.3a Rapid Atrial Pacing for 3 hours increased the incidence of arrhythmia.
In this model – rapid atrial pacing for 3 hours markedly increased the incidence of spontaneous cardiac arrhythmias versus the non-paced control animals. In fact 5/10 rapidly paced animals developed atrial or ventricular tachyarrhythmia during or following the pacing period (see Figure 3-2) which were not observed in the control group (0/7).

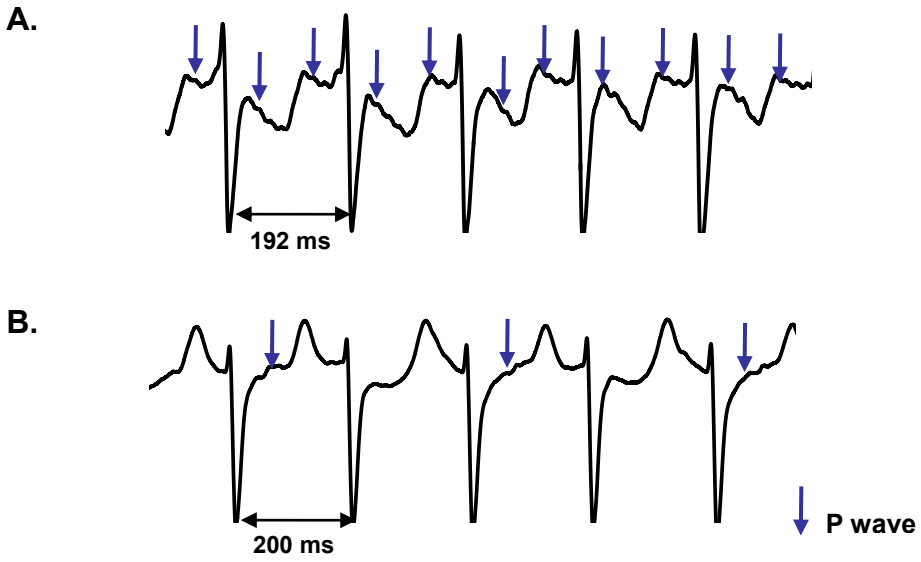

Figure 3-2. Spontaneous atrial and ventricular tachyarrhythmia induced by rapid atrial pacing.
A- Lead III ECG recording of an atrial tachyarrhythmia characterized by multiple p-waves (indicated by vertical arrows) for each QRS beat. **B-** Ventricular tachyarrhythmia characterized by multiple ventricular activations for each p-wave.

3.3b Rapid Atrial Pacing increases pacing threshold.

The mean pacing stimulus thresholds tended to increase for all stimulus durations i.e. more current was required to successfully capture and propagate an excitation wave (see Figure 3-3). Because successful pacing is normally dependent on the excitation of a critical area of membrane above its excitation threshold it would indicate that there is greater impedance to current in the paced animals or that the excitability of the membrane was in some way compromised.

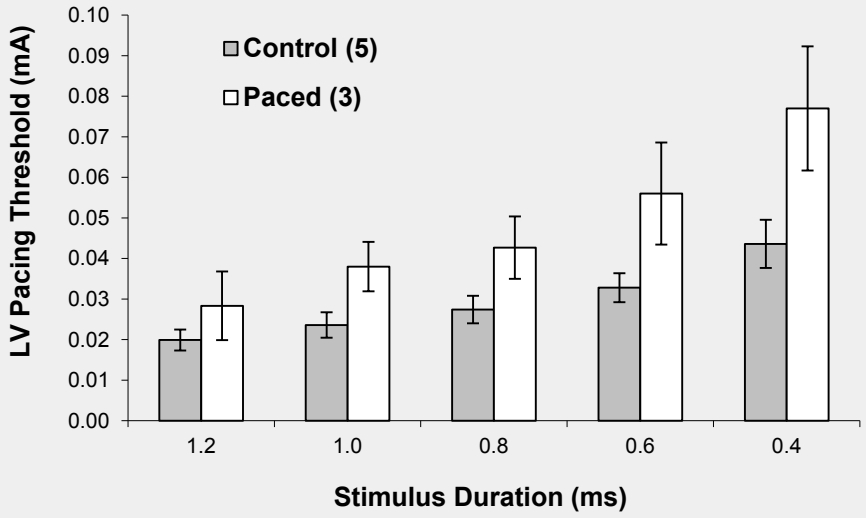

Figure 3-3. LV pacing thresholds tended to increase following 3h rapid atrial pacing. Increased LV pacing thresholds (mean ± SEM) during epicardial mapping suggest that gap junctional conductance is reduced. Sample size (n) is indicated in the legend.

In order to examine this phenomenon we measured ventricular Im_{25} during sinus rhythm (as described previously by Witkowski *et al.* [471]). Im_{25} measures the delay from the point of peak transmembrane current, to its voltage dependent inactivation (return to baseline, orange arrow in Figure 3-4A). This measurement is linearly correlated with measured inward sodium current activation/duration [471], and in the original paper it was delayed by I_{Na} inhibition via KCL infusion (Figure 3-4B). In our model, the Im_{25} tended to be reduced (p=0.14) by rapid pacing (see Figure 3-4C) this would indicate that

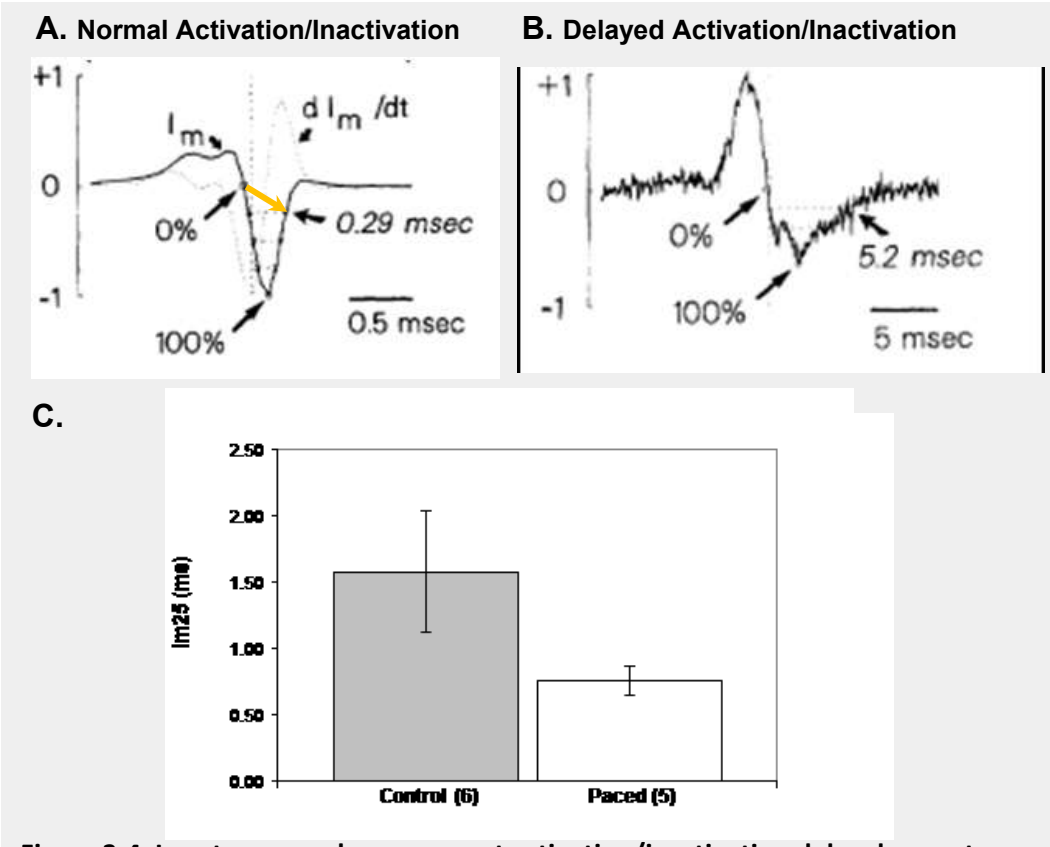

Figure 3-4. Im_{25} transmembrane current activation/inactivation delay does not increase following rapid atrial pacing for 3 hours.
A-B. Representative Im_{25} calculation (from Witkowski FX, *et al. CircRes.* 1993;72:424-39). **A-** Im_{25} is the delay between peak transmembrane current to its voltage dependent inactivation by membrane depolarization. The time between onset (0%) and return to 25% of total current is 0.29ms (arrow). A decrease in this interval indicates faster activation and thus inactivation. **B.** Im_{25} increases with KCL infusion (from 0.3 to 5ms). **C.** Im25 (mean ±SEM) is not significantly altered by rapid pacing for 3 hours, but it tended to decrease. This indicates that sodium channel activity is enhanced or unchanged by rapid pacing. Sample sizes are indicated (n) Paced versus control p=0.14.

sodium channel currents were either up regulated or unchanged in this model. Thus, the increase in pacing threshold observed (in Figure 3-3) probably reflects a change in cellular coupling rather than a decrease in membrane excitability.

3.3c Sub-threshold stimuli decay faster in the paced animals.

When a sub-threshold stimulus was given late in diastole its amplitude appears to be reduced following rapid pacing with increasing distance from the pacing site. This again indicates that junctional coupling was somewhat impaired (see Figure 3-5). This was confirmed using the more accurate technique of calculating

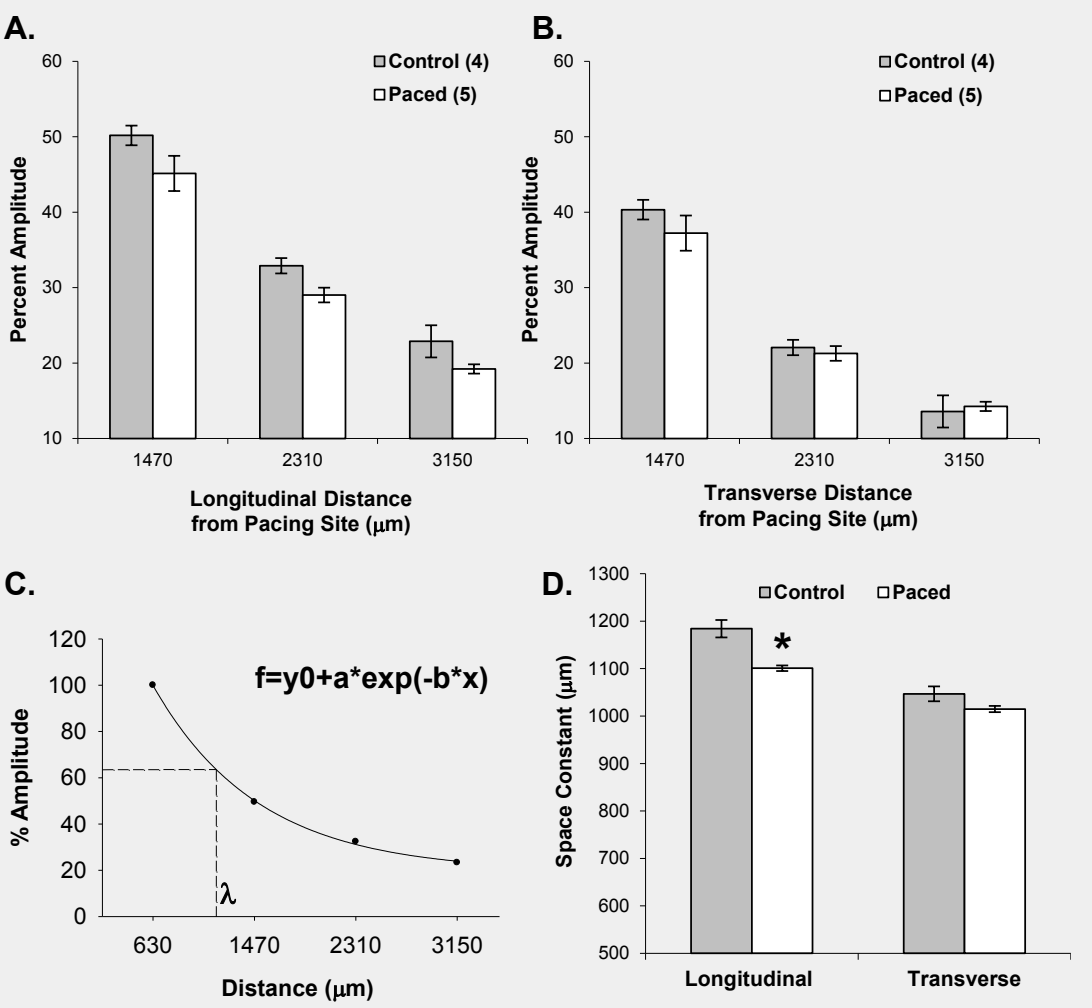

Figure 3-5. Tissue resistivity tends to increase in the rapidly paced animals.
A- Subthreshold stimulus amplitude tends to decline faster in the rapidly paced animals with increasing distance from the pacing site in the longitudinal direction (along the axis of the myocytes) as well as in the B- transverse direction. C- When the individual data is plotted and fit with an exponential decay curve the space constant (λ) is calculated as the distance at which the amplitude decays 63.21% (1/e). D- Following rapid atrial pacing junctional coupling is inhibited the longitudinal direction (*p<0.05) and tended to be lower in the transverse direction..

the space constant, where amplitudes are measured at the same time and fit to curve prior to λ averaging. Based on this technique it is apparent that there is a reduction in longitudinal coupling and a trend to be reduced in the transverse direction. The values we have observed are similar to the predicted ~1mm constant based on classical cable theory [518] as expected. They are also similar to previously reports of ~1500, 800μm in the longitudinal and transverse directions respectively [519].

3.3d Conduction velocity is unchanged.

Despite the increased LV pacing threshold and reduced LV sub-threshold amplitude and space constant there was no significant change in the propagation speed of an activation wavefront between the paced and control animals (see Figure 3-6). In fact there is a slight trend to indicate that conduction velocity may be increased in the longitudinal direction. Based on the reduced junctional coupling in the longitudinal direction this would again indicate that there may be an up regulation of sodium current in these animals as suggested by the Im_{25} measurement. However, even if this were not the case, it is also known from transgenic animals that a reduction of almost 50% in Cx43 in the heterozygous knockouts does not reduce junctional conduction velocity despite their increased susceptibility to arrhythmias [32, 61]. Thus, as with the transgenic models, a reduction in junctional conductance may be contributing to arrhythmia formation here, even in the absence of a change in conduction velocity.

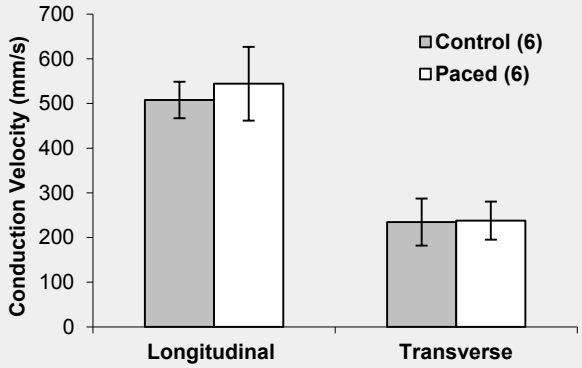

Figure 3-6. Left ventricular conduction velocity was not affected by 3 hours of rapid atrial pacing.

3.3e Rapid Pacing activates AMPK.

The level of threonine-172 phosphorylated (active) α AMPK was increased in the left ventricle by rapid atrial pacing (see Figure 3-7BC). This was correlated with increased activity of AMPK, as measured by ^{32}P incorporation, in the paced animals (see Figure 3-7A), particularly immediately after pacing. With prolonged mapping duration the heart tended to recover over time as would be expected (data not shown).

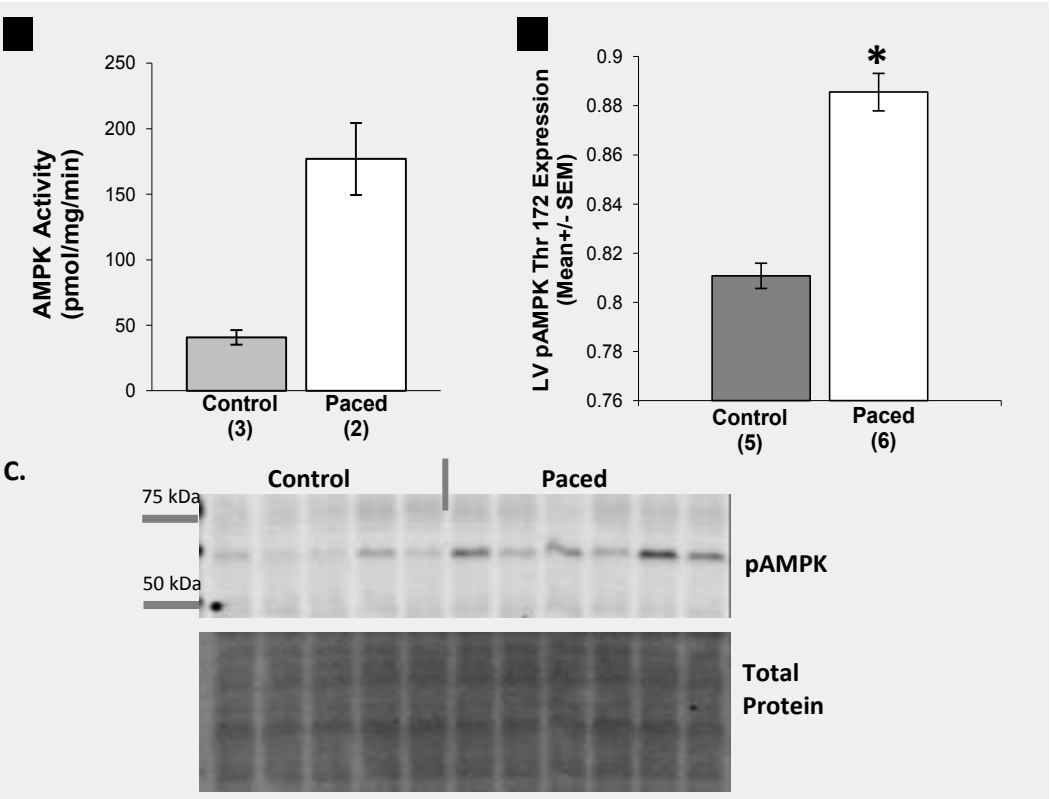

Figure 3-7. AMPK activity is increased by rapid pacing for 3 hours.

A- Mean ±SEM left ventricular AMPK activity assessed by incorporation of ^{32}p into the AMARA (AMPK substrate) peptide is increased immediately after pacing. **B-** Densitometry of phospho-AMPK levels normalized to total Ponceau-S protein (mean ± SEM) from paced and control (sham pacing) animals (*P<0.05). The number of samples used is indicated (n). **C-** Western blot showing the increase in phospho threonine 172 αAMPK (activated AMPK) in the LV after pacing. Equal loading was confirmed by quantifying Ponceau S total protein on the transferred blot.

3.3f Connexin Expression.

As Cx43 represents the primary Cx in the LV myocardium we assessed the effect of rapid atrial pacing on its protein expression. However, despite the reduction in longitudinal junctional conductance (measured by λ), there was no significant difference in the level of Cx43 in the LV (see Figure 3-8A) in either the triton soluble (cytosolic) fraction ($P = 0.267$) or the non-triton soluble (gap junctional plaque/plasma membrane) fraction ($P = 0.128$) within the first 3 hours of rapid pacing. In fact there is a trend to indicate that expression of Cx43 may be increased. This indicates that in this model Cx43 conductance is reduced by other mechanisms, including potential phosphorylation. In the atrial myocardium Cx40 makes up a significant fraction of the Cx expressed although it appears that a majority of the Cx40 in the pig atria is not bound up in junctional plaques (i.e. it is either found in the cytosol, or is expressed at the plasma membrane but not grouped in the junctional plaque). During rapid atrial pacing the expression tended to be reduced in the cytosolic fraction ($P = 0.254$) (see Figure 3-8C). However, the expression is variable, and since frozen samples were not available for all of the atria it would be beneficial to examine these expression changes in further animals (initial analysis of the samples did not include TS/NT fractionation, many of the samples were exhausted prior to this measurement). Additional atrial samples are available but were preserved in formalin, as such they could not be used here for this assay.

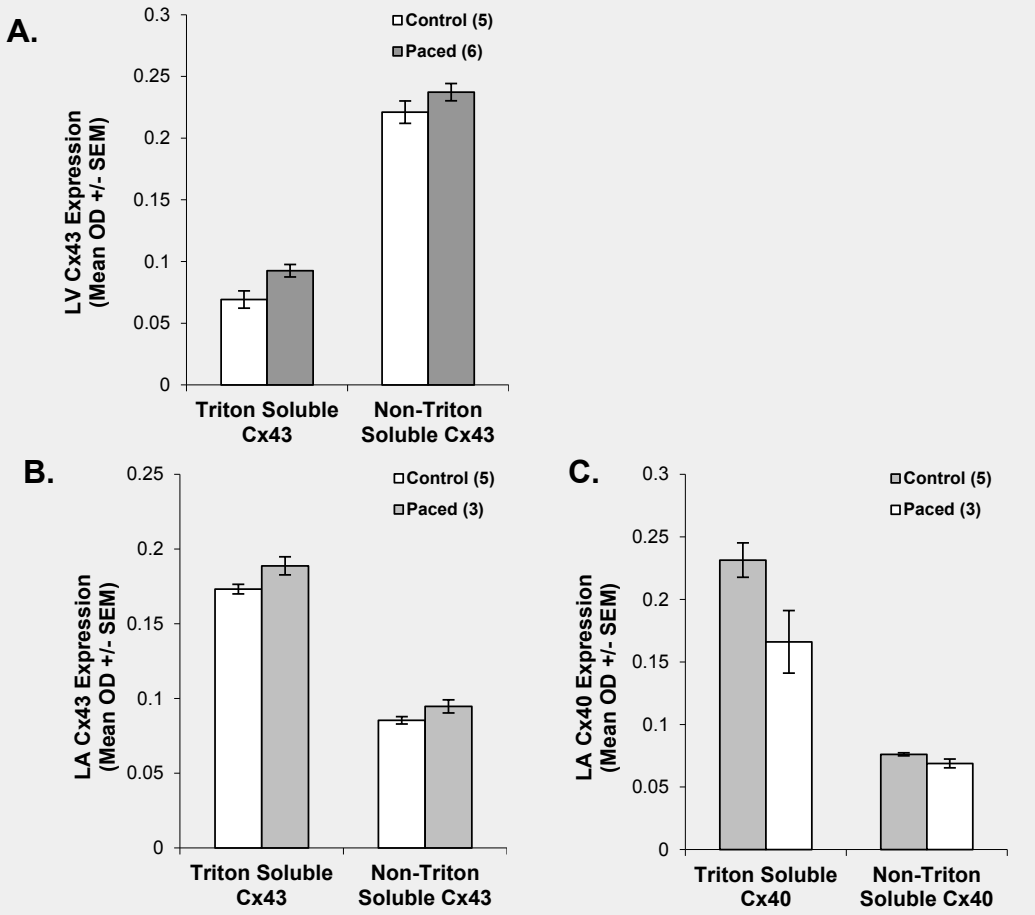

Figure 3-8. Myocardial left ventricular Cx43 is not significantly affected by rapid atrial pacing whereas left atrial Cx40 expression may be reduced.
A. Cx43 tends to be increased versus control following rapid atrial pacing for 3 hours (all normalized to α-tubulin) in both the triton soluble (cytosolic) fraction, as well as Cx43 in the non-triton soluble (plasma membrane/gap junctional plaque). **B.** Atrial Expression of Cx43 tends to be slightly increased after pacing. C. Left atrial Cx40 tends to be reduced. Sample size (n) is indicated in the legend.

As with Cx40, Cx43 was more abundant in the triton soluble fraction of the left atria (Figure 3-8. However, despite the trend to reduced Cx40, LA Cx43 tended to increase with pacing perhaps indicating that any reduction of Cx40 observed is being offset somewhat by Cx43 expression in this model.

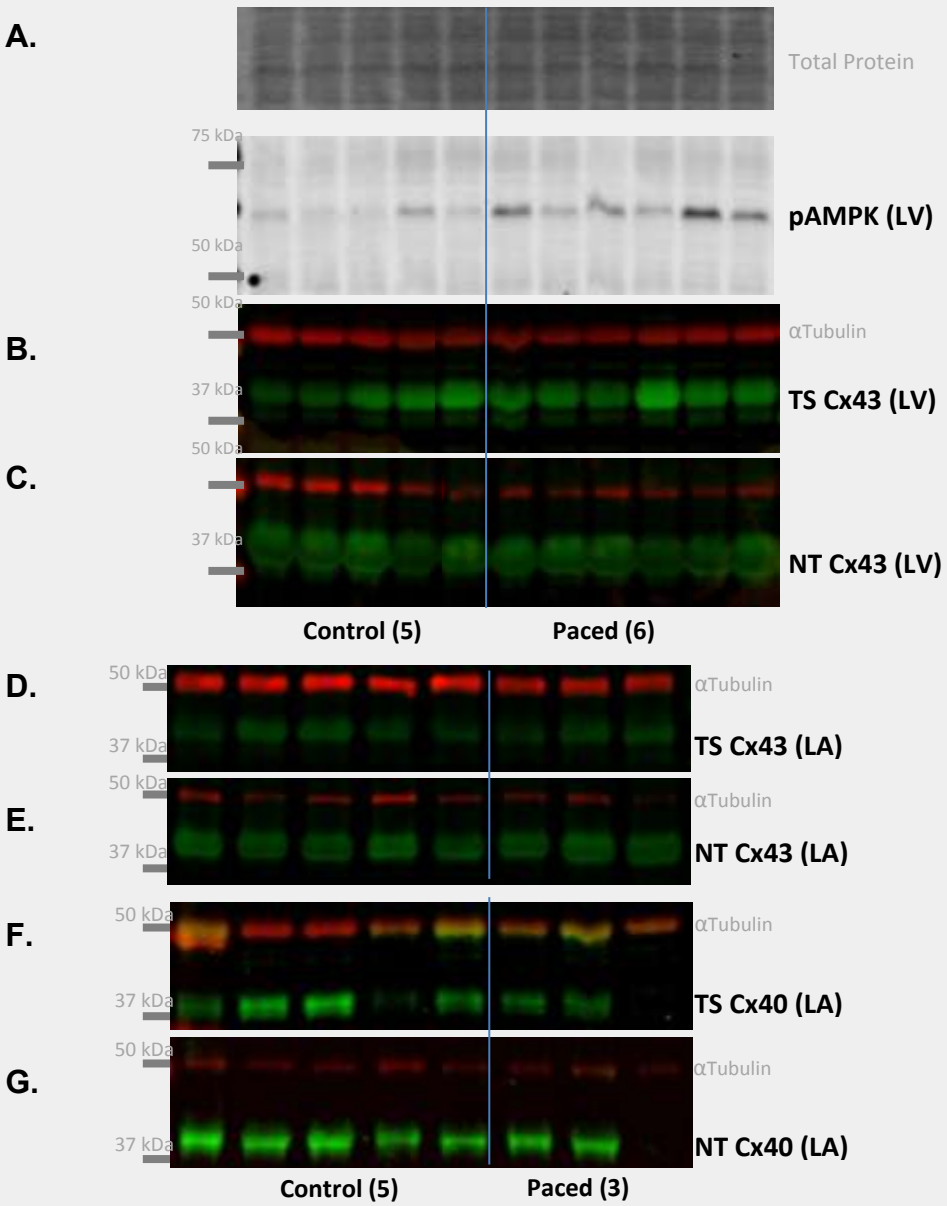

Figure 3-9. Western Blots showing differences in AMPK activation and Cx expression in the LV and LA following rapid pacing.

As quantified in the previous figures: **A.** Western blot showing phospho Thr-172 activation of AMPK (with total protein via Ponceau-S staining shown above). **B-C**. Triton soluble left ventricular Cx43 expression at the end of mapping and non-triton soluble fraction respectively. **D-E**. Triton soluble and Triton insoluble Cx43 expression in LA appendage. **F-G**. Triton soluble and triton insoluble Cx40 expression in the LA respectively. Note that with normalization to loading controls the mean ±SEM are as quantified.

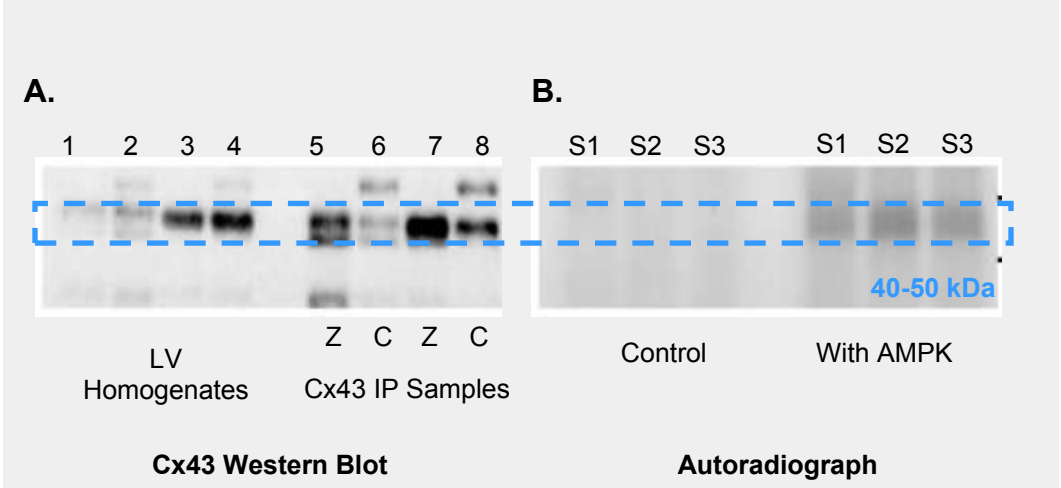

Figure 3-10. Cx43 is phosphorylated by AMPK *in vitro*.
A. Western blot using the Chemicon anti-Cx43 identified Cx43 in whole cell LV homogenates (4 samples lanes 1-4) as well as from samples of Cx43 isolated (by IP) from LV homogenates (lanes 5-8) using two different antibodies (either rabbit Anti-Cx43 (Z)ymed, or mouse anti-Cx43 (C)hemicon). **B-** A portion of these IP samples were mixed with or without purified AMPK in the presence of with radiolabeled phosphorus ^{32}P (for 30 min at 30°C) to show that Cx43 samples were phosphorylated (3 samples shown S1, S2, and S3).

3.3g Phosphorylation of Cx43 in vitro.

We identified (see Figure 3-10A) Cx43 in homogenates from pig LV whole cell homogenates (same strain used in the pacing/mapping studies), and normal Sprague Dawley rat left ventricles using two different antibodies (C)hemicon, and (Z)ymed. Both samples contained Cx43 identified using the Chemicon (C) Cx43 antibody (see Figure 3-10B). When we combined these isolated proteins with commercially available AMPK *in vitro*, we observed the incorporation of ^{32}P into the samples at approximately the same MW as Cx43 (see Figure 3-10C). This indicates that AMPK may phosphorylate Cx43, and thus may alter Cx43 activity in this model.

3.4 Discussion

3.4a Summary of Results

We have demonstrated that AMPK activity is increased in a rapid atrial pacing model, and that in this model frequent spontaneous tachyarrhythmia formation was observed in both the ventricles and atria. It is not yet clear how these arrhythmias are induced. However we do know that the (post-pacing) sinus rate was increased in the rapid pacing group after 3h, and that the Im_{25} duration was not significantly different indicating that the activity of membrane sodium channels was not impaired. It also appears that junctional coupling is reduced in the LV as predicted. This effect does not appear to be dependent on loss of Cx43 expression.

3.4b Rapid Pacing reduces junctional coupling.

Based on the combined data it appears that the amount of current required to pace the LV successfully was increased after 3 hours of atrial pacing. The resistance of the tissue was increased in the longitudinal direction as well as slightly in the transverse direction. Although there was no difference in conduction velocity in this model this is not surprising since there appears to be an increase in sodium channel activity (which may increase conduction velocity). In addition, conduction velocity is a somewhat insensitive marker of junctional activity and it has previously been shown that a reduction of gap junction protein up to 50% does not necessarily reduce conduction velocity despite an increased propensity for arrhythmias [32, 61]. Indicating that, as in our model, arrhythmia formation may occur secondary to a reduction in LV junctional coupling without evidence of a reduction in conduction velocity. The mechanism for this has yet to be explored in detail. Although we were not able to assess action potential duration directly in these studies, it must be assumed that the previously documented changes in sodium, CFTR, and potassium channel alterations which affect action potential duration may be involved in the arrhythmogenic substrate generated (as discussed in section 1.7d). Many of these effects were identified

after these studies were completed, but the effect of decreased junctional conductance would be expected to enhance these mechanisms, allowing potential EADs or DADs formed to propagate, and forming an even more arrhythmogenic substrate.

3.4c The Effect of Mapping Time.

Despite the significant increase in AMPK activity/phosphorylation measured, it is possible that we have actually overestimated the unpaced AMPK activity in this model. Because the basal heart rate after pacing often exceeded 200bpm, it was necessary to use a fast pacing interval during the mapping studies to control for differences in pacing rates (known to alter electrophysiology e.g. refractory periods). Thus, for the duration of epicardial mapping, the 'control' animals were actually being paced at a significantly faster than normal ventricular heart rate (ie 230-240 bpm). Normally there is only a 1-2 second pause of sinus rhythm between mapping runs (10xS1 beats, 1xS2 beat late in diastole, then pause for 2 seconds). As such, it is possible that the AMPK activity of many of the control subjects may be significantly higher than if they had not been mapped at these higher pacing rates. Unfortunately, we could not sample the heart immediately before the mapping study in the majority of animals studied to prevent damage to the heart, thus we cannot empirically confirm this without further study.

Ideally, if these studies were continued, it would be useful to measure the space constant, conduction velocity, and LV/LA monophasic action potential etc. continuously throughout the pacing protocol. This would allow us to make paired correlations in these parameters and get a better estimation of the time course of the reduction in junctional conductance observed. This was not initially apparent, and due to the potential problems with keeping the chest cavity open for prolonged periods of time we opted in later experiments to remain with the initial protocol. In addition, due to the large number of animals required, these improvements were not economically feasible to implement.

3.4d Atrial Effects.

It was not possible to accurately map the atrium due to the size of the mapping array, and difficulty in achieving homogeneous contact pressure for prolonged study. However, it is interesting to note that Cx40 levels tended to be reduced in the left atrium. This may indicate that Cx40 responds differently than Cx43 to AMPK activation. In either case, it would be informative to examine the effects of AMPK activation on Cx40 expression (including immuno-fluorescence localization) and alterations in junctional conductance in the atria in the future.

3.4e Activation of Autophagy.

It has recently been shown that rapid pacing can activate autophagy within 1 day, with increasing intensity out to at least 6 weeks [322]. The authors cite the ability of AMPK to stimulate autophagy [247] and show that AMPK is also increased in their model. The normal function of autophagy is to re-cycle persistent macromolecules (mitochondria, organelles) in the cell, and repair tissues, and cells, under baseline conditions and in response to stress. In our model, we see a significant increase in AMPK activity within 3 hours, and it is probable that markers of autophagy would also be increased. We cannot rule out the possibility that acutely activated autophagy pathways may contribute to the observed effects and further study is warranted.

3.4f Non-specificity of rapid pacing.

We set out in these studies to examine the effect of AMPK activation on cardiac electrophysiology with the expectation that these effects would be mediated by direct phosphorylation of downstream targets like Cx43, and Cx40 as well as (for example) altering protein synthesis via the mTOR pathway. However, due to the nature of the *in vivo* situation it is difficult to ascertain how these complex phenomena are related – rapid pacing has the potential to cause activation of a vast number of protein kinases, protein phosphatases, and signaling pathways. For example, although perhaps not probable when perfusion of the heart is fully

intact aside from the rate dependent decline in coronary perfusion, AMPK activation may have acted in an indirect manner via stimulation of glycolysis to such an extent that it was uncoupled from glucose oxidation potentially leading to myocardial lactic acidosis [520-522], and via fatty acid metabolite build-up [303, 492, 523-526].

Alternately, as with other ion channels (including Cx43, CFTR, and Ryr), phosphorylation at multiple specific sites can be additive – for example with CFTR generating a channel which is progressively more able to open with increasing PKA/β-adrenergic stimulation [437, 439, 444, 446]. Similarly, multi-site phosphorylation of the RyR allows for finely tuned and graded alterations in calcium release, and perturbations of this regulation via hyper-phosphorylation can lead to arrhythmogenesis in heart failure [527-530]. It is also possible that rapid pacing can lead to multiple phosphorylation, and dephosphorylation events on Cx43. In order to tease out the effects one must utilize a system which allows greater control of these variables.

Despite this limitation these studies do provide another potential mechanism whereby rapid pacing and AMPK activation may alter gap junctional conductance leading to an arrhythmogenic substrate. And despite the complex nature of interpreting the results – in the real world it is the combined effect that would be important to a patient. Future studies on these effects in a simpler model that can control for some of these limitations should be very informative and allow us to make more specific cause and effect interpretations.

3.5 Conclusions.

We have shown here for the first time with a pig model of rapid atrial pacing that AMPK may phosphorylate Cx43, that rapid pacing for 3h is able to increase AMPK activity, that LV junctional coupling is reduced without a corresponding change in Cx43 levels, and that Cx40 expression may be reduced in the atria with rapid

pacing. We also show that these effects are present within 3 hours inducing a very arrhythmogenic substrate presumably prior to the onset of any structural remodeling. Based on these findings, we can suggest that commonly encountered clinical tachyarrhythmias regardless of their initial mechanism (whether atrial, AV nodal, or ventricular in origin) may result in the formation of an even more arrhythmogenic substrate in a relatively short period of time due to the activation of AMPK and its effect on junctional conductance and potentially electrical remodeling in general.

3.6 Literature Cited

[1] Bayes de Luna A, Coumel P, Leclercq JF. Ambulatory sudden cardiac death: mechanisms of production of fatal arrhythmia on the basis of data from 157 cases. American Heart Journal. 1989;117:151-9.

[2] Gillum RF. Sudden coronary death in the United States: 1980-1985. Circulation. 1989;79:756-65.

[3] Kavanagh KM, Wyse DG. Ventricular arrhythmias. CMAJ. 1988;138:903-13.

[4] Innerfield RJ. Metformin-associated mortality in U.S. studies. The New England journal of medicine. 1996;334:1611-2; author reply 2-3.

[5] The Cardiac Arrhythmia Suppression Trial I. Special Report, preliminary report: effect of encainide and flecainide on mortality in a randomized trial of arrhythmia suppression after myocardial infarction. New England Journal of Medicine. 1989;321:406-12.

[28] Harris AL. Emerging issues of connexin channels: biophysics fills the gap. Quarterly reviews of biophysics. 2001;34:325-472.

[32] Jalife J, Morley GE, Vaidya D. Connexins and impulse propagation in the mouse heart. Journal of cardiovascular electrophysiology. 1999;10:1649-63.

[36] Dupont E, Ko Y, Rothery S, Coppen SR, Baghai M, Haw M, et al. The gap-junctional protein connexin40 is elevated in patients susceptible to postoperative atrial fibrillation. Circulation. 2001;103:842-9.

[37] Gutstein DE, Morley GE, Tamaddon H, Vaidya D, Schneider MD, Chen J, et al. Conduction slowing and sudden arrhythmic death in mice with cardiac-restricted inactivation of connexin43. Circulation research. 2001;88:333-9.

[38] Vaidya D, Tamaddon HS, Lo CW, Taffet SM, Delmar M, Morley GE, et al. Null mutation of connexin43 causes slow propagation of ventricular activation in the late stages of mouse embryonic development. Circulation research. 2001;88:1196-202.

[39] Lee P, Morley G, Huang Q, Fischer A, Seiler S, Horner JW, et al. Conditional lineage ablation to model human diseases. Proceedings of the National Academy of Sciences of the United States of America. 1998;95:11371-6.

[40] Hagendorff A, Schumacher B, Kirchhoff S, Luderitz B, Willecke K. Conduction disturbances and increased atrial vulnerability in Connexin40-deficient mice analyzed by transesophageal stimulation. Circulation. 1999;99:1508-15.

[41] Verheule S, van Kempen MJ, Postma S, Rook MB, Jongsma HJ. Gap junctions in the rabbit sinoatrial node. American journal of physiology. 2001;280:H2103-15.

[42] Qin D, Zhang ZH, Caref EB, Boutjdir M, Jain P, el Sherif N. Cellular and ionic basis of arrhythmias in postinfarction remodeled ventricular myocardium. CircRes. 1996;79:461-73.

[61] Verheule S, van Batenburg CA, Coenjaerts FE, Kirchhoff S, Willecke K, Jongsma HJ. Cardiac conduction abnormalities in mice lacking the gap junction protein connexin40. Journal of cardiovascular electrophysiology. 1999;10:1380-9.

[106] Kreuzberg MM, Willecke K, Bukauskas FF. Connexin-mediated cardiac impulse propagation: connexin 30.2 slows atrioventricular conduction in mouse heart. Trends in cardiovascular medicine. 2006;16:266-72.

[111] Lopez P, Balicki D, Buehler LK, Falk MM, Chen SC. Distribution and dynamics of gap junction channels revealed in living cells. Cell Commun Adhes. 2001;8:237-42.

[113] Segretain D, Falk MM. Regulation of connexin biosynthesis, assembly, gap junction formation, and removal. Biochim Biophys Acta. 2004;1662:3-21.

[117] Solan JL, Lampe PD. Specific Cx43 phosphorylation events regulate gap junction turnover in vivo. FEBS Lett. 2014.

[118] Laird DW, Puranam KL, Revel JP. Turnover and phosphorylation dynamics of connexin43 gap junction protein in cultured cardiac myocytes. Biochem J. 1991;273(Pt 1):67-72.

[119] Beardslee MA, Laing JG, Beyer EC, Saffitz JE. Rapid turnover of connexin43 in the adult rat heart. Circulation research. 1998;83:629-35.

[123] Laing JG, Beyer EC. The gap junction protein connexin43 is degraded via the ubiquitin proteasome pathway. J Biol Chem. 1995;270:26399-403.

[128] Yeager M, Unger VM, Falk MM. Synthesis, assembly and structure of gap junction intercellular channels. Current opinion in structural biology. 1998;8:517-24.

[206] Hendrickson SC, St.Louis JD, Lowe JE, Abdel-Aleem S. Free fatty acid metabolism during myocardial ischemia and reperfusion. MolCell Biochem. 1997;166:85-94.

[207] Yamada KA, McHowat J, Yan GX, Donahue K, Peirick J, Kleber AG, et al. Cellular uncoupling induced by accumulation of long-chain acylcarnitine during ischemia. Circulation research. 1994;74:83-95.

[208] Barger PM, Kelly DP. Fatty acid utilization in the hypertrophied and failing heart: molecular regulatory mechanisms. AmJMedSci. 1999;318:36-42.

[209] Tian R, Musi N, D'Agostino J, Hirshman MF, Goodyear LJ. Increased adenosine monophosphate-activated protein kinase activity in rat hearts with pressure-overload hypertrophy. Circulation. 2001;104:1664-9.

[210] Pogwizd SM, Corr PB. Biochemical and electrophysiological alterations underlying ventricular arrhythmias in the failing heart. EurHeart J. 1994;15 Suppl D:145-54.

[211] Kudo N, Gillespie JG, Kung L, Witters LA, Schulz R, Clanachan AS, et al. Characterization of 5'AMP-activated protein kinase activity in the heart and its role in inhibiting acetyl-CoA carboxylase during reperfusion following ischemia. Biochim Biophys Acta. 1996;1301:67-75.

[239] Zaha VG, Young LH. AMP-activated protein kinase regulation and biological actions in the heart. Circulation research. 2012;111:800-14.

[247] Kubli DA, Gustafsson AB. Cardiomyocyte health: adapting to metabolic changes through autophagy. Trends in endocrinology and metabolism: TEM. 2014;25:156-64.

[255] Marsin AS, Bouzin C, Bertrand L, Hue L. The stimulation of glycolysis by hypoxia in activated monocytes is mediated by AMP-activated protein kinase and inducible 6-phosphofructo-2-kinase. J Biol Chem. 2002;277:30778-83.

[303] Kantor PF, Dyck JR, Lopaschuk GD. Fatty acid oxidation in the reperfused ischemic heart. The American journal of the medical sciences. 1999;318:3-14.

[310] Hardie DG, Ashford ML. AMPK: regulating energy balance at the cellular and whole body levels. Physiology (Bethesda, Md. 2014;29:99-107.

[322] Yuan Y, Zhao J, Yan S, Wang D, Zhang S, Yun F, et al. Autophagy: A potential novel mechanistic contributor to atrial fibrillation. International journal of cardiology. 2014;172:492-4.

[347] Saez JC, Martinez AD, Branes MC, Gonzalez HE. Regulation of gap junctions by protein phosphorylation. Braz J Med Biol Res. 1998;31:593-600.

[348] Lowenstein WR. Regulation of cell-to-cell communication by phosphorylation. Biochemical Society symposium. 1985;50:43-58.

[423] Hardie DG, Carling D, Carlson M. The AMP-activated/SNF1 protein kinase subfamily: metabolic sensors of the eukaryotic cell? Annual review of biochemistry. 1998;67:821-55.

[430] Temple IP, Inada S, Dobrzynski H, Boyett MR. Connexins and the atrioventricular node. Heart Rhythm. 2013;10:297-304.

[437] Hegedus T, Aleksandrov A, Mengos A, Cui L, Jensen TJ, Riordan JR. Role of individual R domain phosphorylation sites in CFTR regulation by protein kinase A. Biochim Biophys Acta. 2009;1788:1341-9.

[439] Alzamora R, King JD, Jr., Hallows KR. CFTR regulation by phosphorylation. Methods in molecular biology (Clifton, NJ. 2011;741:471-88.

[444] King JD, Jr., Fitch AC, Lee JK, McCane JE, Mak DO, Foskett JK, et al. AMP-activated protein kinase phosphorylation of the R domain inhibits PKA stimulation of CFTR. Am J Physiol Cell Physiol. 2009;297:C94-101.

[446] King JD, Jr., Lee J, Riemen CE, Neumann D, Xiong S, Foskett JK, et al. Role of binding and nucleoside diphosphate kinase A in the regulation of the cystic fibrosis transmembrane conductance regulator by AMP-activated protein kinase. J Biol Chem. 2012;287:33389-400.

[455] Sakamoto J, Barr RL, Kavanagh KM, Lopaschuk GD. Contribution of malonyl-CoA decarboxylase to the high fatty acid oxidation rates seen in the diabetic heart. American journal of physiology. 2000;278:H1196-204.

[465] Kavanagh KM, Guerrero PA, Jugdutt BI, Witkowski FX, Saffitz JE. Electrophysiologic properties and ventricular fibrillation in normal and myopathic hearts. Canadian journal of physiology and pharmacology. 1999;77:510-9.

[466] Balaji S, Hewett KW, Krombach RS, Clair MJ, Ye X, Spinale FG. Inducible lethal ventricular arrhythmias in swine with pacing-induced heart failure. Basic Res Cardiol. 1999;94:496-503.

[467] McElmurray JH, Mukherjee R, Patterson TM, Goldberg A, King MK, Hendrick JW, et al. Comparison of amlodipine or nifedipine treatment with developing congestive heart failure: effects on myocyte contractility. JCard Fail. 2001;7:158-64.

[468] Stephens TJ, Chen ZP, Canny BJ, Michell BJ, Kemp BE, McConell GK. Progressive increase in human skeletal muscle AMPKalpha2 activity and ACC phosphorylation during exercise. Am J Physiol Endocrinol Metab. 2002;282:E688-94.

[469] Saffitz JE, Laing JG, Yamada KA. Connexin expression and turnover : implications for cardiac excitability. Circulation research. 2000;86:723-8.

[470] Salameh A. Life cycle of connexins: regulation of connexin synthesis and degradation. Advances in cardiology. 2006;42:57-70.

[471] Witkowski FX, Kavanagh KM, Penkoske PA, Plonsey R. In vivo estimation of cardiac transmembrane current. CircRes. 1993;72:424-39.

[473] Levine JH, Moore EN, Weisman HF, Kadish AH, Becker LC, Spear JF. Depression of action potential characteristics and a decreased space constant are present in postischemic, reperfused myocardium. JClin Invest. 1987;79:107-16.

[488] Ropelle ER, Pauli JR, Fernandes MF, Rocco SA, Marin RM, Morari J, et al. A central role for neuronal AMP-activated protein kinase (AMPK) and mammalian target of rapamycin (mTOR) in high-protein diet-induced weight loss. Diabetes. 2008;57:594-605.

[489] Brugarolas J, Lei K, Hurley RL, Manning BD, Reiling JH, Hafen E, et al. Regulation of mTOR function in response to hypoxia by REDD1 and the TSC1/TSC2 tumor suppressor complex. Genes & development. 2004;18:2893-904.

[490] Hahn-Windgassen A, Nogueira V, Chen CC, Skeen JE, Sonenberg N, Hay N. Akt activates the mammalian target of rapamycin by regulating cellular ATP level and AMPK activity. J Biol Chem. 2005;280:32081-9.

[491] Kimball SR. Interaction between the AMP-activated protein kinase and mTOR signaling pathways. Medicine and science in sports and exercise. 2006;38:1958-64.

[492] Tripp ME. Developmental cardiac metabolism in health and disease. Pediatric cardiology. 1989;10:150-8.

[493] Chen Y, Hu HZ, Wu JW, Peng QY, Yang G, Liao ZG. [Changes of connexin 43 in rabbit with early myocardial ischemia]. Sichuan da xue xue bao Yi xue ban = Journal of Sichuan University. 2004;35:191-3.

[494] Garcia-Dorado D, Rodriguez-Sinovas A, Ruiz-Meana M. Gap junction-mediated spread of cell injury and death during myocardial ischemia-reperfusion. Cardiovascular research. 2004;61:386-401.

[495] Hatanaka K, Kawata H, Toyofuku T, Yoshida K. Down-regulation of connexin43 in early myocardial ischemia and protective effect by ischemic preconditioning in rat hearts in vivo. Japanese heart journal. 2004;45:1007-19.

[496] Plaisance I, Duthe F, Sarrouilhe D, Herve JC. The metabolic inhibitor antimycin A can disrupt cell-to-cell communication by an ATP- and Ca(2+)-independent mechanism. Pflugers Arch. 2003;447:181-94.

[497] Tansey EE, Kwaku KF, Hammer PE, Cowan DB, Federman M, Levitsky S, et al. Reduction and redistribution of gap and adherens junction proteins after ischemia and reperfusion. The Annals of thoracic surgery. 2006;82:1472-9.

[498] Nattel S, Li D, Yue L. Basic mechanisms of atrial fibrillation--very new insights into very old ideas. AnnuRevPhysiol. 2000;62:51-77.

[499] Van Wagoner DR, Nerbonne JM. Molecular basis of electrical remodeling in atrial fibrillation. JMolCell Cardiol. 2000;32:1101-17.

[500] Li D, Fareh S, Leung TK, Nattel S. Promotion of atrial fibrillation by heart failure in dogs: atrial remodeling of a different sort. Circulation. 1999;100:87-95.

[501] Morillo CA, Klein GJ, Jones DL, Guiraudon CM. Chronic rapid atrial pacing. Structural, functional, and electrophysiological characteristics of a new model of sustained atrial fibrillation. Circulation. 1995;91:1588-95.

[502] Wijffels MC, Kirchhof CJ, Dorland R, Allessie MA. Atrial fibrillation begets atrial fibrillation. A study in awake chronically instrumented goats. Circulation. 1995;92:1954-68.

[503] Ausma J, van dV, Lenders MH, van Ankeren EP, Jongsma HJ, Ramaekers FC, et al. Reverse structural and gap-junctional remodeling after prolonged atrial fibrillation in the goat. Circulation. 2003;107:2051-8.

[504] Ohara K, Miyauchi Y, Ohara T, Fishbein MC, Zhou S, Lee MH, et al. Downregulation of immunodetectable atrial connexin40 in a canine model of chronic left ventricular myocardial infarction: implications to atrial fibrillation. Journal of cardiovascular pharmacology and therapeutics. 2002;7:89-94.

[505] Takeuchi S, Akita T, Takagishi Y, Watanabe E, Sasano C, Honjo H, et al. Disorganization of gap junction distribution in dilated atria of patients with chronic atrial fibrillation. Circ J. 2006;70:575-82.

[506] Wilhelm M, Kirste W, Kuly S, Amann K, Neuhuber W, Weyand M, et al. Atrial distribution of connexin 40 and 43 in patients with intermittent, persistent, and postoperative atrial fibrillation. Heart, lung & circulation. 2006;15:30-7.

[507] Gollob MH. Cardiac connexins as candidate genes for idiopathic atrial fibrillation. Current opinion in cardiology. 2006;21:155-8.

[508] Fialova M, Dlugosova K, Okruhlicova L, Kristek F, Manoach M, Tribulova N. Adaptation of the heart to hypertension is associated with maladaptive gap junction connexin-43 remodelling. Physiol Res. 2007.

[509] Sasano C, Honjo H, Takagishi Y, Uzzaman M, Emdad L, Shimizu A, et al. Internalization and dephosphorylation of connexin43 in hypertrophied right ventricles of rats with pulmonary hypertension. Circ J. 2007;71:382-9.

[510] Kostin S, Dammer S, Hein S, Klovekorn WP, Bauer EP, Schaper J. Connexin 43 expression and distribution in compensated and decompensated cardiac hypertrophy in patients with aortic stenosis. Cardiovascular research. 2004;62:426-36.

[511] Saffitz JE, Kleber AG. Effects of mechanical forces and mediators of hypertrophy on remodeling of gap junctions in the heart. Circulation research. 2004;94:585-91.

[512] Teunissen BE, Jongsma HJ, Bierhuizen MF. Regulation of myocardial connexins during hypertrophic remodelling. European heart journal. 2004;25:1979-89.

[513] Gutstein DE, Morley GE, Vaidya D, Liu F, Chen FL, Stuhlmann H, et al. Heterogeneous expression of Gap junction channels in the heart leads to conduction defects and ventricular dysfunction. Circulation. 2001;104:1194-9.

[514] Spach MS, Heidlage JF, Dolber PC, Barr RC. Changes in anisotropic conduction caused by remodeling cell size and the cellular distribution of gap junctions and Na(+) channels. Journal of electrocardiology. 2001;34 Suppl:69-76.

[515] Peters NS, Green CR, Poole-Wilson PA, Severs NJ. Reduced content of connexin43 gap junctions in ventricular myocardium from hypertrophied and ischemic human hearts. Circulation. 1993;88:864-75.

[516] Lauf U, Giepmans BN, Lopez P, Braconnot S, Chen SC, Falk MM. Dynamic trafficking and delivery of connexons to the plasma membrane and accretion to gap junctions in living cells. Proceedings of the National Academy of Sciences of the United States of America. 2002;99:10446-51.

[517] Beauchamp P, Yamada KA, Baertschi AJ, Green K, Kanter EM, Saffitz JE, et al. Relative contributions of connexins 40 and 43 to atrial impulse propagation in synthetic strands of neonatal and fetal murine cardiomyocytes. Circulation research. 2006;99:1216-24.

[518] Pumir A, Plaza F, Krinsky VI. Effect of an externally applied electric field on excitation propagation in the cardiac muscle. Chaos (Woodbury, NY. 1994;4:547-55.

[519] Akar FG, Roth BJ, Rosenbaum DS. Optical measurement of cell-to-cell coupling in intact heart using subthreshold electrical stimulation. American journal of physiology. 2001;281:H533-42.

[520] Lopaschuk GD. Regulation of carbohydrate metabolism in ischemia and reperfusion. American Heart Journal2000.

[521] Lopaschuk GD. Optimizing cardiac energy metabolism: how can fatty acid and carbohydrate metabolism be manipulated? Coronary artery disease. 2001;12 Suppl 1:S8-11.

[522] Vorperian VR, Wisialowski TA, Deegan R, Roden DM. Effect of hypercapnic acidemia on anisotropic propagation in the canine ventricle. Circulation. 1994;90:456-61.

[523] Apstein CS. Glucose-insulin-potassium for acute myocardial infarction: remarkable results from a new prospective, randomized trial. Circulation. 1998;98:2223-6.

[524] Avitall B, Hare J, Zander G, Lessila C, Dhala A, Deshpande S, et al. Cardioversion, defibrillation, and overdrive pacing of ventricular arrhythmias: the effect of moricizine in dogs with sustained monomorphic ventricular tachycardia. Pacing ClinElectrophysiol. 1993;16:2092-7.

[525] Bonnet D, Martin D, Pascale DL, Villain E, Jouvet P, Rabier D, et al. Arrhythmias and conduction defects as presenting symptoms of fatty acid oxidation disorders in children. Circulation. 1999;100:2248-53.

[526] Schmilinsky-Fluri G, Valiunas V, Willi M, Weingart R. Modulation of cardiac gap junctions: the mode of action of arachidonic acid. J Mol Cell Cardiol. 1997;29:1703-13.

[527] Camors E, Valdivia HH. CaMKII regulation of cardiac ryanodine receptors and inositol triphosphate receptors. Frontiers in pharmacology. 2014;5:101.

[528] Zhang H, Makarewich CA, Kubo H, Wang W, Duran JM, Li Y, et al. Hyperphosphorylation of the cardiac ryanodine receptor at serine 2808 is not involved in cardiac dysfunction after myocardial infarction. Circulation research. 2012;110:831-40.

[529] Ke J, Xiao X, Chen F, He L, Dai MS, Wang XP, et al. Function of the CaMKII-ryanodine receptor signaling pathway in rabbits with left ventricular hypertrophy and triggered ventricular arrhythmia. World journal of emergency medicine. 2012;3:65-70.

[530] Lokuta AJ, Rogers TB, Lederer WJ, Valdivia HH. Modulation of cardiac ryanodine receptors of swine and rabbit by a phosphorylation-dephosphorylation mechanism. The Journal of physiology. 1995;487 (Pt 3):609-22.

Chapter 4 Assessment of cardiac gap junction function in vivo and in vitro: a comparison of current techniques.

This thesis is an original work by Jason Bradley Iden.

No part of this chapter has been previously published.

Surgical procedures were carried out by Jason Iden with assistance from Dr. Gang Liu.
Langendorf perfusion apparatus was designed and built by Jason Iden.

Neonatal cardiac myocytes were isolated and cultured by Jason Iden with help and support of Suzanne Kovacic (Dr. Jason Dyck's laboratory).
Adenoviral constructs were supplied by the University of Alberta Cardiovascular Research Group Adenoviral Core Facility.

Filter design and use of MatLab Signal Processing Toolbox facilitated by Dan Roach.

4.1 Overall Introduction

Due to their structure and physiology the study of cardiac gap junctional communication is difficult and complex. In the *in vivo* setting we are limited to measurements of electrical conduction velocity, and subthreshold measurements of intercellular resistance, or measurements of whole tissue impedance with plunge electrodes. Despite the appealing nature of a physiological preparation there are certain drawbacks to this methodology in terms of limited specificity, and equipment versus animal size. The use of an isolated heart can facilitate both electrical mapping, and the use of pharmacological treatments that are not suitable *in vivo*, while maintaining the benefits of using an intact heart. However, these electrical techniques do impose limitations that can (again) be abrogated to some extent by switching to an optical mapping system.

In utilizing isolated cells, the ability to more effectively alter experimental conditions is the primary benefit, and there are also a large variety of techniques available. One such is the use of cardiac myocyte monolayers with multi-electrode arrays that partially mimic the measurements done *in vivo*. In addition, various fluorescent dyes have been used to evaluate macroscopic (small molecule) conductance. These dyes are typically loaded into a cell or group of cells by scrape loading, microinjection, or co-incubation of two differentially labeled cell populations and the rate of transfer measured in various ways. Measuring electrical intercellular currents by double cell patch clamp is the gold standard. However, it is also the most technically challenging, is very expensive to setup, and difficult to do in a beating cell. During the course of my studies, most of these techniques were used with variable success. Here I will outline the benefits, drawbacks and preliminary data found using each method. In the end, a two cell FRAP method attained the best mix of usability and sensitivity.

4.2 In vivo epicardial electrical mapping.

4.2a Overview and Theoretical Benefits

As with all techniques and methods, one must first evaluate whether the question is suitable to the model. As we were initially interested in the metabolic regulation of cardiac gap junctions, and their effect on arrhythmia formation, we needed a model that was suitable for both evaluation of arrhythmia formation, and the potential changes in cardiac junctional coupling. As such, the principle benefit of *in vivo* epicardial mapping is that it is a physiological model that is most suitable for inferences with respect to a clinical setting.

4.2b Materials and Methods

For detailed methodology please see section 2.2, and 2.12a and results Chapter 3. We utilized a rapid pacing technique to increase cardiac demand and evaluated the changes in cardiac electrophysiology: ECG parameters, alterations in conduction velocity, sodium channel activity, pacing thresholds, tissue resistivity, and calculated the space constant tau (λ).

In combination, these parameters are indicative of junctional coupling. Many of them can be repeatedly measured in the same position on the posterior wall of the LV (where the pericardium can be used to dynamically stabilize the recording electrode array against the heart as it moves during contraction), and where the surface is relatively free of large vessels and nerves that can affect homogenous contact of the array on the myocardial surface.

4.2c Preliminary Results and Discussion

Since this data was already presented in Chapter 3 of this thesis, it will not be repeated here. Overall, the recording of this data was reasonably straightforward. The surgical preparation was feasible, although in order to measure these parameters we required direct access to the heart. As such, there were concerns that extended open chest surgery would place undue stress on the animal that would require the use of larger anesthetic doses for a much

longer period of time. Additionally, it was necessary to maintain 1:1 conduction through the AV node at rates up to 300bpm (which can be inhibited with large doses of sodium pentobarbital). Based on these potential problems, we opted to not open the chest until the end of the 3 hour pacing protocol. This prevented us from repeatedly measuring electrical parameters (space constant, CV, pacing threshold etc.) before during and after pacing.

One of the challenges of this technique is the type of Cx subunits that are measurable. We measured junctional conductance in the LV free wall which is primarily determined by Cx43 activity. However, in order to measure changes in Cx40 we would require a consistent stable position to record from the surface of the atria. This is just not feasible with the recording array used due to its size and the geometry and relative instability of the left atrial appendage spatially and temporally. Furthermore, in the atrial appendage we would be measuring the combination of Cx40 and Cx43 activity which do not always respond in the same way to interventions [531-536]. This technique is even less well suited to measuring the activity of Cx45 which is located in the relatively small nodal regions of the heart, and although certain parameters could be estimated by measuring AVN conduction time via pacing/recording catheters, these regions are best studied in *ex-vivo* preparations, and are formed of a various mixture of Cx40, 43, and Cx45. In addition, the size of an *in vivo* large animal preparation, while a benefit for stability and allowing the use of a larger electrode array, can also introduce several concerning issues. For example, in our case the use of AMPK activating drugs like phenformin can have systemic effects that are not tolerable (eg. induction of lactic acidosis). In addition, the volume of non-clinical drugs like the AMPK inhibitor compound C – are prohibitively expensive when used in a large animal ignoring the additional problems related to drug bioavailability and clearance. To address these concerns, we also explored the possibility of electrically mapping the LV in a murine (rat/mouse) model.

4.3 Langendorf Heart Electrical mapping.

4.3a Overview and Theoretical Benefits

Although realistically, any *in vivo* model would have the same limitation with respect to systemic pharmacological effects. In comparison to the use of large animal studies, the cost of the animal, reduced need for multiple people for surgical procedures, and volumes of pharmacological agents required for a small animal preparation are more reasonable. Unfortunately, the use of our mapping array with a murine *in vivo* model was not possible due to the obstruction of the chest wall with the heart *in situ* that prevented us from mapping the LV effectively. However, using an isolated rat heart *in vitro* model with a custom built Langendorf heart perfusion apparatus we were able to orient the heart such that the posterior LV free wall was in direct contact with the mapping array. In addition, this model allows us to potentially examine the effects of direct perfusion with AMPK or specific junctional conductance altering pharmacological agents without altering systemic metabolism/function using feasible amounts of pharmacological agents.

4.3b Materials and Methods

See section 2.2, and 2.12b for detailed methodology. Hearts were isolated from adult Sprague Dawley rats, the aortic arch was cannulated and the heart was transferred to the Langendorf perfusion apparatus. The heart was perfused with Krebs–Henseleit buffer, under constant pressure, at 37±0.5°C. Epicardial electrical mapping was achieved by placing the anterior surface of the left and right ventricles, or the posterior LV free wall on the mapping array.

4.3c Preliminary Results and Discussion

The preparation was usable, and stable for at least 60-90 minutes (coronary flow/developed pressure). Following an initial 5 min baseline equilibration period coronary flow-rates of ~7-15 ml/min were achieved (60 mmHg constant pressure) with ~10% drop in coronary flow over 60-90minutes.

Measurement of epicardial surface potentials, and a volume conducted ECG in the rat heart was complicated by electrical noise generated in the signal due to the perfusion buffer column which tends to act like an antenna. This was partially prevented by shielding and grounding but not to the extent required with the equipment available (a large Faraday cage may be able to prevent this). The signal to noise ratio in the ECG was also decreased (versus the pig preparation) due to the reduced signal amplitude measured from the smaller heart.

The average measured conduction velocity in this model (longitudinal 0.427 ± 0.0063 m/s, transverse 0.262± 0.0031 m/s, L/T= 1.64 ± 0.023 m/s n=12) was slower than found in the pig model (0.507±0.041 m/s, 0.235±0.053 n=6), and ~60-80% of values reported in the literature using 'Groningen' rats (Long 0.69±0.13 m/s (n=408) Trans 0.33±0.06 (n=468) L/T 2.1±0.4)[537]. In this model, there were sometimes differences in the conduction velocity measured at each point along a straight line (one arm of the array) and the longitudinal to transverse ratio was often difficult to ascertain. However, this was not entirely unexpected. As noted previously, the structural orientation of cardiac myocytes is important because the resistance to current is much lower in the longitudinal direction. Due to the small size of the rat heart there are changes in myocyte orientation over a relatively short distance. Thus, due to the electrode spacing in our array, determination of the longitudinal to transverse orientation was much more difficult relative to the pig preparation. In addition, over this same small scale the myocytes exhibit rotational twisting leading to greater isotropy in the tissue [477]. Our observations are consistent with these properties.

Based on orientation indicated by conduction velocity data we attempted to measure the space constant, in both the longitudinal and transverse directions, to confirm our ability to measure reduced junctional conductance. Hearts were perfused with normal Krebs buffer during baseline measurements and the non-

specific gap junction inhibitor heptanol in Krebs buffer was infused at 1/10 the flow rate resulting in a final concentration of 5 μM for 10 minutes. Although this dosage was not as large as has been used in the literature (up to 2mM), at these higher concentrations the hearts tended to develop arrhythmias almost immediately, and pacing efficacy was almost totally abolished. Throughout the infusion, a continuous repeat of subthreshold mapping signal trains were recorded (input via unipolar pacing into the center electrode, 10x S1 (5ms, 2xthreshold), 1xS2 10ms 1/2 threshold), followed by a short pause of sinus activity (2 seconds). When possible to analyze, these recordings show that combined with a reduction in conduction velocity (see Figure 4-1A), almost complete blockage of sinus activity, and a reduction in pacing efficacy there was a slight but consistent reduction in the space constant in both the longitudinal (828 versus 804 μm) and transverse direction (731 versus 655 μm) (see Figure 4-1C) (n=1). While this is an isolated observation, it is indicative that we can measure a change in junctional conductance.

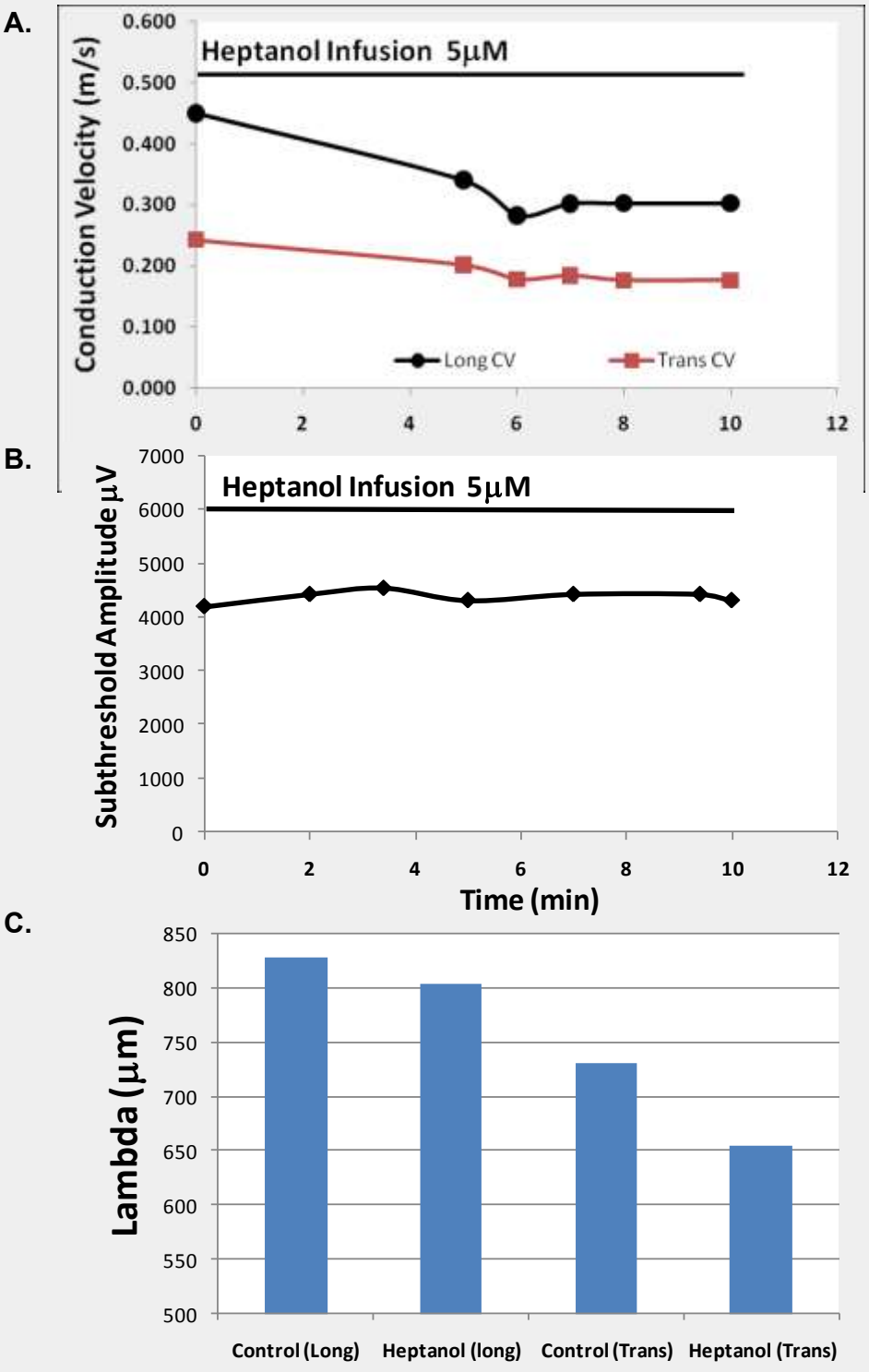

Figure 4-1. Infusion of junctional uncoupler heptanol 5µM reduces junctional coupling in Langendorf perfused rat heart LV.

A. 10 minute infusion of 5µM heptanol reduced conduction velocity. **B.** Based on this figure, it did not initially appear that heptanol infusion reduced subthreshold amplitudes. **C.** However, the space constant (lambda) calculated from this data was reduced, indicating that at the end of 10 minute heptanol perfusion junctional conductance was inhibited in this isolated case.

These findings were difficult to reproduce. In the majority of these studies VT/VF was induced within 2 minutes of heptanol infusion (0.1-3mM) making analysis of CV or space constants difficult. Conduction velocity tended to be reduced in a dose dependent manner. However, there did not appear to be any difference in the amplitude of the S2 pulse with heptanol infusion. To facilitate faster measurement and ease of analysis in certain experiments a bipolar pacing stimulus was used to measure subthreshold amplitude in both the longitudinal and transverse directions. By pacing between two outer electrodes and measuring subthreshold amplitudes in the inner electrodes, the amplitude could be rapidly calculated and used to estimate tissue resistivity over time with various treatments. However, this also made measurement of the space constant impossible as we did not have enough electrodes at a constant distance from the pacing site to allow accurate curve fitting.

Although there is some pericardial serous fluid and some saline from the gauze (used to stabilize the mapping electrode in position on the LV surface in the pig model), comparatively there is much more fluid surrounding a Langendorf perfused rat heart. As such, since Krebs buffer is conductive, it follows that the buffer surrounding the heart may be allowing current to bypass the membrane, and it may act as a current sink, reducing the amplitude measured. To determine what the effective subthreshold voltage amplitude would be in buffer alone the subthreshold mapping stimuli was repeated in normal Krebs buffer 0.9% saline (and decreasing concentrations 1/2, 1/4, 1/8). The resulting subthreshold amplitude was exponentially negatively correlated with conductivity of the buffer used, and was dependent on the distance from the pacing electrode alone, with no change in longitudinal to transverse ratios, as would be expected. In comparison to the space constant measured in the pig (~1100 μm) the normal Krebs buffer space constant was much shorter (~552 μm), with lower conductivity (half normal saline) this space constant was reduced even further to ~536 μm. In buffer alone, the waveform of the subthreshold pulse tended to

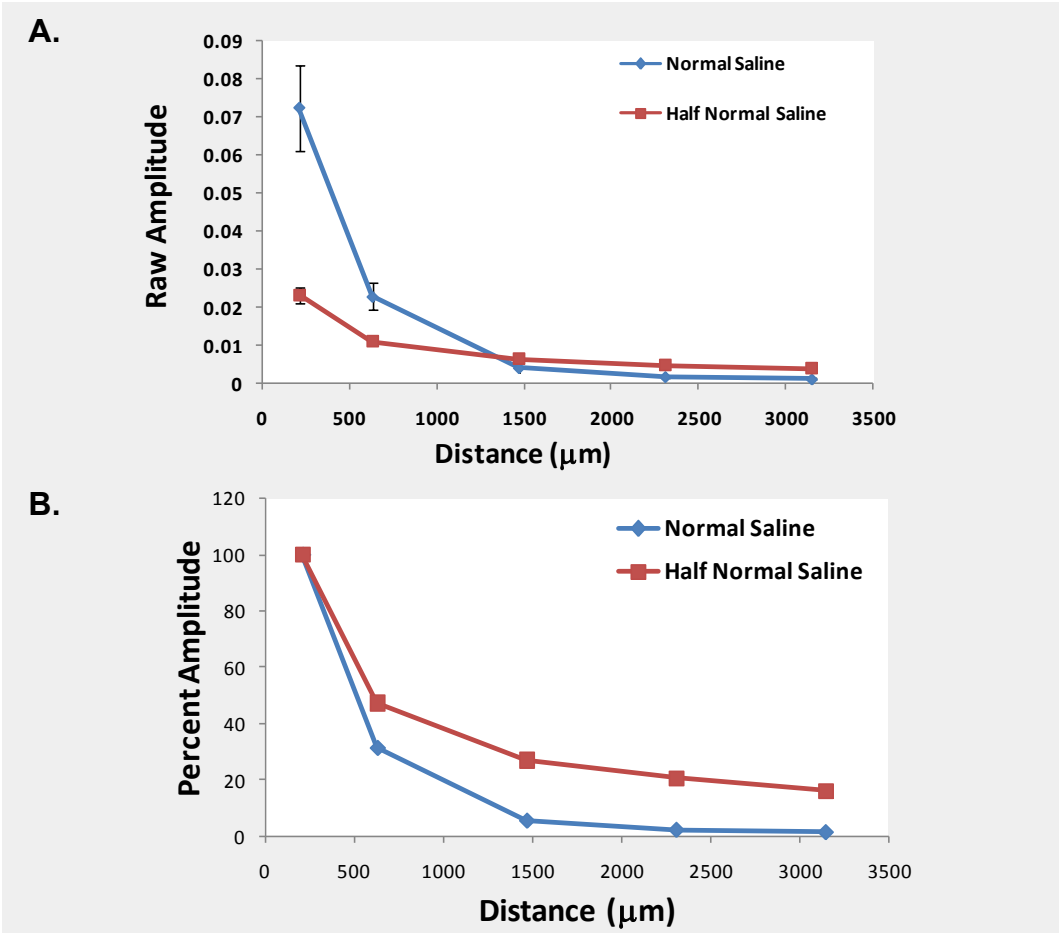

Figure 4-2. Measurement of Subthreshold pulse amplitude in normal saline buffer and half normal saline buffer to measure the space constant.
A. Raw amplitude of subthreshold pulses. **B**. For calculation of the space constant, the amplitude is normalized to the initial (closest electrode amplitude) and the decay rate is determined. Lambda was 552μm and 536 μm for the normal saline, and half normal saline respectively indicating that indeed the lower conductivity saline has greater resistance.

reach a peak negative amplitude which decayed over the course of the pacing duration. Whereas with a heart in place the spike gradually reached a plateau amplitude by the end of the pacing spike duration, as expected during the charging of the membrane capacitance.

To prevent this from occurring, the amount of perfusate was reduced in the compartment containing the heart, and the mapping electrode was placed on the upper (anterior) surface of the heart in order to reduce the potential for buffer short circuit. However, due to the nature of the LV perfusion system with

perfusate exiting the coronary sinus, it was not possible to eliminate this shunting pathway completely. One possible way of addressing this would be the use of a working heart model, which maintains a (mostly) closed system. The removal of the buffer surrounding the heart also prevented the measurement of a volume conducted ECG, and reduced the temperature buffering capacity of the chamber: cooling the heart.

One of the primary drawbacks to this methodology was the frequent arrhythmias that were induced and relatively low percentage of hearts that could actually be utilized fully. The cause of this instability during perfusion was not easily identified. Based on comparisons of buffer systems, pH stability, and temperature, our system was similar to others in the cardiovascular group. As we needed fairly consistent contact with the mapping electrode, it was necessary to lay the entire apparatus on its side. While this orientation is the norm *in vivo* – it was apparent that this did cause a problem as a heart that was totally stable for 90 minutes in perfusion went into VT almost immediately upon attempts to map the heart reducing coronary flow from 8.5 ml/min to 3.5 ml/min indicating that perfusion was reduced. It is also possible that there may be some contamination of the system when using heptanol, as replacing the tubing and fully cleaning after heptanol use was eventually needed to prevent arrhythmia formation during baseline perfusion in subsequent experiments. It was also important to avoid applying excessive pressure on the heart which tended to cause coronary flow to drop, thus also limiting our ability to ensure ideal contact with the mapping array. Due to the problems with mapping the heart and maintaining proper contact, we elected to attempt to measure tissue resistivity with the heart freely hanging in a vertical position.

The four electrode technique has been described previously [475-477]. In brief, a series of 4 small plunge electrodes was placed in the LV free wall at ~1mm intervals. By pacing the exterior two electrodes, and measuring the potential

difference between the inner two, we measured the impedance of the tissue independently of the exterior buffer solution. This measurement also allowed us to more effectively filter the electrical signals, and measure heptanol sensitive junctional conductance almost constantly from the same area. The use of this technique did of course present some difficulty as it was not possible to consistently determine whether we were measuring a longitudinal or transverse orientation to the myocytes. In addition, the electrodes used were built in our laboratory using 75μm Teflon coated platinum wire that had the ends exposed. The wires were mounted on a mesh support with set gaps at 200μm and set in place by epoxy. This mesh support was then placed on the LV and the wires inserted into the LV to a depth of ~1-2mm. Unfortunately, in practice it was difficult to get the support to remain in place consistently, and loss of multiple electrode assemblies due to damage made their use problematic.

In the end, the most significant drawback of these studies was its relatively low success rate. The combination of arrhythmias induced by both buffer contamination, and the orientation of the heart were prohibitive. In addition, it was never possible to completely eliminate the possible formation of a buffer shunting current. To address some of these issues, we attempted to utilize a sensitive optical mapping system developed in our laboratory.

4.4 Optical Mapping of Langendorf perfused rat hearts.

4.4a Overview and Theoretical Benefits

The use of optical mapping systems to measure electrical activity from the heart surface has been documented by a number of groups and was first published by our laboratory in 1997 [480-482]. With this technique, the spatial resolution is very high relative to electrical mapping (5616 sites covering an area of ~7.8x8mm versus 88 in our array). It also removes the requirement for constant contact pressure to keep measured amplitudes consistent. Using the camera in our lab, we have temporal resolution of up to 2.7kfps, but in practice this was often

reduced to ~1000 fps to allow greater CCD saturation (meaning less shot noise). Thus, we have ~1ms temporal resolution, adequate for measurement of local activation waves and comparison of conduction velocity.

It was demonstrated by Akar's group that optical mapping of subthreshold signals was possible, thus allowing evaluation of junctional coupling using this technique [519]. The combined measurement of subthreshold signals, and conduction velocity can indicate myocyte orientation around the pacing site. In addition, since we could visualize conduction in a small area of the heart, this method (in contrast to electrical mapping), allows us to specifically map an area that had been infected with adenovirus for the activation or inhibition of AMPK as needed to address the overall hypothesis of these studies.

4.4b Materials and Methods

Using adult Sprague-Dawley rats, ~20μL of tittered (~1-6 x10^{10} pfu/ml) adenovirus encoding either GFP, or GPF and constitutively active $AMPK_{CA}$ was injected into a single location on the left ventricle. This single injection site was utilized to allow us to measure differences in conduction within a single field of view. Total recovery/treatment time was 72 hours at which point the heart was excised as in the previous section for *in vitro* Langendorf mode perfusion and optical mapping.

Optical mapping procedures have been described in detail in section 2.12d [480-482]. The area of infection was identified, then 75μm Teflon coated gold wire was inserted into the area (and at various locations in the field of view) for unipolar pacing using the cannula as a reference as shown in Figure 4-3F . Hearts were perfused with voltage sensitive di-4ANNEPS to stain the epicardial membrane, and motion artifacts were minimized with 20μM cytochalasin-D (which cleaves filamentous actin), or the much less expensive electromechanical un-coupler butanedione monoxime (BDM). Once properly stained, the area was paced with the subthreshold mapping train as in the previous studies (here we

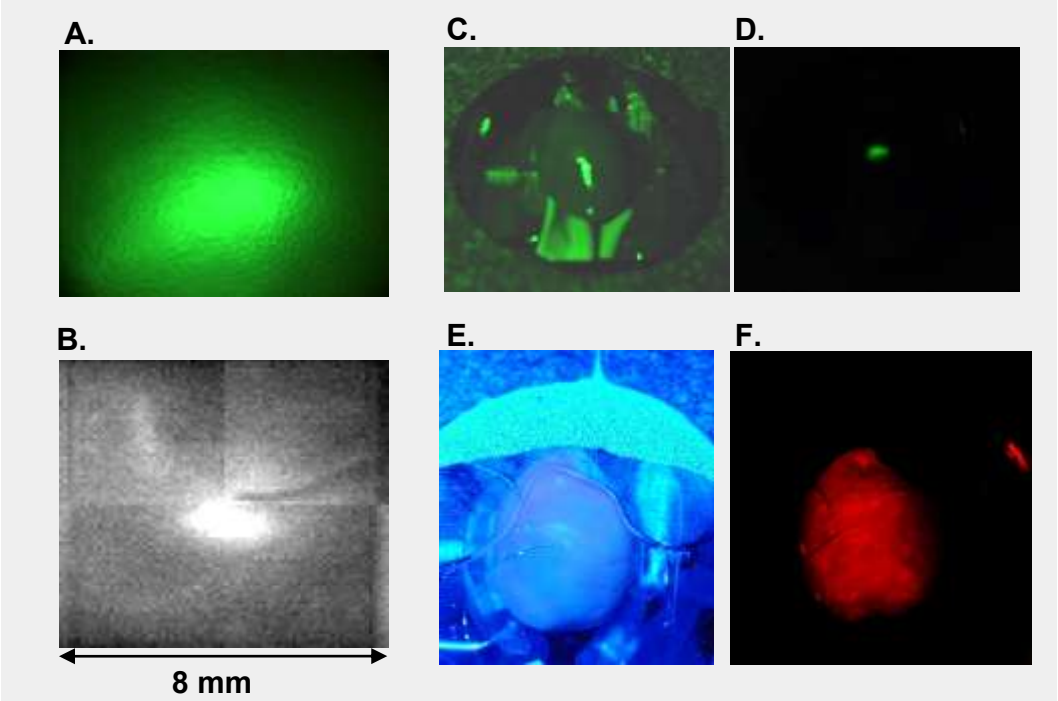

Figure 4-3. Optical mapping setup of Langendorf rat heart.
A. Microscope picture of GFP expression 48h after a typical adenoviral injection (courtesy Dr. P. Light). **B.** CCD image of a similar infection site obtained with the optical mapping camera using a GFP excitation filter set. **C.** Photograph of a heart showing the orientation for comparison with D. **D.** Identification of the GFP infection site. **E.** The injection site (visible as a whitish area in the center) with pacing wires under unfiltered green 500±40 nm excitation light. **F.** Heart stained with di-4ANNEPS viewed through a (>590nm, long pass) red filter.

used a train of 5 S1 pacing stimuli, then one or two subthreshold stimuli 10-20ms duration, followed by a pause of 2 seconds).

4.4c Preliminary Results and Discussion

We were able to easily identify the area of infection (see Figure 4-3D), and pace the area effectively for measurement of conduction velocity. However, initial attempts to measure the subthreshold stimulus were undetectable under normal conditions. As such, due to the long stimulus duration and low threshold for pacing it was necessary to effectively increase the pacing threshold in order to visualize the signal. As such, initially we mapped the LV with normal KCL (4mM), then with high KCL (6-8mM) for subthreshold stimulation (Figure 4-4) as

described by Akar *et al*. [519]. The resulting signal lost much of its signal to noise ratio making it more difficult to analyze.

Signal Processing

Previously in our lab we utilized a fairly crude method of signal processing designed for random fibrillation wavelets. In order to properly analyze this data, a software suite was developed in MatLab v6.5 (Mathworks) as follows.

Initially, since the camera detects a drop in fluorescence with depolarization, the signals must be subtracted from the visual mean fluorescence and then inverted. Previously, this camera was used to measure fibrillating myocardium with constant wavelets in each frame, thus a simple linear mean square fit of the signal was sufficient to control for bleaching of the signal over time. In our case, this was not possible due to the pause pacing used, and the average fluorescence increase during pacing versus the pause. As such, it was necessary to develop a way to isolate the depolarization due to pacing from the baseline prior to correction. This was accomplished by making an initial linear or cubic curve fit, then detecting the onset of the pulse and replacing the data with the previous fit, then sequentially re-fitting the baseline. In general, with ~4-7 iterations, this method allowed us to debleach the signal and prevent the large increase in background noise inherent with the previous technique (that easily drowned out the small subthreshold pulses used).

Once properly debleached, the signals were traditionally normalized to 8 bit (0 to 256) then 5 point median filtered and a movie was generated for analysis. Again, this technique was not sufficiently clean enough to reduce the substantial shot noise inherent with the CCD (especially when using signals from high KCL hearts). Thus we explored two mechanisms of digitally filtering the signal. The first has been described previously, by Simonotto and Furman *et al*. [538, 539], in collaboration with our lab. In this method, the signal is de-constructed using Fourier transform and the higher and lower frequency data was subtracted

(using cutoffs of 2Hz and 16Hz). However, using this technique it was often noted that a harmonic resonance could be generated in the re-constructed signal. As such, we opted to use a two way (forward and backwards, to correct/prevent phase shifts in the signal) finite impulse response filter (FIR) with a low pass cutoff frequency of 32Hz (versus 16Hz to minimize slowing of the upstroke) which were optimized for the sampling frequency of the camera (see Figure 4-4A). In addition, due to residual noise, and movement artifacts, a subsequent process for signal averaging these digitally filtered signals was developed using the peak dV/dt in the mean frame fluorescence as a reference point with summation of 50 frames prior, and 250+ frames following this point. In order to ensure that these digital filtering and processing techniques did not significantly alter the signals, we compared them to raw delta fluorescence and signal averaged raw delta fluorescence signals and found that the noise was significantly reduced by both techniques, yet there was no significant decrease in the rate of the upstroke or time to repolarization noted (see Figure 4-4B).

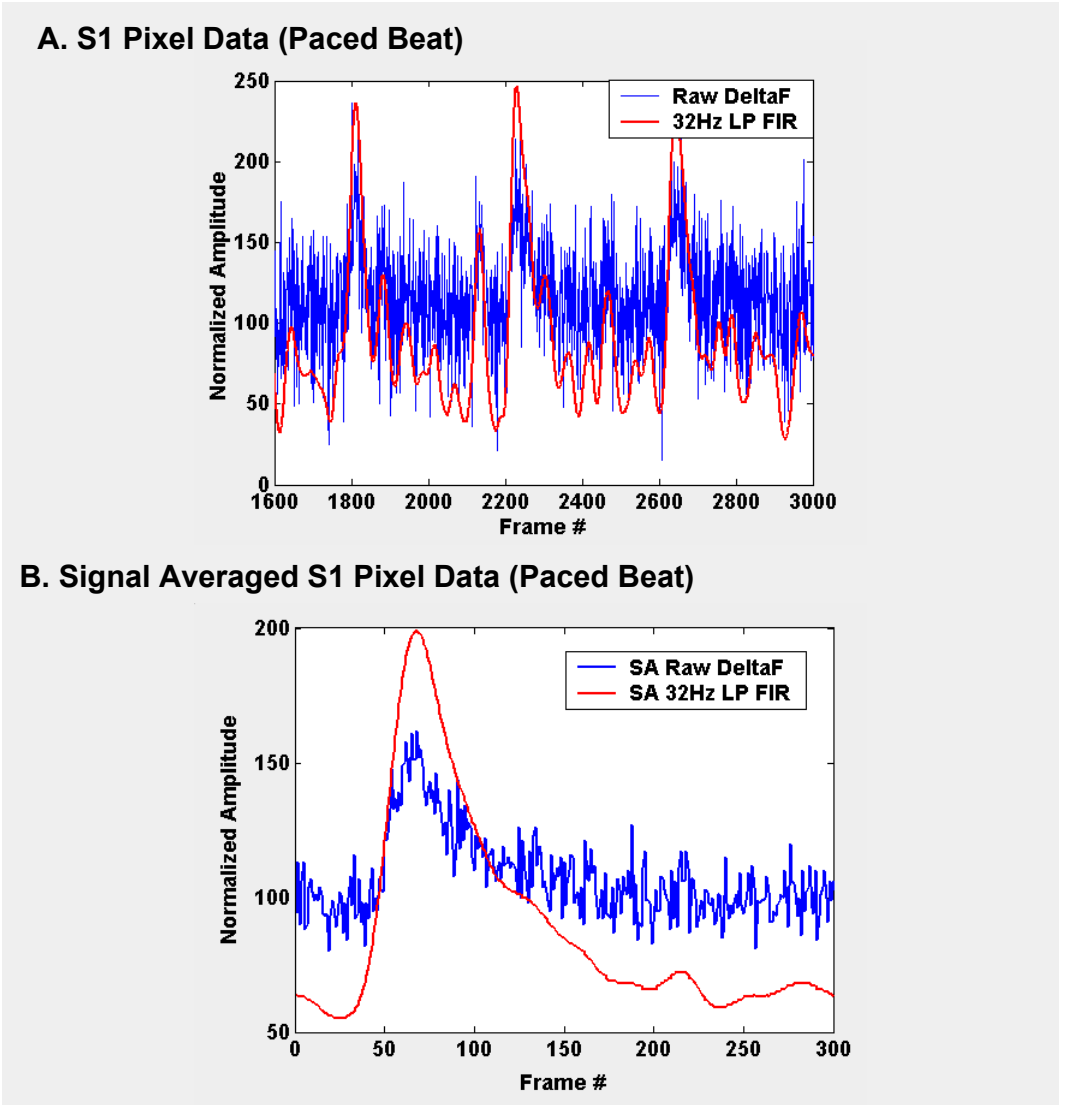

Figure 4-4. Signal Processing of Raw Optical Mapping Data.
A. Inverted and normalized (0 to 256) raw delta fluorescence from a single pixel has high frequency 'shot' noise due to CCD camera, especially with increased KCL concentrations. To remove this noise, the signals are digitally filtered using a Finite Impulse Response (FIR) low pass filter with a 32Hz cutoff frequency. Note that the raw fluorescence tends to have higher background noise due to random low amplitude pixel variance. **B.** To reduce the influence of residual noise and movement artifact in the FIR or Raw Fluorescence signals we signal averaged 50 frames (~50ms) prior to peak mean frame fluorescence to 250 frames after the peak. In this case 9 S1 beats from a single 10,000 frame movie were summed and averaged. Signal averaged S1 beats show similar onset time, and upstroke velocity versus non filtered signals. The clean signals allow us to accurately calculate the activation time (peak dV/dt in upstroke), and significantly increase the sensitivity to a subthreshold pulse.

Conduction Velocity/Activation Patterns

Optical conduction velocity in this model can be calculated by measuring differences in peak amplitude as it changes across a region centered on a pixel of interest, in comparison with the surrounding pixels, from one image to the next. Calculating the plane of the slope of these differences allows us to create a vector indicating the speed, and direction of activation as described previously [484]. In practice, calculation of these vectors, and plotting them in real time, was less informative than initially anticipated (see Figure 4-5). It was noted in these and previous studies that the calculation of the vectors is highly susceptible to noise, tissue orientation, and motion artifact.

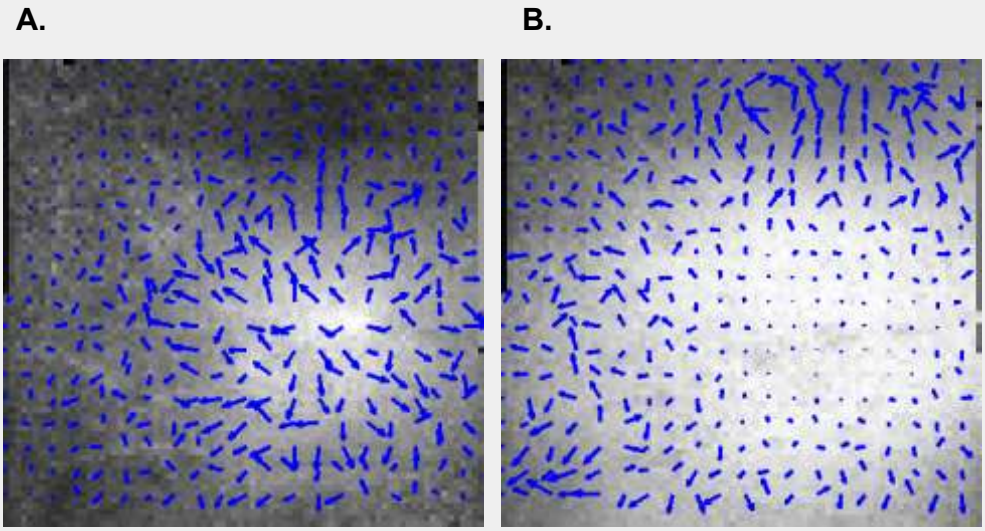

Figure 4-5. Conduction velocity motion vectors of a centrally paced activation.
A. Amplitude/velocity vectors showing changing motion of activation wave front from frame to frame. **B.** Following complete activation (no change in amplitude) there is a decline in the vector size showing, lack of motion in the central 'activated' region.

Alternately we, and others, have demonstrated that it is much easier to see differences in CV using an isochronal activation time map. Although differences were slight, we were able to detect a decrease in conduction velocity in the infected regions as evidenced by crowding of isochrone lines with normal 4.4 mM KCL (see Figure 4-6B,D,E). This decline became more pronounced with increased extracellular KCL (see Figure 4-6C,F). It was also noted in a number of

cases that increasing KCL lead to conduction block, and tended to induce activation around the infected region (see Figure 4-6F). Thus predisposing the region for possible reentry induced arrhythmia. The observation that conduction is normal with low KCL, and impaired as it is increased has been shown recently [540]. Where it was shown that the heart has a fairly large electrical reserve, and that conduction will often break down first in a region with impaired coupling. Unfortunately, a similar effect was noted in both the control GFP infected hearts and the AMPK virus treated hearts, indicating that infection of the region rather than (or in addition to) the activation of AMPK in the region was responsible. It is certainly possible that increased inflammation or damage may have an effect.

Subthreshold Mapping and Calculation of Space Constant (λ)

By using longer pulse durations as in Akar *et al.* in addition to high KCL to increase the pacing threshold (allowing larger input current) visualization of subthreshold signals was achieved. Furthermore, with the much improved signal to noise ratio obtained by recent digital filtration and signal averaging, it was also possible to measure the space constant of electrotonic coupling (λ) (see Figure 4-7). These values were calculated by averaging 3 pixels that run through the center of the region in either the row or column orientation which here correspond to the longitudinal or transverse respectively. Although larger (especially in the longitudinal direction) than previously reported in the guinea pig heart, we observed values of ~3.0± 0.19mm in the longitudinal direction, and 0.99±0.19 in the transverse direction (versus 1.5mm and 0.8mm respectively reported from a guinea pig). These values are also similar to those observed in the transverse orientation in a pig heart. Despite these significant successes, we have so far been unable to compare accurately λ from the infected GFP versus AMPK regions (due to low n numbers of comparable pacing sites), although this may be possible in the future with further analysis.

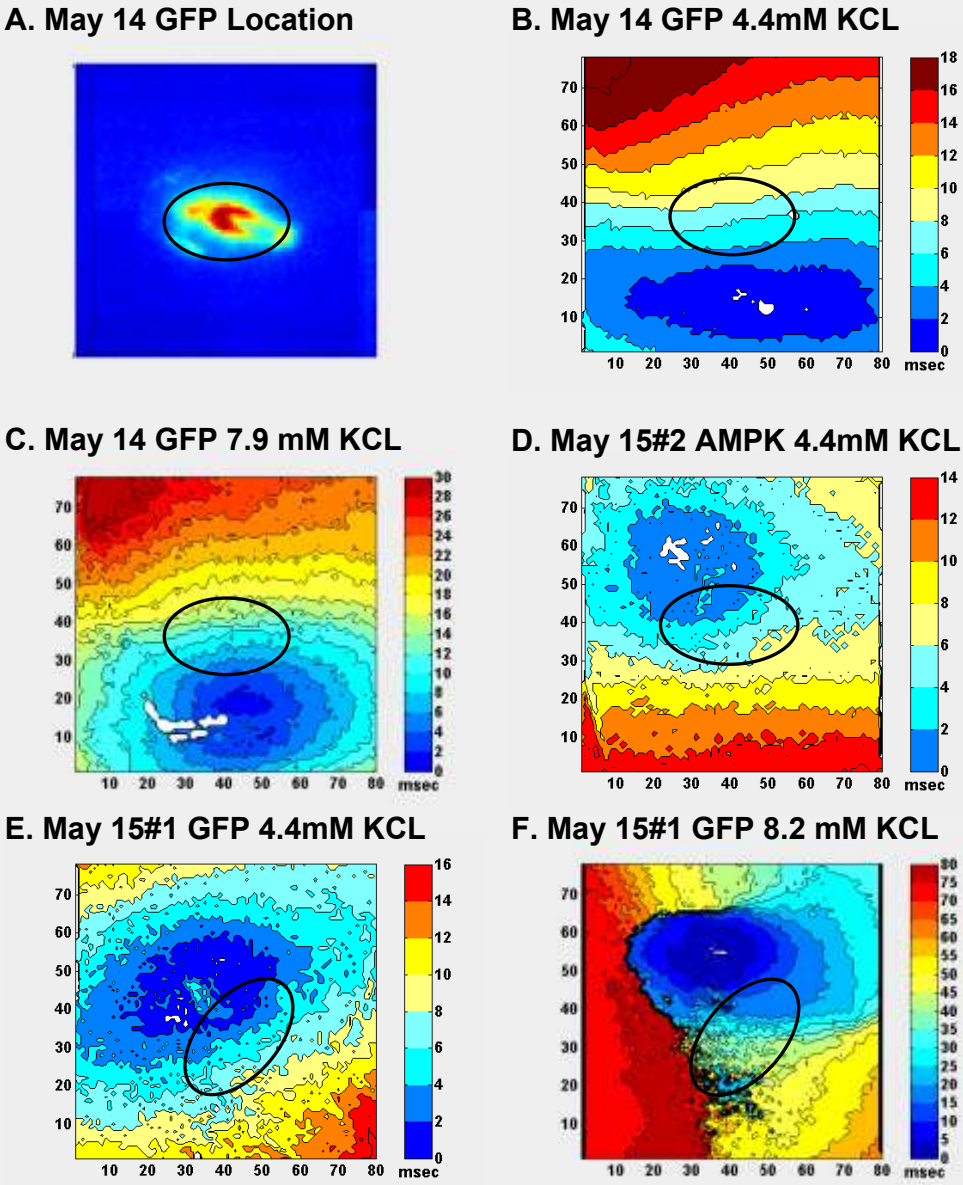

Figure 4-6. Activation of adenoviral infected rat heart.
A. Location of GFP expression (adenoviral infection site) with the optical mapping camera. **B.** Activation of the same region with normal 4.4mM KCl shows a slight slowing in conduction velocity (crowding of 2ms isocrone lines) in that region. **C.** This slowing is more apparent with increased KCl. **D.** Infection with AMPKca virus appears to slow conduction as well, although to a lesser extent in this example. **E.** Relatively normal activation with 4.4mM KCL with some slowing of conduction in the infected region. **F.** Despite reasonably normal activation (E), in some cases increased KCL lead to conduction block and reentry .

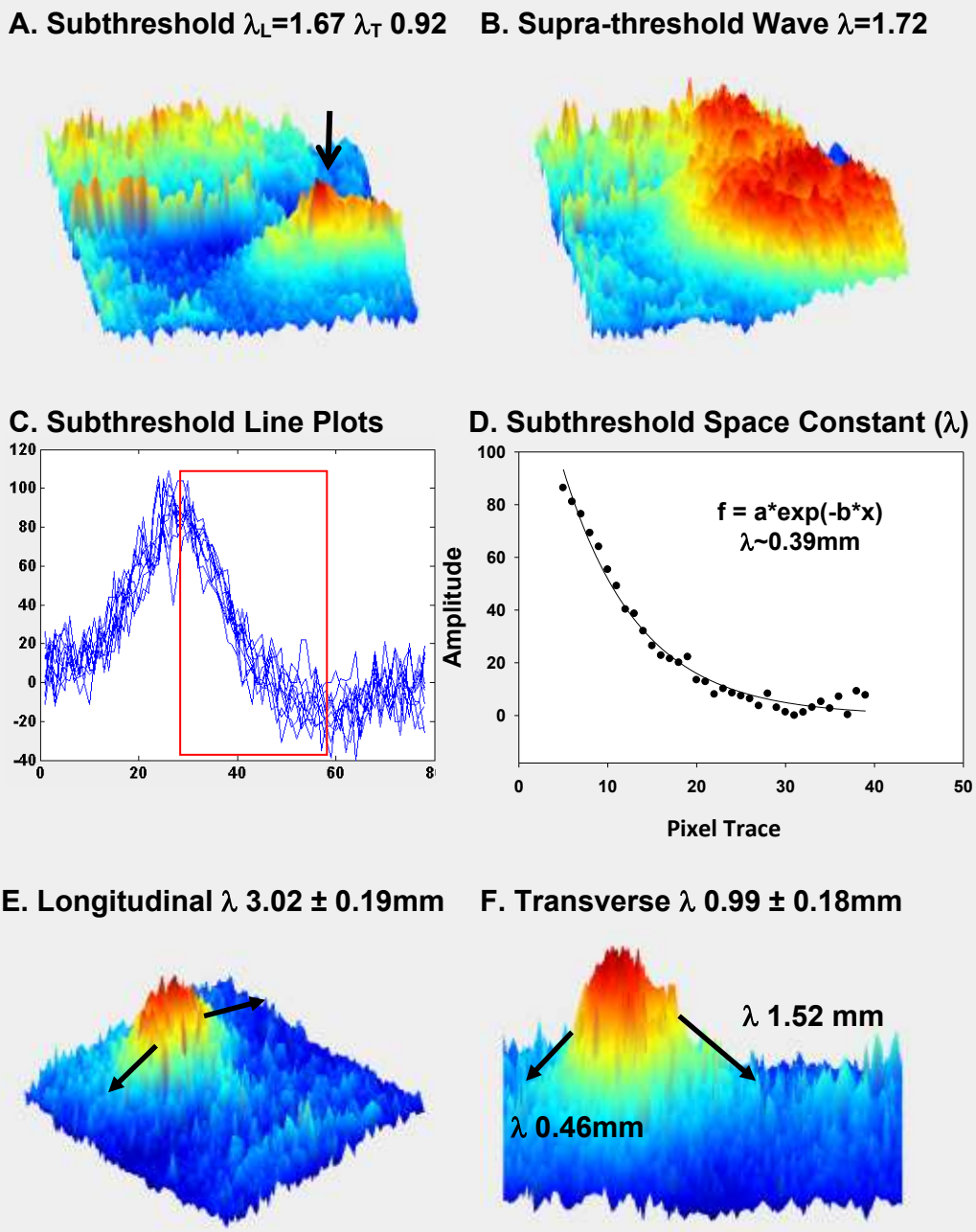

Figure 4-7. Estimation of junctional coupling by subthreshold optical mapping.
A. Surface plot showing Signal Averaged (3) subthreshold pulse (bottom right - arrow) under high KCL perfusion (6-8mM). **B.** Supra-threshold pulse from the same site showing similar decay in amplitude across activation wave front. **C.** Line plots of individual pixel rows across the subthreshold pulse peak. **D.** Exponential decay fit of the mean amplitude from C, λ calculated as distance (#pixels ~0.1mm/pixel) at which the amplitude decays by 1/e (0.3679). **E.** Steady state amplitude at end of 20 ms subthreshold pacing pulse, λ somewhat longer than literature values expected to be 1.5 to 0.8mm long to trans respectively. **F.** In the transverse direction, λ of 0.99 ±.18 mm is similar to the values reported previously.

Since we have used a 5xS1 plus S2, S3 at the most we can signal average 1-3 subthreshold pulses in a typical 10,000 frame movie. In the future, the accuracy and measurement of the subthreshold pulse could be significantly improved by using repeated pulse trains of a single suprathreshold pulse (for amplitude normalization), followed by a subthreshold one. Signal averaging is much more effective with increasing samples (noise reduction ~$1/n^2$). Thus when using up to identical 10 beats the results are much better than that using only 2 or 3 beats as shown here for the subthreshold analysis.

The signal to noise ratio was reduced significantly by the use of KCL (which depolarizes the membrane). To alleviate this perceived degradation of the signal, we also utilized the sodium channel inhibitor lidocaine to increase the pacing threshold while maintaining normal membrane potential. However, in the one experiment, it did not qualitatively appear to significantly increase the signal to noise ratio when processed with the same digital filtration and signal averaging as applied here (data not shown).

Overall Utility and Limitations

Optical mapping was effective in demonstrating activation patterns and conduction velocity changes in these rat hearts, as well as allowing us to visualize sites of infection on the ventricular surface easily. It was also more recently possible to obtain direct measurements of junctional conductance. Previously, this had been thought unattainable due to significant noise artifact in the signals (one significant reason these studies were initially discontinued). One significant drawback to this methodology is the expense of both di-4ANNEPS, and more importantly cytochalasin D which can exceed $300/rat used for proper staining and motion artifact minimization. In the end, following the appreciation that the viral infection caused significant inhibition of junctional conductance non-specifically, possibly by the development of fibrosis, damage during injection, or as noted in later chapters, by an increase in AMPK activity due to infection with the GFP virus, these studies were discontinued. To finalize these studies, it

would be useful to measure histologically whether there was a significant increase in fibrosis or inflammation in these regions that correlated with the changes in conduction observed. For the future, this methodology could in theory be used to examine acute pharmacological AMPK activation or inhibition as initially intended in the rat heart electrical mapping studies that were discontinued.

4.5 Dual Cell Patch Clamp

4.5a Overview and Theoretical Benefits

Dual cell patch clamp is the gold standard method of measuring GJ conductance changes. The standard techniques used in the literature have been reviewed (page 349-361)[28]. The general approach is similar to all whole cell patch clamp methods in mammalian cells. A gigaohm seal is applied using a glass micropipette. The pipette itself is filled with a buffer approximating intracellular conditions, and the membrane under the patch electrode tip is ruptured. The voltage potential of the cell membrane is clamped at a certain value, then the current required to maintain that voltage is measured. In dual cell patching, this process is duplicated on two cells that are attached, thus by clamping one cell at a certain voltage, as you change the other cells voltage, a potential across the two cell membranes (junctional voltage) is measurable. Although there are certain assumptions and corrections that need to be applied (series resistance of the recording electrodes being a major example)[541, 542], with proper conditions and data analysis, one can accurately measure junctional conductance directly. In general, it is best to have low junctional coupling (poorly coupled cells), and minimal electrode resistance to get the most accurate estimate of junctional current (macroscopic junctional conductance). It has also been suggested that a ramp protocol can reduce the effects of initial voltage transient errors on junctional currents [28].

Being able to directly measure junctional conductance readily, repeatedly and accurately allows real time measurement of junctional conductance as experimental conditions change. Under more stringent conditions, with very limited junctional coupling, it is also possible to measure single junction gating events that allow measurement of open probability and single channel conductance. These events are unambiguously measured by seeing an equal and opposite effect in both cells.

This technique does however have its limitations. The generation of very minimally coupled cells is dependent on the number of channels between the cells, and is not easily controlled in many cases without the addition of commonly used uncoupling agents such as heptanol, octanol, or halothane, which are also known to reduce open probability [175, 543, 544]. This has been partially addressed by using custom engineered cell lines that have drug dependent expression of Cx subunits under control of tetracycline or the lac operon system [545]. But they are not readily transferrable to multiple cell lines.

In addition, the success rate for a single cell patch clamp experiment, (assuming relatively strong user proficiency) is in the neighborhood of 20%, thus in order to get two perfectly sealed cells, the rate is $1/5^2$ or ~4% success. This can of course be highly dependent on the cell type being studied as some cells are easier to patch than others. The most studied mammalian cells are the neuronal 2A (N2A), as well as HeLa cell lines. These are used due to their low expression rates for endogenous connexins (although no cell line is completely Cx deficient), as well as their ease of culture, and in the case of N2A cells, their uniform circular shape and thus ease of patching [546, 547].

4.5b Materials and Methods

N2A, HeLa, and Hek293 T-Rex cells were cultured per section 2.3.

Using the MultiClamp system (Axon Instruments), and a Zeiss Axiovert 200M microscope equipped with epifluorescent illumination for green fluorescent protein. Cells were transferred to the heated stage and perfused with Tyrode buffer pH 7.4. Appropriate smooth membrane, well coupled cell pairs for dual cell patch were common using both N2A, and Hek293 cells.

4.5c Preliminary Results and Discussion

In collaboration with Dr. Hank Duff (University of Calgary), and despite the availability of trained and seasoned support staff, the success rate for these initial studies was too low to justify continued experimentation. The major difficulties were due to difficulties forming and maintaining stable gigaohm seals when manipulating the microelectrode to patch two cells. Successful patching was ~10-20%, but with very few successful experiments, and none that were stable enough for a pharmacological before and after treatment analysis. These experiments were discontinued pending review of the methodology and at the suggestion of my supervisory committee. Overall, the technique has been proven in a number of laboratories, but requires significant experimental expertise and a sizable investment in equipment. The use of pharmacological uncoupling agents like cytochalasin-D (to cleave actin microfilaments), and pharmacological means of reducing intracellular calcium to limit contractile function may enable the dual cell study of more physiologically relevant cells in the future as well. If there are significant experimental objectives that need to be clarified (i.e. single channel conductance, open probability etc.), then the investment would be worthwhile, but requiring patience to develop and perfect the technique.

4.6 Macroscopic Junctional Conductance – Dye Transfer Assays

Measurement of junctional conductance without the problems inherent with electrical signal recording is possible by the use of fluorescent dye transfer assays. These assays have been well documented in the gap junction literature and measure 'macromolecular' or 'metabolic' junctional permeability. Junctional permeability to different sized or charged dye molecules depends on the number, Cx type, and their activity/phosphorylation state. It is not always correlated to junctional electrical conductance. For example, Cx40 has a very large unitary electrical conductance, but a very small permeability to negatively charged or large dye molecules [171, 548]. These differences have been shown to functionally distinguish between junctions of different subtype, and can predict the permeability to various signaling molecules like cAMP [29, 167, 549]. As such, permeability to dye is recognized in the literature as being physiologically relevant to intercellular signaling. The primary difference in these dye transfer assays is the method used to incorporate dye into the primary cell(s) but in general they measure junctional conductance by either the number of cells with detectable dye after a certain time period, or the concentration of dye in the recipient cell(s).

4.6a Dye properties

The permeability of various dyes can be linked to their structural properties. For example, the size of the molecule, as well as any charge on a portion of the molecule can have significant effects on its permeability through various connexin subtypes. The properties of the most commonly used dyes are shown in Table 4-1. Generally speaking the smaller dyes are more soluble than larger, and certain Cx subtypes show some selectivity for either positive or negative charges. For example Cx40 has a smaller dye permeability, with cationic selectivity, thus we opted to use calcein blue dye in the majority of the Cx40 studies due to its size and neutral charge, and to allow the use of GFP expressing constructs and viri. For Cx43 which has a larger pore, and is slightly anionic

selective – we used the Alexa dyes, calcein green when labeling with GFP was not an issue, Alexa594 when it was, or calcein blue (for consistency).

Table 4-1. Fluorescent Dye Properties.

Tracer	*MW (Da)*	*Size (Å)*	*Charge*	*Ref.*
Alexa350	349	14.1 x 13.7 x 8.1	-1	
Alexa488	570	14.1 x 13.7 x 11.5	-1(-2, 1)	
Alexa594	759	17.4 x 17 x 14.8	-1(-2, 1)	
Calcein (green)	**623**		**-4(-6,2)**	
Calcein blue	**321**		**0**	
6-carboxyfluorescein (6-CF)	376	12.6 x 12.7 x 8.5	-2	[550]
4,6-diamidino-2-phenyl-indole dihydrochloride (DAPI)	279	15.4 x 6.0	2	[165]
Dichlorofluorescein (DCF)	401	12.3 x 12.7 x 5.5	-1	[550]
Ethidium broimide (EB)	314	11.6 x 9.3	1	[165]
Hydroxycoumarin carboxylic acid (HCCA)	206		-6	
Lucifer yellow (LY)	443	10.6 x 9.5,	-2	[165]
		12.6 x 14 x 5.5		[550]
Neurobiotin (NB)	287	12.7 x 5.4	1	[165]
Propidium iodide (PI)	441	12.9 x 9.3	1	[165]
NBD-m-TMA	139	5.5 Å	1	[168]

4.7 Single Cell Dye Microinjection

4.7a Overview and Theoretical Benefits

This method requires a membrane impermeable dye like lucifer yellow (mw 443, -2 charge) or Alexa594 (mw ~759kDa, -1 charge) that is gap junction permeable. The dye is loaded into a small bore glass microelectrode and then injected into a single cell of a monolayer either by pressure, or by current application. Smaller, less negatively charged dyes like ethidium bromide (mw 314 kDa, +1 charge), or neurobiotin (287kDa, +1 charge) can be used for cation selective Cx40 junctions. These dyes are often mixed with large non-junction permeable dye like dextran (mw 10,000 kDa) conjugated with calcein dye to mark the cell injected. The rate

of junctional conductance is estimated by counting the number of cells which receive a detectable amount of dye in a certain amount of time.

4.7b Materials and Methods

Neonatal cardiac myocytes were isolated as described in section 2.3 for single cell microinjection studies per section 2.13a. They were either untreated, or infected with 10moi adenovirus containing GFP, or $AMPK_{CA}$ for 48h. Treatment with 2-deoxyglucose (5mM) plus oligomycin (5μM) was used to inhibit junctional coupling [413]. During microinjection cells were placed in Tyrode solution pH 7.4 at room temperature.

Single cells in the middle of a field of view were injected with Alexa594, and dye was allowed to diffuse into neighboring cells. Bright field, GFP, Dapi (Hoechst 33342), and CY3 (AlexaFluor 594) channel photographs were acquired in sequence to document the cell injected, whether it was infected with virus, and how many cells were co-expressing Hoechst and AlexaFluor594 (see Figure 4-8).

4.7c Preliminary Results and Discussion

Injection of neonatal cardiac myocytes was reasonably successful but often the cell would be over-loaded or under-loaded depending on the efficacy of dye injection. Variation in junctional conductance was often also apparent within the same dish, where cells that appeared to be tightly bound to their neighbors had unexpectedly very low dye permeability. Treatment of neonatal cardiac myocytes with adenoviral AMPKca was initially thought to reduce junctional coupling relative to GFP virus. However, with 3 different doses of GFP and AMPKca, there did not appear to be a clear trend in the data. Treatment with 5mM 2-deoxyglucose with 5μM oligomycin (to inhibit glucose uptake, and the electron transport chain respectively) caused a time dependent decrease in junctional coupling (presumably by ATP depletion but this was not measured)(see Figure 4-9).

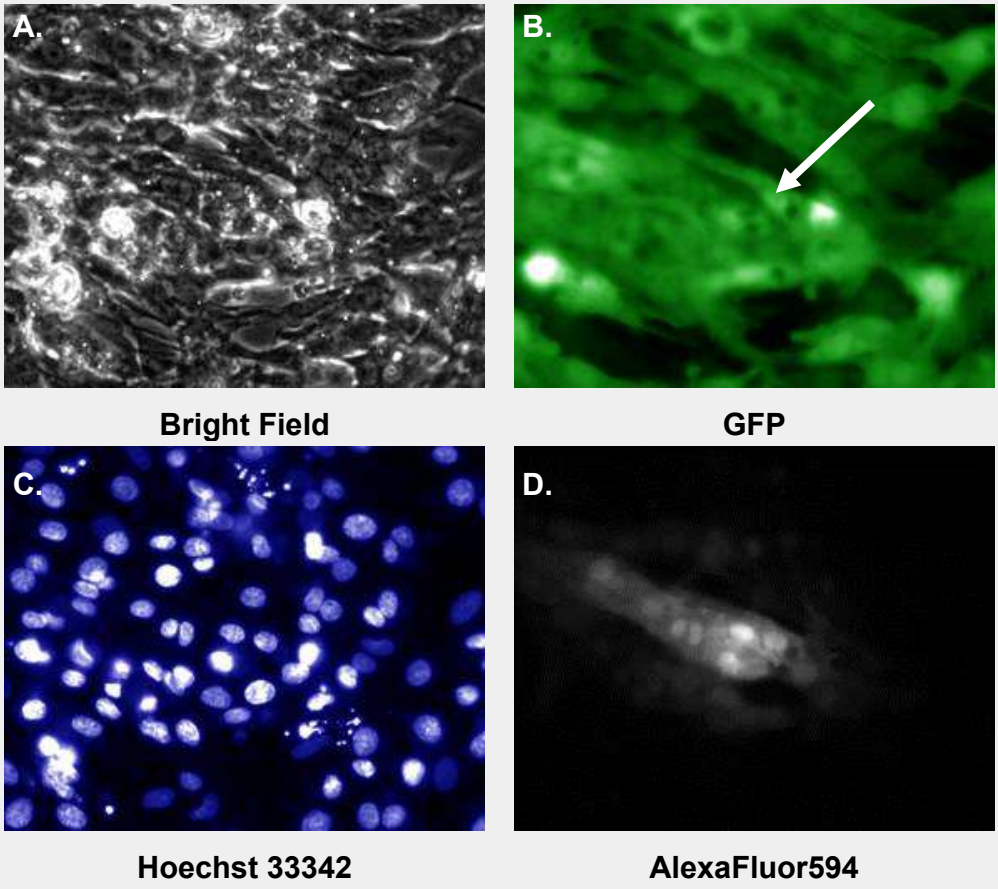

Figure 4-8. Single cell microinjection of AlexaFluor594 dye for the measurement of junctional coupling in neonatal cardiac myocytes.
A. Bright field view of the cells. **B.** Expression of GFP/AMPK virus was confirmed by expression of GFP. Dye was injected into a single cell (white arrow). **C.** Hoechst 33342 allows counting of cells in confluent monolayer. **D.** Dye transfer from injected cell to its neighbors.

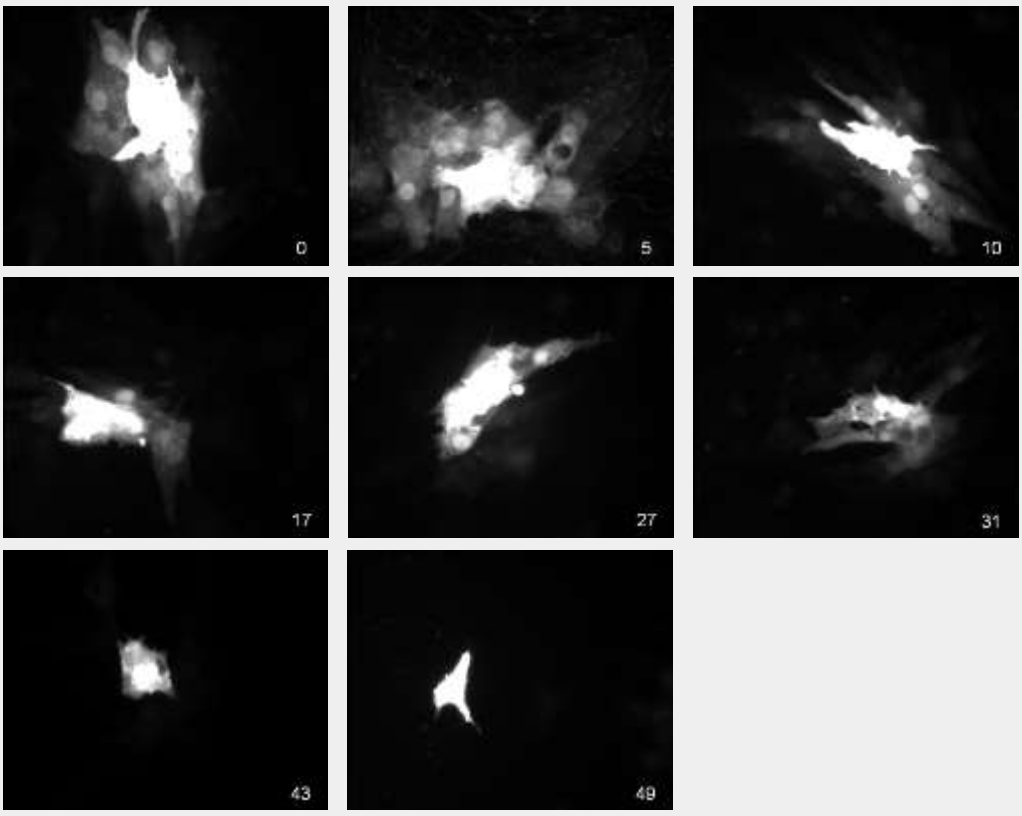

Figure 4-9. Inhibition of junctional coupling by 2-deoxyglucose & 5μM oligomycin in neonatal cardiac myocytes
Representative images of cells injected at time (inset, in minutes) after addition of 2-deoxyglucose (5mM) and oligomycin (5μM) to inhibit glycolysis, and the electron transport chain respectively.

4.7d Drawbacks and Limitations

This methodology is useful but limited due to fairly large variance in the amount of dye injected per cell. This variance can be attributed largely to error in the production of glass microelectrodes thereby producing inconsistent dye diffusion rates. Achieving consistent electrodes was often not possible from pull to pull, as they tended to change over time. The glass microelectrodes also tended to become occluded or break during the injection procedure. In addition, changes in the degree of junctional coupling that are inherent to the system are significant. This variance reduces the precision of the model to detect changes in gap junctional conductance. In addition, these measurements are time

consuming in that repeated injections of 5-10 cells per dish are required. Since a new electrode was often required to minimize loss of loading due to membrane occlusion (debris from injection) this meant that upwards of 10 good electrodes were needed. As stated before, it was not possible to use all electrodes due to variations in the pore size/shape or permeability to dye (tested under fluorescence before use of any electrode during adjustment of compensation pressure). In short, these measurements are useful for detecting gross changes in permeability, as seen with ATP depletion, but less so for more subtle changes in conductance.

4.8 Scrape Loading

4.8a Overview and Theoretical Benefits

Another method of dye transfer is termed scrape loading, in which the same membrane impermeable fluorescent dyes used in the previous section are diluted in a buffer free from calcium. A cell monolayer is then scraped/cut with a scalpel blade, and dye is allowed to access the cells along the cut edge for a certain amount of time prior to rinsing with clean buffer. These cells then pass dye to their neighbors, and the amount of junctional coupling is assessed by the distance (from the cut edge) to which dye transfer is detected. One benefit to this method is that a larger number of cells can be assayed at once, correcting for changes in cell orientation, or cell-cell coupling that can significantly alter results in the single cell injection method.

4.8b Materials and Methodology

See section 2.3, and 2.13b for methodology. Neonatal cardiac myocytes were labeled with Hoechst 33342, rinsed and scored in 3 parallel lines with a scalpel blade then incubated with dye (one GJ permeable, and one not permeable) for 2 minutes, then fixed for subsequent imaging.

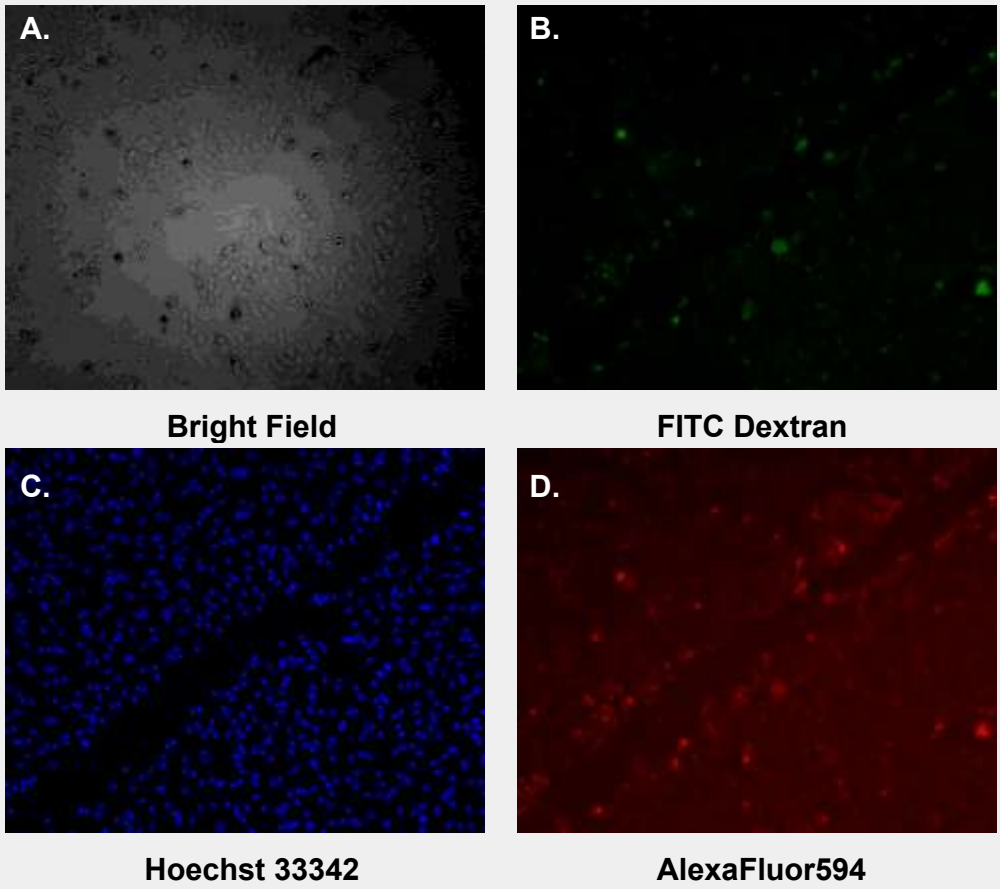

Figure 4-10. Scrape loading of AlexaFluor594 dye for the measurement of junctional coupling in neonatal cardiac myocytes.
A. 10x magnification bright field view of the cells. **B.** FITC Dextran (non-GJ permeable) showing cells damaged by scrape. **C.** Hoechst 33342 allows counting of cells in confluent monolayer. **D.** Dye transfer from damaged cells to their neighbors.

4.8c Preliminary Results and Discussion

Scrape loading was moderately successful (see Figure 4-10) as we could clearly see cells that were labeled with AlexaFluor dye along the scrape line, and that cells nearest the line showed some degree of GJ permeable dye loading. With nuclear staining, it was possible to estimate the number of cells affected. However, it was often either difficult to see the FITC dextran staining, or difficult to differentiate between stained and non-FITC stained cells (which indicates those that received dye directly, and those that were passed dye from stained neighbors). 20x magnification may improve our ability to visualize the FITC-dextran staining, however 40x was too close to see the total cell count. This

methodology may be somewhat insensitive to all but large changes in dye permeability, and better suited for questions of yes/no conductance. It should be noted that these studies could have been optimized, and it would have been useful to titrate the diffusion time, and FITC-dextran concentration to improve the assay sensitivity.

4.9 GapFRAP Dye Transfer.

Another method of measuring kinetics of dye transfer can be assessed by the GapFRAP technique with some modifications to the protocol described previously for Cx43 containing cells [372].

4.9a Materials and Methods

Please see section 2.3 for cell culture, and 2.13d for GapFRAP methodology. Hek293 cells were cultured, and loaded with Cell Trace Calcein Blue AM. Pairs of cells were identified based on defined selection criteria. One cell of the pair was bleached, and 20 subsequent scans were recorded at either 5s (Cx43) or 10s (Cx40) intervals to measure the rate of fluorescence recovery.

4.9b Preliminary Results and Discussion

The collection of data with this technique was straight forward and could be done in any lab with access to a confocal microscope with UV or two photon excitation (for calcein blue, other dyes can be used without these lasers). It is usable with virtually any type of cell including neonatal cardiac myocytes, adult cardiac myocytes, or propagated cell lines for example Hek293 cells as needed. The recovery in Hek293 cells was shown to be heptanol sensitive (see section 5.3f), and induction of Cx40 or Cx43 in these Hek-293 cells increased the degree of coupling significantly.

As with the microinjection technique, due to variations in the amount of cell-cell contact, and differences in cell to cell variation, it was beneficial to measure as large a number of cell pairs as possible. However, in comparison to the other dye

transfer techniques it allows us to measure the actual kinetics of dye exchange between two cells in real time. For these combined reasons (ease of use, cost, and replication) this technique was used for the remainder of the studies presented in this thesis.

4.10 Conclusions

The methods available for measuring gap junctional conductance are varied and have a range of effectiveness. The *in vivo* electrical methods are useful for measuring tissue level systems and we did measure significant differences in the space constant with our 3h rapid pacing protocol. However, it should be noted that in the *in vitro* isolated heart system, we were unable to specifically inhibit junctional conductance and measure a change in space constant (when measured with our electrode array and using an externally applied subthreshold pacing stimulus). In this case, there were concerns with shunting currents etc. that we were not able to eliminate. These issues are not expected to be an issue in the pig model. Some of these issues could be abrogated by using a four plunge electrode method of measuring junctional conductance/tissue resistivity. However, problems (in the rat Langendorf model) with arrhythmogenesis, poor contractility, damage to the heart from the plunge electrodes, as well as noisy signals, and our inability to develop a durable and re-usable electrode system for its continued use were prohibitive in our hands.

Although further study may be necessary, it appears that using the optical mapping system with a central plunge pacing electrode (not an option with the contact mapping array) and the newest techniques for data analysis and processing, we were able to measure junctional conductance optically. However, motion artifacts, the cost of the dye/uncoupling agents, and their potential for significant non-specific effects on other membrane proteins/ion channels etc. made this technique less optimal.

The dye transfer techniques were clearly able to measure junctional conductance specifically, in a way that was heptanol sensitive. These techniques were best represented by the GapFRAP assay in ease of use and reliability while providing actual kinetic information about junctional conductance in real time. Despite limitations due to the number of cells required for statistical analysis, and the number measureable per hour on the scope, it still represents the most feasible of the techniques used to this point in our laboratory. That being said, it would be beneficial to expand these studies utilizing the most recently developed pharmacological tools. For example, the optical mapping studies could be repeated with A-769662, or compound-991, and compound-C to bypass the viral and injection dependent issues. Further, exploration of the dual cell patch clamp protocol would be especially beneficial: it would give us another functional methodology (to validate the dye transfer assay), allow for more detailed analysis of gating and rapid time scale events, and allow for before/after paired analysis. This is a key advantage, as even the GapFRAP technique has the limitation of only being able to measure coupling once or perhaps twice in the same cell pair (photo-bleaching will inevitably lead to damage and changes in the subsequent measurements).

4.11 Literature Cited

[28] Harris AL. Emerging issues of connexin channels: biophysics fills the gap. Quarterly reviews of biophysics. 2001;34:325-472.

[29] Bedner P, Niessen H, Odermatt B, Kretz M, Willecke K, Harz H. Selective permeability of different connexin channels to the second messenger cyclic AMP. J Biol Chem. 2006;281:6673-81.

[165] Elfgang C, Eckert R, Lichtenberg-Frate H, Butterweck A, Traub O, Klein RA, et al. Specific permeability and selective formation of gap junction channels in connexin-transfected HeLa cells. The Journal of cell biology. 1995;129:805-17.

[167] Kanaporis G, Mese G, Valiuniene L, White TW, Brink PR, Valiunas V. Gap junction channels exhibit connexin-specific permeability to cyclic nucleotides. J Gen Physiol. 2008;131:293-305.

[168] Kanaporis G, Brink PR, Valiunas V. Gap junction permeability: selectivity for anionic and cationic probes. Am J Physiol Cell Physiol. 2011;300:C600-9.

[171] Rackauskas M, Verselis VK, Bukauskas FF. Permeability of homotypic and heterotypic gap junction channels formed of cardiac connexins mCx30.2, Cx40, Cx43, and Cx45. American journal of physiology. 2007;293:H1729-36.

[175] He DS, Burt JM. Mechanism and selectivity of the effects of halothane on gap junction channel function. Circulation research. 2000;86:E104-9.

[372] Cameron SJ, Malik S, Akaike M, Lerner-Marmarosh N, Yan C, Lee JD, et al. Regulation of epidermal growth factor-induced connexin 43 gap junction communication by big mitogen-activated protein kinase1/ERK5 but not ERK1/2 kinase activation. J Biol Chem. 2003;278:18682-8.

[413] Turner MS, Haywood GA, Andreka P, You L, Martin PE, Evans WH, et al. Reversible connexin 43 dephosphorylation during hypoxia and reoxygenation is linked to cellular ATP levels. Circulation research. 2004;95:726-33.

[475] Steendijk P, Mur G, van der Velde ET, Baan J. The four-electrode resistivity technique in anisotropic media: theoretical analysis and application on myocardial tissue in vivo. IEEE TransBiomedEng. 1993;40:1138-48.

[476] Padilla F, Garcia-Dorado D, Rodriguez-Sinovas A, Ruiz-Meana M, Inserte J, Soler-Soler J. Protection afforded by ischemic preconditioning is not mediated by effects on cell-to-cell electrical coupling during myocardial ischemia-reperfusion. American journal of physiology. 2003;285:H1909-16.

[477] Baynham TC, Knisley SB. Effective epicardial resistance of rabbit ventricles. AnnBiomedEng. 1999;27:96-102.

[480] Nygren A, Clark RB, Belke DD, Kondo C, Giles WR, Witkowski FX. Voltage-sensitive dye mapping of activation and conduction in adult mouse hearts. AnnBiomedEng. 2000;28:958-67.

[481] Witkowski FX, Leon LJ, Penkoske PA, Giles WR, Spano ML, Ditto WL, et al. Spatiotemporal evolution of ventricular fibrillation. Nature. 1998;392:78-82.

[482] Witkowski FX, Clark RB, Larsen TS, Melnikov A, Giles WR. Voltage-sensitive dye recordings of electrophysiological activation in a Langendorff-perfused mouse heart. CanJCardiol. 1997;13:1077-82.

[484] Guo Q, Mandal MK, Liu G, Kavanagh KM. Cardiac video analysis using Hodge-Helmholtz field decomposition. Computers in biology and medicine. 2006;36:1-20.

[519] Akar FG, Roth BJ, Rosenbaum DS. Optical measurement of cell-to-cell coupling in intact heart using subthreshold electrical stimulation. American journal of physiology. 2001;281:H533-42.

[531] Burt JM, Steele TD. Selective effect of PDGF on connexin43 versus connexin40 comprised gap junction channels. Cell Commun Adhes. 2003;10:287-91.

[532] Cottrell GT, Wu Y, Burt JM. Cx40 and Cx43 expression ratio influences heteromeric/ heterotypic gap junction channel properties. Am J Physiol Cell Physiol. 2002;282:C1469-82.

[533] Haefliger JA, Demotz S, Braissant O, Suter E, Waeber B, Nicod P, et al. Connexins 40 and 43 are differentially regulated within the kidneys of rats with renovascular hypertension. Kidney Int. 2001;60:190-201.

[534] Oyamada Y, Komatsu K, Kimura H, Mori M, Oyamada M. Differential regulation of gap junction protein (connexin) genes during cardiomyocytic differentiation of mouse embryonic stem cells in vitro. Exp Cell Res. 1996;229:318-26.

[535] Johnson TL, Nerem RM. Endothelial connexin 37, connexin 40, and connexin 43 respond uniquely to substrate and shear stress. Endothelium. 2007;14:215-26.

[536] Salameh A, Frenzel C, Boldt A, Rassler B, Glawe I, Schulte J, et al. Subchronic alpha- and beta-adrenergic regulation of cardiac gap junction protein expression. Faseb J. 2006;20:365-7.

[537] Rossi S, Baruffi S, Bertuzzi A, Miragoli M, Corradi D, Maestri R, et al. Ventricular activation is impaired in aged rat hearts. American journal of physiology. 2008;295:H2336-47.

[538] Simonotto JD, Myers SM, Furman MD, Norman WM, Liu Z, DeMarse TB, et al. Coherence analysis over the latent period of epileptogenesis reveal that high-frequency communication is increased across hemispheres in an animal model of limbic epilepsy. Conf Proc IEEE Eng Med Biol Soc. 2006;1:1154-6.

[539] Furman MD, Simonotto JD, Beaver TM, Spano ML, Ditto WL. Using recurrence quantification analysis determinism for noise removal in cardiac optical mapping. IEEE transactions on bio-medical engineering. 2006;53:767-70.

[540] Nygren A, Olson ML, Chen KY, Emmett T, Kargacin G, Shimoni Y. Propagation of the cardiac impulse in the diabetic rat heart: reduced conduction reserve. The Journal of physiology. 2007;580:543-60.

[541] Veenstra RD, Wang HZ, Westphale EM, Beyer EC. Multiple connexins confer distinct regulatory and conductance properties of gap junctions in developing heart. Circulation research. 1992;71:1277-83.

[542] van Rijen HV, van Kempen MJ, Postma S, Jongsma HJ. Tumour necrosis factor alpha alters the expression of connexin43, connexin40, and connexin37 in human umbilical vein endothelial cells. Cytokine. 1998;10:258-64.

[543] Veenstra RD, DeHaan RL. Cardiac gap junction channel activity in embryonic chick ventricle cells. The American journal of physiology. 1988;254:H170-80.

[544] Burt JM, Spray DC. Volatile anesthetics block intercellular communication between neonatal rat myocardial cells. Circulation research. 1989;65:829-37.

[545] Zhong G, Mantel PL, Jiang X, Jarry-Guichard T, Gros D, Labarrere C, et al. LacSwitch II regulation of connexin43 cDNA expression enables gap-junction single-channel analysis. BioTechniques. 2003;34:1034-9, 41-4, 46.

[546] Beblo DA, Wang HZ, Beyer EC, Westphale EM, Veenstra RD. Unique conductance, gating, and selective permeability properties of gap junction channels formed by connexin40. Circulation research. 1995;77:813-22.

[547] Srinivas M, Costa M, Gao Y, Fort A, Fishman GI, Spray DC. Voltage dependence of macroscopic and unitary currents of gap junction channels formed by mouse connexin50 expressed in rat neuroblastoma cells. The Journal of physiology. 1999;517 (Pt 3):673-89.

[548] Valiunas V, Beyer EC, Brink PR. Cardiac gap junction channels show quantitative differences in selectivity. Circulation research. 2002;91:104-11.

[549] Ponsioen B, van Zeijl L, Moolenaar WH, Jalink K. Direct measurement of cyclic AMP diffusion and signaling through connexin43 gap junctional channels. Exp Cell Res. 2007;313:415-23.

[550] Brink PR, Ramanan SV. A model for the diffusion of fluorescent probes in the septate giant axon of earthworm. Axoplasmic diffusion and junctional membrane permeability. Biophys J. 1985;48:299-309.

Chapter 5 Inhibition of human cardiac gap junctions Cx43 and Cx40 by phenformin independent of AMPK activation.

This thesis is an original work by Jason Bradley Iden.

No part of this chapter has been previously published.

Adenoviral constructs were supplied by the University of Alberta Cardiovascular Research Group Adenoviral Core Facility
Some GapFRAP experiments and cell culture maintenance were performed by David Dilworth, experimental design, data analysis and interpretation done by Jason Iden.
Cx isolation, sub-cloning, and stable cell generation done by Jason Iden with guidance from Dr. Jim Lees Miller, and Dr Wayne Chen whose lab supplied the HEK-293 cells.

5.1 Introduction

For a detailed summary on gap junction physiology see section 1.3 and 1.6. Gap junctions are low resistance cell-to-cell pathways that connect cells electrically and allow the exchange of signaling molecules up to 1kDa in size. They are composed of end-to-end hemichannels, each of which is a hexamer of connexin subunits (Cx). The major human cardiac gap junctions include hCx40, hCx43, and hCx45 (Cx30.2 is expressed in murine nodal tissues but not in the human heart [98, 106]). Here we will focus on Cx43 and Cx40. Cx43 is expressed in all but the center of the nodal areas, including the ventricular and atrial working myocardium as well as the purkinje fibers [80-91]. Cx40 is expressed in the atrial myocardium as well as in the specialized conductive pathways of the heart (sinoatrial node, AV node, bundle of His, and purkinje network) [83-90, 92-95].

Junctional conductance is the primary determinant of the passive properties of cardiac electrophysiology and the regional expression of these subtypes confers regional differences in cell coupling. Modifications in the expression, activity and distribution of junctional connexin subunits have repeatedly been shown to be associated with arrhythmias or a pre-disposition for them [36-61]. Further, improving Cx mediated conduction has led to the prevention of arrhythmia in a number of models [68, 70-79].Thus understanding their regulation is necessary to understand the generation, and eventual prevention and treatment of cardiac arrhythmias.

5.1a Phospho-regulation of Connexins.

Connexins are regulated by a number of different processes throughout their life cycle, including long term regulation of gene transcription, acute changes in unitary conductance, and altered rates of both transport and degradation. One of the key mediators is direct phosphorylation of Cx proteins. All Cx proteins contain multiple phosphorylation sites for different protein kinases. Phosphorylation can be constitutive or transient, displays cell and tissue

specificity and affect connexin assembly, trafficking, turnover, permeability and protein-protein interaction (for reviews see [353, 551-556].

5.1b Metabolic Phospo-Regulation of Junctional Conductance.

AMPK phosphorylates serine/threonine residues in response to increased ADP and AMP in the cell (for detailed review see section 1.5). Ultimately it acts as an 'energy sensor' stimulating energy (ATP) production via increased glycolysis, glucose uptake, and fatty acid oxidation, and reducing energy demands by inhibiting numerous pathways including protein synthesis by phospho-inhibition of the mTOR pathway. The full array of phosphorylation targets is of course unknown. We have however previously identified AMPK target sequences in the three major human cardiac connexin isoforms hCx40, hCx43, and hCx45. Using a porcine model of rapid atrial pacing we have also shown that within 3 hours after rapid pacing onset that the AMPK pathway is activated and that this time period is associated with a detrimental effect on junctional conductance. Specifically we observed that expression of Cx40 was reduced in some atria, and LV epicardial junctional conductance was reduced, especially in the longitudinal direction, without a corresponding decrease in Cx43 expression (in fact it tended to increase). We were also able to show that co-incubation of AMPK with Cx43 resulted in incorporation of ^{32}P at approximately the correct MW for the immuno-precipitated connexin substrate. It has also been shown that AMPK can inhibit Cx26 in association with a reduction in Cx26 expression (Xenopus oocyte model) [557]. Combined, these data indicate that the reduction of junctional conductance with rapid pacing may be mediated by reduced unitary Cx conductance due to phosphorylation.

The overall goal of this previous work was to show that AMPK mediated phosphorylation of cardiac gap junctions is responsible for the observed effects. However, the primary drawback of these studies was related to the non-specific effects of rapid pacing (which result in the activation of a number of different

pathways), and the co-expression of Cx subunits in the various tissues of the heart (which prevented us from determining which of the cardiac gap junctions were affected). Thus, in order to re-examine the potential regulation of the cardiac gap junctions by phosphorylation, we attempt here to isolate the various connexins and utilize more precise alterations of kinase activity. In this chapter we will be focusing on potential phospho-regulation of Cx43 and Cx40, the primary passive determinants of conduction in the ventricular and atrial myocardium respectively. We utilize adenoviral, and pharmacological mediated modification of AMPK activity with isolated human variants of Cx40 and Cx43 expressed in human Hek293 cells.

5.2 Materials and Methods

For detailed methodology see chapter 2 sections 2.3 (cell lines and culture) and 2.10 (cloning and selection).

5.2a Cloning and Expression of Cx40 and Cx43

The human Cx40, and Cx43 genes were purchased from the ATCC, cloned and incorporated into the pZeroBlunt vector and sequenced. They were then directionally sub-cloned into the pTRACER vector for transient co-expression with GFP and initial screening studies. For stable transfection the Cx40 and Cx43 genes were then sub-cloned into the T-Rex pcDNA5/Frt/TO vector.

5.2b Transient Cx Transfection.

Neuronal 2A cells (N2A) were transiently transfected for 24 hours with the pTRACER vector. Expression of Cx40 and Cx43 were measured by western blot and functional activity was confirmed in a few cases by microinjection of membrane impermeable Alexa594 dye into one cell of a pair expressing GFP.

5.2c Generation of stable Cx40 and Cx43 Hek293 cells.

See section 2.10d. Cx40 or Cx43 were incorporated into Hek293 cells at a single genomic Flp recombinase (FRT) integration site under the control of a

tetracycline inducible promoter. Cell clones were tested for incorporation, and expressed Cx40 or Cx43 when induced with tetracycline/doxycycline (1μg/ml media).

5.2d Activation of AMPK.

Per section 2.14, modification of AMPK activity was achieved by adenoviral mediated expression of GFP (negative control), $AMPK_{CA}$ or $AMPK_{DN}$ [435, 486]. Pharmacologically AMPK activation was also achieved by treating cells for 2h with 1mM AICAR, or 10mM phenformin as described previously [325, 326, 487].

5.2e Cell Homogenization.

Cells were lysed in a general lysis buffer (see section 2.5) supplemented with either 1% triton X-100, or NP-40 detergent with protease and phosphatase inhibitors.

5.2f Triton Soluble/Insoluble Fractionation.

See section 2.5. Cells were scraped in lysis buffer without detergent. Cell homogenates were separated for triton soluble (TS) vs. non-triton soluble (NTS) fractions, normalized to TS total protein concentration.

5.2g Western Blotting.

Following the techniques outlined in section 2.9 specific antibodies were utilized as follows: Cx40 expression was measured using two different Cx40 antibodies – goat anti-Cx40 (SC-20466 Santa Cruz Biotechnology, La Jolla, CA, USA) with an epitope in the CT (SC-CT), and rabbit anti-Cx40 (Ab1726 Chemicon Temecula, CA, USA) which also binds to an epitope in the c-terminus. Goat anti-Cx40 was used for western blotting unless otherwise indicated. Cx43 expression was measured using mouse anti-Cx43 (Chemicon MAB-3068) with an epitope in the c-terminal region, and confirmed with rabbit anti-Cx43 (Zymed Laboratories) which binds to another c-terminal epitope.

5.2h Immuno-fluorescence.

Following the methods outlined in section 2.11, Cx40 was detected using goat anti-Cx40 (Santa Cruz) antibodies at 0.2 μg/mL with 1:400 donkey anti-goat IgG conjugated with Alexa488, or with 1:100 rabbit anti-Cx40 (Chemicon) and 1:400 goat anti-rabbit conjugated with Alexa488. Cx43 was detected using mouse anti-Cx43 (Chemicon) primary, with goat anti-mouse IgG conjugated with Alexa594, or rabbit anti-Cx43 (Zymed) with donkey anti-rabbit conjugated with Alexa488.

Images were obtained using an LSM 510 confocal microscope at 63x magnification with an oil immersion lens (630x total magnification).

5.2i GapFRAP Dye Transfer.

Per section 2.13d, the kinetics of dye transfer were assessed by the GapFRAP technique. Hek293 cells were cultured, and loaded with Cell Trace Calcein Blue AM. Pairs of cells were identified based on defined selection criteria. One cell of the pair was bleached, and 20 subsequent scans were recorded at either 5s (Cx43) or 10s (Cx40) intervals to measure the rate of fluorescence recovery.

5.2j Statistical Analysis.

A two way repeated measures analysis of variance with a post-hoc Holm-Sidak test (Sigma Stat 3.5) for specific comparisons was used to test for statistically significant differences in fluorescence recovery and a two-tailed t-test was used to examine changes in protein expression.

5.3 Results

5.3a Transient Expression of hCx40, and hCx43 in N2A cells.

We chose to utilize two non-cardiac cell lines for Cx expression. This is not ideal is some ways, namely – that they are not cardiac cells. Unfortunately, the use of cardiac cells is limited as (1) there are very few culturable (vs. primary culture) human cardiac cell lines available: H9C2, HL-1, and stem cells are possible but they can be exceedingly difficult (and expensive in the case of stem cells) to maintain in stable cell culture. Stem cells also need to be partially differentiated each time. Cardiac fibroblasts are also possible, but they are usually of murine origin, and (2) typically express multiple Cx subtypes, which are expressed to higher levels than in other 'communication deficient' cell lines making the interpretation of results more difficult. (3) Unless the cells are of human origin, they contain murine Cx, with multiple sequence differences, including the lack of some human putative Cx phosphorylation sites. The N2A cell line, although it is also limited in some of these ways, is frequently used in Cx literature, is known for its ability to express isolated Cx cells, and it has a morphology that facilitates dual cell patch clamp (one of the key techniques we hope to use in the future), as such it was chosen for initial transient transfection, and was planned to be used in stable cell generation.

Following transfection of neuronal 2A (N2A) cells with Cx40, or Cx43, which co-expressed GFP, we identified the expression of Cx40 and Cx43 by western blot (data not shown). In these cells, transfection efficiency was approximately 30-60% with an optimal DNA:Fugene6 ratio of 3:2. By plating the cells at low density, we were able to identify very limited numbers of cell pairs that both expressed GFP and hence were coupled by either Cx40 or Cx43. Functional coupling was assessed in a few of these cell pairs by the transfer of membrane impermeable AlexaFluor 594 dye from a patch clamp pipette into one cell and following its staining into the adjoining cell or cells. Based on this method we observed dye transfer between cell pairs expressing Cx40 or Cx43, whereas the

non-transfected cells were not able to transfer this particular dye to any significant extent. Unfortunately, due to the low transfection efficiency and use of GFP to also label cells infected with viral particles, it was not possible to use this method effectively. Instead we opted to generate stable cell lines. We made some attempt to generate an N2A cell line with a stable integration point, and inducible (necessary for dual cell patch clamp single channel assessment) Cx expression using the Invitrogen Flp-In system. These attempts were not successful in the short term. As such we elected to proceed with the commercially available Hek-293 T-Rex cell line, expressing either hCx40 or hCx43 from a known single stable integration site until such time as other options became available.

5.3b Heterologous Expression of Cx40 and Cx43 in Hek293 cells.

Initial Hek293 colony screening was done to confirm the expression of Cx40 or Cx43, with negative beta galactosidase staining, indicative of insertion into the single stable integration site. A single stable cell line of each Cx type was chosen and propagated for these studies and will be designated Cx40, Cx43 or Hek293 respectively. Gene expression was induced in the Hek293 cells with 1-2 μg/mL doxycycline within 12 hours, for at least 24h after which these expression levels begin to decline, presumably due to the 24h half-life of doxycycline in solution. As such, generally a 24h induction period was used for consistency.

Both Cx40 and Cx43 are known to be expressed as multiple isoforms depending on the degree of post translational modification, and they are also known to run somewhat faster than might be expected based purely on their molecular weight (as confirmed in the N2A cell expression). As with most membrane bound proteins, connexins are translated in the rough endoplasmic reticulum (ER) and then transported to the cis, medial and later trans Golgi network where they undergo folding, oligomerization, and partial post-translational modifications (including phosphorylation) leading to the formation of a mature hexamer [558].

Musil *et al* have shown that Cx proteins associated with the internal ER/golgi membranes are soluble in 1% triton [364, 559] whereas the larger fully phosphorylated Cx bound to the plasma membrane in gap junction plaques are not. This allows us to determine whether Cx40/43 is being properly formed and transferred to the plasma membrane where it can form a functional gap junction.

Western blots for Cx40 and Cx43 protein show expression in both the triton soluble ER/Golgi/cytosolic fraction as well as in the non-triton soluble membrane bound fraction (see Figure 5-1). A second antibody for either Cx40 or Cx43 was used to confirm the identity of the bands (data not shown). The proportion of insoluble to soluble Cx appears to be dependent on cell density and the time of incubation. The majority of Cx protein in confluent cells, following a 24-48h induction period was associated with the non-triton soluble fraction (NTS), with a greater proportion of the protein present as the 'slower migrating/larger' isoforms. However, at lower cellular densities (60-80% confluent as used for functional studies and immuno-fluorescence) a significant triton soluble (TS) fraction is observed as shown in Figure 5-1.

5.3c Endogenous Phosphorylation of Heterologous Cx40 and Cx43.

As expected, there are multiple isoforms of both Cx40 and Cx43 expressed in the Hek293 cells. The three major isoforms of Cx43 have been previously identified as P0, P1, and P2 in order of increasing size and maturity. The smallest P0 is the non-phosphorylated ER/Golgi associated isoform, whereas the slower P1 and P2 isoforms are normally associated with the trans Golgi and plasma membrane respectively – all three of these isoforms are formed when Cx43 is expressed in these Hek293 cells (see Figure 5-1A,C). Similarly – the upper Cx40 band in Figure 5-1B,D represents the largest 'phosphorylated' Cx40 isoform which would be located at the gap junctional plaques along the cell to cell border. As expected the non-triton soluble fraction (NTS) contained primarily the largest P2 Cx43

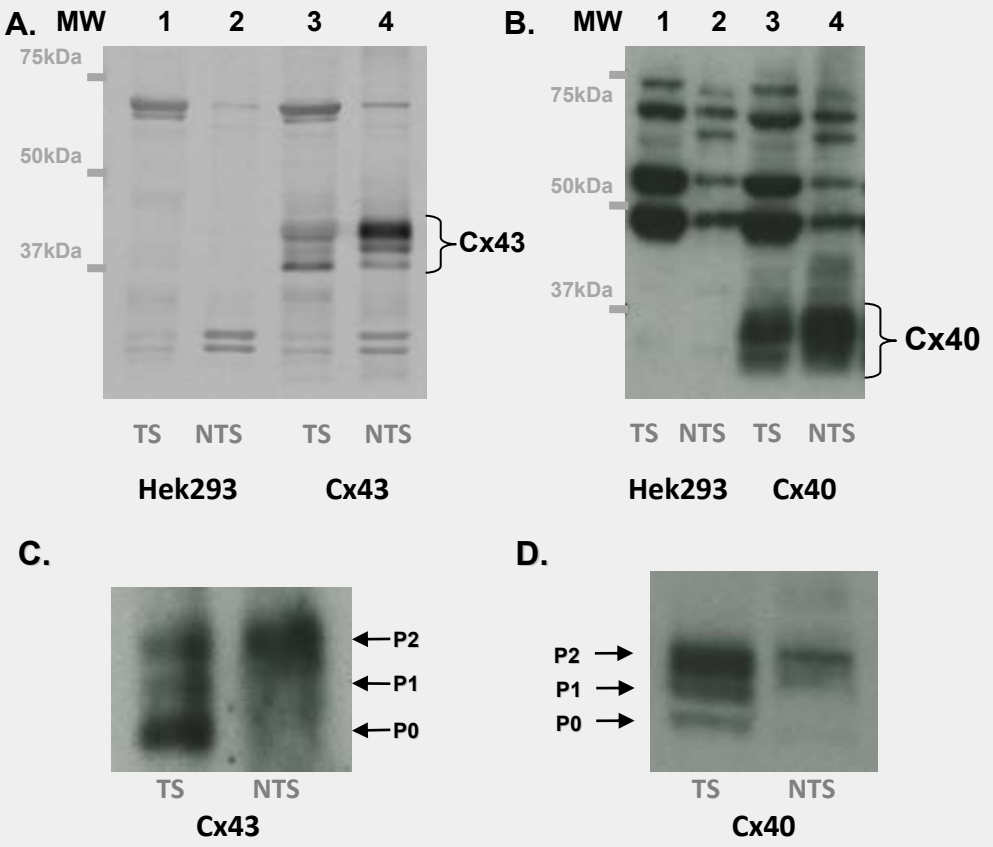

Figure 5-1. Cx40 and Cx43 protein expression in Hek293 cells.
A- Cx43 expression in both the triton soluble (TS) and triton insoluble (NTS) Hek293 cell fractions. There is no detectable endogenous Cx43 expressed in Hek293 (see lane 1,2) and expression of Cx43 is induced by doxycycline (see lanes 3,4). In general, numerous non-specific bands are observed with both the Cx40 and Cx43 antibodies used, however they do not interfere with the Cx signal. **B**- Doxycycline (1μg/mL) induced Cx40 expression in the triton soluble (TS) and non-triton soluble (NTS) fractions. As with Cx43 there is no endogenous expression of Cx40 in Hek293 cells (lane 1,2) versus the stably transfected cell line (lanes 3,4). **C.** Representative samples of Cx43 expressed in Hek293 form multiple phosphorylated isoforms P0, P1, and P2 in both the triton soluble (TS) intracellular organelle fraction and non-triton soluble (NTS) plasma membrane fraction. The NTS fraction contains primarily the largest P1,2 isoforms as expected. **D.** Despite oft blurring of the separate forms, this sample of Cx40 expression shows the formation of different phosphorylated Cx40 isoforms. As with Cx43, the fully phosphorylated P2 and P1 isoforms are found at the cell-cell border. However, they are not easily separable (without arbitrarily creating selection artifacts) in most cases.

and Cx40 isoforms (see Figure 5-1C) although some are also found in the triton soluble fractions as well. It is not easy to quantifiably separate the P1 and P2 isoforms of either variety, and in the case of Cx40 it is difficult to separate even the P0 from the P1 and P2 isoforms (Figure 5-1D) without inducing a selection

artifact. As such for quantification purposes, we do not measure them separately here.

5.3d Cx43 and Cx40 expressed in Hek293 are found at the cell-cell border and co-localized with intracellular organelles.

Immuno-fluorescent staining of Cx43 (see Figure 5-2) and Cx40 (see Figure 5-3) shows that Cx40/43 (green staining) is primarily located at the cell-cell borders as well as in the cytosolic compartment in bright punctate patterns. Some of this staining appears to be localized to perinuclear intracellular organelles resembling the Golgi, or ER as would be expected. Staining of the non-induced Cx40 or Cx43 cells resembles that of the parental non-transfected Hek293 cells (see panel A Figure 5-2, and Figure 5-3). Diffuse Cx staining observed in non-induced cells is likely non-specific.

5.3e Expression of Cx45 in non-transfected Hek293 cells.

Cx40 expression in non-transfected/induced cells was undetectable in overexposed western blots (as in Figure 5-1B). However, previous reports indicated that Hek293 cells express small amounts of either Cx43 or Cx45 [372, 420, 459-461]. Cytosolic Cx43 was not detectable by immunofluorescence microscopy or by western blot in triton soluble cell homogenate fractions even when using up to 100 μg of total protein per lane (data not shown). However, some punctate staining of appositional membranes was observed with Cx45 immunofluorescent staining. This was correlated with detection of a doublet Cx45 band in Cx40 immuno-precipitate samples that was not detectable in Hek-293 cell homogenate (data not shown). Combined these observations indicate that low levels of Cx45 may be expressed in these cells.

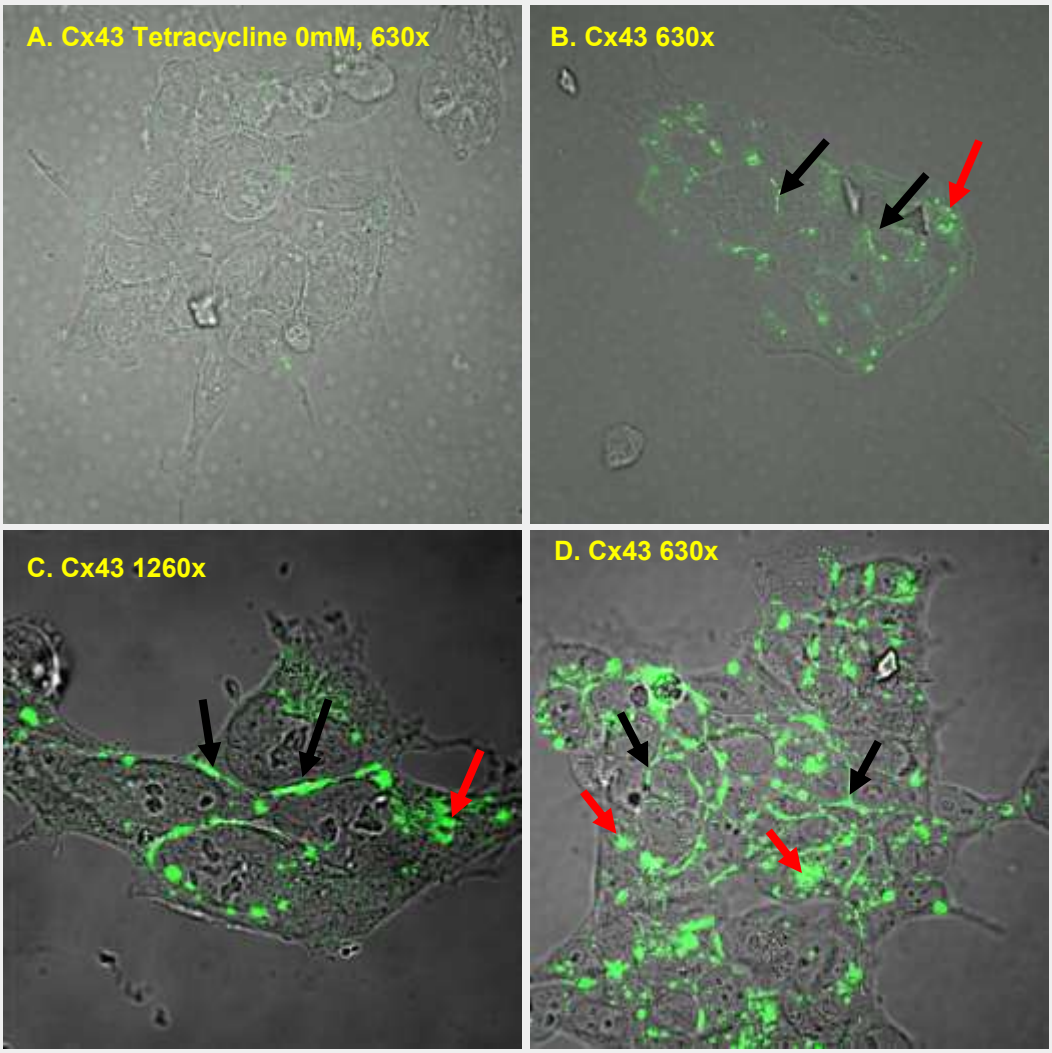

Figure 5-2. Cx43 is expressed in Hek293 cells at the cell-cell borders and in cellular organelles.

A- Cx43 cells without tetracycline induced expression stained with rabbit anti-Cx43 (green). **B-D** Cx43 Hek293 cells treated with 1mM tetracycline. **B-** Note Cx43 at the cell-cell border (black arrows) and in perinuclear golgi like organelles (red arrows). **C-** Larger magnification image of Cx43 expression. **D-** Another antibody (mouse anti-Cx43) confirms the localization of Cx43 in these Hek293 cells.

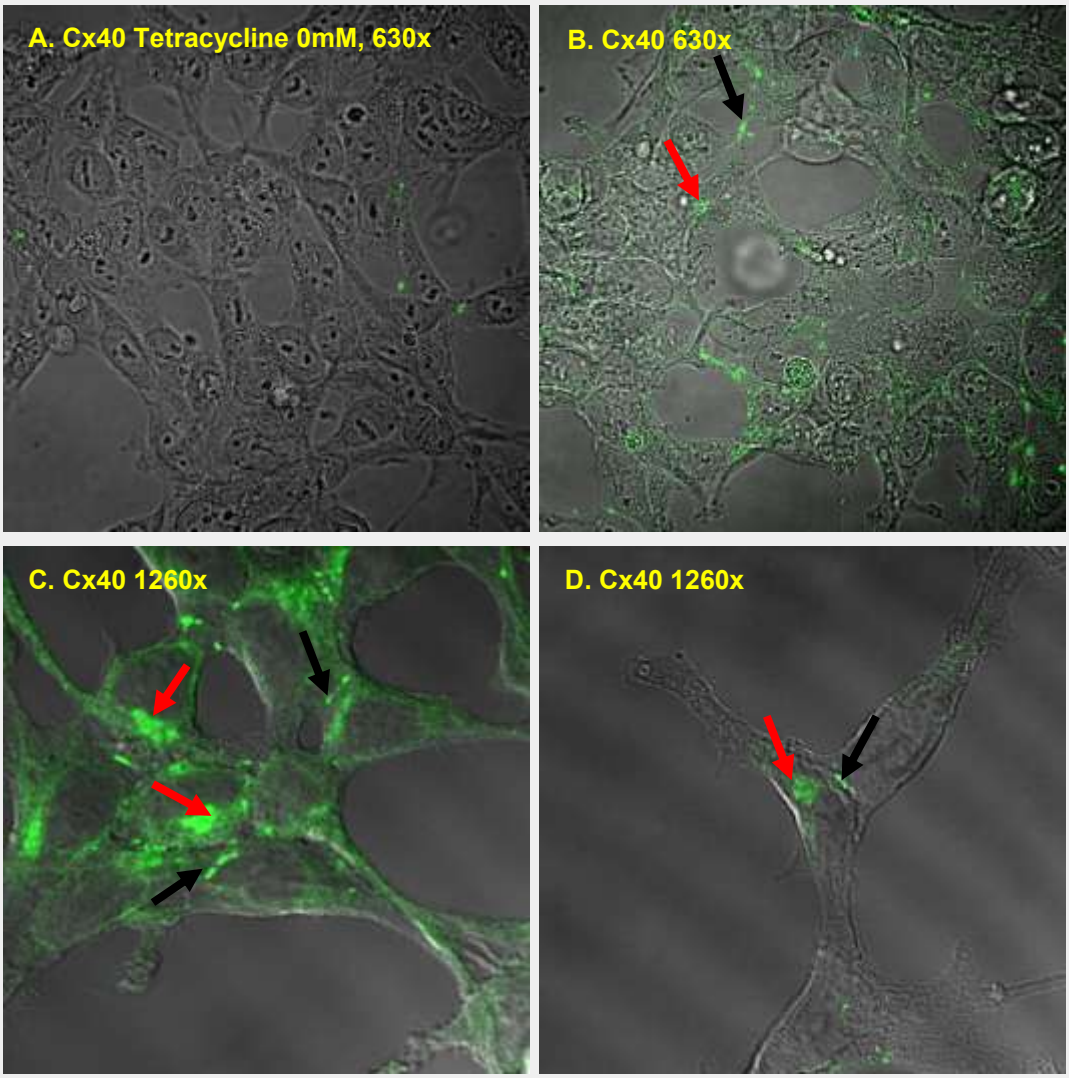

Figure 5-3. Cx40 is expressed in Hek293 cells at the cell-cell border and within intra-cellular organelles.

A- Representative photograph of Cx40 cells without tetracycline induced expression stained with rabbit anti-Cx40 (green). **B-D.** Cx40 Hek293 cells treated with 1mM tetracycline. **B-** Cx40 is expressed at the cell-cell border (black arrows) and inside the cell (Red arrows). **C-** Cx40 expression at the cell border (black arrows) and in perinuclear golgi like organelles (red arrows) was confirmed by using a second (goat anti-Cx40 antibody) **D-** Clear picture showing Cx40 expression at both the cell border and in a round perinuclear organelle resembling a golgi body (goat anti-Cx40).

5.3f Expression of Cx40 or Cx43 increases Hek293 junctional conductance.

Functionally we confirmed the presence of an endogenous junctional conductance in these Hek293 cells presumably due to low levels of Cx45 expression. The commonly used non-specific gap junction uncoupler heptanol was used to show that dye transfer is gap junction mediated (see Figure 5-4) and that inhibition of gap junctions in general reduced the dye recovery to the levels observed for single cells (ratio calculated to a nearby non-bleached cell). Induction of Cx40 or Cx43 expression significantly increased the rate of junctional dye conductance and hence recovery (see Figure 5-4A). In the case of Cx43, the rate of conductance required a faster sampling time (5s versus 10s) to observe the bleach and recovery. However, despite this difference in sampling interval it was possible to extract parameters suitable for comparison by fitting each curve to an exponential (rise to max) function. Based on these curve fit data it is apparent that the predicted plateau of fluorescence recovery was somewhat higher in the Cx40 and Cx43 groups relative to the untransfected cells (70 versus ~100) (see Figure 5-4B). There was no difference between maximal recovery level between Cx40 and Cx43 groups as would be expected. Further, the rate of recovery indicated by the fast 'tau' or time to reach 50% of the plateau (see Figure 5-4C) was much higher in transfected cells with Cx40 being almost twice as quick to recover versus Hek293 cells ($p=0.0000442$) and Cx43 almost 4 fold faster than Cx40 ($p=0.0372$).

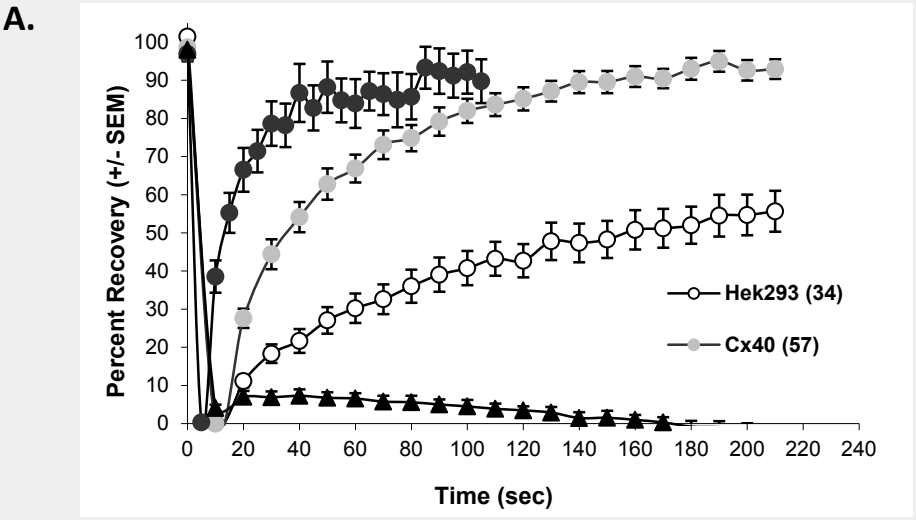

Figure 5-4. Gap Junctional conductance of calcein blue dye is significantly increased by expression of Cx40 and Cx43 following 24h treatment with 1µg/ml doxycycline. **A-** Ratio of bleached/donor cell fluorescence showing the rates of recovery. Inhibition of gap junctional conductance with 2mM heptanol (5min) shows that the dye recovery is gap junction dependent (similar to bleached single cells). **B,C-** Fitting each curve to an exponential function allows calculation of the predicted plateau of recovery, and time to reach 50% recovery (tau), allowing comparison of Cx40 to Cx43. Mean ±SEM shown. *p<0.05, **p<0.01, ***p<0.001. The number of cell pairs used for each group is indicated (n).

5.4 Viral Modulation of Cx40 and Cx43

The use of adenoviral agents to specifically activate or inactivate AMPK has been documented [435, 486, 560, 561]. We have used three separate constructs that affect the alpha subunit of the AMPK complex. They are designated $AdAMPK_{CA}$,

which co-expresses green fluorescent protein along with a mutated catalytic alpha subunit, with the phospho-threonine 172 site mutated to an aspartic acid (T172D), and the β-subunit binding region removed, as described previously [435]. This activates the enzyme permanently. The opposite effect is induced by expression of the $AdAMPK_{DN}$ which encodes an AMPK alpha subunit without the active kinase region. By expressing this subunit (either $\alpha 1$ or $\alpha 2$) we competitively reduce the activity of AMPK. The third variant expresses only the GFP protein as an infection control. Using a multiplicity of infection (moi) of 1-10 (1-10 viral particles per cell) we discovered that a majority of the Hek293 cells died at doses of greater than 2 moi. Using 1 moi it was visually confirmed that ~60-80 percent of cells expressed GFP with a 24 hour pretreatment.

To examine the effects of viral manipulation of AMPK activity on Cx43 conductance, Cx43 expressing cells were infected with adenovirus (1 moi) and morphologically healthy cell pairs were identified with at least one visually expressing GFP (double stained cells were used when possible). Surprisingly junctional conductance was significantly inhibited by infection with any of the adenoviral constructs (see Figure 5-5A). Similar results were observed when cells expressing Cx40 were tested, where again, all three viral infections caused a significant reduction in Cx40 conductance (see Figure 5-5B). Interestingly infection with the AMPK activating adenovirus appears to inhibit conductance to a lesser extent than DN, or GFP only virus (although the n is small) (see Figure 5-5B).

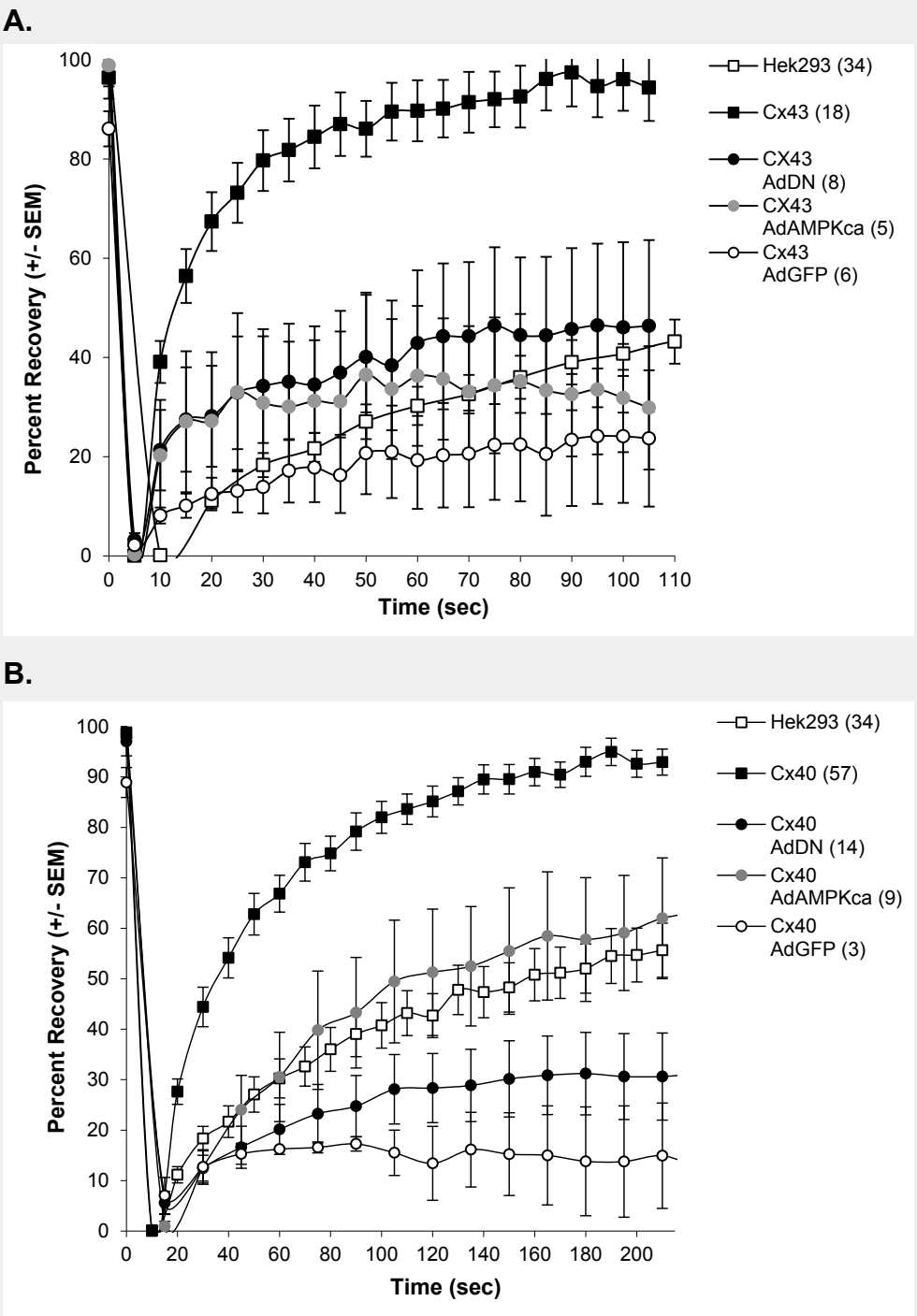

Figure 5-5. 24 hour pre-treatment with adenovirus non-specifically reduces junctional coupling significantly in both Cx43 and Cx40 expressing cells.
A. Pre-treatment with adenoviral GFP, $AMPK_{CA}$ and $AMPK_{DN}$ reduced Cx43 conductance to a level similar to or less than non-transfected Hek293 cells. **B.** Cx40 activity was similarly reduced below that of non-transfected Hek293 activity by pre-treatment with adenovirus.

In order to discern how viral infection was affecting AMPK activity, we infected Hek293 cells for 24h at ~1-5 moi (double DN was double concentration). We measured phospho-S79-Acetyl-CoA carboxylase (activated ACC) the originally

identified AMPK target, as well as phospho-Thr-172 AMPK (activated AMPK), and total α-AMPK expression (see Figure 5-6). These results show that all of our adenoviral constructs induced ACC phosphorylation similarly, without increasing pAMPK. Although there was some loading variance, the total ACC signal, which

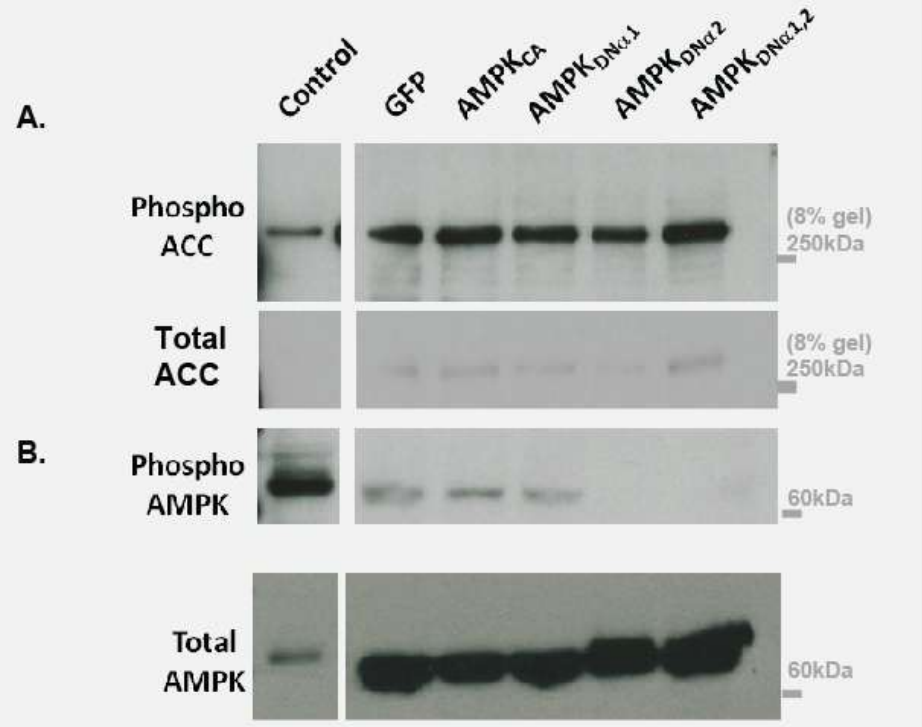

Figure 5-6. 24 hour pre-treatment with adenovirus increases AMPK activity and expression versus non-infected Hek293 cells.
A. Representative western blots following pre-treatment with adenoviral GFP, AMPKCA and AMPKDN (either α1, or α2) increased phosphoS79 ACC (a known AMPK target). ACC ran above the 250kDa marker (8% gel) 260 vs. 280kDa was not distinguishable and faint non-specific binding was observed due to long exposure time for control group. Total ACC signal was significantly degraded by strip and re-probe procedure affecting our ability to quantify the blot. Alternate loading controls were utilized in subsequent experiments. **B.** It also appears to reduce phospho-Thr172 AMPK versus non-infected Hek293 cells. Confirmation of increased mutant AMPK is shown in the bottom panel, and it indicates that the GFP virus non-specifically increases AMPK expression. Quantification of the signal was not pursued as the use of the virus was discontinued.

should be much larger than the p-ACC, was much reduced during the strip and re-probe procedure, this necessitated the use of alternate control proteins in subsequent blots. The abolition of p-AMPK signal with the viral AMPK constructs is expected as these constructs do not have phosphorylate-able Thr-172 sites. Total AMPK (measuring both wild type and mutant forms) showed that adenoviral infection increased AMPK expression. Based on this data, it appears that the viral stocks have been contaminated with the DN variant as we see increased expression of 63kDa AMPK in both GFP and $AMPK_{CA}$ treatments (the CA form would be ~35kDa, and was not measured here). Since only the DN or wildtype form is this size we must assume that the CA form may not have been present, or that the empty GFP vector similarly increased expression of wild type AMPK as described by Sambandam *et. al.* using H9C2 (atrial) cells [562]. This unexpected limitation prevented us from proceeding with further work using the AMPK viri, and may be a function of either viral contamination, or induced AMPK expression due to infection alone.

5.5 Pharmacological Manipulation of AMPK Activity

Although the viral manipulation of AMPK activity was hampered by increased AMPK activity in even the GFP expressing cells there was a significant decrease in Cx activity overall. To confirm whether activation of AMPK was responsible for these changes we required another method of increasing AMPK activity. Two commonly used pharmacological agents AICAR, and phenformin have both been shown to increase AMPK activity by two separate mechanisms - AICAR by acting as a stable AMP analogue, and phenformin by a multi-targeted pathway.

5.5a Activation of AMPK by phenformin and AICAR in Hek293 cells.

The ability of AICAR and phenformin to alter AMPK activity was confirmed by measuring phospho-Ser79-ACC, and phospho-Thr172-AMPK (see Figure 5-7A and representative blots in Figure 5-10). Treatment with both AICAR and phenformin raised pACC 1.5-2 fold that of control samples. Phospho-AMPK levels increased

A. P- ACC

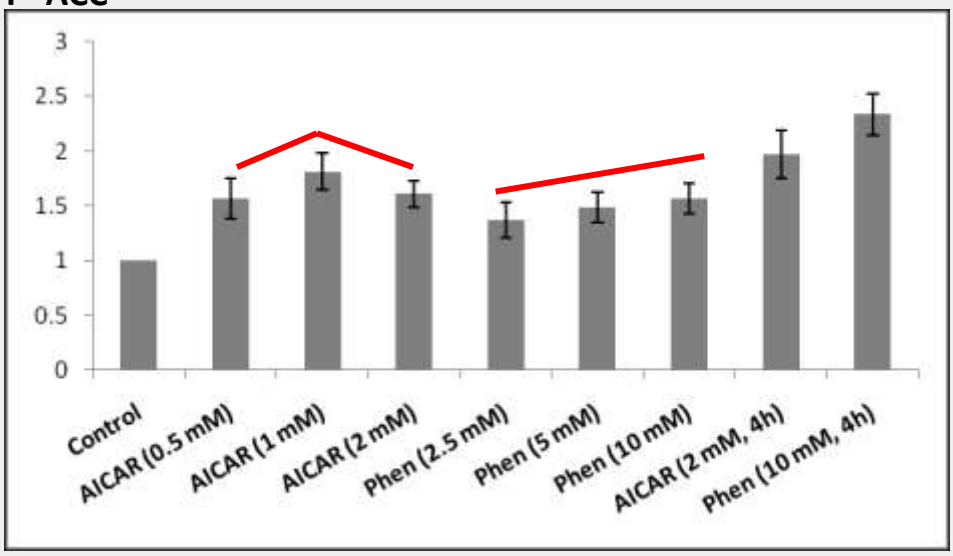

B. P- AMPK

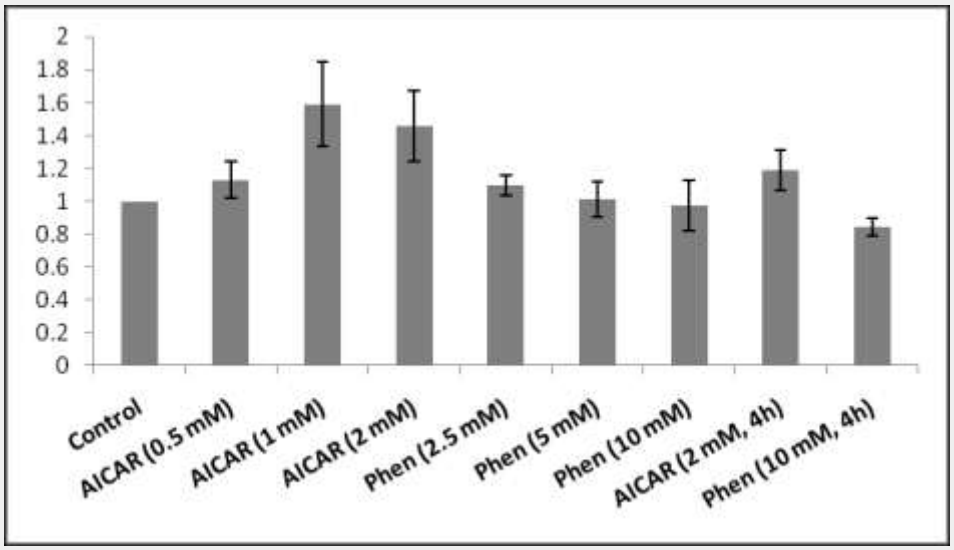

Figure 5-7. Phenformin and AICAR significantly increase AMPK activity in Hek293. **A.** Phospo-ACC is increased in cells treated with AICAR and phenformin (normalized to Golgin97 loading control) mean+/- SEM. These effects appear to be time and dosage dependent as expected. Although not dramatic, AICAR treatment again appears to affect P-ACC to a greater degree at 1.0 versus 2.0mM. **B.** Phospo-AMPK is increased in cells treated with AICAR (normalized to Actin loading control) mean+/- SEM. Abundance of Phospho-AMPK is less affected by phenformin treatment in these cells despite significant increase in P-ACC. This may indicate a reduction in total AMPK expression, or may be due to the difference in mechanism between AICAR and phenformin.

with AICAR but not phenformin treatment when normalized to Golgin97 (Figure 5-10B). These time course, and dose responses were generated following preliminary results that indicated that pACC and p-AMPK were both activated by AICAR and phenformin with the median 2h dose (data not shown), as such the activity level of Cx40 and Cx43 were measured at that dose and pre-treatment time.

5.5b Activation of AMPK by phenformin alters Cx43 conductance but AICAR has no effect.

Two hour pre-treatment of Cx43 expressing cells with AICAR (2mM) did not significantly alter Cx43 activity although it did tend to speed up the tau slightly (see Figure 5-8B). Phenformin on the other hand, significantly reduced Cx43 activity and the calculated tau (see Figure 5-8) p= 0.00676 vs. Cx43).

5.5c Phenformin reduces Cx40 activity but AICAR has no effect.

Treatment of Cx40 expressing cells with AICAR had no effect on Cx40 activity, whereas phenformin for the same 2h pre-treatment reduced Cx40 activity and significantly increased the calculated tau (see Figure 5-9). Although not tested in the Cx43 experiments, here we also show that treatment of the wildtype Hek293 cells with both phenformin and AICAR had no effect (see Figure 5-9A,B).

A.

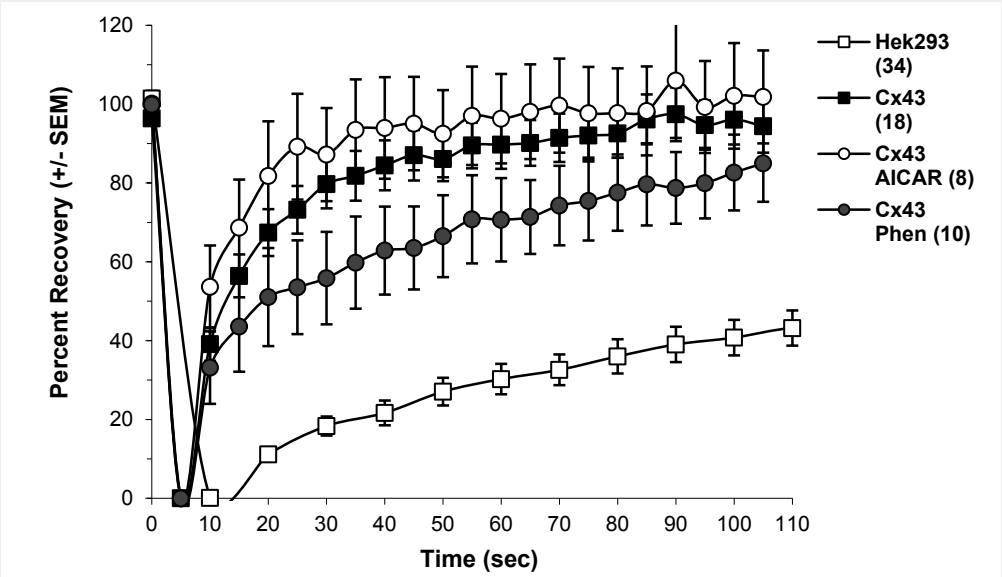

B.

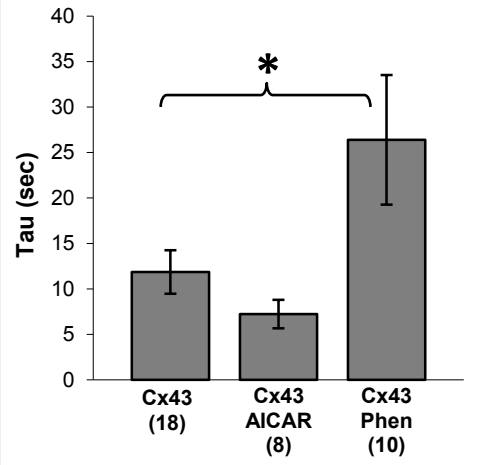

Figure 5-8. Phenformin inhibits Cx43 mediated junctional coupling.
A. 2h pre-treatment with 10mM phenformin tended to decrease Cx43 mediated junctional conductance whereas activation of AMPK with AICAR (2 mM) shows no change or tended to increase it. B. Calculated tau (time to reach 50%) is significantly increased in the phenformin treated group, and somewhat reduced by AICAR. * $p<0.01$ vs. Cx43 (tau increase = lower activity, delayed equilibration).

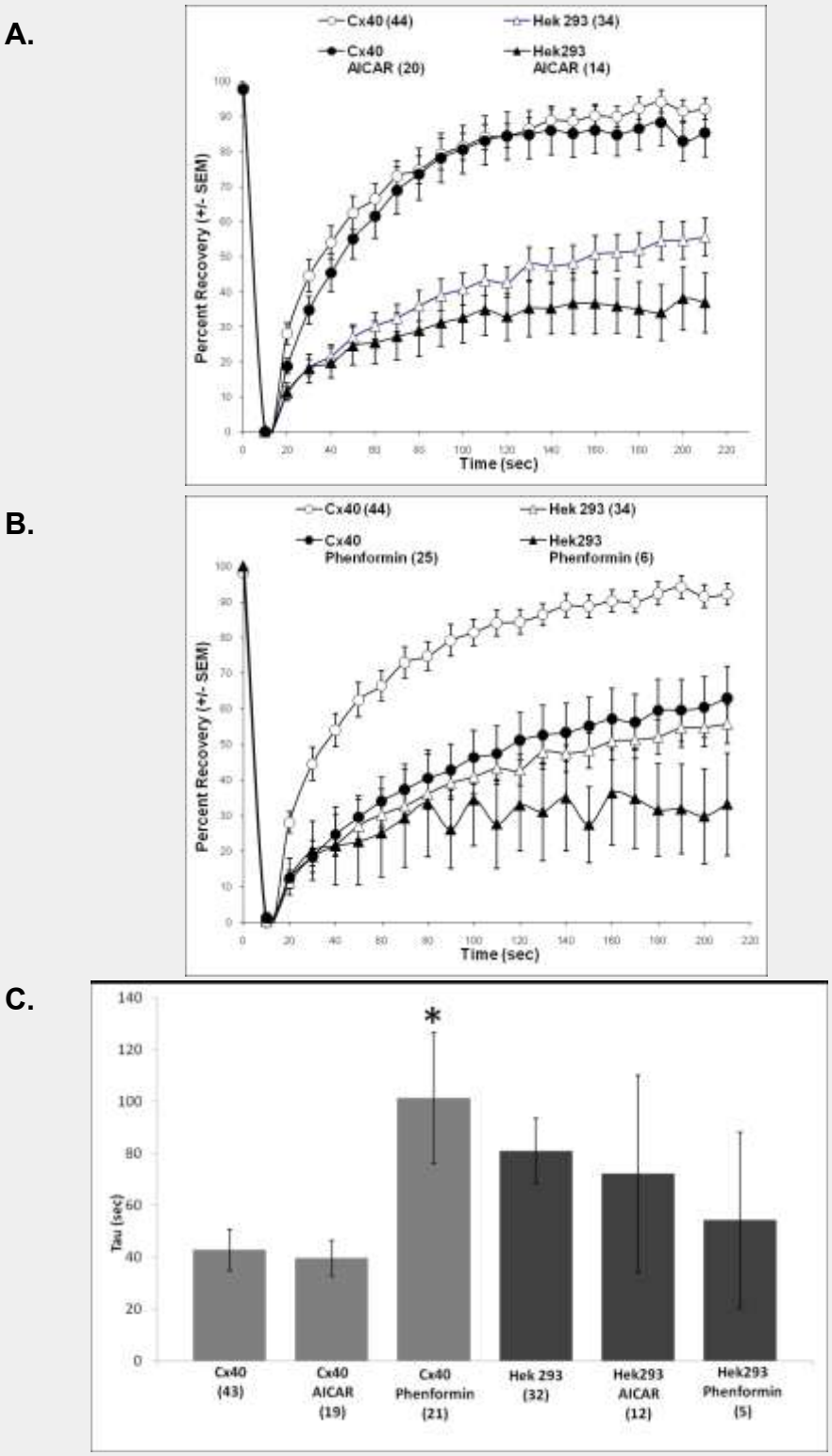

Figure 5-9. Phenformin significantly reduces Cx40 activity.
A. Fluorescence recovery in cells pre-treated with 2mM AICAR for 2 hours. **B.** Activity plots from cells treated with 10mM phenformin. **C.** Pre-treatment with the AMPK activating drug phenformin reduces Cx40 activity and increases the time to reach 50% recovery (tau). *p<0.01 vs. Cx40 expressing cells.

5.5d Cx43 expression is normal in cells treated with phenformin, and AICAR

NT Cx43 expression tends to be reduced by phenformin or AICAR in time and concentration dependent manner (i.e. less P1 and P2 are found in gap junction plaques) (see Figure 5-11A and representative blots in Figure 5-10). These changes are correlated with observed alterations in AMPK activity such that as AMPK activity is increased, NTS Cx43 expression is decreased (i.e. AMPK activity is lower in the 1.0mM versus 2.0mM AICAR treatment, and Cx43 expression is reduced likewise). Cx43 P0 expression tends to mirror the changes in P1 and P2, although to a lesser extent. Furthermore, as Cx43 P1 and P2 are reduced in the NTS fraction, Cx43 P1 and P2 were increased in the TS fraction indicating that these isoforms are being internalized, or not being transported to the membrane. When the time of treatment was extended to 4h, Cx43 expression was again inhibited by phenformin, but not by AICAR indicating that there may be a difference in these treatments.

5.5e Cx40 expression is reduced in cells treated with phenformin

Similar to the effect on Cx43, 2h pre-treatment with both phenformin and AICAR (to a lesser extent) decreased the expression of NTS Cx40 (see Figure 5-12a). Surprisingly, this tended to be maximal at 2.5mM, and partially prevented with increasing concentrations of phenformin, but not when the treatment was extended to 4h. As with the Cx43 internalization, changes in Cx40 NTS expression were correlated with altered expression in the TS fraction as would be expected (see Figure 5-12b phenformin 2.5, 5, 10mM, AICAR 0.5mM). In general, this may indicate that Cx40 has been translocated or internalized due to AMPK activation.

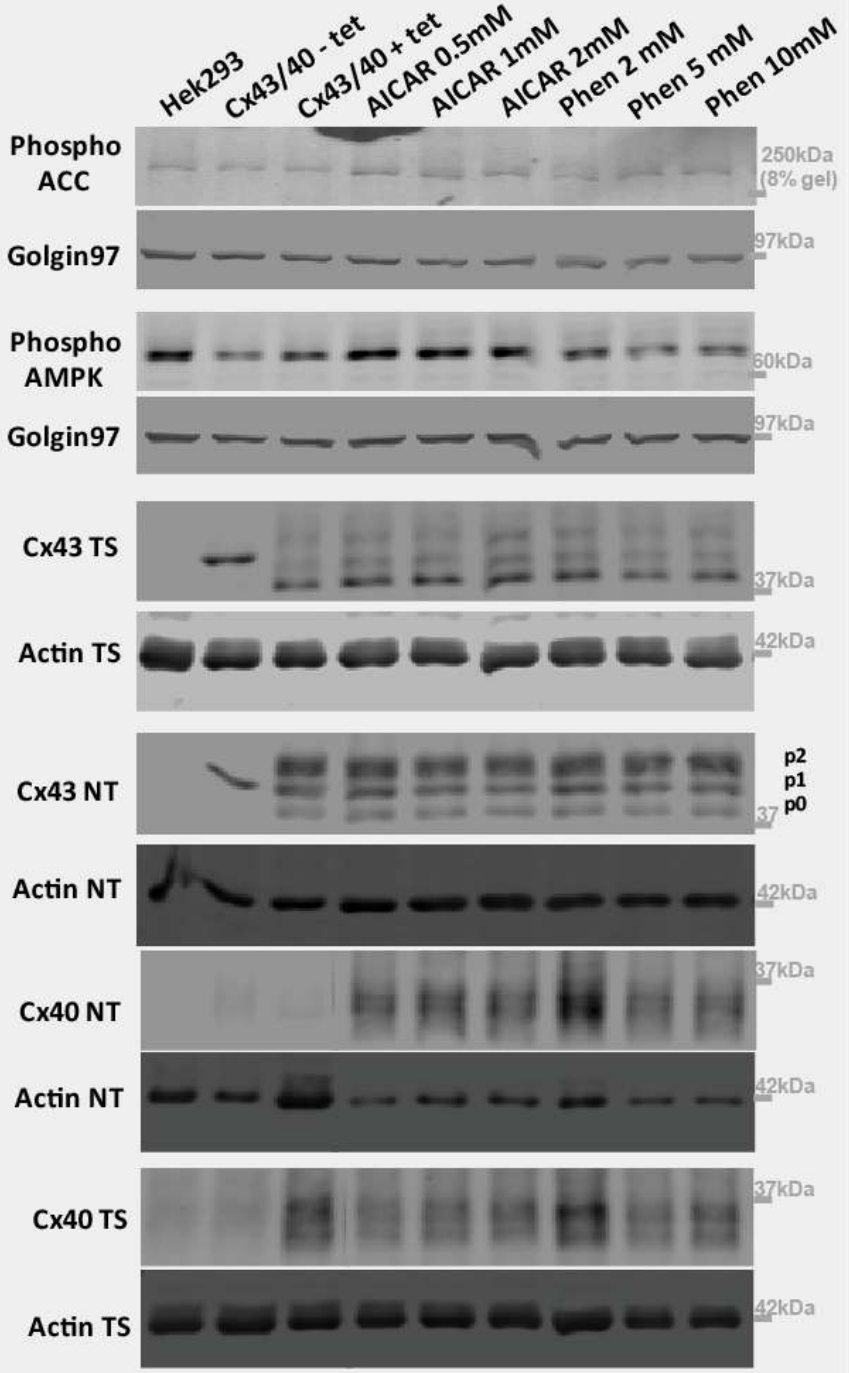

Figure 5-10. Representative Western blots

Representative western blots showing correlated expression of various proteins in Hek293 cells pre-treated with 2mM AICAR, or 10mM phenformin for 2 hours (as quantified in Figure 5-7,Figure 5-11, and Figure 5-12). Phospho-ACC (s79), and Phospho-AMPK were correlated to Golgin 97 expression for loading (as their non-Phos. forms could not be measured simultaneously on the Licor Imaging station). Total protein loading was confirmed by Ponceau-S staining. Any variation in sample loading as depicted above were corrected in the mean data summarized in the above mentioned figures. Note that a single band was excised in the Cx40 blots to maintain continuity with drug treatments (between lanes 3,4).

A. Cx43 Non-Triton Soluble Protein Expression

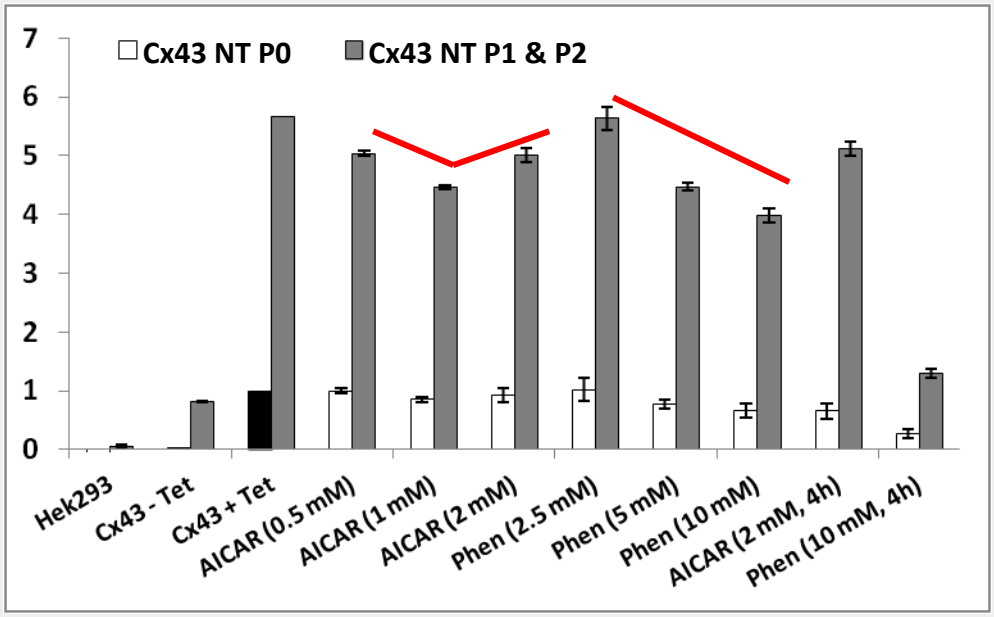

B. Cx43 Triton Soluble Protein Expression

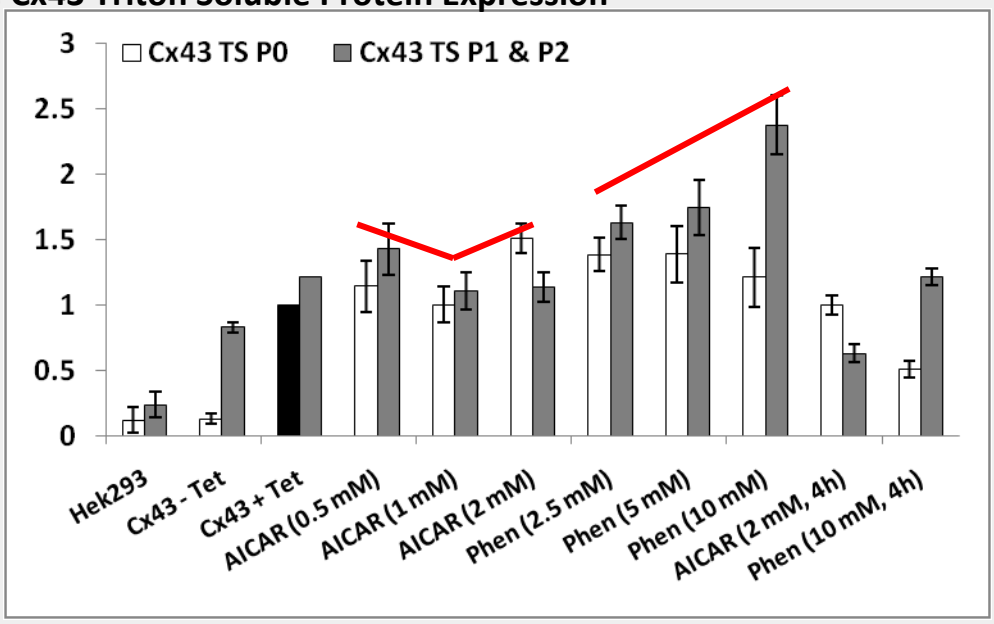

Figure 5-11. Cx43 Protein Expression is reduced by phenformin, and AICAR.
As per Figure 5-7, and Figure 5-10, phenformin and AICAR significantly increase AMPK activity in Hek293, this is accompanied by a decrease in Cx43 expression. **A.** Non-Triton soluble Cx43 expression normalized to control P0 Cx43+Tet cells (**black bar**). Mean fold difference in expression +/- SEM, n=3 shown. Expression of Cx43 at the cell-cell border, bound to gap junction plaques, is reduced by AMPK activation. This reduction is time and concentration dependent. **B.** Triton soluble Cx43 expression normalized to P0 Cx43+Tet (**black bar**). Mean fold difference in expression is shown +/- SEM, n=3. Based on the reduction in Cx43 expressed in the NTS fraction, we also observe an increase in Cx43 in the Cytosolic fraction indicating possible internalization. At later time points cytosolic expression is also reduced.

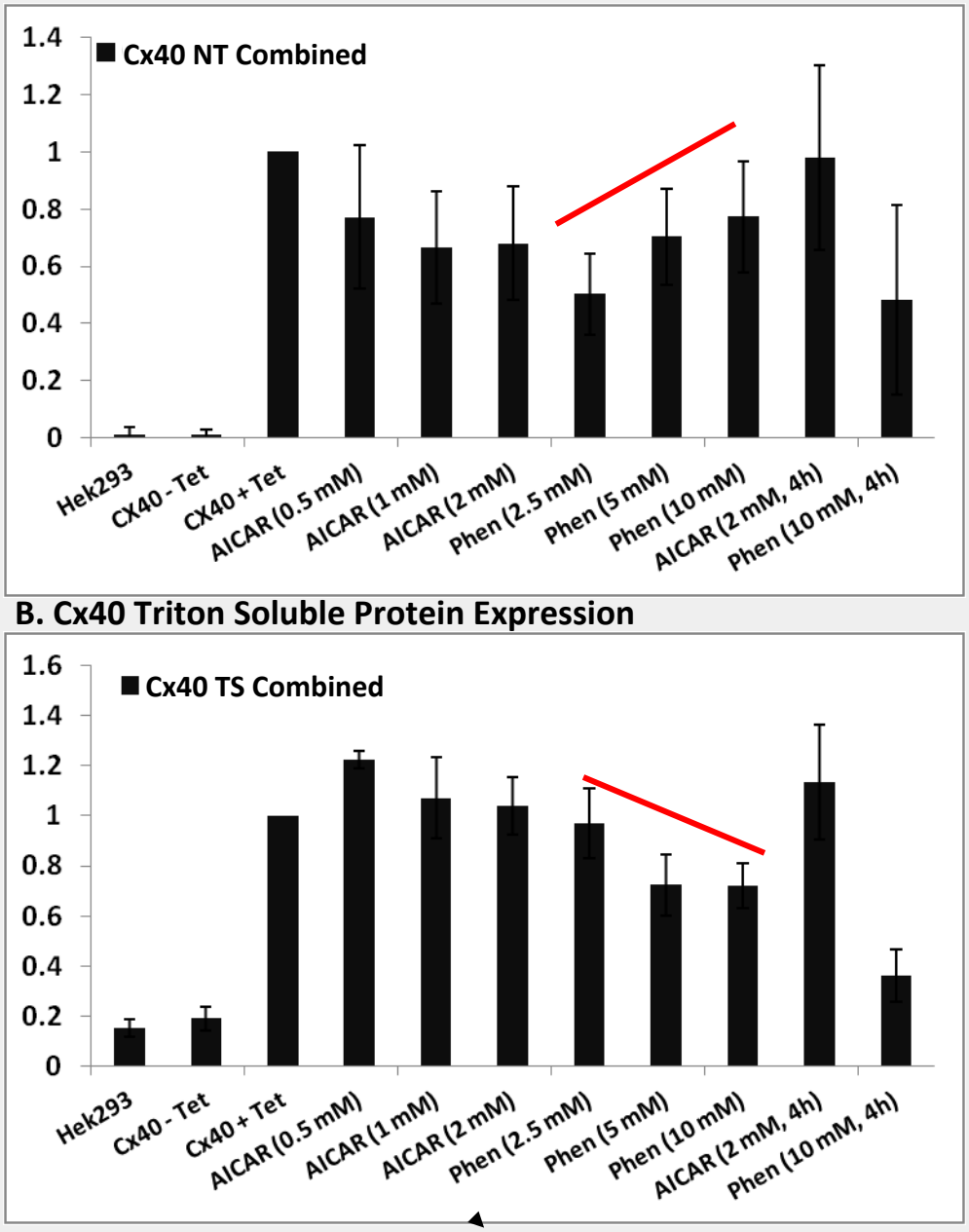

Figure 5-12. Cx40 expression at the cell-cell border is altered by AICAR and phenformin.

As per Figure 5-7, and Figure 5-10,, phenformin and AICAR both activate AMPK activity. **A.** Treatment with phenformin or AICAR reduces the expression of Cx40 in the NTS fraction (normalized to Actin expression to account for differences in gel loading, and to Cx40+Tet for comparison between treatment throughout). This decrease is partially prevented by increasing does of phenformin (red arrow). **B.** Cytosolic Cx40 expression is reduced in phenformin treated cells (5, 10mM), and differentially affected in AICAR treated cells. In all cases, altered NTS Cx40 is reflected by a concomitant inverse change in TS Cx40 (red arrow). Mean fold difference in expression +/- SEM, n=3 shown.

5.5f Cx40 Immuno- fluorescence localization is not significantly altered by 2h treatment with either phenformin, or AICAR.

Qualitatively it consistently appeared that more Cx40 staining was found in the intracellular compartment when treated with AICAR. This agrees with the observed change in Cx40 TS versus NT expression. Cx40 expression and localization do not appear to be significantly altered by phenformin when examined by fluorescence microscopy (see Figure 5-13). In general, most of the phenformin treated cells examined show some expression of Cx40 at the cell-cell interface. Again, this would be consistent with the changes in expression in the TS versus NT fraction observed with 10mM phenformin treatment. Overall, there appears to be a disconnect between the observed differences in Cx40 activity, relative to the observed changes in expression or localization. This may indicate that there is another mechanism involved.

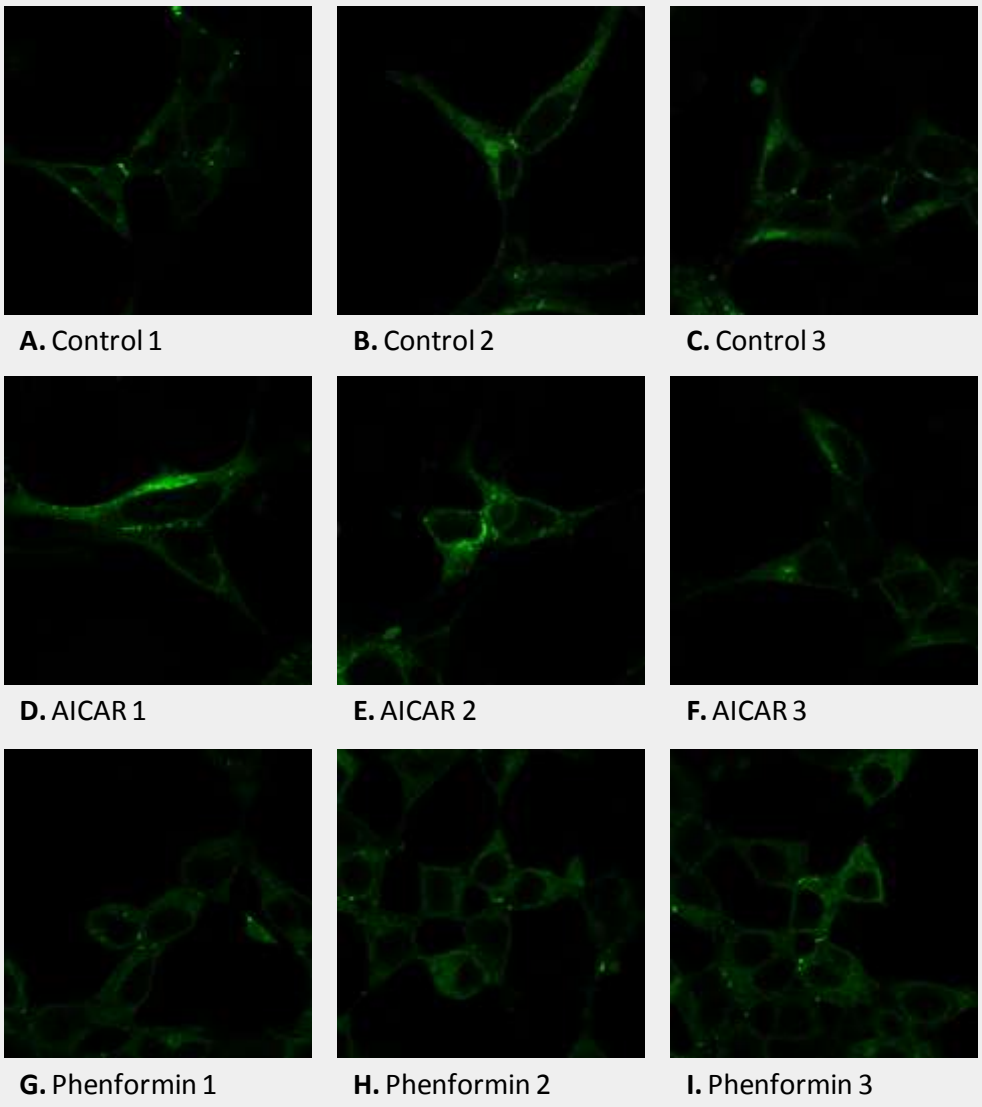

Figure 5-13. Phenformin and AICAR do not alter localization of Cx40.
A-C. Three examples of Cx40 expression in Cx40 cells. **D-F.** Three examples of Cx40 expression following 2h AICAR 2mM pre-treatment. **G-I.** Three examples of Cx40 expression following 2h phenformin 10mM pre-treatment. In all cases – Cx40 is found at the cell-cell interface as well as in cellular organelles in both control and drug treated cells.

5.6 Discussion

5.6a Summary of Results.

We have generated an inducible stable system for the expression of Cx40 and Cx43 in Hek293 cells, with normal processing, localization, and activity; facilitating the passage of fluorescent dye between cells. This model was used to evaluate the effect of adenoviral and pharmacological regulation of AMPK and how they affect Cx40 and Cx43 expression as follows.

Adenoviral Activation of AMPK

We have shown here that adenoviral infection causes significant reductions in both Cx40 and Cx43 conductance. Infection is correlated with significant up regulation of AMPK activity and expression, in a non-construct dependent manner, which was partially inhibited by the $AMPK_{DN}$ construct. Thus, our data support the idea that AMPK may partially mediate the inhibition of Cx activity, but we cannot rule out the possibility that non-AMPK mediated effects are also important with this treatment. It should be noted that viral infection via swine influenza, cyto-megalovirus, and others has been shown to increase Cx43 degradation, decrease Cx expression and activity [563]. Due to these limitations we cannot make a definitive conclusion on AMPK mediated Cx regulation based on this limited data set.

Cx43 and Pharmacological activation of AMPK

Measurement of markers of AMPK activity (phospho-ACC, and phospho-AMPK) indicate that pharmacological pre-treatment with both phenformin and AICAR increased AMPK activity in these cells (although AICAR may have been more effective in some cases). As decreased NTS Cx43 expression was correlated with increasing AMPK activity, and this was correlated with a concomitant increase in TS Cx43 expression, it would indicate that some of the NTS P1 and P2 Cx43 was being internalized in response to both phenformin and AICAR.

However, as Cx43 activity was significantly inhibited by phenformin, and was not affected by AICAR, this would also indicate that these two treatments have a very different functional effect that may be independent of AMPK activation. This difference may be related to differential activation of AMPK, or to their differing mechanism of action (see section 4.6b to follow).

Cx40 and Pharmacological Activation of AMPK.

As with Cx43, AICAR had little effect on Cx40 activity, whereas phenformin significantly impaired the functional activity of Cx40. Again, AICAR treatment tended to transiently reduce the expression of NTS Cx40 (not at 4 hours). This was associated with a concomitant change in TS Cx40. This may suggest that AICAR was transiently inducing the internalization of, or preventing the transfer of Cx40 to the junctional plaque. As this decrease was not reflected in junctional activity, it would indicate that the Cx40 at the membrane was active and able to maintain the typical level of conductance between cells.

With phenformin treatment, NTS Cx40 expression was reduced at the junctional plaque (similar to the extent observed with AICAR). This effect surprisingly appeared to be maximal at 2.5mM and was partially prevented by increasing concentrations of phenformin (from 2.5-10mM). As this effect was mirrored in the TS internal membrane fraction, it again indicates that there was some movement of Cx40 between the internal membrane fraction and the junctional plaque. Further study on the dosage and time dependent effects of AICAR would be beneficial.

Since AICAR and phenformin have differential effects on functional activity it would appear that AMPK activation (and thus phosphorylation of Cx proteins), is not entirely responsible for the alterations in Cx40 or Cx43 activity observed. However, both the pharmacological and adenoviral treatments affect a large number of signaling pathways, and both Cx40 and Cx43 are affected in different/complex ways by each of these pathways. Thus, it is likely that the

different response is due to differences in their mechanism of action. The following section will outline how these mechanisms might affect Cx function.

5.6b Differential Mechanistic actions of Phenformin

To understand how phenformin may be affecting junctional conductance in our model, it is necessary to examine its mechanism of action. Phenformin is a biguanide compound developed along with buformin to mimic the effects of other guanine analogues from the *Galea officinalis* plant extract used for the treatment of diabetes. They were both removed from the market due to their high risk for inducing lactic acidosis in patients - a classical indicator of mitochondrial inhibition. Clinically, phenformin is thought to act on various systems including: inhibition of mitochondrial respiration, reduced oxidative and nitrative stress, repressed mitochondrial permeability, and increased AMPK activity in the liver and skeletal muscle (which in turn stimulates glycolysis, glucose uptake, oxidative phosphorylation, and beta oxidation of fatty acids, as well as reducing protein synthesis).

Phenformin inhibits Complex I of the electron transport chain.

It was confirmed by Dykens *et al.* that phenformin inhibits complex I of the electron transport chain [564]. They showed that mitochondrial respiration was inhibited when cells were treated with 25μM phenformin (IC50 of 13μM) for 24 hours, a reduction that was ~80% as effective as the potent electron transport chain complex I inhibitor rotenone (5μM). Phenformin also caused extracellular acidification to the proportional degree (80% rotenone effect). It was also noted that transient increases in reactive oxidative molecules were observed at 24h but dropped off with higher doses, or longer time periods, indicating that oxidative free radical damage may play a role earlier in the time course, or that when complex I is inhibited further oxidative stress is prevented. It was further shown that isolated complex I (but not the others) was inhibited by phenformin with an IC50 of 1.5mM. As the authors note, the lower doses required for inhibition of intact mitochondria agree with previous observations that

phenformin is accumulated in the cell by 4 fold [565] and in the mitochondria by up to 100 fold [566]. Thus a 400 fold bioaccumulation in the mitochondria versus extracellular concentration is likely. With the phenformin concentration used in our study (10mM for 2h), we would expect a profound inhibition of mitochondrial respiration in our model with potentially reduced oxidative stress [564].

ATP is not limiting.

Despite significantly reduced mitochondrial activity, it has also been reported that ATP levels are not drastically reduced by phenformin [567] which was also confirmed by Dykens *et al.* [564]. They showed that when treated with 25μM phenformin for 24h cells grown in glucose media (as ours were) retained 80% of their resting ATP levels. This is in contrast to cells grown in galactose that are almost totally deprived of ATP (presumably since galactose cannot be used for glycolysis). This is most likely due to the fact that AMPK can stimulate glucose uptake by causing GLUT4 translocation, and stimulation of glycolysis via phosphorylation of phosphofructokinase-2 [294] to the point that only a 20% reduction in ATP is observed.

Uncoupled glycolysis may cause acute intracellular acidosis, and or calcium accumulation reducing junctional conductance.

Due to this massively increased glycolytic rate that is completely uncoupled from glucose oxidation we would expect a significant accumulation of lactate in these cells. Although Lactate levels are now thought to be maintained at an equilibrium point with pyruvate in the cytosol, this requires it to be shuttled into the mitochondria for use as an Acetyl-CoA energy source (via PDH), or converted back into pyruvate (consuming NAD^+), both of which may be limiting with inhibition of the ETC here [568, 569]. Furthermore, because we are using a closed non-circulating system, and the conversion of glycolytic pyruvate to lactate results in the production of $2H^+$ per molecule of glucose used, it is assumed that acute acidosis may occur within the cell (as shown previously with

phenformin treatment [564]). This acidosis was not sufficient to affect media color following 2h of phenformin treatment, but may have if the treatment was prolonged. Further to the drop in intracellular pH, the excess cytosolic H^+ will also trigger activity of the sodium hydrogen exchanger, and in turn increase sodium-calcium exchange thus increasing intracellular calcium concentration. In combination, there will be an increase in local H^+ and the potential accumulation of calcium to various degrees in these cells, in many ways mimicking the effects of ischemia in the heart.

Inhibition of gap junctional conductance by low pH and high calcium.
The effects of pH and calcium (for review see Peracchia *et al.* [570]) have been extensively examined in the realm of ischemia such that it has been demonstrated quite effectively that gap junctional conductance can be acutely and reversibly inhibited by lowered intracellular pH [28, 139, 153, 571-576]. It is also known that increased intracellular calcium concentration can reduce junctional conductance within seconds [28]. In many cases these phenomena are related such that lower pH or higher calcium combined often increase the inhibitory effect (as may be the case in our model).

Mechanistically, it has been demonstrated that low pH can induce protonation of the Cx43 molecule (H95) resulting in decreased conductance [573]. This was followed by studies demonstrating that the c-terminal tail region of Cx43 can bind to the cytoplasmic loop region leading to junctional closure in response to low pH [153, 156, 158]. It was also shown that intracellular acidification causes the formation of protonated taurine that can interact with the pore forming region of the Cx hexamer [571].

Via a similar interaction, it was also shown that increased intracellular calcium leads to the direct binding of calmodulin (CaM) to a number of different connexin isoforms leading to junctional obstruction. In the case of Cx43 this was recently shown to occur on the cytoplasmic loop domain (aa. 136-158) [577]. In

addition, activation of calcium calmodulin dependent protein kinase II CaMKII has been shown to directly phosphorylate Cx32 leading to junctional closure [578] indicating that activation of this kinase could have further effects on Cx40 or Cx43 junctional coupling that are undocumented at this time.

In summary, these combined effects of phenformin (increased glycolysis, lowered intracellular pH, and calcium accumulation) probably explain or partially explain the reduced Cx40 and Cx43 conductance observed in our model. This pathway does not necessarily explain the reduction observed with adenovirus where mitochondrial respiration should be reasonably intact and normal coupling between glycolysis and glucose oxidation may be expected. However, not all of the effects of phenformin are mediated by reduced mitochondrial activity. Activation of AMPK by phenformin and AICAR are also dependent upon the activation of multiple (and sometimes different) upstream signaling pathways. By the same rationale, adenoviral infection is also thought to affect a number of different cellular processes. Although the effect of adenoviral infection on the pathways which activate AMPK are generally difficult to ascertain (since most studies use GFP virus as a control for infection) the following sections will outline some of the pathways known to be activated upstream of AMPK which may affect junctional conductance.

5.6c Upstream Signaling and AMPK

Although AMPK is activated allosterically by AMP, and profoundly in response to increased AMP:ATP ratios, stimulants such as ischemia, insulin, metformin, and hyperosmotic stress have all been proposed to activate AMPK activity without altering the total ADP/AMP:ATP ratio [338, 579-582]. Many of these diverse stimuli alter the activity of upstream kinases that in turn phosphorylate αAMPK on Thr-172 stimulating its activity. So far these include LKB1, and CAMKKβ [583]. Other potential upstream kinases have been proposed but have not yet been confirmed [338]. These may include p38 MAPK which is thought in some cases to

act upstream of AMPK activation [584], and Tak1 which has been shown to phosphorylate AMPK *in vitro* [585] but may in fact modulate LKB1 activity on AMPK [344].

5.6d LKB1 and AMPK

Although there is some variation, activators of AMPK including phenformin, and AICAR do not activate AMPK in HeLa cells which lack LKB1, but do so if an active LKB1 is expressed in these cells [339]. Similarly, in embryonic stem cells lacking LKB1, activation of AMPK for 2h by AICAR (2mM), metformin (10mM) and phenformin (2mM) is eliminated [586] and phosphorylation of ACC is reduced in the AICAR and metformin treated cells. This phenomenon is also observed in skeletal muscle that lacks LKB1 [587]. These data would indicate that LKB1 acts upstream of the drug induced AMPK activation observed. However, in cells lacking LKB1, AMPK phosphorylation is not totally inhibited, and it was also shown that AMPK phosphorylation and activity can be stimulated in HeLa cells by AICAR independent of LKB1 activity [588]. In addition to the inhibition of mitochondrial activity Hek293 cells express LKB1 [589] so the activation of AMPK in response to phenformin/ AICAR/ adenoviral infection is most likely partially LKB1 dependent in our model.

There is currently no direct link between LKB1 activation and connexin activity or junctional conductance. However, it has been shown that LKB1 can control cell structure, polarity, and of course nutrient usage and cellular metabolism (for review see Hezel and Bardeesy [590]) via its control of the AMPK family of kinases and other kinase pathways. LKB1 can induce cell polarity by localizing ZO1 and p120 catenin into junctional complexes (which also include connexins and gap junctions). It was further shown that LKB1 dependent activation of AMPK with AICAR can speed up the formation of tight junctions, and inhibition (by DN virus) can reduce the formation of tight junctions in part by inhibition of the mTOR pathway (also causing increased protein synthesis). Thus, if anything,

activation of LKB1 would be expected to increase the development of junctional plaques and presumably increase Cx trafficking to the plasma membrane. Obviously this is not the overall effect in our model indicating that it is either not relevant here, or that it may be a compensating effect in opposition to the calcium and pH dependent inhibition of junctional conductance. Further study would be required to prove or disprove this hypothesis.

AICAR stimulation of AMPK has also been implicated in regulating the transport of vesicles containing both GLUT4 transporters, and as yet unknown cargos to the plasma membrane by phosphorylation of AS160 proteins whereas phenformin does not [591, 592]. Although merely conjecture, this brings up the possibility that AICAR stimulated cells may be increasing expression of junctional proteins at the plasma membrane, whereas phenformin does not. But in either case, this study highlights the fact that in some cases AMPK activation by AICAR is not equivalent to the AMPK activation by phenformin, or presumably the effect of adenoviral infection, each of which may have particular upstream activators and outcomes.

5.6e CAMKKβ and AMPK

The activation of AMPK by non-LKB1 AMPK kinases is one possible explanation for these differential effects. One such kinase is calcium calmodulin kinase kinase (CaMKKβ) which has also been shown to phosphorylate αAMPK at Thr172. CaMKK is activated by increased intracellular Ca^{++} bound to calmodulin (CaM), and this has been linked to thrombin activation of AMPK in endothelial cells (Stahmann N 2006), and a similar response is seen in T-lymphocytes who are activated by binding to the T-cell antigen receptor [593]. Although there is no evidence indicating that phenformin or adenoviral infection activates CaMKKβ directly, based on the partial phosphorylation of AMPKα Thr-172 in HeLa cells, it cannot be ruled out. In addition it is expected that accumulation of intracellular calcium would activate CaM and CaMKKβ with phenformin in our model possibly

contributing to AMPK activation, and/or altered junctional conductance. However, the observation that CaMKII increased the activity of Cx43 in spinal cord astrocytes without altering its expression or localization [594], that Cx43 is phosphorylated by CAMKKII at multiple sites [392] and that Cx36 conductance is upregulated by CAMKKβ [595] would argue that if anything CaMKII/CaMKKβ phosphorylation is complex, and it may be acting in opposition to the observed Cx inhibition but again this remains to be demonstrated.

5.6f Inhibition of junctional communication by p38 MAPK

Downstream activation of p38 MAPK has been shown in response to metformin and AMPK activation [596] and p38 MAPK activation with anisomycin is known to phosphorylate Cx43 reducing its conductance [597, 598]. Thus activation of p38 MAPK may contribute to the observed reduction in junctional conductance observed with adenoviral infection as well as phenformin treatment. However, once again, the determination of whether p38 is indeed activated, or whether inhibition of this pathway would partially prevent the reduction in junctional conductance will require further study.

5.6g Pathway interactions.

As shown above, there is a vast array of potentially activated pathways in the response to phenformin, AICAR, or adenoviral infection. This complex array is further complicated by the fact that many of these pathways have interacting components. For example, inhibition of LKB1 by PKA results in reduced AMPK activity, and inhibition of AMPK by the AKT pathway removes mTOR phosphorylation and leads to increased protein synthesis. Other possible points of interaction include activation of AMPK by stimulation of EGF receptors, activation of PKC (via TPA), or activation of IGF (by insulin) [599].

5.6h Phospho-regulation of Connexins

It is clear that Cx proteins are profoundly regulated by phosphorylation at multiple sometimes interacting sites (for reviews see [353, 551, 556]). Thus it can

be difficult to ascertain what the effects of phosphorylation on any one site would be. In terms of Cx43, it has been shown that it can be phosphorylated in the c-terminal tail by a number of kinases including PKA, PKC, MAPK and tyrosine kinases. Some of these phosphorylation events are associated with increased activity (PKA), some with reduced activity (tyrosine kinase, p38 MAPK). Although less well known relative to Cx43 it has been proposed that Cx40 is phosphorylated and stimulated by PKA at as yet unconfirmed phosphorylation sites [416, 417]. As described in the introduction, there are a large number of potential sites in Cx40, for PKC, PKA, MAPK, AMPK and others. In addition, phosphorylation is a balance between kinase activity, and phosphatase activity. We have not assessed the activation of either PP2a, or PP2B which have been shown to affect Cx43 phosphorylation status [404, 409, 600]. As such it is difficult to predict how activation of any of these interrelated kinases and phosphatases by the aforementioned signaling pathways will affect phosphorylation and activity of either Cx40 or Cx43 in our model without further more precise study.

5.6i Limitations and Future Directions.

In the short term, there is a significant amount of work needed to determine which of these pathways is most important to the reduction of junctional conductance in this particular model. As mentioned, the relative activation level of AMPK may play a larger role than we have suggested thus far. The activity of Cx40 and Cx43 would ideally be re-evaluated with each drug dose and time to correlate with the measured Cx expression and AMPK activity level. Methodologically, it would be better to measure AMPK activity directly rather than using p-ACC as a proxy measurement, this would alleviate problems with loading, strip and re-probe controls etc. The use of more specific pharmacological activators (A-769662, or compound 991), and the AMPK inhibitor compound C would allow for more specific alteration in AMPK activity than we were able to utilize here. The use of markers for the Golgi Apparatus,

Endoplasmic Reticulum, and endosomal degradation vesicles would allow us to better correlate the changes in expression with their actual localization.

To examine the potential mechanisms of phenformin inhibition, it would be useful to examine the relative pH/calcium levels in these cells following phenformin/adenoviral treatment to show that they are indeed increased. Based on the literature, and personal observations, we could expect that direct AMPK mediated phosphorylation of connexins may stimulate their activity (eg. AICAR tended to decrease tau from 10s to 7s in Cx43). By utilizing HeLa cells (lacking upstream LKB1 activity), we could unmask potential direct effects while maintaining the inhibition due to acidification/calcium accumulation. Furthermore, the isolation of some of these effects may be possible by utilizing more specific alterations in the Cx molecules, including for example removal of potential phosphorylation sites, calmodulin binding sites, or protonated residues which would be expected to block these various pathways.

Generation of a stable N2A cell platform is a key goal to reduce the effects of the background junctional conductance. We could also examine the baseline conductance in the Hek-293 cells via dual cell patch clamp. This would allow us to measure single channel conductance events (different for Cx43 and Cx45) and identify the Cx involved. By examining the distribution of single channel events with our Cx43 and Cx40 Hek-293 cells we can estimate the proportion of the junctions that are heterotypically mixed (based on protein expression this would be very low).

5.7 Summary and Conclusions-

Based on these studies, we cannot say that AMPK does not phosphorylate either Cx40 or Cx43. However, activating AMPK alone (by AICAR) does not seem to inhibit junctional coupling as we initially hypothesized. As noted, there are a significant number of pathways that may be affected by phenformin activation

which can be specific and inconsistent with AICAR induced effects and may or may not share common effectors with adenoviral infection. At this point we can suggest that the inhibition of Cx40 and Cx43 in response to phenformin is potentially due to the combined stimulation of glycolysis and inhibition of mitochondrial activity leading to increased acidosis and proton production or calcium accumulation in the cytosol. This may be dependent on calmodulin binding to Cx43/Cx40 directly or the interaction of the c-terminal tail of Cx40/43 with the cytoplasmic loop causing junctional closure. There are also significant concurrent alterations in signaling pathways that may or may not alter Cx phosphorylation/activity directly. Including circumstantial evidence that would indicate that AMPK activation may have some stimulatory effect on junctional conductance that is masked in our model. Finally, junctional inhibition by adenoviral infection is significant, but without further study we cannot make any conclusion as to the potential cause at this time.

5.8 Literature Cited

[28] Harris AL. Emerging issues of connexin channels: biophysics fills the gap. Quarterly reviews of biophysics. 2001;34:325-472.

[36] Dupont E, Ko Y, Rothery S, Coppen SR, Baghai M, Haw M, et al. The gap-junctional protein connexin40 is elevated in patients susceptible to postoperative atrial fibrillation. Circulation. 2001;103:842-9.

[37] Gutstein DE, Morley GE, Tamaddon H, Vaidya D, Schneider MD, Chen J, et al. Conduction slowing and sudden arrhythmic death in mice with cardiac-restricted inactivation of connexin43. Circulation research. 2001;88:333-9.

[38] Vaidya D, Tamaddon HS, Lo CW, Taffet SM, Delmar M, Morley GE, et al. Null mutation of connexin43 causes slow propagation of ventricular activation in the late stages of mouse embryonic development. Circulation research. 2001;88:1196-202.

[39] Lee P, Morley G, Huang Q, Fischer A, Seiler S, Horner JW, et al. Conditional lineage ablation to model human diseases. Proceedings of the National Academy of Sciences of the United States of America. 1998;95:11371-6.

[40] Hagendorff A, Schumacher B, Kirchhoff S, Luderitz B, Willecke K. Conduction disturbances and increased atrial vulnerability in Connexin40-deficient mice analyzed by transesophageal stimulation. Circulation. 1999;99:1508-15.

[41] Verheule S, van Kempen MJ, Postma S, Rook MB, Jongsma HJ. Gap junctions in the rabbit sinoatrial node. American journal of physiology. 2001;280:H2103-15.

[42] Qin D, Zhang ZH, Caref EB, Boutjdir M, Jain P, el Sherif N. Cellular and ionic basis of arrhythmias in postinfarction remodeled ventricular myocardium. CircRes. 1996;79:461-73.

[43] Dhillon PS, Chowdhury RA, Patel PM, Jabr R, Momin AU, Vecht J, et al. The Relationship between Connexin Expression and Gap Junction Resistivity in Human Atrial Myocardium. Circ Arrhythm Electrophysiol. 2014.

[44] Yan J, Kong W, Zhang Q, Beyer EC, Walcott G, Fast VG, et al. c-Jun N-terminal kinase activation contributes to reduced connexin43 and development of atrial arrhythmias. Cardiovascular research. 2013;97:589-97.

[45] Paul M, Wichter T, Gerss J, Arps V, Schulze-Bahr E, Robenek H, et al. Connexin expression patterns in arrhythmogenic right ventricular cardiomyopathy. Am J Cardiol. 2013;111:1488-95.

[46] Lubkemeier I, Requardt RP, Lin X, Sasse P, Andrie R, Schrickel JW, et al. Deletion of the last five C-terminal amino acid residues of connexin43 leads to lethal ventricular arrhythmias in mice without affecting coupling via gap junction channels. Basic research in cardiology. 2013;108:348.

[47] Lubkemeier I, Andrie R, Lickfett L, Bosen F, Stockigt F, Dobrowolski R, et al. The Connexin40A96S mutation from a patient with atrial fibrillation causes decreased atrial conduction velocities and sustained episodes of induced atrial fibrillation in mice. J Mol Cell Cardiol. 2013;65:19-32.

[48] Wu W, Li Y, Lu Z, Hu X. Increased susceptibility to ischemia-induced ventricular tachyarrhythmias in depressed rats: Involvement of reduction of connexin 43. Experimental and therapeutic medicine. 2012;3:192-4.

[49] Makita N, Seki A, Sumitomo N, Chkourko H, Fukuhara S, Watanabe H, et al. A connexin40 mutation associated with a malignant variant of progressive familial heart block type I. Circ Arrhythm Electrophysiol. 2012;5:163-72.

[50] Jansen JA, Noorman M, Musa H, Stein M, de Jong S, van der Nagel R, et al. Reduced heterogeneous expression of Cx43 results in decreased Nav1.5 expression and reduced sodium current that accounts for arrhythmia vulnerability in conditional Cx43 knockout mice. Heart Rhythm. 2012;9:600-7.

[51] Delmar M, Makita N. Cardiac connexins, mutations and arrhythmias. Current opinion in cardiology. 2012;27:236-41.

[52] Wirka RC, Gore S, Van Wagoner DR, Arking DE, Lubitz SA, Lunetta KL, et al. A common connexin-40 gene promoter variant affects connexin-40 expression in human atria and is associated with atrial fibrillation. Circ Arrhythm Electrophysiol. 2011;4:87-93.

[53] Strom M, Wan X, Poelzing S, Ficker E, Rosenbaum DS. Gap junction heterogeneity as mechanism for electrophysiologically distinct properties across the ventricular wall. American journal of physiology. 2010;298:H787-94.

[54] Soltysinska E, Olesen SP, Christ T, Wettwer E, Varro A, Grunnet M, et al. Transmural expression of ion channels and transporters in human nondiseased and end-stage failing hearts. Pflugers Arch. 2009;459:11-23.

[55] Chaldoupi SM, Loh P, Hauer RN, de Bakker JM, van Rijen HV. The role of connexin40 in atrial fibrillation. Cardiovascular research. 2009;84:15-23.

[56] Sato T, Ohkusa T, Honjo H, Suzuki S, Yoshida MA, Ishiguro YS, et al. Altered expression of connexin43 contributes to the arrhythmogenic substrate during the development of heart failure in cardiomyopathic hamster. American journal of physiology. 2008;294:H1164-73.

[57] Leaf DE, Feig JE, Vasquez C, Riva PL, Yu C, Lader JM, et al. Connexin40 imparts conduction heterogeneity to atrial tissue. Circulation research. 2008;103:1001-8.

[58] Danik SB, Liu F, Zhang J, Suk HJ, Morley GE, Fishman GI, et al. Modulation of cardiac gap junction expression and arrhythmic susceptibility. Circulation research. 2004;95:1035-41.

[59] VanderBrink BA, Sellitto C, Saba S, Link MS, Zhu W, Homoud MK, et al. Connexin40-deficient mice exhibit atrioventricular nodal and infra-Hisian conduction abnormalities. Journal of cardiovascular electrophysiology. 2000;11:1270-6.

[60] Bevilacqua LM, Simon AM, Maguire CT, Gehrmann J, Wakimoto H, Paul DL, et al. A targeted disruption in connexin40 leads to distinct atrioventricular conduction defects. J Interv Card Electrophysiol. 2000;4:459-67.

[61] Verheule S, van Batenburg CA, Coenjaerts FE, Kirchhoff S, Willecke K, Jongsma HJ. Cardiac conduction abnormalities in mice lacking the gap junction protein connexin40. Journal of cardiovascular electrophysiology. 1999;10:1380-9.

[68] Remo BF, Qu J, Volpicelli FM, Giovannone S, Shin D, Lader J, et al. Phosphatase-resistant gap junctions inhibit pathological remodeling and prevent arrhythmias. Circulation research. 2011;108:1459-66.

[70] O'Quinn MP, Palatinus JA, Harris BS, Hewett KW, Gourdie RG. A peptide mimetic of the connexin43 carboxyl terminus reduces gap junction remodeling and induced arrhythmia following ventricular injury. Circulation research. 2011;108:704-15.

[71] Bikou O, Thomas D, Trappe K, Lugenbiel P, Kelemen K, Koch M, et al. Connexin 43 gene therapy prevents persistent atrial fibrillation in a porcine model. Cardiovascular research. 2011;92:218-25.

[72] Zhang QY, Wang W, Shi QX, Li YL, Huang JH, Yao Y, et al. Antiarrhythmic effect mediated by kappa-opioid receptor is associated with Cx43 stabilization. Crit Care Med. 2010;38:2365-76.

[73] Unuma K, Shintani-Ishida K, Tsushima K, Shimosawa T, Ueyama T, Kuwahara M, et al. Connexin-43 redistribution and gap junction activation during forced restraint protects against sudden arrhythmic death in rats. Circ J. 2010;74:1087-95.

[74] Quan XQ, Bai R, Lu JG, Patel C, Liu N, Ruan Y, et al. Pharmacological Enhancement of Cardiac Gap Junction Coupling Prevents Arrhythmias in Canine LQT2 Model. Cell Commun Adhes. 2009:1-10.

[75] Roell W, Lewalter T, Sasse P, Tallini YN, Choi BR, Breitbach M, et al. Engraftment of connexin 43-expressing cells prevents post-infarct arrhythmia. Nature. 2007;450:819-24.

[76] Stahlhut M, Petersen JS, Hennan JK, Ramirez MT. The antiarrhythmic peptide rotigaptide (ZP123) increases connexin 43 protein expression in neonatal rat ventricular cardiomyocytes. Cell Commun Adhes. 2006;13:21-7.

[77] Haugan K, Miyamoto T, Takeishi Y, Kubota I, Nakayama J, Shimojo H, et al. Rotigaptide (ZP123) improves atrial conduction slowing in chronic volume overload-induced dilated atria. Basic & clinical pharmacology & toxicology. 2006;99:71-9.

[78] Dhein S, Larsen BD, Petersen JS, Mohr FW. Effects of the new antiarrhythmic peptide ZP123 on epicardial activation and repolarization pattern. Cell Commun Adhes. 2003;10:371-8.

[79] Weng S, Lauven M, Schaefer T, Polontchouk L, Grover R, Dhein S. Pharmacological modification of gap junction coupling by an antiarrhythmic peptide via protein kinase C activation. Faseb J. 2002;16:1114-6.

[80] Herve JC, Sarrouilhe D. Protein phosphatase modulation of the intercellular junctional communication: importance in cardiac myocytes. Progress in biophysics and molecular biology. 2006;90:225-48.

[81] Veenstra RD. Developmental changes in regulation of embryonic chick heart gap junctions. J Membr Biol. 1991;119:253-65.

[82] van Kempen MJ, Fromaget C, Gros D, Moorman AF, Lamers WH. Spatial distribution of connexin43, the major cardiac gap junction protein, in the developing and adult rat heart. Circulation research. 1991;68:1638-51.

[83] Gourdie RG, Green CR, Severs NJ, Thompson RP. Immunolabelling patterns of gap junction connexins in the developing and mature rat heart. Anatomy and embryology. 1992;185:363-78.

[84] Kanter HL, Laing JG, Beau SL, Beyer EC, Saffitz JE. Distinct patterns of connexin expression in canine Purkinje fibers and ventricular muscle. Circulation research. 1993;72:1124-31.

[85] Oosthoek PW, Viragh S, Mayen AE, van Kempen MJ, Lamers WH, Moorman AF. Immunohistochemical delineation of the conduction system. I: The sinoatrial node. Circulation research. 1993;73:473-81.

[86] Oosthoek PW, Viragh S, Lamers WH, Moorman AF. Immunohistochemical delineation of the conduction system. II: The atrioventricular node and Purkinje fibers. Circulation research. 1993;73:482-91.

[87] Davis LM, Kanter HL, Beyer EC, Saffitz JE. Distinct gap junction protein phenotypes in cardiac tissues with disparate conduction properties. J Am Coll Cardiol. 1994;24:1124-32.

[88] Gros DB, Jongsma HJ. Connexins in mammalian heart function. Bioessays. 1996;18:719-30.

[89] Davis LM, Rodefeld ME, Green K, Beyer EC, Saffitz JE. Gap junction protein phenotypes of the human heart and conduction system. Journal of cardiovascular electrophysiology. 1995;6:813-22.

[90] Van Kempen MJ, Vermeulen JL, Moorman AF, Gros D, Paul DL, Lamers WH. Developmental changes of connexin40 and connexin43 mRNA distribution patterns in the rat heart. Cardiovascular research. 1996;32:886-900.

[91] Severs NJ, Bruce AF, Dupont E, Rothery S. Remodelling of gap junctions and connexin expression in diseased myocardium. Cardiovascular research. 2008;80:9-19.

[92] Bastide B, Neyses L, Ganten D, Paul M, Willecke K, Traub O. Gap junction protein connexin40 is preferentially expressed in vascular endothelium and conductive bundles of rat myocardium and is increased under hypertensive conditions. Circulation research. 1993;73:1138-49.

[93] De Maziere A, Analbers L, Jongsma HJ, Gros D. Immunoelectron microscopic visualization of the gap junction protein connexin 40 in the mammalian heart. European journal of morphology. 1993;31:51-4.

[94] Gros D, Jarry-Guichard T, Ten Velde I, de Maziere A, van Kempen MJ, Davoust J, et al. Restricted distribution of connexin40, a gap junctional protein, in mammalian heart. Circulation research. 1994;74:839-51.

[95] Delorme B, Dahl E, Jarry-Guichard T, Marics I, Briand JP, Willecke K, et al. Developmental regulation of connexin 40 gene expression in mouse heart correlates with the differentiation of the conduction system. Dev Dyn. 1995;204:358-71.

[98] Kreuzberg MM, Liebermann M, Segschneider S, Dobrowolski R, Dobrzynski H, Kaba R, et al. Human connexin31.9, unlike its orthologous protein connexin30.2 in the mouse, is not detectable in the human cardiac conduction system. Journal of Molecular and Cellular Cardiology. 2009;46:553-9.

[106] Kreuzberg MM, Willecke K, Bukauskas FF. Connexin-mediated cardiac impulse propagation: connexin 30.2 slows atrioventricular conduction in mouse heart. Trends in cardiovascular medicine. 2006;16:266-72.

[139] Morley GE, Taffet SM, Delmar M. Intramolecular interactions mediate pH regulation of connexin43 channels. Biophys J. 1996;70:1294-302.

[153] Duffy HS, Sorgen PL, Girvin ME, O'Donnell P, Coombs W, Taffet SM, et al. pH-dependent intramolecular binding and structure involving Cx43 cytoplasmic domains. J Biol Chem. 2002;277:36706-14.

[156] Duffy HS, Ashton AW, O'Donnell P, Coombs W, Taffet SM, Delmar M, et al. Regulation of connexin43 protein complexes by intracellular acidification. Circulation research. 2004;94:215-22.

[158] Sorgen PL, Duffy HS, Spray DC, Delmar M. pH-dependent dimerization of the carboxyl terminal domain of Cx43. Biophys J. 2004;87:574-81.

[294] Marsin AS, Bertrand L, Rider MH, Deprez J, Beauloye C, Vincent MF, et al. Phosphorylation and activation of heart PFK-2 by AMPK has a role in the stimulation of glycolysis during ischaemia. CurrBiol. 2000;10:1247-55.

[325] Sakamoto K, Goransson O, Hardie DG, Alessi DR. Activity of LKB1 and AMPK-related kinases in skeletal muscle: effects of contraction, phenformin, and AICAR. Am J Physiol Endocrinol Metab. 2004;287:E310-7.

[326] Zhang L, He H, Balschi JA. Metformin and phenformin activate AMP-activated protein kinase in the heart by increasing cytosolic AMP concentration. American journal of physiology. 2007;293:H457-66.

[338] Altarejos JY, Taniguchi M, Clanachan AS, Lopaschuk GD. Myocardial ischemia differentially regulates LKB1 and an alternate 5'-AMP-activated protein kinase kinase. J Biol Chem. 2005;280:183-90.

[339] Hawley SA, Boudeau J, Reid JL, Mustard KJ, Udd L, Makela TP, et al. Complexes between the LKB1 tumor suppressor, STRAD alpha/beta and MO25 alpha/beta are upstream kinases in the AMP-activated protein kinase cascade. Journal of biology. 2003;2:28.

[344] Xie M, Zhang D, Dyck JR, Li Y, Zhang H, Morishima M, et al. A pivotal role for endogenous TGF-beta-activated kinase-1 in the LKB1/AMP-activated protein kinase energy-sensor pathway. Proceedings of the National Academy of Sciences of the United States of America. 2006;103:17378-83.

[353] Lampe PD, Lau AF. The effects of connexin phosphorylation on gap junctional communication. The international journal of biochemistry & cell biology. 2004;36:1171-86.

[364] Musil LS, Goodenough DA. Biochemical analysis of connexin43 intracellular transport, phosphorylation, and assembly into gap junctional plaques. The Journal of cell biology. 1991;115:1357-74.

[372] Cameron SJ, Malik S, Akaike M, Lerner-Marmarosh N, Yan C, Lee JD, et al. Regulation of epidermal growth factor-induced connexin 43 gap junction communication by big mitogen-activated protein kinase1/ERK5 but not ERK1/2 kinase activation. J Biol Chem. 2003;278:18682-8.

[392] Huang RY, Laing JG, Kanter EM, Berthoud VM, Bao M, Rohrs HW, et al. Identification of CaMKII phosphorylation sites in Connexin43 by high-resolution mass spectrometry. Journal of proteome research. 2011;10:1098-109.

[404] Ai X, Pogwizd SM. Connexin 43 downregulation and dephosphorylation in nonischemic heart failure is associated with enhanced colocalized protein phosphatase type 2A. Circulation research. 2005;96:54-63.

[409] Singh D, Lampe PD. Identification of connexin-43 interacting proteins. Cell Commun Adhes. 2003;10:215-20.

[416] van Rijen HV, van Veen TA, Hermans MM, Jongsma HJ. Human connexin40 gap junction channels are modulated by cAMP. Cardiovascular research. 2000;45:941-51.

[417] Hoffmann A, Gloe T, Pohl U, Zahler S. Nitric oxide enhances de novo formation of endothelial gap junctions. Cardiovascular research. 2003;60:421-30.

[420] Butterweck A, Gergs U, Elfgang C, Willecke K, Traub O. Immunochemical characterization of the gap junction protein connexin45 in mouse kidney and transfected human HeLa cells. J Membr Biol. 1994;141:247-56.

[435] Light PE, Wallace CH, Dyck JR. Constitutively active adenosine monophosphate-activated protein kinase regulates voltage-gated sodium channels in ventricular myocytes. Circulation. 2003;107:1962-5.

[459] Dang X, Jeyaraman M, Kardami E. Regulation of connexin-43-mediated growth inhibition by a phosphorylatable amino-acid is independent of gap junction-forming ability. Mol Cell Biochem. 2006;289:201-7.

[460] Gemel J, Lin X, Veenstra RD, Beyer EC. N-terminal residues in Cx43 and Cx40 determine physiological properties of gap junction channels, but do not influence heteromeric assembly with each other or with Cx26. Journal of cell science. 2006;119:2258-68.

[461] Lin X, Gemel J, Beyer EC, Veenstra RD. Dynamic model for ventricular junctional conductance during the cardiac action potential. American journal of physiology. 2005;288:H1113-23.

[486] Woods A, Azzout-Marniche D, Foretz M, Stein SC, Lemarchand P, Ferre P, et al. Characterization of the role of AMP-activated protein kinase in the regulation of glucose-activated gene expression using constitutively active and dominant negative forms of the kinase. Mol Cell Biol. 2000;20:6704-11.

[487] Woollhead AM, Scott JW, Hardie DG, Baines DL. Phenformin and 5-aminoimidazole-4-carboxamide-1-beta-D-ribofuranoside (AICAR) activation of AMP-activated protein kinase inhibits transepithelial Na+ transport across H441 lung cells. The Journal of physiology. 2005;566:781-92.

[551] Moreno AP, Lau AF. Gap junction channel gating modulated through protein phosphorylation. Progress in biophysics and molecular biology. 2007;94:107-19.

[552] Herve JC, Dhein S. Pharmacology of cardiovascular gap junctions. Advances in cardiology. 2006;42:107-31.

[553] King TJ, Lampe PD. Temporal regulation of connexin phosphorylation in embryonic and adult tissues. Biochim Biophys Acta. 2005;1719:24-35.

[554] Laird DW. Connexin phosphorylation as a regulatory event linked to gap junction internalization and degradation. Biochim Biophys Acta. 2005;1711:172-82.

[555] Moreno AP. Connexin phosphorylation as a regulatory event linked to channel gating. Biochim Biophys Acta. 2005;1711:164-71.

[556] Solan JL, Lampe PD. Connexin phosphorylation as a regulatory event linked to gap junction channel assembly. Biochim Biophys Acta. 2005;1711:154-63.

[557] Alesutan I, Sopjani M, Munoz C, Fraser S, Kemp BE, Foller M, et al. Inhibition of connexin 26 by the AMP-activated protein kinase. J Membr Biol. 2011;240:151-8.

[558] Sarma JD, Wang F, Koval M. Targeted gap junction protein constructs reveal connexin-specific differences in oligomerization. J Biol Chem. 2002;277:20911-8.

[559] Musil LS, Goodenough DA. Multisubunit assembly of an integral plasma membrane channel protein, gap junction connexin43, occurs after exit from the ER. Cell. 1993;74:1065-77.

[560] An Z, Wang H, Song P, Zhang M, Geng X, Zou MH. Nicotine-induced Activation of AMP-activated Protein Kinase Inhibits Fatty Acid Synthase in 3T3L1 Adipocytes: A ROLE FOR OXIDANT STRESS. J Biol Chem. 2007;282:26793-801.

[561] Wang W, Yang X, Lopez dSI, Carling D, Gorospe M. Increased AMP:ATP ratio and AMP-activated protein kinase activity during cellular senescence linked to reduced HuR function. JBiolChem. 2003;278:27016-23.

[562] Sambandam N, Steinmetz M, Chu A, Altarejos JY, Dyck JR, Lopaschuk GD. Malonyl-CoA decarboxylase (MCD) is differentially regulated in subcellular compartments by 5'AMP-activated protein kinase (AMPK). Studies using H9c2 cells overexpressing MCD and AMPK by adenoviral gene transfer technique. European journal of biochemistry / FEBS. 2004;271:2831-40.

[563] Eugenin EA. Role of connexin/pannexin containing channels in infectious diseases. FEBS Lett. 2014;588:1389-95.

[564] Dykens JA, Jamieson J, Marroquin L, Nadanaciva S, Billis PA, Will Y. Biguanide-induced mitochondrial dysfunction yields increased lactate production and cytotoxicity of aerobically-poised HepG2 cells and human hepatocytes in vitro. Toxicology and applied pharmacology. 2008.

[565] Wang DS, Kusuhara H, Kato Y, Jonker JW, Schinkel AH, Sugiyama Y. Involvement of organic cation transporter 1 in the lactic acidosis caused by metformin. Molecular pharmacology. 2003;63:844-8.

[566] Davidoff F. Effects of guanidine derivatives on mitochondrial function. 3. The mechanism of phenethylbiguanide accumulation and its relationship to in vitro respiratory inhibition. J Biol Chem. 1971;246:4017-27.

[567] Owen MR, Doran E, Halestrap AP. Evidence that metformin exerts its anti-diabetic effects through inhibition of complex 1 of the mitochondrial respiratory chain. Biochem J. 2000;348 Pt 3:607-14.

[568] Kane DA. Lactate oxidation at the mitochondria: a lactate-malate-aspartate shuttle at work. Frontiers in neuroscience. 2014;8:366.

[569] Rogatzki MJ, Ferguson BS, Goodwin ML, Gladden LB. Lactate is always the end product of glycolysis. Frontiers in neuroscience. 2015;9:22.

[570] Peracchia C. Chemical gating of gap junction channels; roles of calcium, pH and calmodulin. Biochim Biophys Acta. 2004;1662:61-80.

[571] Bevans CG, Harris AL. Regulation of connexin channels by pH. Direct action of the protonated form of taurine and other aminosulfonates. J Biol Chem. 1999;274:3711-9.

[572] Abudara V, Jiang RG, Eyzaguirre C. Acidic regulation of junction channels between glomus cells in the rat carotid body. Possible role of [Ca(2+)](i). Brain research. 2001;916:50-60.

[573] Ek JF, Delmar M, Perzova R, Taffet SM. Role of histidine 95 on pH gating of the cardiac gap junction protein connexin43. Circulation research. 1994;74:1058-64.

[574] Ek-Vitorin JF, Calero G, Morley GE, Coombs W, Taffet SM, Delmar M. PH regulation of connexin43: molecular analysis of the gating particle. Biophys J. 1996;71:1273-84.

[575] Gu H, Ek-Vitorin JF, Taffet SM, Delmar M. UltraRapid communication : coexpression of connexins 40 and 43 enhances the pH sensitivityof gap junctions: A model for synergistic interactions among connexins. Circulation research. 2000;86:1100.

[576] Morley GE, Ek-Vitorin JF, Taffet SM, Delmar M. Structure of connexin43 and its regulation by pHi. Journal of cardiovascular electrophysiology. 1997;8:939-51.

[577] Zhou Y, Yang W, Lurtz MM, Ye Y, Huang Y, Lee HW, et al. Identification of the calmodulin binding domain of connexin 43. J Biol Chem. 2007;282:35005-17.

[578] Saez JC, Nairn AC, Czernik AJ, Spray DC, Hertzberg EL, Greengard P, et al. Phosphorylation of connexin 32, a hepatocyte gap-junction protein, by cAMP-dependent protein kinase, protein kinase C and Ca2+/calmodulin-dependent protein kinase II. European journal of biochemistry / FEBS. 1990;192:263-73.

[579] Beauloye C, Marsin AS, Bertrand L, Krause U, Hardie DG, Vanoverschelde JL, et al. Insulin antagonizes AMP-activated protein kinase activation by ischemia or anoxia in rat hearts, without affecting total adenine nucleotides. FEBS Lett. 2001;505:348-52.

[580] Fryer LG, Parbu-Patel A, Carling D. The Anti-diabetic drugs rosiglitazone and metformin stimulate AMP-activated protein kinase through distinct signaling pathways. J Biol Chem. 2002;277:25226-32.

[581] Hawley SA, Gadalla AE, Olsen GS, Hardie DG. The antidiabetic drug metformin activates the AMP-activated protein kinase cascade via an adenine nucleotide-independent mechanism. Diabetes. 2002;51:2420-5.

[582] Itani SI, Saha AK, Kurowski TG, Coffin HR, Tornheim K, Ruderman NB. Glucose autoregulates its uptake in skeletal muscle: involvement of AMP-activated protein kinase. Diabetes. 2003;52:1635-40.

[583] Carling D, Sanders MJ, Woods A. The regulation of AMP-activated protein kinase by upstream kinases. Int J Obes (Lond). 2008;32 Suppl 4:S55-9.

[584] Jaswal JS, Gandhi M, Finegan BA, Dyck JR, Clanachan AS. p38 mitogen-activated protein kinase mediates adenosine-induced alterations in myocardial glucose utilization via 5'-AMP-activated protein kinase. American journal of physiology. 2007;292:H1978-85.

[585] Momcilovic M, Hong SP, Carlson M. Mammalian TAK1 activates Snf1 protein kinase in yeast and phosphorylates AMP-activated protein kinase in vitro. J Biol Chem. 2006;281:25336-43.

[586] Huang X, Wullschleger S, Shpiro N, McGuire VA, Sakamoto K, Woods YL, et al. Important role of the LKB1-AMPK pathway in suppressing tumorigenesis in PTEN-deficient mice. Biochem J. 2008;412:211-21.

[587] Sakamoto K, McCarthy A, Smith D, Green KA, Grahame HD, Ashworth A, et al. Deficiency of LKB1 in skeletal muscle prevents AMPK activation and glucose uptake during contraction. EMBO J. 2005;24:1810-20.

[588] Sun Y, Connors KE, Yang DQ. AICAR induces phosphorylation of AMPK in an ATM-dependent, LKB1-independent manner. Mol Cell Biochem. 2007.

[589] Dokladda K, Green KA, Pan DA, Hardie DG. PD98059 and U0126 activate AMP-activated protein kinase by increasing the cellular AMP:ATP ratio and not via inhibition of the MAP kinase pathway. FEBS Lett. 2005;579:236-40.

[590] Hezel AF, Bardeesy N. LKB1; linking cell structure and tumor suppression. Oncogene. 2008;27:6908-19.

[591] Geraghty KM, Chen S, Harthill JE, Ibrahim AF, Toth R, Morrice NA, et al. Regulation of multisite phosphorylation and 14-3-3 binding of AS160 in response to IGF-1, EGF, PMA and AICAR. Biochem J. 2007;407:231-41.

[592] Chen S, Murphy J, Toth R, Campbell DG, Morrice NA, Mackintosh C. Complementary regulation of TBC1D1 and AS160 by growth factors, insulin and AMPK activators. Biochem J. 2008;409:449-59.

[593] Tamas P, Hawley SA, Clarke RG, Mustard KJ, Green K, Hardie DG, et al. Regulation of the energy sensor AMP-activated protein kinase by antigen receptor and Ca2+ in T lymphocytes. The Journal of experimental medicine. 2006;203:1665-70.

[594] Pina-Benabou MH, Srinivas M, Spray DC, Scemes E. Calmodulin kinase pathway mediates the K+-induced increase in Gap junctional communication between mouse spinal cord astrocytes. JNeurosci. 2001;21:6635-43.

[595] Del Corsso C, Iglesias R, Zoidl G, Dermietzel R, Spray DC. Calmodulin dependent protein kinase increases conductance at gap junctions formed by the neuronal gap junction protein connexin36. Brain research. 2012;1487:69-77.

[596] Saeedi R, Parsons HL, Wambolt RB, Paulson K, Sharma V, Dyck JR, et al. Metabolic actions of metformin in the heart can occur by AMPK-independent mechanisms. American journal of physiology. 2008;294:H2497-506.

[597] Leykauf K, Durst M, Alonso A. Phosphorylation and subcellular distribution of connexin43 in normal and stressed cells. Cell Tissue Res. 2003;311:23-30.

[598] Ogawa T, Hayashi T, Kyoizumi S, Kusunoki Y, Nakachi K, MacPhee DG, et al. Anisomycin downregulates gap-junctional intercellular communication via the p38 MAP-kinase pathway. Journal of cell science. 2004;117:2087-96.

[599] Louden E, Chi MM, Moley KH. Crosstalk between the AMP-activated kinase and insulin signaling pathways rescues murine blastocyst cells from insulin resistance. Reproduction. 2008;136:335-44.

[600] Gerner L, Youssef G, O'Shaughnessy RF. The protein phosphatase 2A regulatory subunit Ppp2r2a is required for Connexin-43 dephosphorlyation during epidermal barrier acquisition. Exp Dermatol. 2013;22:754-6.

Chapter 6 Mutation of putative PKC, cAMP, and AMPK phosphorylation sites alters human Cx40 conductance.

This is an original work by Jason Iden
.
Portions of this chapter have been submitted for publication to:
The Journal of Biological Chemistry (under review).
with Editorial contributions by Dr. Katherine M. Kavanagh, Dr. Paul Lampe, and Dr. Henry Duff.

Mutations and constructs were designed and built by Jason Iden with guidance from
Dr. Jim Lees Miller (in the Lab of Dr. Henry Duff), University of Calgary

Blinded observations for immunofluorescence expression were done by
Dr. Katherine M. Kavanagh, and Dr. Henry Duff.

A portion of GapFRAP studies, and cell culture maintenance were carried out by
Dr. David Dilworth under supervision of Jason Iden.

6.1 Introduction

Gap junctions are low resistance cell-to-cell pathways that connect cells electrically and chemically through the exchange of signaling molecules up to 1kDa in size. They are composed of connexin proteins arranged as a hexamer termed a connexon (or hemi-channel) in one membrane that docks with a connexon in an adjacent cell's membrane forming a cell-to-cell channel. All connexin proteins have a similar structural organization [127-133]: four α-helical transmembrane domains (M1-4), two extracellular loops (E1, E2), a cytoplasmic loop (CL) and N- and C- termini (NT, CT) facing the cytosol (see Figure 6-1A). The greatest isoform specific variation occurs in the three intracellular regulatory domains. These domains are structurally flexible, can interact with other proteins or domains within the connexon, and are thought to adjust conformation affecting conductance parameters (e.g., channel diameter, open probability, and membrane stability) [133]. The N-terminal (NT) domain is important for voltage sensitivity, and permeability: forming a pore funnel and ring (Asp3, Trp4, Phe6) when open and a plug like domain when closed [131-136]. The cytoplasmic loop (CL) domain is thought to interact with the C-terminal (CT) domain in a "particle-receptor" model important for gating of the channel [137-140]. The CT is also important for protein-protein interactions, both with itself, with other connexin subunits, and with various structural and regulatory proteins in the same vicinity.

Connexins are phosphoproteins containing multiple phosphorylation sites modified by various protein kinases. Phosphorylation can be constitutive or transient and display cell and tissue specificity. Phosphorylation is known to affect connexin assembly, trafficking, turnover, permeability and protein-protein interaction in a complex manner [350, 352, 551, 554, 556, 601].

Normal Cx40 expression and function is critical for the proper development and maturation of the heart in particular the electrical conduction system [602], and

vasculature [603]. Altered expression and function of Cx40 also results in arrhythmia formation in the hearts of knockout mice [40, 604-607]. In humans, abnormal Cx40 expression and function are linked to altered conduction and the formation of atrial arrhythmias including atrial fibrillation [608-613]. In addition, atrial fibrillation is also associated with increased phosphorylation of Cx40 but the specific sites affected and the upstream kinase(s) have not been identified [614].

To date there is no direct evidence demonstrating Cx40 phosphorylation associated with changes in expression, conductance, trafficking, gating, or stability as has been shown for some other gap junction subunit proteins. However, human Cx40 electrical conductance and permeability to Lucifer yellow dye are stimulated by cAMP in two different cell lines (HUVEC and SKHep1 transfected with human Cx40). This effect is PKA dependent (sensitive to inhibition by H89), phosphorylation mediated (correlates with a phosphorylation-dependent shift in SDS-PAGE mobility), and protein translocation dependent (sensitive to brefelden A) [615, 616].

Based on evidence suggesting regulatory phosphorylation of Cx40, and the wealth of data demonstrating the regulatory importance of gap junction phosphorylation, we sought to examine the phosphorylation dependent regulation of Cx40 by site directed mutagenesis.

We first examined the Cx40 sequence for potential phosphorylation sites and then 3D modeled Cx40 to see if those sites were accessible. Based on these analyses, we mutated 4 sites to either aspartic acid (d) or alanine (a) to simulate constitutively phosphorylated and de-phosphorylated states respectively [459, 617, 618]. We found mutation at three of these sites had dramatic effects on Cx40 localization and channel permeability.

6.2 Materials and Methods

For general chemicals, and cell culture conditions see section 2.1, and 2.3.

Per section 2.10, a Hek293 cell line was generated to express human Cx40 from a single stable FRT integration site under control of a tetracycline inducible promoter.

6.2a Identification of Human Cx40 Phosphorylation Sites.

The Cx40 sequence was scanned for putative phosphorylation sites using the neural net program NetPhos2.0 [462] and NetPhosK [463] with a sensitivity (Sn) of 79% and specificity (Sp) of 91% for known PKA sites, Sn82%, Sp89% for CK2 sites, and Sn82%, Sp97% for S6K [464, 619]. Based on the probability scores for each potential phosphorylation site and their localization within the Cx subunit we chose 4 of a possible 25 sites exceeding 50% probability for phosphorylation.

6.2b In-silico Modeling.

The Cx40 sequence, (± mutation) was submitted to the SWISS-MODEL bioinformatics server [620, 621], generating energy minimized/ optimized, sequence homology template protein models. The Cx40 models were based on the Cx26 3.5Å template 2zw3.1.A [132] with sequence homology of 63% covering residues 3-233 (CT 233-346 truncated) with a QMQE score of 0.46.

The generated structures were visualized using PyMOL (Molecular Graphics System, Version 1.5.0.4, Schrödinger, LLC). Solvent accessible surface charge calculations were done with the Pymol Adaptive Poisson-Boltzmann Solver (APBS plugin)[622], and PDB2PQR[623] with dielectrics for solvent 80 and protein 2, respectively. The Porewalker software server was used to calculate the average pore diameter at 50 points along the z(pore)-axis for quantification [624].

6.2c Site directed mutagenesis.

See section 2.10e. Mutations were incorporated into the Cx40 sequence to modify the putative phosphorylation sites to either alanine (a) or aspartic acid (d) mimicking dephosphorylation or phosphorylation respectively.

6.2d Cell Homogenization.

Cells were lysed in a general lysis buffer (see section 2.5) supplemented with either 1% triton X-100, or NP-40 detergent with protease and phosphatase inhibitors, then separated into triton soluble (TS) or non-triton soluble (NTS) fractions, normalized to TS total protein concentration.

6.2e Western Blotting.

Following the techniques outlined in section 2.9 specific antibodies were selected as follows: Goat anti-Cx40 SC-20466 (Santa Cruz Biotechnology, La Jolla, CA, USA), with AlexaFluor conjugated secondary antibodies. Equal loading was confirmed on the same blot by measuring actin expression (rabbit anti-pan Actin, Sigma-Aldrich) using another secondary antibody that was simultaneously detected with a LI-COR Odyssey scanner (LI-COR Biosciences, Lincoln, NB, USA).

6.2f Immuno-fluorescence.

Per detailed methodology section 2.11, Cx40 was detected using goat anti-Cx40 (Santa Cruz) antibodies at 0.2 μg/ml. Golgi organelles were stained with mouse anti-golgin97 at 1:200. Depending on whether dual triple or single staining protocols were being used we chose different secondary antibodies. Goat anti-mouse IgG conjugated with Alexa594 (red) was used to identify Golgi, and rabbit anti-goat IgG or donkey anti-mouse IgG conjugated to Alexa488 (green) were used to stain Cx proteins. Nuclei were stained with Hoechst 3342. Images were obtained using a Leica DMRXA2 upright fluorescence microscope equipped with an Andor iXon+ DU-855k camera, at 1000x total magnification with an oil immersion lens. Images were scored for degree of expression (0-4), with 0 representing no expression, and 4 representing multiple (>3) junctional plaques

visible at the cell-cell border, or co-localized with Golgi staining. Each border/Golgi was scored individually by 2 blinded observers, and the median, 25th percentile, and 75th percentile were plotted (box) with max and min value whiskers indicated. Inter-observer variability was very low ($R^2 = 0.9764$).

6.2g GapFRAP Dye Transfer.

Per section 2.13d, the kinetics of dye transfer were assessed by the GapFRAP technique. Hek293 cells were cultured, and loaded with Cell Trace Calcein Blue AM. Pairs of cells were identified based on defined selection criteria. One cell of the pair was bleached, and 20 subsequent scans were recorded at 10s intervals to measure the rate of fluorescence recovery.

6.2h Statistical Analysis.

Per section 2.15, we used a repeated measures ANOVA to compare GapFRAP recovery curves, and a one way ANOVA on ranks with post-hoc Dunn's analysis was used to quantify differences in immunofluorescence labeling.

6.3 Results

6.3a In Silico Modeling

As shown in 1, the NetPhosK analysis predicted a number potential phosphorylation sites. We chose to further examine four: threonine 19 (t19), contained in the n-terminus near the first transmembrane domain; serine 120 (s120) and serine 122 (s122), located in the cytoplasmic loop domain; and serine 349 (s349), found in the c-terminal domain (see Figure 6-1A,C). These sites are consensus sequences for protein kinase C (PKC), cAMP dependent protein kinase (PKA) and amp-activated protein kinase (AMPK) among others (a PPSP server analysis matched these sites to 10,11,9,17 different kinases respectively)[619].

Table 6-1. NetPhosK Predicted Cx40 Phosphorylation Sites**.**

Site	Kinase	Score	Site	Kinase	Score
S-18	PKA	0.53	T-262	p38MAPK	0.56
T-19	*PKC	0.79	S-289	DNAPK	0.6
T-27	PKC	0.58	S-289	ATM	0.53
T-39	PKC	0.55	T-307	CKI	0.51
S-43	CKII	0.56	T-307	p38MAPK	0.54
Y-66	EGFR	0.55	S-328	GSK3	0.5
S-86	PKA	0.58	S-328	cdk5	0.63
T-99	PKC	0.86	S-339	PKC	0.83
S-120	PKA	0.79	S-345	RSK	0.63
S-122	*DNAPK	0.51	S-345	PKC	0.86
Y-125	SRC	0.52	S-345	PKA	0.79
S-134	CKII	0.64	S-345	*PKG	0.53
T-181	PKC	0.52	S-348	PKC	0.89
T-181	cdc2	0.5	S-349	*PKC	0.77
S-188	p38MAPK	0.54	S-349	cdc2	0.52
S-188	PKA	0.59	S-353	CKII	0.52
S-188	GSK3	0.51	S-357	PKC	0.61
T-202	PKC	0.53	* AMPK Site Match		

In order to predict the likelihood that the identified phosphorylation sites would be accessible, in areas likely to have functional implications, and evaluate potential conformational changes, we modeled the 3D structure of Cx40. The generated Cx40 structures shared a 63% sequence homology to the crystalized Cx26 with the majority of the differences in the flexible CL loop domain (not visible in the Cx26 crystal structure). The dodecameric structure is shown in cartoon representation in Figure 6-1A. The relative locations of the NT tail in the pore center, with cytoplasmic extensions forming the CL, and the truncated CT are visible. Each individual Cx subunit is colored sequentially, with the mutation sites visible in the cartoon representation as spheres. The solvent accessible surface charge was calculated and is shown in Figure 6-1B. The end on view (left panel) shows a mixture of positive, neutral, and negative areas leading into the central pore. The longitudinal cross section (right panel) shows the channel

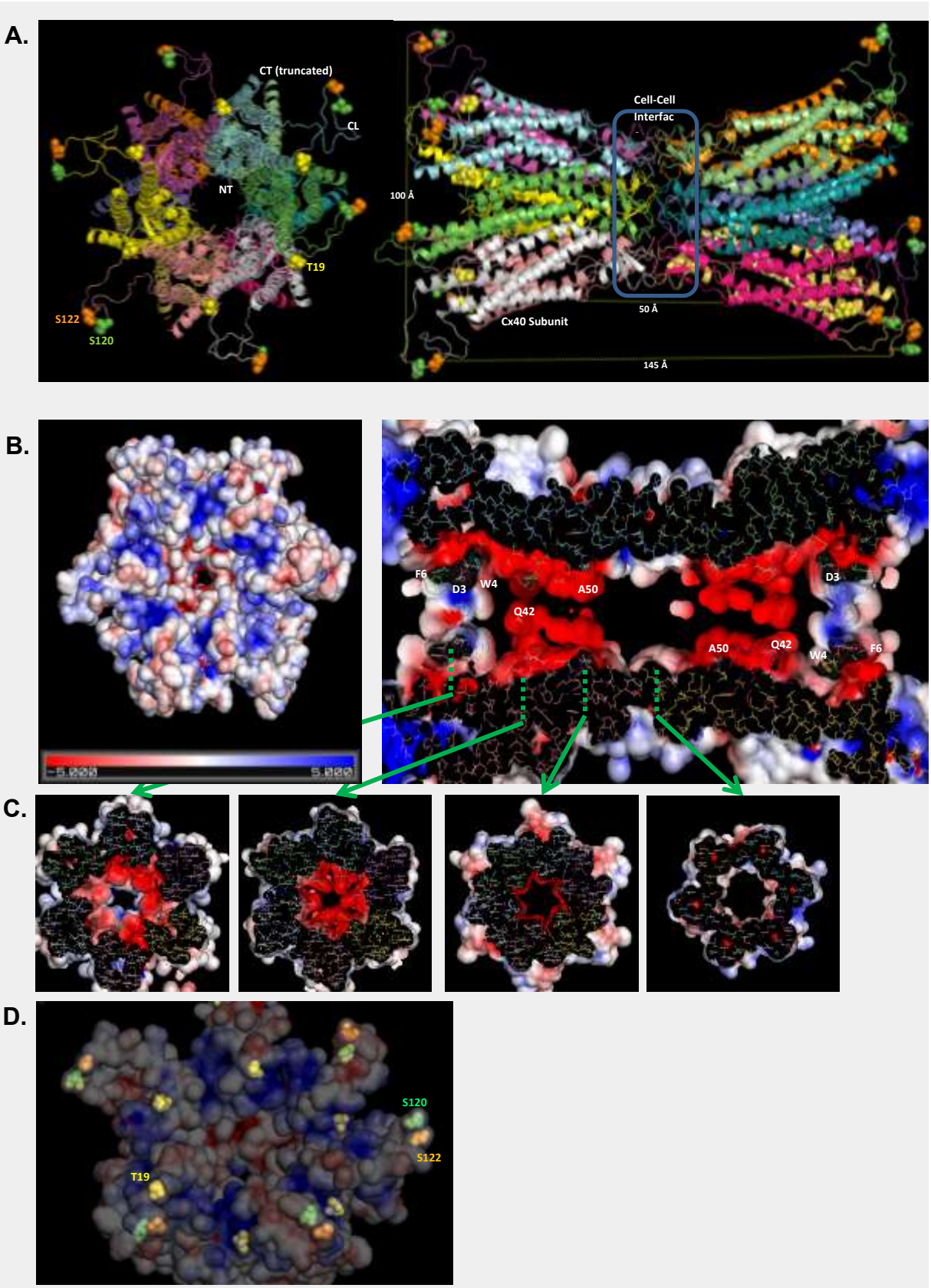

Figure 6-1. Human Cx 40 3D modelled structure (3.5 Å resolution).

Figure 6-1. Human Cx 40 3D modelled structure (3.5 Å resolution).
See previous page. **A-** *In silico* structural model of human Cx40 as generated by "SWISS-MODEL" servers using 3.5 Å Cx26 as a model template. Individual Cx40 subunits are colored sequentially. Within an individual subunit the n-terminal (NT), cytoplasmic loop (CL), and truncated c-terminal (CT) domains are visible. The location of mutation sites are shown with atom spheres. The distance between residues are indicated by yellow dotted lines (rounded to the nearest angstrom Å). **B.** Calculated solvent accessible surface charge for modeled Cx40 gap junction. Left panel - Short axis, the cytoplasmic half of one connexon is shown (end on) with a mix of positive (blue), neutral (white) and negative (red) charges visible in the cytoplasmic pore vestibule. Right panel – 10 Å deep, longitudinal cross section of pore channel surface charge model along pore axis. Key residues which limit the pore diameter are indicated. **C.** Serial sections showing relative pore size and surface charge moving inward from cytosol at points indicated by green dashed lines (F6/D3/W4 ring, Q42, A50, central pore vestibule). **D.** Mutation of sites T19 (yellow), S120 (green), and S122 (orange) are shown as atom spheres with semi-transparent surface charge superimposed. All three sites are expected to be solvent accessible.

path, including a pore funnel with minimal diameter at the level of Asp3 (D3), Trp4 (W4), Phe6 (F6). The modeled NT domain does not include the NT Met1, or Gly2 residues which are expected to be cleaved and acetylated respectively in Cx40 [625]. The modeled diameter is smaller than predicted by an equilibrated Cx26 structure (shown subsequently) in which the NT constriction is relaxed considerably [626]. This funnel area has regions of positive, neutral and negative charge, and (combined with expected G2 acetylation) the negative charge on D3 is thought to mediate cation selectivity [133, 626]. Past this constriction, primarily negatively charged residues line the channel and Glu42 (Q42) forms a ring of constriction approx. 10Å inside the pore funnel. In the equilibrated model this area is the limiting channel diameter [626]. Ala50 (A50) forms the final constriction prior to the extracellular central pore vestibule. The relative channel diameters (including surface charge) in these areas are shown as serial cross sections in C. Figure 6-1D shows the accessibility of the mutation sites chosen for potential kinase mediated phosphorylation. All three of the sites are solvent accessible, and the s122 and s120 sites are particularly well exposed.

6.3b Heterologous Expression of Cx40 in Hek293 cells Increases Dye Permeability.

Expression of Cx40 was induced in Hek293 cells by 1-2µg/mL doxycycline. Induction of Cx40 expression significantly increased junctional conductance (see Figure 6-2A). Functionally we confirmed the presence of an endogenous baseline junctional conductance in these Hek293 cells. The commonly used non-specific gap junction uncoupler heptanol was used to show that dye transfer is gap junction mediated and that inhibition of gap junctions in general reduced the Δ-fluorescence ratio (dye conductance) to the ratio observed between a bleached single cell/nearby single cell.

6.3c Wildtype Cx40 expressed in Hek293 is found at the cell-cell border and co-localized with intracellular organelles.

Immuno-fluorescent staining of Cx40 using commercial antibodies (Santa Cruz goat Anti-CT SC-CT shown here, and Chemicon Ab-1726, rabbit anti-Cx40 CT) showed that Cx40 (green staining) was found to be primarily located at the cell – cell borders as well as in cytosolic membrane compartments (see Figure 6-2B-D) in bright punctate patterns. Some of this staining appears to be localized to organelles including the Golgi which are co-stained with anti-golgin97 (red) (see Figure 6-2B-D) and possibly the endoplasmic reticulum which is normally found in the perinuclear region.

6.3d Heterologous Expression of Cx40 in Hek293 cells – Protein Expression.

Identification of Cx40 was confirmed by western blotting (see Figure 6-2E). Two separate commercial antibodies (see methods section 6.2e) against Cx40 (comparison data not shown) both identified the same doxycycline induced 35-40 kDa protein, with little to no interference from non-induced protein bands. This is consistent with previous observations that show that several connexins run slightly faster than predicted on SDS page gels relative to their expected molecular size [361].

To further show that Cx40 is being properly synthesized and trafficked to the plasma membrane/plasmalemma where it accumulates into gap junction plaques, we examined the Triton solubility of Cx40 in these different cellular compartments. Musil *et al.* showed that Cx proteins associated with the internal ER/Golgi membranes are soluble in 1% triton (TS) whereas Cx bound to the plasma membrane in gap junction plaques are not [364, 559]. Furthermore, connexins, like many other proteins, often show retarded migration upon phosphorylation [364, 559]. In the Hek293 cells used here, wildtype Cx40 protein is found, via western immunoblotting, in both the TS ER/Golgi/cytosol fraction as well as in the non-triton soluble (NTS) membrane fraction (see Figure 6-2E). In both fractions, Cx40 forms differentially phosphorylated isoforms, as indicated by differences in migration in SDS-PAGE, shown more clearly in Figure 6-2F where the typical isoforms P0, P1, and P2 are visible (although we are unable to quantitatively separate them). Previous studies have shown that the Cx40 [627] and Cx43 isoforms co-migrate when treated with alkaline phosphatase indicating that the banding is phosphorylation dependent [364, 559].

Figure 6-2. Heterologous expression of functional Cx40 in Hek293 cells.
See next page. **A-** Treatment with 1µg/ml doxycycline induced Cx40 activity in Hek293 cells, significantly increasing dye transfer between cell pairs. Mean ± SEM fluorescence (recipient/donor %) shown. Inhibition of gap junctions with 2mM heptanol (5min) prevented recovery of fluorescence. Overall Hek293 vs. Cx40 p=1.5x10-11. The number of cell pairs used for each group is indicated in the legend (n). B-D- Cx40 is expressed in Hek293 cells at the cell-cell borders and inside the cell within the Golgi and other organelles. **B-** Non-transfected Hek293 cells. **C-** Cx40 Hek293 cells (1^{o} rabbit anti-Cx40). Note in C- Cx40 in perinuclear Golgi like organelles (yellow arrows) and in gap junction plaques (green arrow). Note in **D-** Single cells of the same line (as C.) tend to contain primarily Golgi- localized Cx40 staining versus normal staining in cell pairs. **E-** Western blot, using the same antibody as in B-D, shows that there is no endogenous expression of Cx40 in Hek293 cells (lane 1,2,4,5). Treatment with doxycycline (1µg/mL) induced Cx40 expression in the (membrane bound) non-triton soluble (NTS) fractions and (intracellular) triton soluble (TS) fractions (lanes 3, 6 respectively).

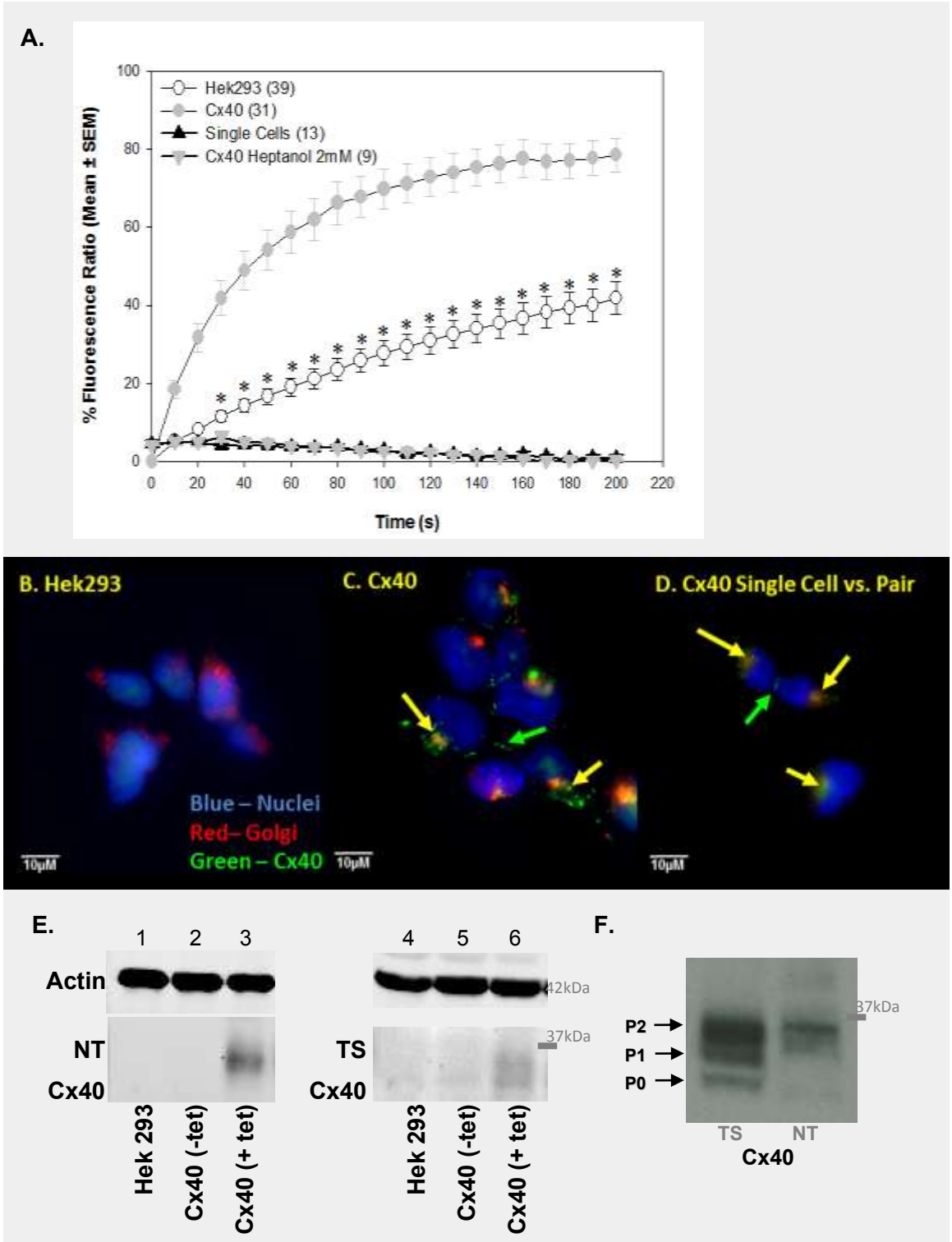

Figure 6-2. Heterologous expression of functional Cx40 in Hek293 cells.

6.3e Endogenous expression of Cx45.

In an attempt to identify the Cx responsible for the background conductance observed in Figure 6-2A we examined endogenous expression of Cx43, and Cx45 which have been previously reported in small amounts in other Hek293 cells [372, 420, 459-461]. Neither Cx43 nor Cx45 were detectable by immunofluorescence or by western blot in triton soluble cell homogenate fractions even when using up to 100µg of total protein per lane (data not shown). However, when amplified by co-precipitation with anti-Cx40, we were able to identify very low levels of Cx45 (data not shown). Co-precipitation of Cx43 by the same methods was not detectable. Immuno-fluorescent staining of Cx45 was not obvious in these cells, but some punctate staining of appositional membranes was observed. Background staining of Cx43 was not observed (data not shown).

6.4 Mutation of Putative hCx40 Phosphorylation sites

6.4a Phosphorylation of s122 is required for normal function and the s122a mutant has reduced plasmalemmal expression.

Mutation of the putative AMPK/DNAPK phosphorylation site at s122 to mimic de-phosphorylation (s122a) reduced Cx40 conductance markedly (Figure 6-3A). The activity of the phosphomimetic s122d was comparable to wildtype. Cx40 plasmalemmal and Golgi expression of s122a protein was significantly reduced (Figure 6-3C,E,F). Expression of the s122d mutant was normal in both fractions and immunofluorescence staining was similar relative to wildtype Cx40. As these observations match the change in function observed, it would indicate that phosphorylation of s122 is required for normal function and the lack of gap junction formation underlies the reduced communication of this mutant.

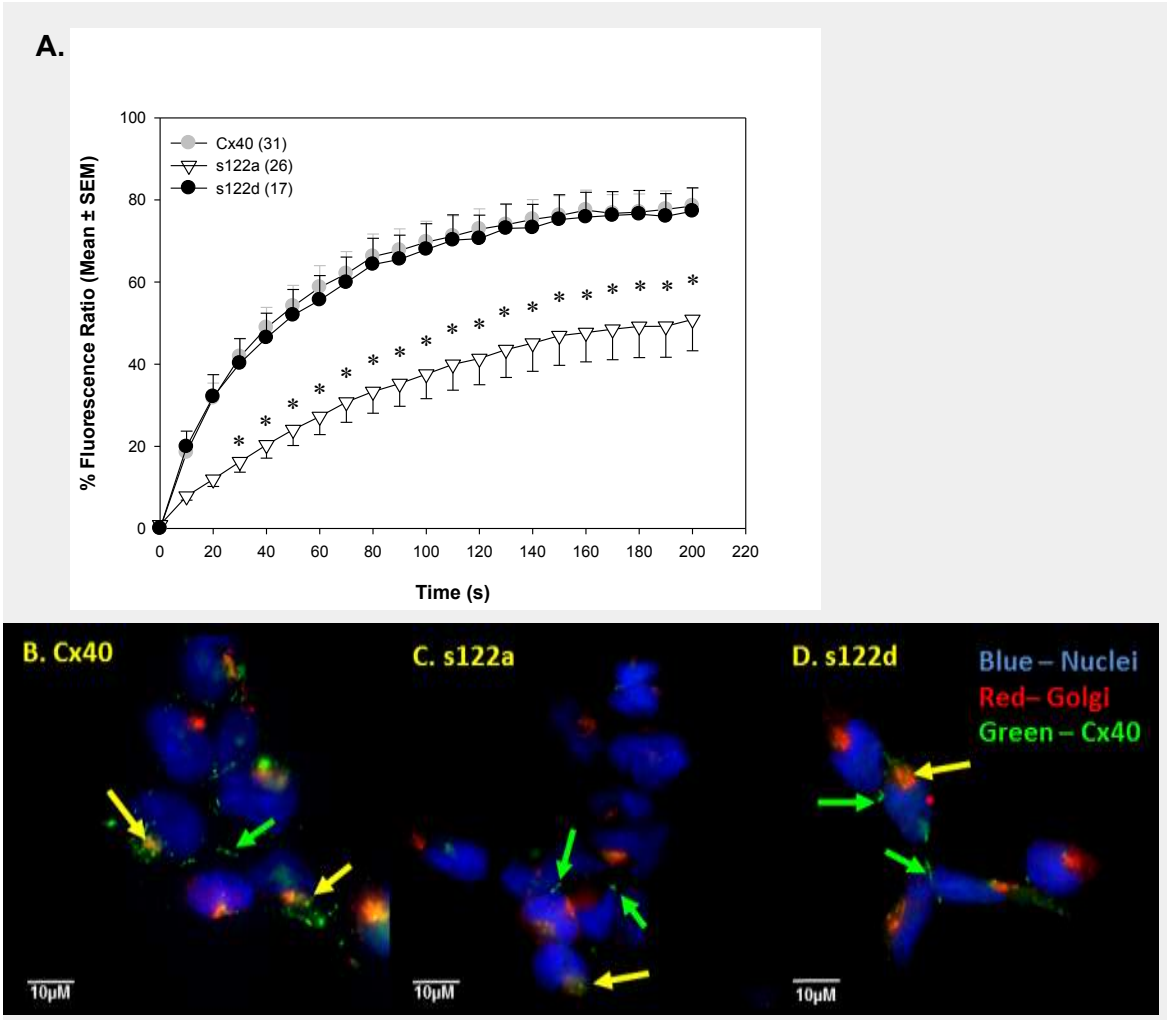

Figure 6-3. Phosphorylation of Cx40 s122 (s122d) is required for normal activity.

Figure 6-3. Phosphorylation of Cx40 s122 (s122d) is required for normal activity.

See previous page. **A-** Preventing phosphorylation of this cytoplasmic loop residue (s122a) inhibits calcein blue dye conductance significantly (overall p=1.8x10-6). * indicates p<0.05 vs. Cx40 at each time point. **B-D**- Mutation of Cx40 s122 to mimic de-phosphorylation (s122a) reduced the expression of Cx40. Localization of **B-**Cx40, **C-**Cx40 s122a and **D-**Cx40 s122d mutants. Both mutants traffic to the plasma membrane to some extent (green arrow/stain) and are found in the Golgi (yellow arrow). **E-F** The expression of s122a was reduced at the cell-cell border and in the Golgi apparatus. s122d expression was similar to wildtype Cx40 based on blinded analysis of immunofluorescence scored for degree of expression. *p <0.05 vs. wildtype Cx40.).

We also examined the surface charge distribution, and limiting pore diameter of the modeled structures of these mutants (Figure 6-4). The charge distribution in the central cytoplasmic vestibule is fairly consistent between Cx40 and the mutants, with an increase in negative charge in the distal areas of the cytoplasmic loop in the s122d mutant as expected. The diameter of the pore funnel (D3,W4,F6) ring appears to be slightly smaller in the s122 mutants (Figure 6-4B right panel), and (~z=12-13) in the corresponding quantified data (Figure 6-4D). In the Glu42 region, mutation affected the pore diameter with s122a>s122d>Cx40 (~z=18-19). In addition, there appears to be a greater concentration of negative charge in the pore funnel region in the s122a vs. s122d/Cx40. Combined these data indicate that some conformational change may also have occurred.

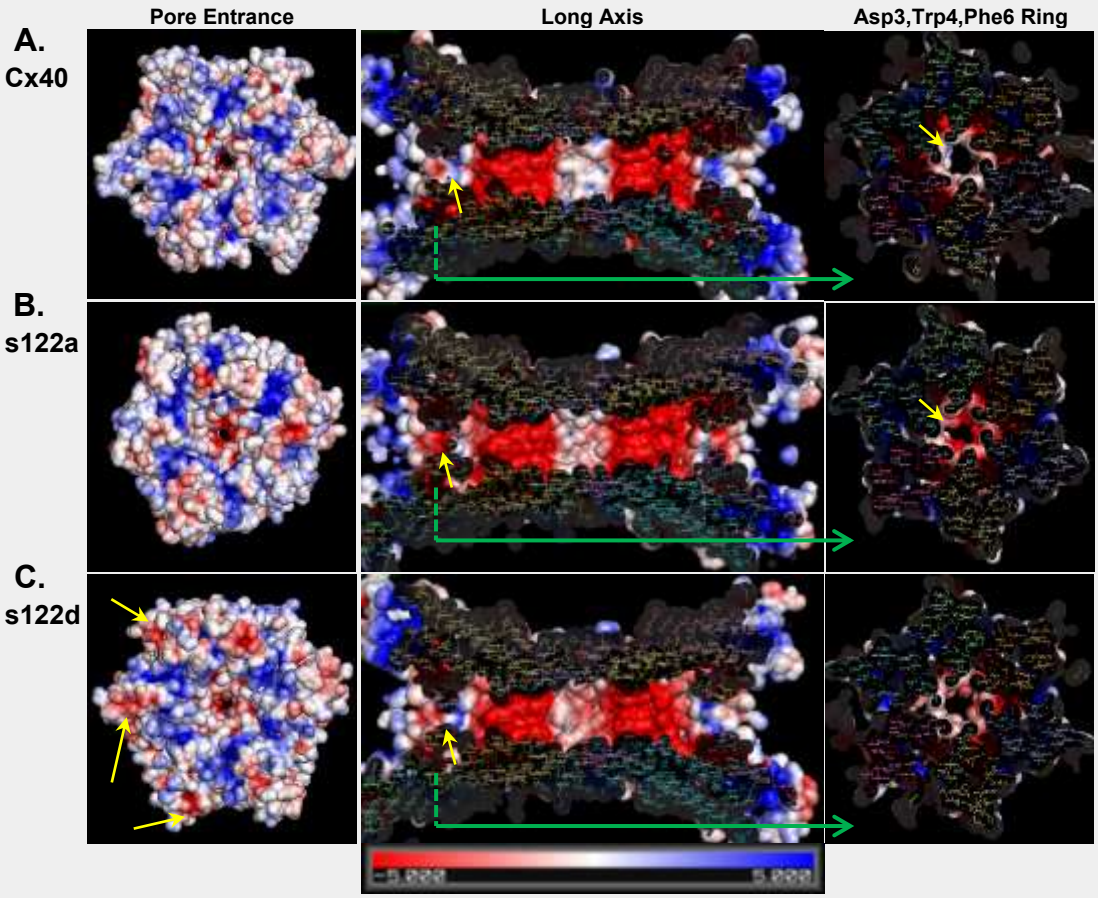

Figure 6-4. Structural modeling of Cx40s122 mutants.

A-C. Solvent accessible surface charge model of Cx40 (A), s122a (B), and s122d (C). Left panel shows the cytoplasmic pore vestibule (end on view), the central panel shows the longitudinal cross section along the pore channel axis, and right panel shows a cross section of the D3/Q4/F6 ring (10 Å depth). **Left panel -** The cytoplasmic pore funnel domains appear similar between Cx40 and the s122 mutants with greater negative charge in the region near the s122d mutant (yellow arrows). **Central panel -** There is a change in the surface charge near the D3,W4,F6 ring with more intense negative (red) charge density in the s122a mutant versus the Cx40 and s122d mutant (yellow arrows). **Right panel -** This change was confirmed when examining the full circumference of the D3/W4/F6 ring. In the s122a mutant there is a greater overall negative charge density (more red and less neutral/white around the pore in B vs. A/C). There also appears to be a decrease in positive (blue) charge density (yellow arrow A vs. B). **D.** Porewalker average diameter profile indicates that the mutants have a similar modeled pore size.

6.4b Phosphorylation of s120 reduced junctional conductance without altering plasmalemmal expression.

In contrast to the previous example, mutation of the s120 (putative PKA) phosphorylation site in the cytoplasmic loop region of Cx40 to mimic phosphorylation (s120d) reduced Cx40 mediated dye conductance, whereas the s120a mutant was similar to wildtype (Figure 6-5A). Immunofluorescence staining indicates that both the s120a and s120d mutants are expressed at the cell-cell borders as well as in cytoplasmic organelles (Figure 6-5B-D). Quantitation of the immunofluorescent data confirms that there was no significant difference in plasmalemmal expression. This may indicate that the reduced function of the s120d mutant reflects a decrease in junctional permeability. In fact, in addition to some changes in the pore lining surface charge distribution, the modeled limiting pore diameter reflected the permeability: Cx40>s120a>>s120d (Figure 6-6A-C right panel, and z~12-13 in the corresponding quantified data Figure 6-6D). There did not appear to be any change in the Glu42 region (~z=18-19). Combined these data indicate that phosphorylation produced a conformational change that limited the permeability of Cx40 channels formed with s120d.

Figure 6-5. Phosphomimetic mutation of Cx40 s120 reduced calcein blue dye permeability without altering Cx40 expression at the cell membrane.
See next page. **A-** Cx40 functional activity was significantly reduced in s120d mutant, p= 0.0044 vs. Cx40. The dephosphorylation mimic (s120a) had no effect (overall p=0.881). * indicates p<0.05 vs. Cx40 at each time point. The number of cell pairs examined is indicated in the legend (n). **B-D-** Localization of B-Cx40, C- Cx40 s120a and D-Cx40 s120d mutants. Relative to the expression of wildtype Cx40 both mutants (green arrows/staining) appear to traffic to the plasma membrane normally. Again perinuclear staining is apparent (yellow arrow). **E-F** Cx40 expression based on blinded analysis of immunofluorescence scored for degree of expression. **E-** s120a and s120d are expressed to a similar degree at the plasma membrane. **F-** Golgi localized expression of s120a and s120d is significantly reduced. *p <0.05 vs. wildtype Cx40.

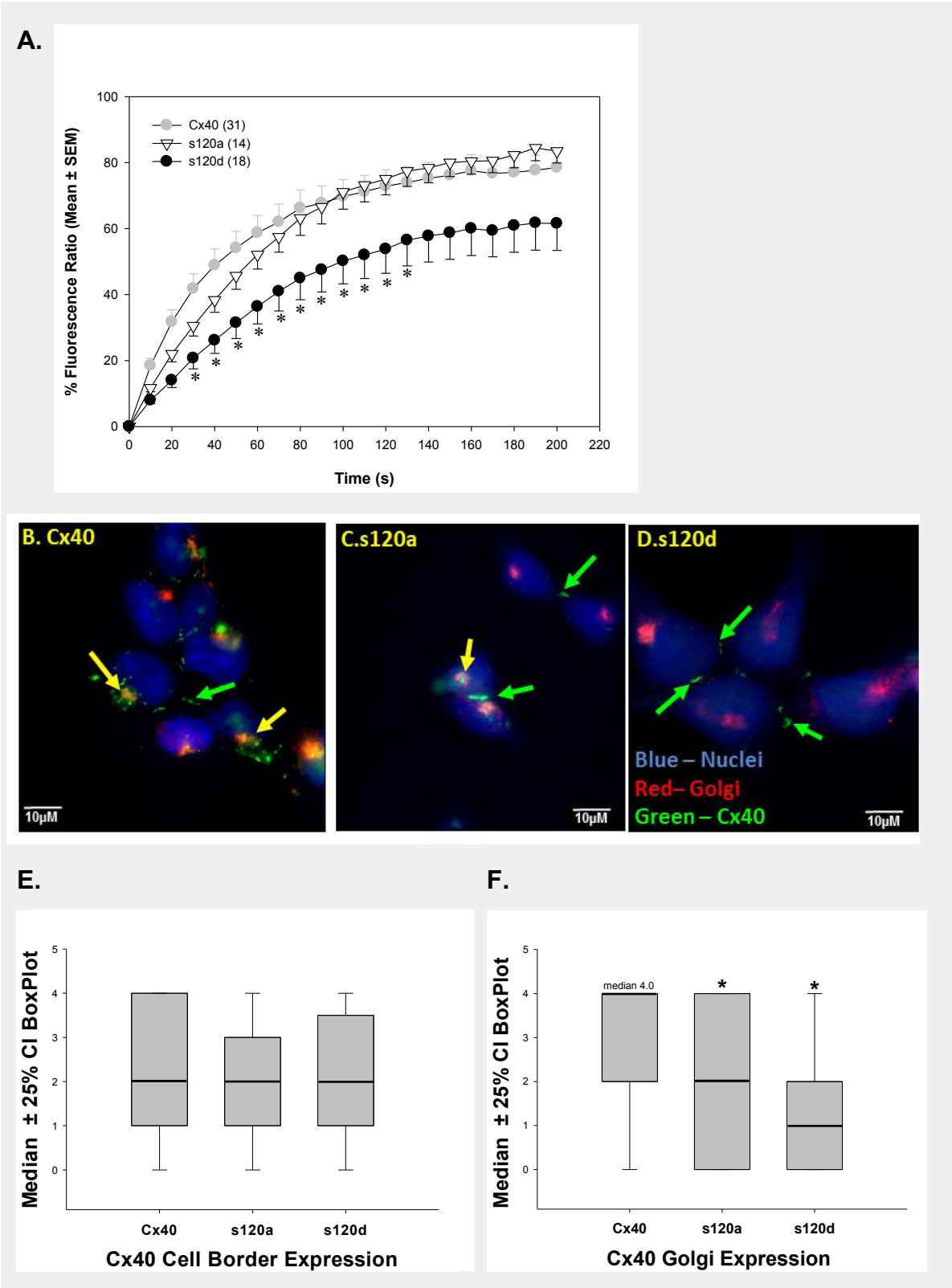

Figure 6-5. Phosphomimetic mutation of Cx40 s120 reduced calcein blue dye permeability without altering Cx40 expression at the cell membrane.

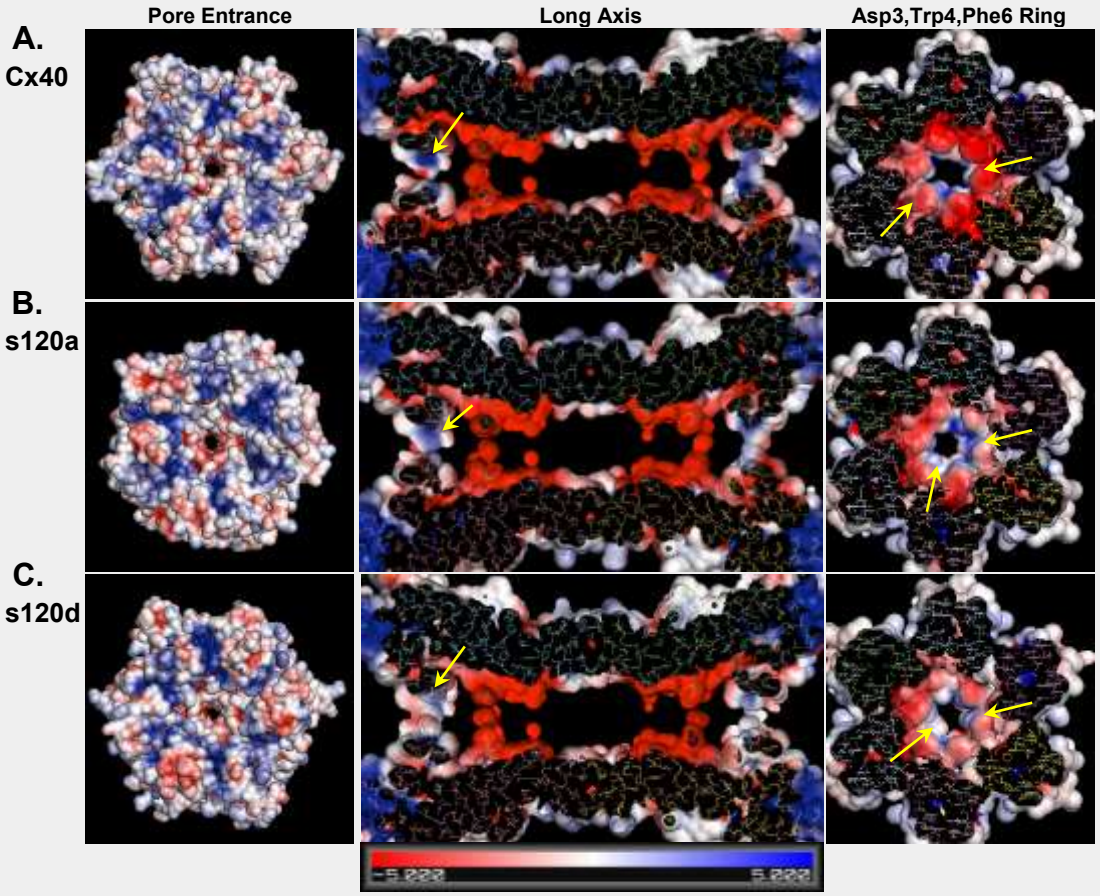

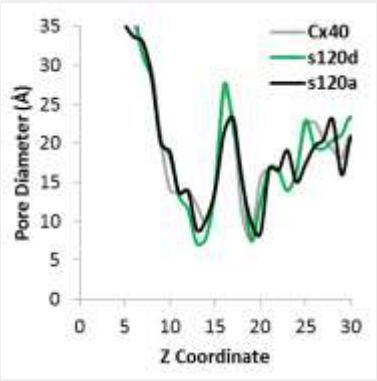

Figure 6-6. Structural modeling of Cx40s120 mutants.
A-C. Solvent accessible surface charge models of Cx40 (A), s120a (B), and s120d (C). **Left Panel -** The cytoplasmic vestibule domains appear similar between Cx40 and the s120 mutants. **Central Panel -** It appears that there is a change in the surface charge near the D3,W4,F6 ring with diffuse positive (blue, yellow arrow) in s120a, and more negative (red) and greater neutral (white) charge area in the s120d mutant. **Right Panel -** Full pore circumference at D3/W4/F6 (10Å slice depth). The Cx40 image shows more intense negative (red) charge density in the outermost funnel versus either mutant (right panel A, yellow arrows). There is more positive charge deeper into the funnel in the s120a and more neutral charge density in the s120d mutant (yellow arrows) indicating a change in the underlying structural conformation. The s120d mutant also had the smallest pore limiting diameter forming more of a slit versus Cx40 or s120a. **D.** Porewalker average diameter calculation profile.

6.4c Mutation of s349 to mimic phosphorylation (s349a) or dephosphorylation (s349a) has no effect on Cx40 conductance

Mutation of the putative PKC/AMPK phosphorylation site at serine 349 in the c-terminal tail region of Cx40 had no significant effect on dye permeability (Figure 6-7A). Both mutants were visibly able to form apparent gap junctional plaques (Figure 6-7B-D), and staining was evident in some perinuclear regions. Quantitatively, there was no significant difference in the expression of these mutants in the plasmalemma fraction (data not shown). We were not able to model this region of the Cx protein as it was not visible in the published Cx26 crystal structure.

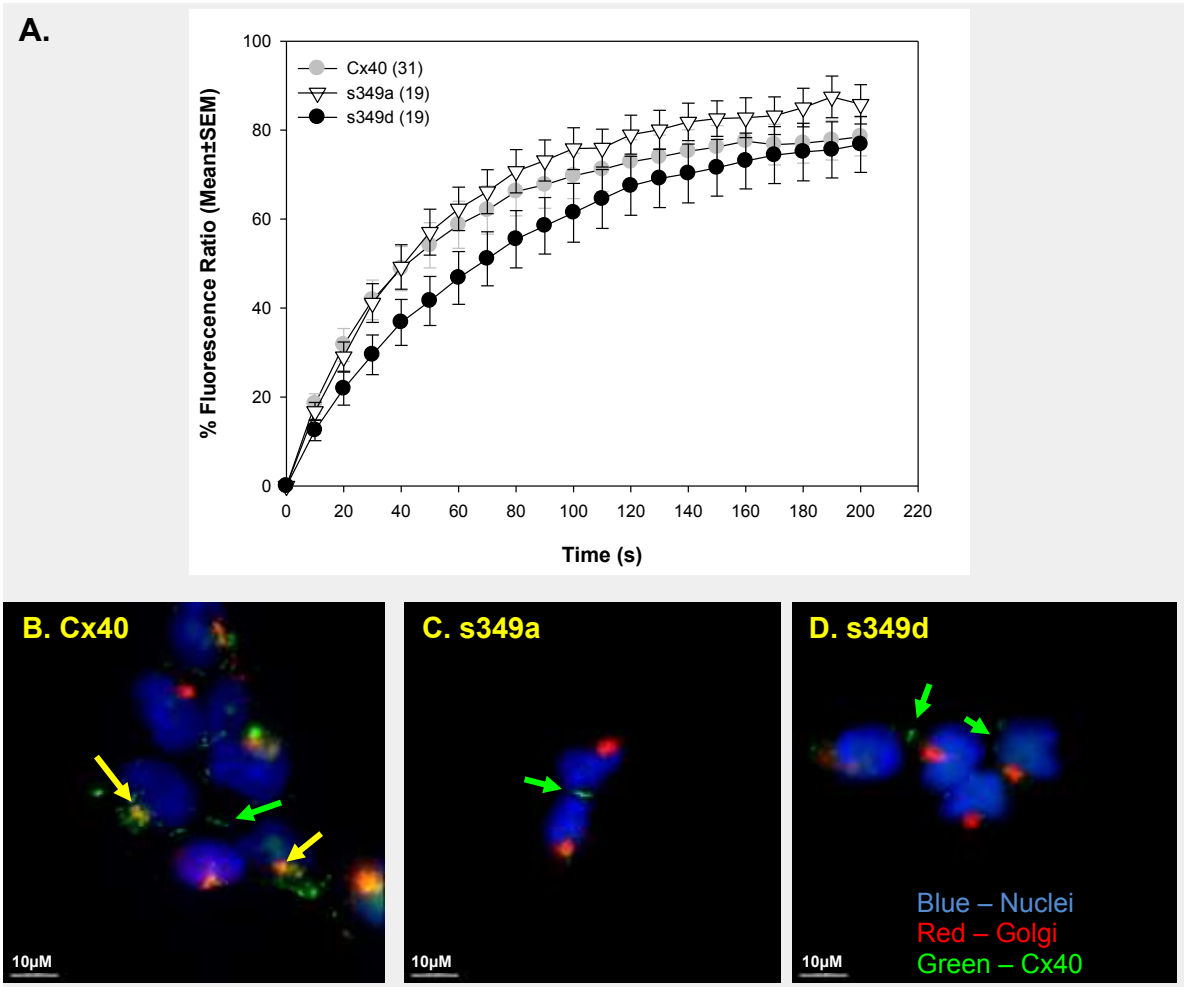

Figure 6-7. Cx40 permeability and expression are not affected by mutation of Cx40 s349.
A- Calcein blue dye transfer, was not statistically different between s349a/d versus Cx40. The number of cell pairs examined is indicated in the legend (n). **B-D.** Localization of **B-** Cx40, **C-** Cx40 S349a and **D-** Cx40 S349d mutants. Both s349a and s349d mutants formed visible gap junctions (green arrows) and their distribution was similar to Cx40.

6.4d Mutation of Threonine-19 to mimic phosphorylation reduces junctional conductance and expression at the cell-cell border

Mimicry of dephosphorylation by mutation to alanine (t19a) had no statistically significant effect on the overall rate of dye transfer between t19a containing cells (Figure 6-8A). However, the t19d mutation significantly reduced the dye permeability of the channels (including a dominant negative reduction in the minimal background conductance).

The ability of these mutants to be synthesized and their intracellular trafficking was examined by immunofluorescence. Figure 6-8B-F shows that the level of cell-cell border expression matches the functional activity trend, with expression of Cx40 > t19a >>t19d (Figure 6-8E). These results likely indicate that disruption of proper Cx40 trafficking is responsible for the reduction of junctional conductance. There also appears to be a reduction in the Golgi expression of both mutants (Cx40>t19a>t19d; median 4 vs. 2, vs. 0 respectively). Qualitatively, some of the t19d signal was located in a perinuclear region that was not associated with Golgi staining indicating that the intracellular distribution may be affected by these mutations. In addition to some changes in the surface charge distribution in both the cytoplasmic vestibule and the pore funnel domains, the size of the limiting pore diameter was reduced in the modeled proteins in a manner that corresponded to the permeability differences observed

Figure 6-8. Calcein Blue dye conductance is markedly reduced after mutation of Cx40 t19 to mimic phosphorylation (t19d).

See next page. **A.** Dye transfer, overall t19d vs. Cx40 p=1.1x10-10. Mutation to mimic dephosphorylation (t19a) had no effect overall (p=0.063 vs. Cx40).*indicates p<0.05 (t19d vs. Cx40) at individual time points. t19d was also significantly reduced vs. Hek293 background conductance (overall p=0.025). The number of cell pairs examined is indicated in the legend (n). **B-D.** Localization of B- Cx40, C- Cx40 t19a and D- Cx40 t19d mutants. In comparison to t19a, the t19d tended to be located in cytoplasmic/intracellular compartments including the Golgi (yellow arrow) as well as in perinuclear regions (possibly ER) (indicated by white arrow). **E-F.** Cx40 expression based on blinded analysis of immunofluorescence scored for degree of expression. **E.** Expression of t19a is somewhat reduced, and t19d almost non-existent at the cell-cell border. **F.** Golgi expression of t19a and t19d are significantly reduced vs. Cx40. *p <0.05 vs. wildtype Cx40.

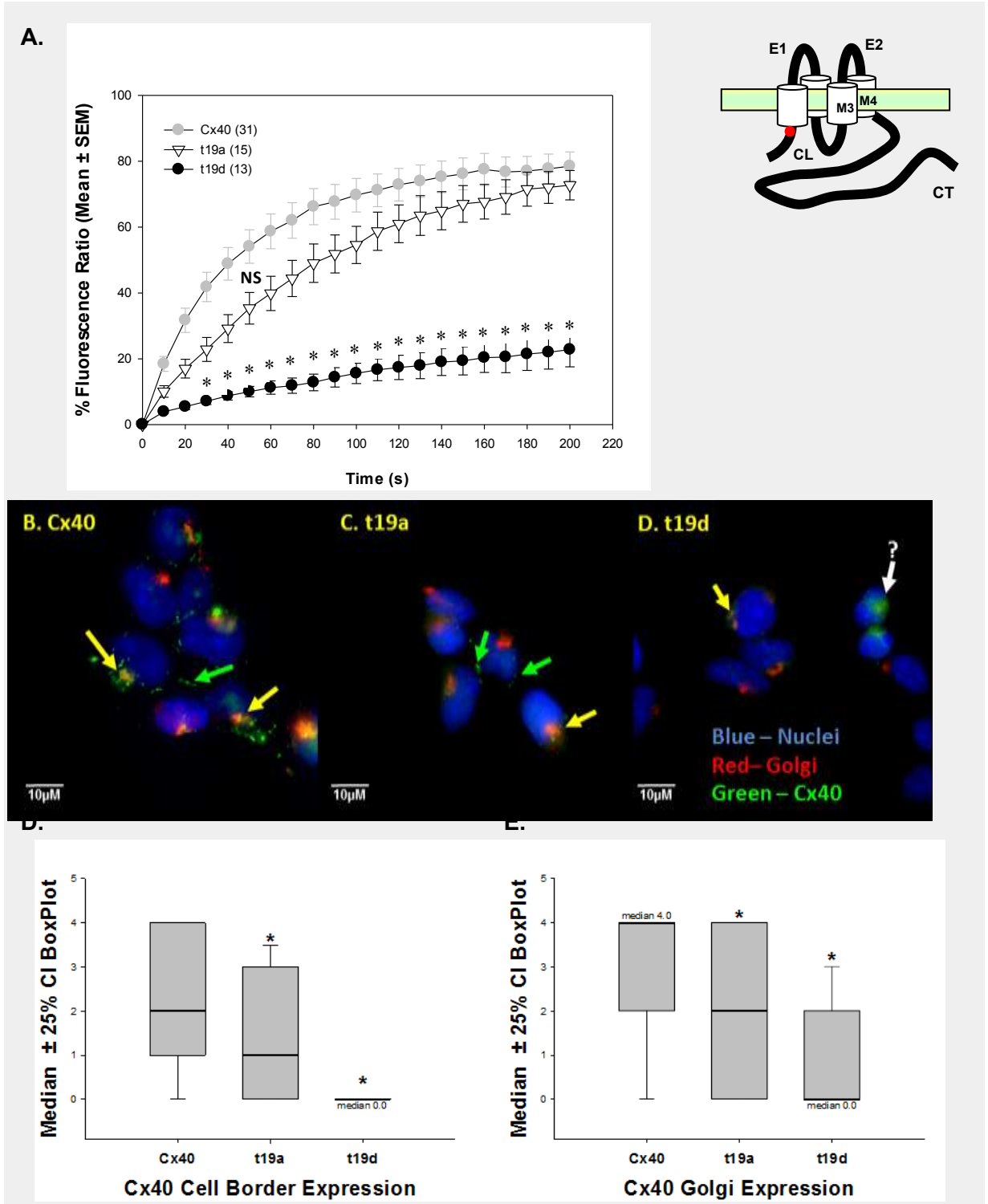

Figure 6-8. Calcein Blue dye conductance is markedly reduced after mutation of Cx40 t19 to mimic phosphorylation (t19d).

with (Cx40=t19a>>t19d) as shown in Figure 6-9A-C right panels, and z~12-13 in the corresponding quantified data Figure 6-9D). Combined, these data would indicate that phosphorylation at t19 causes a conformational change that affects Cx40 protein localization.

6.5 Discussion

6.5a Cx40 Mutations affecting Cx40 function.

Collectively, the current data suggest that human Cx40 is regulated significantly by the mutation of three previously uncharacterized putative phosphorylation targets; t19 in the n-terminal segment, and s120, and s122 in the cytoplasmic loop domain. The effects appear to be mediated by changes in expression, localization, and potentially by conformational changes in the gap junction structure. Phosphorylation has been predominantly studied in the CT domain, however the CL domain of Cx56 [628] and the NT domain of Cx43 in brain tissues [393] have been reported to be phosphorylated. To date, regulatory phosphorylation of human cardiac connexins within these domains has not been demonstrated.

6.5b Connexin Phosphoregulation

There is an abundance of scientific literature (most commonly with Cx43) showing the gain of function, loss of function, and altered expression, half-life, permeability, protein-protein interaction, or cellular localization due to phosphorylation of specific Cx residues [117, 351-353, 551, 554, 556]. Specifically: (1) activation of PKA/cAMP leads to phosphorylation of Cx43 s364, and s365 necessary for translocation from the trans-Golgi to the plasma membrane and activation of Cx43 conductance [160, 352, 384, 387, 394].

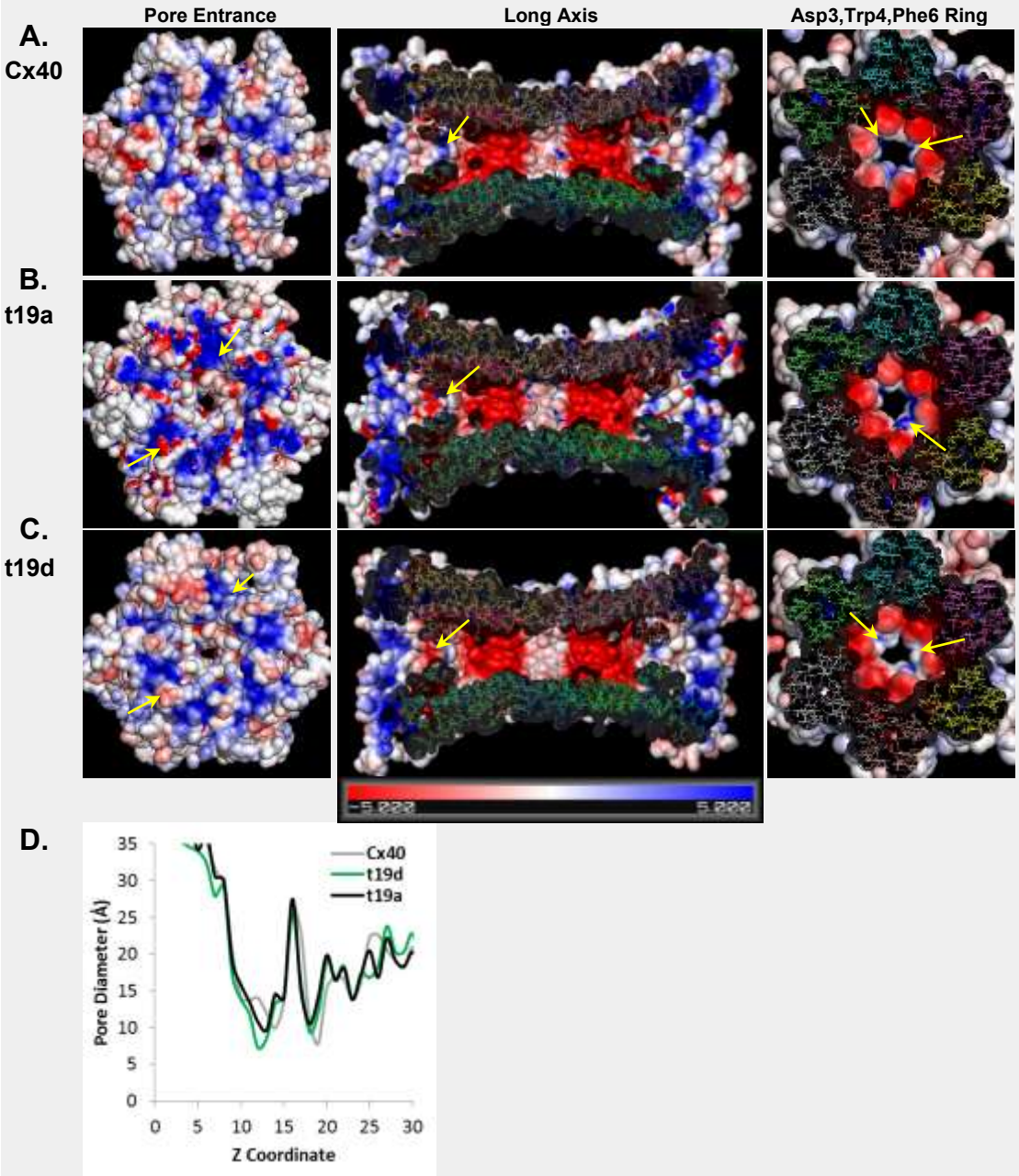

Figure 6-9. Structural modeling of Cx40t19 mutants.

A-C. Solvent accessible surface charge model of Cx40 (A), t19a (B), and t19d (C). **Left Panel -** It appears that there are larger surface charge gradients in the t19a cytoplasmic pore vestibule , with more intense positive/blue, and negative /red in the central areas (B vs. A, yellow arrow), and more neutral (white) charge density in the distal regions. **Central Panel -** There appears to be more variation near the D3,W4,F6 ring in both t19 mutants (greater negative charge (red) in some areas, yellow arrows vs. Cx40). **Right Panels -** Full pore circumference at D3/W4/F6 (10Å slice depth). There appears to be a greater concentration of positive (blue) charge in some areas (t19a yellow arrow versus Cx40, t19d). Combined these changes indicate an alteration in the underlying structural conformation. The conductance of the t19d and t19a mutant appear to follow the limiting diameter in this region with Cx40>t19a>t19d in cross sectional area. **D.** Porewalker average diameter profile. Cx40=t19a>t19d.

(2) PKA mediated phosphorylation of Cx50 at s395 causes an increase in conductance which was attenuated by mutation of the site to alanine [629]. (3) Accretion of Cx43 into GJ plaques is induced by Akt dependent phosphorylation of Cx43 at s373 which was blocked by its mutation to alanine, and by genetic inhibition of Akt [117, 122]. (4) Activation of PKC (via phorbol ester) leads to phosphorylation of Cx43 at s262 and s368 and down regulation of Cx43 activity (including its unitary electrical conductance) [163, 362, 399, 400]. These studies outline similar pathways to those affected here that are modified by phosphorylation, and support the premise that mutation of putative phosphorylation sites can block and mimic their effects.

Alterations in junctional conductance can be related to altered expression or localization, altered activity (open probability, pore diameter) despite normal expression, or some combination of the two. The reduced activity of the s122a mutant appears to be dependent on its reduced expression at the cell-cell border, with potential changes in the surface charge in the pore funnel domain.

The decrease in conductance of 120d cannot be explained by a defect in expression or trafficking. Both s120 mutants are expressed normally at the cell-cell border. However, the functional activity of the s120d mutant is impaired significantly and this impairment corresponded to a reduction in the modeled pore funnel diameter indicating that a conformational change results.

In vitro studies have demonstrated that activation of cAMP and PKA can lead to an increase in Cx40 activity [615, 616]. The s120d mutant leads to a decrease in terminal conductance unrelated to plasmalemmal expression. Thus 120d is not a likely candidate to be responsible for the PKA mediated increase in conductance. However, the ability to phosphorylate s122 appears necessary for normal conductance.

It appears that various putative phosphorylation sites may regulate Cx40 function via different mechanisms. For example the t19d mutation results in a protein that does not accumulate in Golgi and is not properly transported to the plasmalemma indicating the protein might be less stable. The inability to phosphorylate s122 (s122a), results in an inability to traffic the protein from the Golgi to the plasmalemma. In contrast phosphorylation of s120d causes normal plasmalemmal expression but conductance is reduced. This suggests a direct effect on gating or selectivity of plasmalemmal Cx40.

The connexin CT and CL domains are known to modify channel opening probability [630] affecting dye permeability [631], and have been shown to interact in a particle receptor fashion induced by low pH [152, 153, 630]. The region of Cx43 proposed to be the CT receptor corresponds to CL residues 119-144. Based on our modeled structures, this region has a loop domain which contains s120, and s122 at the tip of the formed loop. As such, these residues are proposed to be in a particularly vital area for the interaction of the CT and the CL. Previous studies have shown that v-SRC (tyrosine kinase) can interact with the Cx43 CL, modulating its interaction with the CT domain, and affecting junctional permeability [152]. In addition, it has been shown previously that CL phosphorylation of Cx56 induces junctional closure in a PKC dependent manner [628]. From these data and our observations, we suggest that phosphorylation of the CL at s122 and s120 likely represents a previously unrecognized regulatory mechanism affecting Cx40 activity. Experimental analysis of the interaction between these domains of Cx40 would be beneficial.

Based on previously documented limitations in the Cx26 crystal structure [626] it is likely that our model indicates a smaller than experimentally observed pore diameter. However, one of the limits of Cx structural biology at this time is the lack of structural data on closed vs. open channels [133]. As such, our model could also allow the experimental confirmation that s120d mutant Cx40 and wild

type Cx40 have different crystal structures and perhaps shed some light on the structure of the pore funnel domain in general.

6.5c Limitations

Although we have identified three novel sites where phosphorylation might be expected, these are putative phosphorylation sites. No direct evidence is provided that these sites are endogenously phosphorylated, moreover simultaneous phosphorylation of multiple binding sites could result in complex phenotypes.

6.6 Conclusions

We have demonstrated for the first time that mutation of putative phosphorylation sites in the cytoplasmic loop may be a significant factor in regulating Cx40 via multiple mechanisms.

6.7 Acknowledgements

Technical assistance provided by Jim Lees Miller, and David Dilworth. T-Rex Flpin cells were gratefully provided in collaboration with the laboratory of S.R. Wayne Chen.

6.8 Literature Cited

[40] Hagendorff A, Schumacher B, Kirchhoff S, Luderitz B, Willecke K. Conduction disturbances and increased atrial vulnerability in Connexin40-deficient mice analyzed by transesophageal stimulation. Circulation. 1999;99:1508-15.

[117] Solan JL, Lampe PD. Specific Cx43 phosphorylation events regulate gap junction turnover in vivo. FEBS Lett. 2014.

[122] Dunn CA, Su V, Lau AF, Lampe PD. Activation of Akt, not connexin 43 protein ubiquitination, regulates gap junction stability. J Biol Chem. 2012;287:2600-7.

[127] Unger VM, Kumar NM, Gilula NB, Yeager M. Projection structure of a gap junction membrane channel at 7 A resolution. Nature structural biology. 1997;4:39-43.

[128] Yeager M, Unger VM, Falk MM. Synthesis, assembly and structure of gap junction intercellular channels. Current opinion in structural biology. 1998;8:517-24.

[129] Unger VM, Kumar NM, Gilula NB, Yeager M. Three-dimensional structure of a recombinant gap junction membrane channel. Science. 1999;283:1176-80.

[130] Kronengold J, Trexler EB, Bukauskas FF, Bargiello TA, Verselis VK. Single-channel SCAM identifies pore-lining residues in the first extracellular loop and first transmembrane domains of Cx46 hemichannels. J Gen Physiol. 2003;122:389-405.

[131] Maeda S, Tsukihara T. Structure of the gap junction channel and its implications for its biological functions. Cell Mol Life Sci. 2011;68:1115-29.

[132] Maeda S, Nakagawa S, Suga M, Yamashita E, Oshima A, Fujiyoshi Y, et al. Structure of the connexin 26 gap junction channel at 3.5 A resolution. Nature. 2009;458:597-602.

[133] Oshima A. Structure and closure of connexin gap junction channels. FEBS Lett. 2014.

[134] Beyer EC, Lipkind GM, Kyle JW, Berthoud VM. Structural organization of intercellular channels II. Amino terminal domain of the connexins: sequence, functional roles, and structure. Biochim Biophys Acta. 2012;1818:1823-30.

[135] Oh S, Rubin JB, Bennett MV, Verselis VK, Bargiello TA. Molecular determinants of electrical rectification of single channel conductance in gap junctions formed by connexins 26 and 32. J Gen Physiol. 1999;114:339-64.

[136] Purnick PE, Oh S, Abrams CK, Verselis VK, Bargiello TA. Reversal of the gating polarity of gap junctions by negative charge substitutions in the N-terminus of connexin 32. Biophys J. 2000;79:2403-15.

[137] Stergiopoulos K, Alvarado JL, Mastroianni M, Ek-Vitorin JF, Taffet SM, Delmar M. Hetero-domain interactions as a mechanism for the regulation of connexin channels. Circulation research. 1999;84:1144-55.

[138] Zhou L, Kasperek EM, Nicholson BJ. Dissection of the molecular basis of pp60(v-src) induced gating of connexin 43 gap junction channels. The Journal of cell biology. 1999;144:1033-45.

[139] Morley GE, Taffet SM, Delmar M. Intramolecular interactions mediate pH regulation of connexin43 channels. Biophys J. 1996;70:1294-302.

[140] Ek-Vitorin JF, Burt JM. Structural basis for the selective permeability of channels made of communicating junction proteins. Biochim Biophys Acta. 2013;1828:51-68.

[152] Duffy HS, Delmar M, Coombs W, Tafftet SM, Hertzberg EL, Spray DC. Functional demonstration of connexin-protein binding using surface plasmon resonance. Cell Commun Adhes. 2001;8:225-9.

[153] Duffy HS, Sorgen PL, Girvin ME, O'Donnell P, Coombs W, Taffet SM, et al. pH-dependent intramolecular binding and structure involving Cx43 cytoplasmic domains. J Biol Chem. 2002;277:36706-14.

[160] Solan JL, Marquez-Rosado L, Sorgen PL, Thornton PJ, Gafken PR, Lampe PD. Phosphorylation at S365 is a gatekeeper event that changes the structure of Cx43 and prevents down-regulation by PKC. The Journal of cell biology. 2007;179:1301-9.

[163] Ek-Vitorin JF, King TJ, Heyman NS, Lampe PD, Burt JM. Selectivity of connexin 43 channels is regulated through protein kinase C-dependent phosphorylation. Circulation research. 2006;98:1498-505.

[350] Chen VC, Gouw JW, Naus CC, Foster LJ. Connexin multi-site phosphorylation: mass spectrometry-based proteomics fills the gap. Biochim Biophys Acta. 2013;1828:23-34.

[351] Marquez-Rosado L, Solan JL, Dunn CA, Norris RP, Lampe PD. Connexin43 phosphorylation in brain, cardiac, endothelial and epithelial tissues. Biochim Biophys Acta. 2012;1818:1985-92.

[352] Solan JL, Lampe PD. Connexin43 phosphorylation: structural changes and biological effects. Biochem J. 2009;419:261-72.

[353] Lampe PD, Lau AF. The effects of connexin phosphorylation on gap junctional communication. The international journal of biochemistry & cell biology. 2004;36:1171-86.

[361] Kadle R, Zhang JT, Nicholson BJ. Tissue-specific distribution of differentially phosphorylated forms of Cx43. Mol Cell Biol. 1991;11:363-9.

[362] Solan JL, Fry MD, TenBroek EM, Lampe PD. Connexin43 phosphorylation at S368 is acute during S and G2/M and in response to protein kinase C activation. Journal of cell science. 2003;116:2203-11.

[364] Musil LS, Goodenough DA. Biochemical analysis of connexin43 intracellular transport, phosphorylation, and assembly into gap junctional plaques. The Journal of cell biology. 1991;115:1357-74.

[372] Cameron SJ, Malik S, Akaike M, Lerner-Marmarosh N, Yan C, Lee JD, et al. Regulation of epidermal growth factor-induced connexin 43 gap junction communication by big mitogen-activated protein kinase1/ERK5 but not ERK1/2 kinase activation. J Biol Chem. 2003;278:18682-8.

[384] Yogo K, Ogawa T, Akiyama M, Ishida-Kitagawa N, Sasada H, Sato E, et al. PKA implicated in the phosphorylation of Cx43 induced by stimulation with FSH in rat granulosa cells. J Reprod Dev. 2006;52:321-8.

[387] TenBroek EM, Lampe PD, Solan JL, Reynhout JK, Johnson RG. Ser364 of connexin43 and the upregulation of gap junction assembly by cAMP. The Journal of cell biology. 2001;155:1307-18.

[393] Wisniewski JR, Nagaraj N, Zougman A, Gnad F, Mann M. Brain phosphoproteome obtained by a FASP-based method reveals plasma membrane protein topology. Journal of proteome research. 2010;9:3280-9.

[394] Yogo K, Ogawa T, Akiyama M, Ishida N, Takeya T. Identification and functional analysis of novel phosphorylation sites in Cx43 in rat primary granulosa cells. FEBS Lett. 2002;531:132-6.

[399] Richards TS, Dunn CA, Carter WG, Usui ML, Olerud JE, Lampe PD. Protein kinase C spatially and temporally regulates gap junctional communication during human wound repair via phosphorylation of connexin43 on serine368. The Journal of cell biology. 2004;167:555-62.

[400] Hund TJ, Lerner DL, Yamada KA, Schuessler RB, Saffitz JE. Protein kinase Cepsilon mediates salutary effects on electrical coupling induced by ischemic preconditioning. Heart Rhythm. 2007;4:1183-93.

[420] Butterweck A, Gergs U, Elfgang C, Willecke K, Traub O. Immunochemical characterization of the gap junction protein connexin45 in mouse kidney and transfected human HeLa cells. J Membr Biol. 1994;141:247-56.

[459] Dang X, Jeyaraman M, Kardami E. Regulation of connexin-43-mediated growth inhibition by a phosphorylatable amino-acid is independent of gap junction-forming ability. Mol Cell Biochem. 2006;289:201-7.

[460] Gemel J, Lin X, Veenstra RD, Beyer EC. N-terminal residues in Cx43 and Cx40 determine physiological properties of gap junction channels, but do not influence heteromeric assembly with each other or with Cx26. Journal of cell science. 2006;119:2258-68.

[461] Lin X, Gemel J, Beyer EC, Veenstra RD. Dynamic model for ventricular junctional conductance during the cardiac action potential. American journal of physiology. 2005;288:H1113-23.

[462] Blom N, Gammeltoft S, Brunak S. Sequence and structure-based prediction of eukaryotic protein phosphorylation sites. Journal of molecular biology. 1999;294:1351-62.

[463] Blom N, Sicheritz-Ponten T, Gupta R, Gammeltoft S, Brunak S. Prediction of post-translational glycosylation and phosphorylation of proteins from the amino acid sequence. Proteomics. 2004;4:1633-49.

[464] Huang HD, Lee TY, Tzeng SW, Horng JT. KinasePhos: a web tool for identifying protein kinase-specific phosphorylation sites. Nucleic acids research. 2005;33:W226-9.

[551] Moreno AP, Lau AF. Gap junction channel gating modulated through protein phosphorylation. Progress in biophysics and molecular biology. 2007;94:107-19.

[554] Laird DW. Connexin phosphorylation as a regulatory event linked to gap junction internalization and degradation. Biochim Biophys Acta. 2005;1711:172-82.

[556] Solan JL, Lampe PD. Connexin phosphorylation as a regulatory event linked to gap junction channel assembly. Biochim Biophys Acta. 2005;1711:154-63.

[559] Musil LS, Goodenough DA. Multisubunit assembly of an integral plasma membrane channel protein, gap junction connexin43, occurs after exit from the ER. Cell. 1993;74:1065-77.

[601] Lampe PD, Lau AF. The effects of connexin phosphorylation on gap junctional communication. IntJBiochemCell Biol. 2004;36:1171-86.

[602] Gu H, Smith FC, Taffet SM, Delmar M. High incidence of cardiac malformations in connexin40-deficient mice. CircRes. 2003;93:201-6.

[603] Simon AM, McWhorter AR. Vascular abnormalities in mice lacking the endothelial gap junction proteins connexin37 and connexin40. DevBiol. 2002;251:206-20.

[604] Kirchhoff S, Nelles E, Hagendorff A, Kruger O, Traub O, Willecke K. Reduced cardiac conduction velocity and predisposition to arrhythmias in connexin40-deficient mice. Curr Biol. 1998;8:299-302.

[605] Verheule S, van Batenburg CA, Coenjaerts FE, Kirchhoff S, Willecke K, Jongsma HJ. Cardiac conduction abnormalities in mice lacking the gap junction protein connexin40. JCardiovascElectrophysiol. 1999;10:1380-9.

[606] Tamaddon HS, Vaidya D, Simon AM, Paul DL, Jalife J, Morley GE. High-resolution optical mapping of the right bundle branch in connexin40 knockout mice reveals slow conduction in the specialized conduction system. CircRes. 2000;87:929-36.

[607] van Rijen HV, van Veen TA, van Kempen MJ, Wilms-Schopman FJ, Potse M, Krueger O, et al. Impaired conduction in the bundle branches of mouse hearts lacking the gap junction protein connexin40. Circulation. 2001;103:1591-8.

[608] Gollob MH, Jones DL, Krahn AD, Danis L, Gong XQ, Shao Q, et al. Somatic mutations in the connexin 40 gene (GJA5) in atrial fibrillation. The New England journal of medicine. 2006;354:2677-88.

[609] Groenewegen WA, Firouzi M, Bezzina CR, Vliex S, van Langen IM, Sandkuijl L, et al. A cardiac sodium channel mutation cosegregates with a rare connexin40 genotype in familial atrial standstill. Circulation research. 2003;92:14-22.

[610] Firouzi M, Ramanna H, Kok B, Jongsma HJ, Koeleman BP, Doevendans PA, et al. Association of human connexin40 gene polymorphisms with atrial vulnerability as a risk factor for idiopathic atrial fibrillation. Circulation research. 2004;95:e29-33.

[611] Firouzi M, Bierhuizen MF, Kok B, Teunissen BE, Jansen AT, Jongsma HJ, et al. The human Cx40 promoter polymorphism -44G-->A differentially affects transcriptional regulation by Sp1 and GATA4. Biochim Biophys Acta. 2006;1759:491-6.

[612] Hauer RN, Groenewegen WA, Firouzi M, Ramanna H, Jongsma HJ. Cx40 polymorphism in human atrial fibrillation. Advances in cardiology. 2006;42:284-91.

[613] Juang JM, Chern YR, Tsai CT, Chiang FT, Lin JL, Hwang JJ, et al. The association of human connexin 40 genetic polymorphisms with atrial fibrillation. International journal of cardiology. 2007;116:107-12.

[614] Nao T, Ohkusa T, Hisamatsu Y, Inoue N, Matsumoto T, Yamada J, et al. Comparison of expression of connexin in right atrial myocardium in patients with chronic atrial fibrillation versus those in sinus rhythm. Am J Cardiol. 2003;91:678-83.

[615] van Rijen HV, van Veen TA, Hermans MM, Jongsma HJ. Human connexin40 gap junction channels are modulated by cAMP. CardiovascRes. 2000;45:941-51.

[616] Hoffmann A, Gloe T, Pohl U, Zahler S. Nitric oxide enhances de novo formation of endothelial gap junctions. CardiovascRes. 2003;60:421-30.

[617] Doble BW, Dang X, Ping P, Fandrich RR, Nickel BE, Jin Y, et al. Phosphorylation of serine 262 in the gap junction protein connexin-43 regulates DNA synthesis in cell-cell contact forming cardiomyocytes. Journal of cell science. 2004;117:507-14.

[618] Patel LS, Mitchell CK, Dubinsky WP, O'Brien J. Regulation of gap junction coupling through the neuronal connexin Cx35 by nitric oxide and cGMP. Cell Commun Adhes. 2006;13:41-54.

[619] Xue Y, Li A, Wang L, Feng H, Yao X. PPSP: prediction of PK-specific phosphorylation site with Bayesian decision theory. BMC bioinformatics. 2006;7:163.

[620] Bordoli L, Kiefer F, Arnold K, Benkert P, Battey J, Schwede T. Protein structure homology modeling using SWISS-MODEL workspace. Nat Protoc. 2009;4:1-13.

[621] Biasini M, Bienert S, Waterhouse A, Arnold K, Studer G, Schmidt T, et al. SWISS-MODEL: modelling protein tertiary and quaternary structure using evolutionary information. Nucleic acids research. 2014;42:W252-8.

[622] Baker NA, Sept D, Joseph S, Holst MJ, McCammon JA. Electrostatics of nanosystems: Application to microtubules and the ribosome. Proceedings of the National Academy of Sciences. 2001;98:10037-41.

[623] Dolinsky TJ, Nielsen JE, McCammon JA, Baker NA. PDB2PQR: an automated pipeline for the setup of Poisson–Boltzmann electrostatics calculations. Nucleic acids research. 2004;32:W665-W7.

[624] Pellegrini-Calace M, Maiwald T, Thornton JM. PoreWalker: A Novel Tool for the Identification and Characterization of Channels in Transmembrane Proteins from Their Three-Dimensional Structure. PLoS computational biology. 2009;5:e1000440.

[625] Shearer D, Ens W, Standing K, Valdimarsson G. Posttranslational modifications in lens fiber connexins identified by off-line-HPLC MALDI-quadrupole time-of-flight mass spectrometry. Investigative ophthalmology & visual science. 2008;49:1553-62.

[626] Kwon T, Harris AL, Rossi A, Bargiello TA. Molecular dynamics simulations of the Cx26 hemichannel: evaluation of structural models with Brownian dynamics. J Gen Physiol. 2011;138:475-93.

[627] Matesic D, Tillen T, Sitaramayya A. Connexin 40 expression in bovine and rat retinas. Cell Biol Int. 2003;27:89-99.

[628] Berthoud VM, Beyer EC, Kurata WE, Lau AF, Lampe PD. The gap-junction protein connexin 56 is phosphorylated in the intracellular loop and the carboxy-terminal region. European journal of biochemistry / FEBS. 1997;244:89-97.

[629] Liu J, Ek Vitorin JF, Weintraub ST, Gu S, Shi Q, Burt JM, et al. Phosphorylation of connexin 50 by protein kinase A enhances gap junction and hemichannel function. J Biol Chem. 2011;286:16914-28.

[630] Seki A, Duffy HS, Coombs W, Spray DC, Taffet SM, Delmar M. Modifications in the biophysical properties of connexin43 channels by a peptide of the cytoplasmic loop region. Circulation research. 2004;95:e22-8.

[631] Manthey D, Banach K, Desplantez T, Lee CG, Kozak CA, Traub O, et al. Intracellular domains of mouse connexin26 and -30 affect diffusional and electrical properties of gap junction channels. J Membr Biol. 2001;181:137-48.

Chapter 7 Overall discussion.

This thesis chapter is an original work by Jason Iden.
No portions of this chapter have been previously published.

We set out to discover if AMPK activation had any effect on junctional conductance. We now know that rapid pacing and various other AMPK activating stimuli do indeed alter junctional activity, although in complex ways. We also provide evidence suggesting novel phosphorylation dependent regulatory sites in human Cx40. The major findings of each of the main projects are summarized below. Future areas of study that are required will be discussed.

7.1 Summary of Significant Findings

7.1a Porcine Rapid Atrial Pacing Model

We have demonstrated that LV gap junctional conductance is decreased by rapid atrial pacing for 3 hours without a corresponding change in Cx43 levels, and that Cx40 expression may be reduced in the atria with rapid pacing. In this model, frequent spontaneous tachyarrhythmia formation was observed in both the ventricles and atria with rapid pacing, presumably prior to the onset of any structural remodeling. We also demonstrate that this phenomenon is associated with increased AMPK activity in the myocardial tissue, and that Cx43 may be phosphorylated by AMPK *in vitro*. Based on these findings, we can suggest that commonly encountered clinical tachyarrhythmias whether supraventricular or ventricular in origin may result in the formation of an even more arrhythmogenic substrate in a relatively short period of time. This effect may be due to the activation of AMPK and its effect on junctional conductance and electrical remodeling. However, when utilizing a large animal surgical model, it is impossible to control for all aspects (much like the pathophysiological setting in patients), and a number of confounding variables could be involved. As discussed in section 3.4f, pH, ischemia, other kinases, multiple phosphorylation sites etc. may play a role in our model. In order to address these issues, further research is warranted.

7.1b Future Directions

Over the past few years, it has become increasingly apparent that autophagy can play a significant role in heart function [247], and that AMPK pays a significant role in its regulation as outlined in section 1.5i. This has recently been highlighted in a brief report by Yuan *et al.* whereby they show remarkably similar effects (vs. the Chapter 3 pig experiments) in a chronic rapidly paced canine model (6 weeks) [322]. They show a similar degree of AMPK activation in the 1 day pacing group in comparison to our 3h results, and imply that over 6 weeks – excessive autophagy can result in atrial remodelling and an arrhythmogenic substrate. Although we do not see a decrease in Cx43, and the remodeling effects may not be profound at only 3h, I would be remiss to not assess the activation of autophagy in our LV and LA tissue samples by measuring LC3B expression. With these results, our data would also provide further evidence that the atrial remodeling and arrhythmogenic substrate is in fact generated much sooner than might be expected.

It would also be imperative to examine the Akt, and AMPK mediated axis controlling autophagy, and assess whether the decline in Cx function observed in our model is associated with a decrease in Akt activity, as well as an increase in AMPK activity on these pathways. This would allow us to eliminate some of the mechanistic ambiguity, and could be assessed in our model post-hoc by measuring expression of the AMPK and Akt targets (phospho-) p-TSC1, p-Raptor, p-mTOR, p-ULK1 (s317 and s777 vs. s757), p-Beclin1, and other markers of this pathway which Yuen *et al*. have not yet assessed fully.

Based on these pathways, one possible mediator of our observed effects in the pacing model is the inhibition of p-Cx43$_{373}$. As elegantly elucidated by Solon, Dunn, and Lampe, Cx43 is acutely regulated by Akt mediated phosphorylation of s373, promoting GJ accretion and permeability [117, 122]. As Akt and AMPK play such a profound role in the regulation of metabolism, protein expression, and

now autophagy, it would be interesting to examine their status in this model (as outlined above) with respect to potential effects on Cx43. Recent evidence indicates that metformin inhibits Akt signaling, and this is prevented by AMPK inhibition with compound C [632] although in other studies, AMPK is activated with no change in downstream Akt target phosphorylation [633]. Akt activation can also phosphorylate and prevent the LKB1 dependent activation of AMPK [232, 634, 635]. Due to the competing pathways regulated by AMPK and Akt, it is possible that Akt may be affected in our model, as such p-Cx43$_{373}$ may be altered. It is also probable that phosphorylation and dephosphorylation of other sites may be affected, including PKC/MAPK dependent phosphorylation of s279/s282 and s368 known to close Cx43 channels [138, 163, 388, 402, 551]. Although we did not have access to the array of Cx43 phospho-site specific antibodies at the time these studies were completed, it would be useful to compare the relative expression levels of those now available in a rapid pacing model.

In order to continue these studies, and make meaningful mechanistic conclusions, we would need to consider whether a small animal model might be utilized, either *in vivo* with appropriately sized electrical mapping apparatus, or in a Langendorf/working heart model utilizing other measurements of Cx function (tissue resistivity, or optical mapping). This would allow us to use genetic models (Akt, AMPK, CamK, MAPK: KO/KI/KD models) to assess the effects on Cx in the heart, even to the point of using newly developed induction powered pacemakers to implement chronic rapid pacing in a mouse model [636]. At the very least, it would be useful to examine Cx function in isolated cells from these models, ventricular (Cx43), or atrial / endothelial cells (which express Cx40) via GapFRAP.

7.1c Pharmacological and Viral Treatments to Alter AMPK

In order to examine Cx40 and Cx43 conductance in a more controlled system, we generated transient vectors to express the human variant of these cardiac connexins in mammalian cell lines. We further stably expressed these junctions in an inducible system to allow greater control and stability of expression in Hek293 cells. These cells express either human Cx40 or hCx43 with tetracycline/doxycycline induction with normal processing, localization, and activity (allowing dye transfer between Hek293 cells that show only minimal ability to do this normally).

By treating these cells with previously characterized AMPK altering adenovirus, we hoped to observe changes in Cx40 or Cx43 activity. In this case, we did indeed observe a decrease in junctional activity, but it was to a similar degree as observed with GFP expressing control virus alone, indicating that the effect was general to adenoviral infection. The mediators of this effect have not been elucidated at this time, but they may involve activation of upstream stress responsive pathways due to the viral infection. One potential mediator of these effects is the v-Src tyrosine kinase previously induced with Rous sarcoma virus [637] known to phosphorylate and inactivate Cx43 via multiple MAPK and tyrosine kinase dependent methods [138, 163, 388, 402, 551]. Although it is beyond the scope of this project, this observation and examining the potential mechanism could become relevant to cardiovascular risk as gene therapy trials are completed and follow-up studies continue (155 trials in the cardiovascular field, with 33% of all trials mediated by adenoviral or adeno-associated viral vectors) [638, 639].

Pharmacological activation of AMPK with AICAR has very little effect on Cx40 or Cx43 activity as measured in these cells. Its impact on Cx expression and distribution is complex. Expression of P1 and P2 isoforms decreased with increasing AMPK activity at the junctional plaque (in both Cx43 and to a greater

extent Cx40). There was some evidence of Cx43 internalization and a shift in the overall phosphorylation level. This may indicate that the AMPK/Akt pathways (identified above), may be playing a role. It also highlights the potential for CL phosphorylation to play a role in Cx40 although at this time we have not yet assessed whether our mutants could block the AICAR mediated effects. It would also argue that if they are affected by the same pathways, that Cx40 may be a target for Akt/ZO-1 dependent regulation as shown with Cx43. Examination of Cx40 to identify potential Akt mediated phosphorylation is of prime interest for future studies.

Activation with phenformin on the other hand, significantly inhibited both Cx40 and Cx43 activity. In the case of Cx43, this decrease was reflected by internalization, or inhibition of trafficking to the junctional plaque. It was also inversely proportional to AMPK activity. In the case of combined Cx40 expression (P0, P1, and P2), junctional plaque expression was also reduced significantly. However, there also appears to be a dose dependent partial prevention of the inhibition with increasing concentrations of phenformin at 2 hours, but which was not apparent at 4 hours.

We proposed that the effects of phenformin on Cx activity are at least partially due to a direct effect on permeability as opposed to the decrease in expression at the junctional plaque. We base this on the observation that AICAR shows a similar decrease (in expression) which is not reflected in junctional activity. The other possibility is that the Cx40 and Cx43 conductance/permeability is activated by AICAR, preventing a reduction in function despite decreased expression. It would be beneficial to examine the p-Cx43$_{s373}$ levels in phenformin treated cells to determine if downregulation of its phosphorylation plays a role in the observed effect, and if so, whether mutation of this site to alanine can prevent this portion.

One possible mechanism of indirect phenformin mediated Cx inhibition involves glycolytic uncoupling, and intracellular acidification/calcium accumulation, both of which are known to inhibit Cx43 and Cx40 junctional conductance [156, 570]. The specific mechanism of this response may be explored in future studies. Specifically, measurement of intracellular calcium/pH can be achieved at least qualitatively with fluorescent dyes. It is also possible to mutate the residues currently known to induce pH sensitivity to see if the functional response is prevented. It is also possible that prevention of calcium accumulation may prevent the reduction in junctional conductance due to phenformin. This may be achieved by calcium sequestration, inhibition of either L-type calcium channels, or the sodium calcium exchanger. In short, although phenformin can significantly lower Cx40 and Cx43 activity, more study would be required to determine the mechanism.

The availability of new compounds which selectively bind and activate AMPK (A-769662, compound 991), combined with inhibition of AMPK via compound C would allow us to examine the effects of AMPK activation without many of the non-specific effects of phenformin, and to a lesser extent AICAR.

7.1d Mutation of Putative phosphorylation sites in Cx40

Mutation of putative phosphorylation sites in Cx40 were initially designed to determine if AMPK phosphorylation would affect Cx40 activity or expression in the absence of confounding pathway interactions, and imprecise pharmacological manipulations. We chose to focus on Cx40 as most of the information on Cx phosphorylation has been examined in Cx43. As such, Cx40 mutation results are more novel, and increasingly more clinically relevant as Cx40 can have a significant role in atrial electrophysiology. As part of these studies, we also included a putative hCx40 cAMP (PKA) phosphorylation site (s120), which was expected to increase Cx40 expression and activity.

Mutation of the n-terminal putative AMPK phosphorylation site t19 significantly reduced Cx40 activity and expression in a dominant negative fashion (reducing endogenous Cx activity as well). It also appears to prevent trafficking to the plasma membrane, or leads to its immediate internalization, and degradation of Cx40. At this point we assume that Cx40 is non-phosphorylated at this residue, and as such phosphorylation would be expected to inhibit conductance and increase internalization. Further experimentation may elucidate these differences.

The rationale for continuing to study this mutant is as follows: t19 is highly conserved among Cx subtypes (Cx31.9 being the only human exception), although it is known as t19 in the 'α family' of Cx (Cx40, 43, 45 etc.) and as t18 in the 'β Cx family' (Cx32, 30, 26 etc.). It is recognized as both an AMPK, and PKC consensus target, and PKC activation is capable of blocking the formation of new GJ acutely [376]. As such, there is reason to believe that this residue is an important site in all human connexins, and if it is modified post-translationally at all, it could be a mediator for this phenomenon. This could also argue that, as the site is conserved in all Cx, it may be integral to normal structure/function. In addition, the decrease in expression observed with both the t19a and t19d mutants (although their activity remained non-significantly different) suggests that prevention of phosphorylation resulted in an activated Cx40. It was also shown recently that s5 on the Cx43 NT is phosphorylated *in vivo* (brain samples), indicating that t19 perhaps should have been identified in the same sample, but was not observed in this system. That being said, many known sites were not identified (including s255, s262, s279, s282, s313, and s373) and many new sites were (see). It could also be argued that phosphorylation of this residue would induce rapid closure/internalization, and hence may explain its absence from the phospho-proteome [393].

The following table shows the NetPhosK relative probability score for these two NT residues based on the neural net of known sites in their consensus database. While this is not evidence that Cx40 t19 or s5 site are phosphorylated (and false positive predictions are frequent), it does indicate that Cx43 and 40 may share regulatory sites where their sequences are similar.

Table 7-1. NetPhosK Analysis of Human Cx40 and Cx43 NT Residues

Site	Kinase	Cx43 Score	Cx40 Score
S-5	CaM-II	0.45	0.44
S-5	GSK3	0.44	0.44
T-19	PKC	0.58	0.79
T-19	CaM-II	0.43	0.46
T-19	cdc2	0.46	0.48
T-19	GSK3	0.44	0.44

In order to elucidate its potential function, the first step would be to identify whether GJ assembly is blocked in the wildtype Cx40 by PKC activation, then if so, whether the t19a mutant is protected from this form of regulation. It would also be useful to generate a phospho-specific antibody to p-Cx40$_{t19}$ which would allow us to determine if the site is actually phosphorylated *in vivo*. A c-terminal GFP tagged Cx40 mutant (CT) would also allow us to follow its movements in real time (as shown with other Cx-GFP chimera) [640].

7.1e Cytoplasmic Loop Phosphorylation

Mutation of the two sites in the cytoplasmic loop resulted in complex phenotypes that are expected to affect Cx40 function. Mutation to mimic phosphorylation of s120 (s120d), was expected to increase Cx activity and translocation to the plasma membrane as proposed in earlier cAMP/PKA dependent studies on Cx40. However, this was not the case, which begs the question – is s120 a phosphorylation target for PKA. To answer this question, it would be useful to mutate the other putative PKA site – s345. Then based on

their ability to induce translocation, with and without cAMP treatment, we could at least determine if the s120 site is active, or whether the cAMP mediated effects are non-specific.

This brings up the fact that as a general rule, mutational analysis should always be interpreted with caution until a discrete pathway or effect can be blocked by the mutation. This is a key limitation of these studies to this point, and one that will only be rectified by further research. One particular way that I would endeavor to address these limitations given the time and resources, would be to combine the mutants with various pharmacological, and pathophysiological treatments, which would indicate those that are most relevant to the physiological setting, and thus most relevant to pursue. I can submit that in very preliminary trials – there was no prevention of the phenformin inhibition by mutation to s122d. Again this evidence strengthens the position that Cx40 inhibition (in this case) is not dependent on AMPK activation, as opposed to the downstream affects from other systems (glycolytic uncoupling, pH, calcium accumulation).

As with the previous mutation, it would be useful to generate phospho-site specific antibodies to each of the Cx40 mutants in order to assess the presence of phosphorylated forms *in vivo*, and examine their expression and trafficking in real time (with a CT-GFP tagged protein), then inhibit various spots in the protein trafficking pathways, for example by inhibiting Cx degradation/internalization (with bafilomycin). With these data we could then determine if the rate of internalization is increased, and whether the mutated junctions are being sent to the plasma membrane at all.

A frequent theme in Cx phospho regulation is the ‘gatekeeper’ effect in which phosphorylation on one site can prevent the sequential phosphorylation on another nearby. The s120 and s122 mutations appear to mimic this effect, with one activator and one inhibitor near one another. In order to determine if these

sites interact, it would be necessary to follow their movement and attempt to measure a change in phospho-status at very specific times. This requires that we utilize phospho-site specific antibodies to assess the level of phosphorylation, or improve our ability to isolate and examine the Cx40 phospho-proteome reliably. To this date, isolation of Cx40 for mass spectrometry (MS) sequence analysis, and tandem mass spectrometry have been hampered by the overwhelming presence of cytosolic actin (42kDa) in gel purified samples. In order to bypass this limitation, it would be necessary to (1) generate a novel tagged mutant (which is large enough to escape the contamination) or; (2) by digesting isolated gel purified proteins in the Cx40 band range with hydroxylamine, it is expected that we would generate four small Cx40 subunits (aa. 1-140, 141-273, 273-325, and 325-358) which could be further HPLC purified and sequenced leaving actin as 363aa and 12aa fragments). Using these novel tools, and presuming that initial screening indicate that one or both is phosphorylated *in vivo*, it would be possible to examine the kinetics of phosphorylation for s122 when s120 is phosphorylated/dephosphorylated and vice versa.

To this point, we have not yet assessed single channel conductance, or open probabilities in these mutants. As such we cannot exclude the possibility that there may be other effects that are so far undetectable in our hands. Should the above studies confirm the *in vivo* phosphorylation on one or more of these sites, confirmation of their single channel conductance characteristics would be warranted.

7.1f Methodological Considerations

Based on preliminary findings, the most effective technique that was utilized in this thesis was a combination of *in vivo* electrical mapping using a large animal model, and cell pair GapFRAP to measure isolated conductance between cells. However, in many cases there was potential for improved efficacy. For example, with the use of new signal processing techniques we were able to significantly

improve on initial optical mapping results indicating that this technique may actually be quite effective.

The efficacy of dye mapping techniques can be evaluated by their reproducibility, and the amount of uncontrolled variation encountered. Based on these criteria they could be ranked in order of effectiveness (1) GapFRAP, (2) scrape loading, and (3) single cell microinjection. As mentioned previously exploitation of the dual cell patch clamp methodology would be useful to explore some of the more specific alterations in junctional physiology (with more practice) and the most recent mutant junctional cell lines. This would allow us to examine before/after drug treatments, with and without blockade of phosphorylation sites, and with/without inhibitors of the various protein phosphatases. There are however still limitations to GapFRAP' s general effectiveness, as it was fairly time consuming requiring large numbers of cell pairs for statistical analysis. There is also the possible matter of altered perm-selectivity. In all of but a handful of the studies referenced here, we utilized the cell-trace blue dye. This was initially necessary as we needed a small neutral or positively charged dye to assess Cx40 conductance rapidly. However, due to its small size, and neutral charge, it may have been less sensitive to changes in permeability as well. It would be advantageous to utilize a mixture of permeants – especially in the case of Cx43 which showed very fast recovery to this dye in future studies.

7.2 Biophysical Implications

We have shown that certain residues in the n-, cytoplasmic loop, and c-terminal locations of Cx40 can be affected by mutation or phosphorylation. One of the key regulatory events in Cx physiology is due to the interaction of the CL and CT areas. An important area for future study would be to examine if there is a significant interaction between the CT and CL in Cx40. Then, presuming there is one, it is probable that mutation/post-translational modification will affect

binding constants between these regions in an isolated *in vitro* system as shown previously for Cx43 [152, 158]. From a structural standpoint, one of the key limitations of this field is the lack of crystalized structures in the open and closed configuration. Study of the differences in the crystal structures from the s120 and s122 mutants would potentially allow us to see the conformational shifts predicted by the 3D modeling.

7.3 Clinical Implications

With the prevalence of tachyarrhythmia, it is of paramount importance that we continue to examine how and where the cardiac electrophysiological substrate is affected. Our results would indicate that junctional coupling may be reduced, and that it may be dependent on sodium/calcium accumulation, or via reduced localized pH in the heart. Determination of whether these effects are sufficient to explain the results or whether direct phosphorylation on particular residues function to resist these effects is unknown.

7.4 Evolutionary Perspectives and Novel Data

With respect to our original hypothesis, although many models which correlated with AMPK activation, and Cx inhibition were identified, we were not able to prove that AMPK mediated a decrease in junctional conductance. This may be due to the limiting fact that we were never in a position to inhibit AMPK activity with compound-C. The lack of Cx inhibition with AICAR indicated that activation of AMPK on its own, does not appear to instigate an immediate reduction in junctional conductance expected to induce arrhythmia formation.

It is interesting however, that some 14 years after the initial outline of this project was formed, in addition to the earlier report from Turner et. al [413] (which in 2004 inconclusively proposed that AMPK was not a factor in Cx43 regulation – see section 1.6b), that I have finally found three papers that link cardiac Cx function with AMPK activity all published after Jan 2015 (and a fourth

in 2014, which suggests that AMPK activation or mTOR inhibition prevented a Cx43 downregulation in diabetic nephropathy [641]).

In the first, Ma *et al*. published a report in Jan 2015, outlining that inhibition of AMPK activation with conpound-C leads to increased Cx43 mRNA expression in ischemic astroglial cells, where Cx43 is normally downregulated [642]. The authors suggested that NFkB as a potential mediator of this Cx43 downregulation. This is intriguing as most of our work has been focused on post-translational phosphorylation pathways rather than transcriptional ones.

The second paper provides evidence that early in ischemia AMPK activation is associated with Cx43 degradation and reduced dye permeability in cardiac myocytes, which is prevented partially (for up to 2h) by AMPK inhibition via compound-C [643]. Here the authors propose that AMPK induced a protective inhibition that prevented passage of detrimental signals to the surrounding cells.

The last is a report that AMPKα1 activity regulates cardiac gap junction Cx43 during pressure overload induced hypertrophy [644]. In which $AMPK_{\alpha 1KO}$ knockout mice were surgically induced by aortic banding to develop cardiac hypertrophy. In this case, Cx43 expression was reduced in wild type, but less so in $AMPK_{\alpha 1KO}$ mice. The hearts showed signs of arrhythmia, electrical heterogeneity, increased refractory period, and reduced conduction which were abrogated by the $AMPK_{\alpha 1}$ knockout. The authors did note that conduction velocities were decreased in both long and transverse directions in the AMPK knockout mice in both control and hypertrophied groups.

Although it may act indirectly in some cases, it appears that AMPK activation via a variety of means, leads to Cx43 downregulation, and an arrhythmogenic substrate.

It also appears that science has caught up to our original premise.

7.5 Overall Conclusion & Clinical Implications

The importance of gap junctional communication in cardiac arrhythmias is clear, and many facets of their dysfunction in structural heart disease and organ development are not even apparent- yet at this time we do not know how gap junctions are regulated even under simple conditions where only one small facet of such diseases are under examination. Clearly the situation in the heart is even more complex, but by understanding the mechanism behind some of these regulatory and signaling events in a simple system we can better predict how junctions react in a more general form. The studies outlined in this proposal will give us better tools to examine gap junction gating mechanisms and get us closer to a fuller understanding of junctional gating under a variety of conditions and thus guide our approach to the treatment of their dysfunction more intelligently.

7.6 Literature Cited

[117] Solan JL, Lampe PD. Specific Cx43 phosphorylation events regulate gap junction turnover in vivo. FEBS Lett. 2014.

[122] Dunn CA, Su V, Lau AF, Lampe PD. Activation of Akt, not connexin 43 protein ubiquitination, regulates gap junction stability. J Biol Chem. 2012;287:2600-7.

[138] Zhou L, Kasperek EM, Nicholson BJ. Dissection of the molecular basis of pp60(v-src) induced gating of connexin 43 gap junction channels. The Journal of cell biology. 1999;144:1033-45.

[152] Duffy HS, Delmar M, Coombs W, Tafftet SM, Hertzberg EL, Spray DC. Functional demonstration of connexin-protein binding using surface plasmon resonance. Cell Commun Adhes. 2001;8:225-9.

[156] Duffy HS, Ashton AW, O'Donnell P, Coombs W, Taffet SM, Delmar M, et al. Regulation of connexin43 protein complexes by intracellular acidification. Circulation research. 2004;94:215-22.

[158] Sorgen PL, Duffy HS, Spray DC, Delmar M. pH-dependent dimerization of the carboxyl terminal domain of Cx43. Biophys J. 2004;87:574-81.

[163] Ek-Vitorin JF, King TJ, Heyman NS, Lampe PD, Burt JM. Selectivity of connexin 43 channels is regulated through protein kinase C-dependent phosphorylation. Circulation research. 2006;98:1498-505.

[232] Soltys CL, Kovacic S, Dyck JR. Activation of cardiac AMP-activated protein kinase by LKB1 expression or chemical hypoxia is blunted by increased Akt activity. American journal of physiology. 2006;290:H2472-9.

[247] Kubli DA, Gustafsson AB. Cardiomyocyte health: adapting to metabolic changes through autophagy. Trends in endocrinology and metabolism: TEM. 2014;25:156-64.

[322] Yuan Y, Zhao J, Yan S, Wang D, Zhang S, Yun F, et al. Autophagy: A potential novel mechanistic contributor to atrial fibrillation. International journal of cardiology. 2014;172:492-4.

[376] Lampe PD. Analyzing phorbol ester effects on gap junctional communication: a dramatic inhibition of assembly. The Journal of cell biology. 1994;127:1895-905.

[388] Solan JL, Lampe PD. Connexin 43 in LA-25 cells with active v-src is phosphorylated on Y247, Y265, S262, S279/282, and S368 via multiple signaling pathways. Cell Commun Adhes. 2008;15:75-84.

[393] Wisniewski JR, Nagaraj N, Zougman A, Gnad F, Mann M. Brain phosphoproteome obtained by a FASP-based method reveals plasma membrane protein topology. Journal of proteome research. 2010;9:3280-9.

[402] Cottrell GT, Lin R, Warn-Cramer BJ, Lau AF, Burt JM. Mechanism of v-Src- and mitogen-activated protein kinase-induced reduction of gap junction communication. Am J Physiol Cell Physiol. 2003;284:C511-20.

[413] Turner MS, Haywood GA, Andreka P, You L, Martin PE, Evans WH, et al. Reversible connexin 43 dephosphorylation during hypoxia and reoxygenation is linked to cellular ATP levels. Circulation research. 2004;95:726-33.

[551] Moreno AP, Lau AF. Gap junction channel gating modulated through protein phosphorylation. Progress in biophysics and molecular biology. 2007;94:107-19.

[570] Peracchia C. Chemical gating of gap junction channels; roles of calcium, pH and calmodulin. Biochim Biophys Acta. 2004;1662:61-80.

[632] Xue J, Zhang H, Liu W, Liu M, Shi M, Wen Z, et al. Metformin inhibits growth of eutopic stromal cells from adenomyotic endometrium via AMPK activation and subsequent inhibition of AKT phosphorylation: a possible role in the treatment of adenomyosis. Reproduction. 2013;146:397-406.

[633] Kristensen JM, Treebak JT, Schjerling P, Goodyear L, Wojtaszewski JF. Two weeks of metformin treatment induces AMPK dependent enhancement of insulin-stimulated glucose uptake in mouse soleus muscle. Am J Physiol Endocrinol Metab. 2014.

[634] Zhang Y, Han X, Hu N, Huff AF, Gao F, Ren J. Akt2 knockout alleviates prolonged caloric restriction-induced change in cardiac contractile function through regulation of autophagy. J Mol Cell Cardiol. 2013.

[635] Hawley SA, Ross FA, Gowans GJ, Tibarewal P, Leslie NR, Hardie DG. Phosphorylation by Akt within the ST loop of AMPK-alpha1 down-regulates its activation in tumour cells. Biochem J. 2014.

[636] Laughner JI, Marrus SB, Zellmer ER, Weinheimer CJ, MacEwan MR, Cui SX, et al. A fully implantable pacemaker for the mouse: from battery to wireless power. PLoS ONE. 2013;8:e76291.

[637] Mitra SS, Xu J, Nicholson BJ. Coregulation of multiple signaling mechanisms in pp60v-Src-induced closure of Cx43 gap junction channels. J Membr Biol. 2012;245:495-506.

[638] Muona K, Makinen K, Hedman M, Manninen H, Yla-Herttuala S. 10-year safety follow-up in patients with local VEGF gene transfer to ischemic lower limb. Gene therapy. 2012;19:392-5.

[639] Wirth T, Parker N, Yla-Herttuala S. History of gene therapy. Gene. 2013;525:162-9.

[640] Jordan K, Solan JL, Dominguez M, Sia M, Hand A, Lampe PD, et al. Trafficking, assembly, and function of a connexin43-green fluorescent protein chimera in live mammalian cells. Molecular biology of the cell. 1999;10:2033-50.

[641] Guo YN, Wang JC, Cai GY, Hu X, Cui SY, Lv Y, et al. AMPK-mediated downregulation of connexin43 and premature senescence of mesangial cells under high-glucose conditions. Exp Gerontol. 2014;51:71-81.

[642] Ma Y, Bu J, Dang H, Sha J, Jing Y, Shan-Jiang A, et al. Inhibition of adenosine monophosphate-activated protein kinase reduces glial cell-mediated inflammation and induces the expression of Cx43 in astroglias after cerebral ischemia. Brain research. 2015.

[643] Martins-Marques T, Catarino S, Zuzarte M, Marques C, Matafome P, Pereira P, et al. Ischemia-induced autophagy leads to degradation of gap junction protein Connexin43 in cardiomyocytes. Biochem J. 2015.

[644] Alesutan I, Voelkl J, Stockigt F, Mia S, Feger M, Primessnig U, et al. AMP-activated protein kinase alpha1 regulates cardiac gap junction protein connexin 43 and electrical remodeling following pressure overload. Cell Physiol Biochem. 2015;35:406-18.

7.7 Combined Literature Cited

[1] Bayes de Luna A, Coumel P, Leclercq JF. Ambulatory sudden cardiac death: mechanisms of production of fatal arrhythmia on the basis of data from 157 cases. American Heart Journal. 1989;117:151-9.

[2] Gillum RF. Sudden coronary death in the United States: 1980-1985. Circulation. 1989;79:756-65.

[3] Kavanagh KM, Wyse DG. Ventricular arrhythmias. CMAJ. 1988;138:903-13.

[4] Innerfield RJ. Metformin-associated mortality in U.S. studies. The New England journal of medicine. 1996;334:1611-2; author reply 2-3.

[5] The Cardiac Arrhythmia Suppression Trial I. Special Report, preliminary report: effect of encainide and flecainide on mortality in a randomized trial of arrhythmia suppression after myocardial infarction. New England Journal of Medicine. 1989;321:406-12.

[6] Deo R, Albert CM. Epidemiology and genetics of sudden cardiac death. Circulation. 2012;125:620-37.

[7] Betensky BP, Dixit S. Sudden cardiac death in patients with nonischemic cardiomyopathy. Indian heart journal. 2014;66s1:S35-s45.

[8] Nikolic G, Bishop RL, Singh JB. Sudden death recorded during Holter monitoring. Circulation. 1982;66:218-25.

[9] Maisel WH, Stevenson LW. Atrial fibrillation in heart failure: epidemiology, pathophysiology, and rationale for therapy. Am J Cardiol. 2003;91:2D-8D.

[10] Khazanie P, Liang L, Qualls LG, Curtis LH, Fonarow GC, Hammill BG, et al. Outcomes of medicare beneficiaries with heart failure and atrial fibrillation. JACC Heart failure. 2014;2:41-8.

[11] Echt DS, Armstrong K, Schmidt P, Oyer PE, Stinson EB, Winkle RA. Clinical experience, complications, and survival in 70 patients with the automatic implantable cardioverter/defibrillator. Circulation. 1985;71:289-96.

[12] Mirowski M. The automatic implantable cardioverter-defibrillator: An overview. Journal of the American College of Cardiology. 1985;6:461-6.

[13] Tchou PJ, Kadri N, Anderson J, Caceres JA, Jazayeri M, Akhtar M. Automatic implantable cardioverter defibrillators and survival of patients with left ventricular dysfunction and malignant ventricular arrhythmias. Annals of Internal Medicine. 1988;109:529-34.

[14] Wyse DG, Waldo AL, DiMarco JP, Domanski MJ, Rosenberg Y, Schron EB, et al. A comparison of rate control and rhythm control in patients with atrial fibrillation. NEnglJMed. 2002;347:1825-33.

[15] Wyse DG. Rhythm versus Rate Control Trials in Atrial Fibrillation. JCardiovascElectrophysiol. 2003;14 Suppl 9:S35-S9.

[16] Wyse DG. Rhythm management in atrial fibrillation: less is more. JAmCollCardiol. 2003;41:1703-6.

[17] Hoyt RH, Cohen ML, Saffitz JE. Distribution and three-dimensional structure of intercellular junctions in canine myocardium. CircRes. 1989;64:563-74.

[18] Kieval RS, Spear JF, Moore EN. Gap junctional conductance in ventricular myocyte pairs isolated from postischemic rabbit myocardium. Circulation research. 1992;71:127-36.

[19] Luke RA, Saffitz JE. Remodeling of ventricular conduction pathways in healed canine infarct border zones. The Journal of clinical investigation. 1991;87:1594-602.

[20] Odegarden S. Organization of connexons and gap junctions in human heart cells. Acta Physiology Scandanavia. 1991;S599:61-70.

[21] Saffitz JE, Corr PB, Sobel BE. Arrhythmogenesis and ventricular dysfunction after myocardial infarction. Is anomalous cellular coupling the elusive link? Circulation. 1993;87:1742-5.

[22] Roth BJ. Influence of a perfusing bath on the foot of the cardiac action potential. CircRes. 2000;86:E19-E22.

[23] Yaniv Y, Lakatta EG, Maltsev VA. From two competing oscillators to one coupled-clock pacemaker cell system. Frontiers in physiology. 2015;6:28.

[24] Catterall WA. Voltage-gated calcium channels. Cold Spring Harbor perspectives in biology. 2011;3:a003947.

[25] Schmitt N, Grunnet M, Olesen SP. Cardiac potassium channel subtypes: new roles in repolarization and arrhythmia. Physiological reviews. 2014;94:609-53.

[26] Saffitz JE, Davis LM, Darrow BJ, Kanter HL, Laing JG, Beyer EC. The molecular basis of anisotropy: role of gap junctions. Journal of cardiovascular electrophysiology. 1995;6:498-510.

[27] Valderrabano M. Influence of anisotropic conduction properties in the propagation of the cardiac action potential. Progress in biophysics and molecular biology. 2007;94:144-68.

[28] Harris AL. Emerging issues of connexin channels: biophysics fills the gap. Quarterly reviews of biophysics. 2001;34:325-472.

[29] Bedner P, Niessen H, Odermatt B, Kretz M, Willecke K, Harz H. Selective permeability of different connexin channels to the second messenger cyclic AMP. J Biol Chem. 2006;281:6673-81.

[30] Valiunas V, Polosina YY, Miller H, Potapova IA, Valiuniene L, Doronin S, et al. Connexin-specific cell-to-cell transfer of short interfering RNA by gap junctions. The Journal of physiology. 2005;568:459-68.

[31] Neijssen J, Herberts C, Drijfhout JW, Reits E, Janssen L, Neefjes J. Cross-presentation by intercellular peptide transfer through gap junctions. Nature. 2005;434:83-8.

[32] Jalife J, Morley GE, Vaidya D. Connexins and impulse propagation in the mouse heart. Journal of cardiovascular electrophysiology. 1999;10:1649-63.

[33] Beyer EC, Davis LM, Saffitz JE, Veenstra RD. Cardiac intercellular communication: consequences of connexin distribution and diversity. Braz J Med Biol Res. 1995;28:415-25.

[34] Kanter HL, Beyer EC, Saffitz JE. Structural and molecular determinants of intercellular coupling in cardiac myocytes. Microsc Res Tech. 1995;31:357-63.

[35] Kleber AG, Rudy Y. Basic mechanisms of cardiac impulse propagation and associated arrhythmias. Physiological reviews. 2004;84:431-88.

[36] Dupont E, Ko Y, Rothery S, Coppen SR, Baghai M, Haw M, et al. The gap-junctional protein connexin40 is elevated in patients susceptible to postoperative atrial fibrillation. Circulation. 2001;103:842-9.

[37] Gutstein DE, Morley GE, Tamaddon H, Vaidya D, Schneider MD, Chen J, et al. Conduction slowing and sudden arrhythmic death in mice with cardiac-restricted inactivation of connexin43. Circulation research. 2001;88:333-9.

[38] Vaidya D, Tamaddon HS, Lo CW, Taffet SM, Delmar M, Morley GE, et al. Null mutation of connexin43 causes slow propagation of ventricular activation in the late stages of mouse embryonic development. Circulation research. 2001;88:1196-202.

[39] Lee P, Morley G, Huang Q, Fischer A, Seiler S, Horner JW, et al. Conditional lineage ablation to model human diseases. Proceedings of the National Academy of Sciences of the United States of America. 1998;95:11371-6.

[40] Hagendorff A, Schumacher B, Kirchhoff S, Luderitz B, Willecke K. Conduction disturbances and increased atrial vulnerability in Connexin40-deficient mice analyzed by transesophageal stimulation. Circulation. 1999;99:1508-15.

[41] Verheule S, van Kempen MJ, Postma S, Rook MB, Jongsma HJ. Gap junctions in the rabbit sinoatrial node. American journal of physiology. 2001;280:H2103-15.

[42] Qin D, Zhang ZH, Caref EB, Boutjdir M, Jain P, el Sherif N. Cellular and ionic basis of arrhythmias in postinfarction remodeled ventricular myocardium. CircRes. 1996;79:461-73.

[43] Dhillon PS, Chowdhury RA, Patel PM, Jabr R, Momin AU, Vecht J, et al. The Relationship between Connexin Expression and Gap Junction Resistivity in Human Atrial Myocardium. Circ Arrhythm Electrophysiol. 2014.

[44] Yan J, Kong W, Zhang Q, Beyer EC, Walcott G, Fast VG, et al. c-Jun N-terminal kinase activation contributes to reduced connexin43 and development of atrial arrhythmias. Cardiovascular research. 2013;97:589-97.

[45] Paul M, Wichter T, Gerss J, Arps V, Schulze-Bahr E, Robenek H, et al. Connexin expression patterns in arrhythmogenic right ventricular cardiomyopathy. Am J Cardiol. 2013;111:1488-95.

[46] Lubkemeier I, Requardt RP, Lin X, Sasse P, Andrie R, Schrickel JW, et al. Deletion of the last five C-terminal amino acid residues of connexin43 leads to lethal ventricular arrhythmias in mice without affecting coupling via gap junction channels. Basic research in cardiology. 2013;108:348.

[47] Lubkemeier I, Andrie R, Lickfett L, Bosen F, Stockigt F, Dobrowolski R, et al. The Connexin40A96S mutation from a patient with atrial fibrillation causes decreased atrial conduction velocities and sustained episodes of induced atrial fibrillation in mice. J Mol Cell Cardiol. 2013;65:19-32.

[48] Wu W, Li Y, Lu Z, Hu X. Increased susceptibility to ischemia-induced ventricular tachyarrhythmias in depressed rats: Involvement of reduction of connexin 43. Experimental and therapeutic medicine. 2012;3:192-4.

[49] Makita N, Seki A, Sumitomo N, Chkourko H, Fukuhara S, Watanabe H, et al. A connexin40 mutation associated with a malignant variant of progressive familial heart block type I. Circ Arrhythm Electrophysiol. 2012;5:163-72.

[50] Jansen JA, Noorman M, Musa H, Stein M, de Jong S, van der Nagel R, et al. Reduced heterogeneous expression of Cx43 results in decreased Nav1.5 expression and reduced sodium current that accounts for arrhythmia vulnerability in conditional Cx43 knockout mice. Heart Rhythm. 2012;9:600-7.

[51] Delmar M, Makita N. Cardiac connexins, mutations and arrhythmias. Current opinion in cardiology. 2012;27:236-41.

[52] Wirka RC, Gore S, Van Wagoner DR, Arking DE, Lubitz SA, Lunetta KL, et al. A common connexin-40 gene promoter variant affects connexin-40 expression in human atria and is associated with atrial fibrillation. Circ Arrhythm Electrophysiol. 2011;4:87-93.

[53] Strom M, Wan X, Poelzing S, Ficker E, Rosenbaum DS. Gap junction heterogeneity as mechanism for electrophysiologically distinct properties across the ventricular wall. American journal of physiology. 2010;298:H787-94.

[54] Soltysinska E, Olesen SP, Christ T, Wettwer E, Varro A, Grunnet M, et al. Transmural expression of ion channels and transporters in human nondiseased and end-stage failing hearts. Pflugers Arch. 2009;459:11-23.

[55] Chaldoupi SM, Loh P, Hauer RN, de Bakker JM, van Rijen HV. The role of connexin40 in atrial fibrillation. Cardiovascular research. 2009;84:15-23.

[56] Sato T, Ohkusa T, Honjo H, Suzuki S, Yoshida MA, Ishiguro YS, et al. Altered expression of connexin43 contributes to the arrhythmogenic substrate during the development of heart failure in cardiomyopathic hamster. American journal of physiology. 2008;294:H1164-73.

[57] Leaf DE, Feig JE, Vasquez C, Riva PL, Yu C, Lader JM, et al. Connexin40 imparts conduction heterogeneity to atrial tissue. Circulation research. 2008;103:1001-8.

[58] Danik SB, Liu F, Zhang J, Suk HJ, Morley GE, Fishman GI, et al. Modulation of cardiac gap junction expression and arrhythmic susceptibility. Circulation research. 2004;95:1035-41.

[59] VanderBrink BA, Sellitto C, Saba S, Link MS, Zhu W, Homoud MK, et al. Connexin40-deficient mice exhibit atrioventricular nodal and infra-Hisian conduction abnormalities. Journal of cardiovascular electrophysiology. 2000;11:1270-6.

[60] Bevilacqua LM, Simon AM, Maguire CT, Gehrmann J, Wakimoto H, Paul DL, et al. A targeted disruption in connexin40 leads to distinct atrioventricular conduction defects. J Interv Card Electrophysiol. 2000;4:459-67.

[61] Verheule S, van Batenburg CA, Coenjaerts FE, Kirchhoff S, Willecke K, Jongsma HJ. Cardiac conduction abnormalities in mice lacking the gap junction protein connexin40. Journal of cardiovascular electrophysiology. 1999;10:1380-9.

[62] Danik SB, Rosner G, Lader J, Gutstein DE, Fishman GI, Morley GE. Electrical remodeling contributes to complex tachyarrhythmias in connexin43-deficient mouse hearts. Faseb J. 2008;22:1204-12.

[63] van Rijen HV, Eckardt D, Degen J, Theis M, Ott T, Willecke K, et al. Slow conduction and enhanced anisotropy increase the propensity for ventricular tachyarrhythmias in adult mice with induced deletion of connexin43. Circulation. 2004;109:1048-55.

[64] Yao JA, Gutstein DE, Liu F, Fishman GI, Wit AL. Cell coupling between ventricular myocyte pairs from connexin43-deficient murine hearts. Circulation research. 2003;93:736-43.

[65] Bagwe S, Berenfeld O, Vaidya D, Morley GE, Jalife J. Altered right atrial excitation and propagation in connexin40 knockout mice. Circulation. 2005;112:2245-53.

[66] Alcolea S, Jarry-Guichard T, de Bakker J, Gonzalez D, Lamers W, Coppen S, et al. Replacement of connexin40 by connexin45 in the mouse: impact on cardiac electrical conduction. Circulation research. 2004;94:100-9.

[67] Wolfle SE, Schmidt VJ, Hoepfl B, Gebert A, Alcolea S, Gros D, et al. Connexin45 cannot replace the function of connexin40 in conducting endothelium-dependent dilations along arterioles. Circulation research. 2007;101:1292-9.

[68] Remo BF, Qu J, Volpicelli FM, Giovannone S, Shin D, Lader J, et al. Phosphatase-resistant gap junctions inhibit pathological remodeling and prevent arrhythmias. Circulation research. 2011;108:1459-66.

[69] Keevil VL, Huang CL, Chau PL, Sayeed RA, Vandenberg JI. The effect of heptanol on the electrical and contractile function of the isolated, perfused rabbit heart. Pflugers Arch. 2000;440:275-82.

[70] O'Quinn MP, Palatinus JA, Harris BS, Hewett KW, Gourdie RG. A peptide mimetic of the connexin43 carboxyl terminus reduces gap junction remodeling and induced arrhythmia following ventricular injury. Circulation research. 2011;108:704-15.

[71] Bikou O, Thomas D, Trappe K, Lugenbiel P, Kelemen K, Koch M, et al. Connexin 43 gene therapy prevents persistent atrial fibrillation in a porcine model. Cardiovascular research. 2011;92:218-25.

[72] Zhang QY, Wang W, Shi QX, Li YL, Huang JH, Yao Y, et al. Antiarrhythmic effect mediated by kappa-opioid receptor is associated with Cx43 stabilization. Crit Care Med. 2010;38:2365-76.

[73] Unuma K, Shintani-Ishida K, Tsushima K, Shimosawa T, Ueyama T, Kuwahara M, et al. Connexin-43 redistribution and gap junction activation during forced restraint protects against sudden arrhythmic death in rats. Circ J. 2010;74:1087-95.

[74] Quan XQ, Bai R, Lu JG, Patel C, Liu N, Ruan Y, et al. Pharmacological Enhancement of Cardiac Gap Junction Coupling Prevents Arrhythmias in Canine LQT2 Model. Cell Commun Adhes. 2009:1-10.

[75] Roell W, Lewalter T, Sasse P, Tallini YN, Choi BR, Breitbach M, et al. Engraftment of connexin 43-expressing cells prevents post-infarct arrhythmia. Nature. 2007;450:819-24.

[76] Stahlhut M, Petersen JS, Hennan JK, Ramirez MT. The antiarrhythmic peptide rotigaptide (ZP123) increases connexin 43 protein expression in neonatal rat ventricular cardiomyocytes. Cell Commun Adhes. 2006;13:21-7.

[77] Haugan K, Miyamoto T, Takeishi Y, Kubota I, Nakayama J, Shimojo H, et al. Rotigaptide (ZP123) improves atrial conduction slowing in chronic volume overload-induced dilated atria. Basic & clinical pharmacology & toxicology. 2006;99:71-9.

[78] Dhein S, Larsen BD, Petersen JS, Mohr FW. Effects of the new antiarrhythmic peptide ZP123 on epicardial activation and repolarization pattern. Cell Commun Adhes. 2003;10:371-8.

[79] Weng S, Lauven M, Schaefer T, Polontchouk L, Grover R, Dhein S. Pharmacological modification of gap junction coupling by an antiarrhythmic peptide via protein kinase C activation. Faseb J. 2002;16:1114-6.

[80] Herve JC, Sarrouilhe D. Protein phosphatase modulation of the intercellular junctional communication: importance in cardiac myocytes. Progress in biophysics and molecular biology. 2006;90:225-48.

[81] Veenstra RD. Developmental changes in regulation of embryonic chick heart gap junctions. J Membr Biol. 1991;119:253-65.

[82] van Kempen MJ, Fromaget C, Gros D, Moorman AF, Lamers WH. Spatial distribution of connexin43, the major cardiac gap junction protein, in the developing and adult rat heart. Circulation research. 1991;68:1638-51.

[83] Gourdie RG, Green CR, Severs NJ, Thompson RP. Immunolabelling patterns of gap junction connexins in the developing and mature rat heart. Anatomy and embryology. 1992;185:363-78.

[84] Kanter HL, Laing JG, Beau SL, Beyer EC, Saffitz JE. Distinct patterns of connexin expression in canine Purkinje fibers and ventricular muscle. Circulation research. 1993;72:1124-31.

[85] Oosthoek PW, Viragh S, Mayen AE, van Kempen MJ, Lamers WH, Moorman AF. Immunohistochemical delineation of the conduction system. I: The sinoatrial node. Circulation research. 1993;73:473-81.

[86] Oosthoek PW, Viragh S, Lamers WH, Moorman AF. Immunohistochemical delineation of the conduction system. II: The atrioventricular node and Purkinje fibers. Circulation research. 1993;73:482-91.

[87] Davis LM, Kanter HL, Beyer EC, Saffitz JE. Distinct gap junction protein phenotypes in cardiac tissues with disparate conduction properties. J Am Coll Cardiol. 1994;24:1124-32.

[88] Gros DB, Jongsma HJ. Connexins in mammalian heart function. Bioessays. 1996;18:719-30.

[89] Davis LM, Rodefeld ME, Green K, Beyer EC, Saffitz JE. Gap junction protein phenotypes of the human heart and conduction system. Journal of cardiovascular electrophysiology. 1995;6:813-22.

[90] Van Kempen MJ, Vermeulen JL, Moorman AF, Gros D, Paul DL, Lamers WH. Developmental changes of connexin40 and connexin43 mRNA distribution patterns in the rat heart. Cardiovascular research. 1996;32:886-900.

[91] Severs NJ, Bruce AF, Dupont E, Rothery S. Remodelling of gap junctions and connexin expression in diseased myocardium. Cardiovascular research. 2008;80:9-19.

[92] Bastide B, Neyses L, Ganten D, Paul M, Willecke K, Traub O. Gap junction protein connexin40 is preferentially expressed in vascular endothelium and conductive bundles of rat myocardium and is increased under hypertensive conditions. Circulation research. 1993;73:1138-49.

[93] De Maziere A, Analbers L, Jongsma HJ, Gros D. Immunoelectron microscopic visualization of the gap junction protein connexin 40 in the mammalian heart. European journal of morphology. 1993;31:51-4.

[94] Gros D, Jarry-Guichard T, Ten Velde I, de Maziere A, van Kempen MJ, Davoust J, et al. Restricted distribution of connexin40, a gap junctional protein, in mammalian heart. Circulation research. 1994;74:839-51.

[95] Delorme B, Dahl E, Jarry-Guichard T, Marics I, Briand JP, Willecke K, et al. Developmental regulation of connexin 40 gene expression in mouse heart correlates with the differentiation of the conduction system. Dev Dyn. 1995;204:358-71.

[96] Coppen SR, Dupont E, Rothery S, Severs NJ. Connexin45 expression is preferentially associated with the ventricular conduction system in mouse and rat heart. Circulation research. 1998;82:232-43.

[97] van Veen TA, van Rijen HV, Jongsma HJ. Electrical conductance of mouse connexin45 gap junction channels is modulated by phosphorylation. Cardiovascular research. 2000;46:496-510.

[98] Kreuzberg MM, Liebermann M, Segschneider S, Dobrowolski R, Dobrzynski H, Kaba R, et al. Human connexin31.9, unlike its orthologous protein connexin30.2 in the mouse, is not detectable in the human cardiac conduction system. Journal of Molecular and Cellular Cardiology. 2009;46:553-9.

[99] Bukauskas FF, Kreuzberg MM, Rackauskas M, Bukauskiene A, Bennett MV, Verselis VK, et al. Properties of mouse connexin 30.2 and human connexin 31.9 hemichannels: implications for atrioventricular conduction in the heart. Proceedings of the National Academy of Sciences of the United States of America. 2006;103:9726-31.

[100] Nielsen PA, Kumar NM. Differences in expression patterns between mouse connexin-30.2 (Cx30.2) and its putative human orthologue, connexin-31.9. FEBS Lett. 2003;540:151-6.

[101] Sohl G, Nielsen PA, Eiberger J, Willecke K. Expression profiles of the novel human connexin genes hCx30.2, hCx40.1, and hCx62 differ from their putative mouse orthologues. Cell Commun Adhes. 2003;10:27-36.

[102] Nielsen PA, Beahm DL, Giepmans BN, Baruch A, Hall JE, Kumar NM. Molecular cloning, functional expression, and tissue distribution of a novel human gap junction-forming protein, connexin-31.9. Interaction with zona occludens protein-1. J Biol Chem. 2002;277:38272-83.

[103] White TW, Srinivas M, Ripps H, Trovato-Salinaro A, Condorelli DF, Bruzzone R. Virtual cloning, functional expression, and gating analysis of human connexin31.9. Am J Physiol Cell Physiol. 2002;283:C960-70.

[104] Belluardo N, White TW, Srinivas M, Trovato-Salinaro A, Ripps H, Mudo G, et al. Identification and functional expression of HCx31.9, a novel gap junction gene. Cell Commun Adhes. 2001;8:173-8.

[105] Kreuzberg MM, Schrickel JW, Ghanem A, Kim JS, Degen J, Janssen-Bienhold U, et al. Connexin30.2 containing gap junction channels decelerate impulse propagation through the atrioventricular node. Proceedings of the National Academy of Sciences of the United States of America. 2006;103:5959-64.

[106] Kreuzberg MM, Willecke K, Bukauskas FF. Connexin-mediated cardiac impulse propagation: connexin 30.2 slows atrioventricular conduction in mouse heart. Trends in cardiovascular medicine. 2006;16:266-72.

[107] Kohl P, Gourdie RG. Fibroblast–myocyte electrotonic coupling: Does it occur in native cardiac tissue?(). Journal of Molecular and Cellular Cardiology. 2014;70:37-46.

[108] Gaudesius G, Miragoli M, Thomas SP, Rohr S. Coupling of cardiac electrical activity over extended distances by fibroblasts of cardiac origin. Circulation research. 2003;93:421-8.

[109] Dhein S, Seidel T, Salameh A, Jozwiak J, Hagen A, Kostelka M, et al. Remodeling of cardiac passive electrical properties and susceptibility to ventricular and atrial arrhythmias. Frontiers in physiology. 2014;5:424.

[110] Miragoli M, Gaudesius G, Rohr S. Electrotonic modulation of cardiac impulse conduction by myofibroblasts. Circulation research. 2006;98:801-10.

[111] Lopez P, Balicki D, Buehler LK, Falk MM, Chen SC. Distribution and dynamics of gap junction channels revealed in living cells. Cell Commun Adhes. 2001;8:237-42.

[112] Falk MM, Lauf U. High resolution, fluorescence deconvolution microscopy and tagging with the autofluorescent tracers CFP, GFP, and YFP to study the structural composition of gap junctions in living cells. Microsc Res Tech. 2001;52:251-62.

[113] Segretain D, Falk MM. Regulation of connexin biosynthesis, assembly, gap junction formation, and removal. Biochim Biophys Acta. 2004;1662:3-21.

[114] Flores CE, Nannapaneni S, Davidson KG, Yasumura T, Bennett MV, Rash JE, et al. Trafficking of gap junction channels at a vertebrate electrical synapse in vivo. Proceedings of the National Academy of Sciences of the United States of America. 2012;109:E573-82.

[115] Zhang SS, Shaw RM. Trafficking highways to the intercalated disc: new insights unlocking the specificity of connexin 43 localization. Cell Commun Adhes. 2014;21:43-54.

[116] Laird DW. The gap junction proteome and its relationship to disease. Trends in cell biology. 2010;20:92-101.

[117] Solan JL, Lampe PD. Specific Cx43 phosphorylation events regulate gap junction turnover in vivo. FEBS Lett. 2014.

[118] Laird DW, Puranam KL, Revel JP. Turnover and phosphorylation dynamics of connexin43 gap junction protein in cultured cardiac myocytes. Biochem J. 1991;273(Pt 1):67-72.

[119] Beardslee MA, Laing JG, Beyer EC, Saffitz JE. Rapid turnover of connexin43 in the adult rat heart. Circulation research. 1998;83:629-35.

[120] Li X, Su V, Kurata WE, Jin C, Lau AF. A novel connexin43-interacting protein, CIP75, which belongs to the UbL-UBA protein family, regulates the turnover of connexin43. J Biol Chem. 2008;283:5748-59.

[121] Traub O, Look J, Paul D, Willecke K. Cyclic adenosine monophosphate stimulates biosynthesis and phosphorylation of the 26 kDa gap junction protein in cultured mouse hepatocytes. Eur J Cell Biol. 1987;43:48-54.

[122] Dunn CA, Su V, Lau AF, Lampe PD. Activation of Akt, not connexin 43 protein ubiquitination, regulates gap junction stability. J Biol Chem. 2012;287:2600-7.

[123] Laing JG, Beyer EC. The gap junction protein connexin43 is degraded via the ubiquitin proteasome pathway. J Biol Chem. 1995;270:26399-403.

[124] Laing JG, Tadros PN, Westphale EM, Beyer EC. Degradation of connexin43 gap junctions involves both the proteasome and the lysosome. Exp Cell Res. 1997;236:482-92.

[125] Laing JG, Tadros PN, Green K, Saffitz JE, Beyer EC. Proteolysis of connexin43-containing gap junctions in normal and heat-stressed cardiac myocytes. Cardiovascular research. 1998;38:711-8.

[126] Gaietta G, Deerinck TJ, Adams SR, Bouwer J, Tour O, Laird DW, et al. Multicolor and electron microscopic imaging of connexin trafficking. Science. 2002;296:503-7.

[127] Unger VM, Kumar NM, Gilula NB, Yeager M. Projection structure of a gap junction membrane channel at 7 A resolution. Nature structural biology. 1997;4:39-43.

[128] Yeager M, Unger VM, Falk MM. Synthesis, assembly and structure of gap junction intercellular channels. Current opinion in structural biology. 1998;8:517-24.

[129] Unger VM, Kumar NM, Gilula NB, Yeager M. Three-dimensional structure of a recombinant gap junction membrane channel. Science. 1999;283:1176-80.

[130] Kronengold J, Trexler EB, Bukauskas FF, Bargiello TA, Verselis VK. Single-channel SCAM identifies pore-lining residues in the first extracellular loop and first transmembrane domains of Cx46 hemichannels. J Gen Physiol. 2003;122:389-405.

[131] Maeda S, Tsukihara T. Structure of the gap junction channel and its implications for its biological functions. Cell Mol Life Sci. 2011;68:1115-29.

[132] Maeda S, Nakagawa S, Suga M, Yamashita E, Oshima A, Fujiyoshi Y, et al. Structure of the connexin 26 gap junction channel at 3.5 A resolution. Nature. 2009;458:597-602.

[133] Oshima A. Structure and closure of connexin gap junction channels. FEBS Lett. 2014.

[134] Beyer EC, Lipkind GM, Kyle JW, Berthoud VM. Structural organization of intercellular channels II. Amino terminal domain of the connexins: sequence, functional roles, and structure. Biochim Biophys Acta. 2012;1818:1823-30.

[135] Oh S, Rubin JB, Bennett MV, Verselis VK, Bargiello TA. Molecular determinants of electrical rectification of single channel conductance in gap junctions formed by connexins 26 and 32. J Gen Physiol. 1999;114:339-64.

[136] Purnick PE, Oh S, Abrams CK, Verselis VK, Bargiello TA. Reversal of the gating polarity of gap junctions by negative charge substitutions in the N-terminus of connexin 32. Biophys J. 2000;79:2403-15.

[137] Stergiopoulos K, Alvarado JL, Mastroianni M, Ek-Vitorin JF, Taffet SM, Delmar M. Hetero-domain interactions as a mechanism for the regulation of connexin channels. Circulation research. 1999;84:1144-55.

[138] Zhou L, Kasperek EM, Nicholson BJ. Dissection of the molecular basis of pp60(v-src) induced gating of connexin 43 gap junction channels. The Journal of cell biology. 1999;144:1033-45.

[139] Morley GE, Taffet SM, Delmar M. Intramolecular interactions mediate pH regulation of connexin43 channels. Biophys J. 1996;70:1294-302.

[140] Ek-Vitorin JF, Burt JM. Structural basis for the selective permeability of channels made of communicating junction proteins. Biochim Biophys Acta. 2013;1828:51-68.

[141] Spray DC, White RL, Mazet F, Bennett MV. Regulation of gap junctional conductance. The American journal of physiology. 1985;248:H753-64.

[142] Rubin JB, Verselis VK, Bennett MV, Bargiello TA. Molecular analysis of voltage dependence of heterotypic gap junctions formed by connexins 26 and 32. Biophys J. 1992;62:183-93; discussion 93-5.

[143] White TW, Bruzzone R, Paul DL. The connexin family of intercellular channel forming proteins. Kidney Int. 1995;48:1148-57.

[144] Spray DC, Harris AL, Bennett MV. Equilibrium properties of a voltage-dependent junctional conductance. J Gen Physiol. 1981;77:77-93.

[145] Lin X, Crye M, Veenstra RD. Regulation of connexin43 gap junctional conductance by ventricular action potentials. Circulation research. 2003;93:e63-73.

[146] Bukauskas FF, Angele AB, Verselis VK, Bennett MV. Coupling asymmetry of heterotypic connexin 45/ connexin 43-EGFP gap junctions: properties of fast and slow gating mechanisms. Proceedings of the National Academy of Sciences of the United States of America. 2002;99:7113-8.

[147] Moreno AP. Biophysical properties of homomeric and heteromultimeric channels formed by cardiac connexins. Cardiovascular research. 2004;62:276-86.

[148] Verselis VK, Ginter CS, Bargiello TA. Opposite voltage gating polarities of two closely related connexins. Nature. 1994;368:348-51.

[149] Bukauskas FF, Bukauskiene A, Bennett MV, Verselis VK. Gating properties of gap junction channels assembled from connexin43 and connexin43 fused with green fluorescent protein. Biophys J. 2001;81:137-52.

[150] Anumonwo JM, Taffet SM, Gu H, Chanson M, Moreno AP, Delmar M. The carboxyl terminal domain regulates the unitary conductance and voltage dependence of connexin40 gap junction channels. Circulation research. 2001;88:666-73.

[151] Moreno AP, Chanson M, Elenes S, Anumonwo J, Scerri I, Gu H, et al. Role of the carboxyl terminal of connexin43 in transjunctional fast voltage gating. Circulation research. 2002;90:450-7.

[152] Duffy HS, Delmar M, Coombs W, Tafftet SM, Hertzberg EL, Spray DC. Functional demonstration of connexin-protein binding using surface plasmon resonance. Cell Commun Adhes. 2001;8:225-9.

[153] Duffy HS, Sorgen PL, Girvin ME, O'Donnell P, Coombs W, Taffet SM, et al. pH-dependent intramolecular binding and structure involving Cx43 cytoplasmic domains. J Biol Chem. 2002;277:36706-14.

[154] Sorgen PL, Duffy HS, Cahill SM, Coombs W, Spray DC, Delmar M, et al. Sequence-specific resonance assignment of the carboxyl terminal domain of Connexin43. Journal of biomolecular NMR. 2002;23:245-6.

[155] Delmar M, Coombs W, Sorgen P, Duffy HS, Taffet SM. Structural bases for the chemical regulation of Connexin43 channels. Cardiovascular research. 2004;62:268-75.

[156] Duffy HS, Ashton AW, O'Donnell P, Coombs W, Taffet SM, Delmar M, et al. Regulation of connexin43 protein complexes by intracellular acidification. Circulation research. 2004;94:215-22.

[157] Sorgen PL, Duffy HS, Sahoo P, Coombs W, Delmar M, Spray DC. Structural changes in the carboxyl terminus of the gap junction protein connexin43 indicates signaling between binding domains for c-Src and zonula occludens-1. J Biol Chem. 2004;279:54695-701.

[158] Sorgen PL, Duffy HS, Spray DC, Delmar M. pH-dependent dimerization of the carboxyl terminal domain of Cx43. Biophys J. 2004;87:574-81.

[159] Lampe PD, Cooper CD, King TJ, Burt JM. Analysis of Connexin43 phosphorylated at S325, S328 and S330 in normoxic and ischemic heart. Journal of cell science. 2006;119:3435-42.

[160] Solan JL, Marquez-Rosado L, Sorgen PL, Thornton PJ, Gafken PR, Lampe PD. Phosphorylation at S365 is a gatekeeper event that changes the structure of Cx43 and prevents down-regulation by PKC. The Journal of cell biology. 2007;179:1301-9.

[161] Lampe PD, TenBroek EM, Burt JM, Kurata WE, Johnson RG, Lau AF. Phosphorylation of connexin43 on serine368 by protein kinase C regulates gap junctional communication. The Journal of cell biology. 2000;149:1503-12.

[162] Moreno AP, Saez JC, Fishman GI, Spray DC. Human connexin43 gap junction channels. Regulation of unitary conductances by phosphorylation. Circulation research. 1994;74:1050-7.

[163] Ek-Vitorin JF, King TJ, Heyman NS, Lampe PD, Burt JM. Selectivity of connexin 43 channels is regulated through protein kinase C-dependent phosphorylation. Circulation research. 2006;98:1498-505.

[164] Eckert R. Gap-junctional single-channel permeability for fluorescent tracers in mammalian cell cultures. Biophys J. 2006;91:565-79.

[165] Elfgang C, Eckert R, Lichtenberg-Frate H, Butterweck A, Traub O, Klein RA, et al. Specific permeability and selective formation of gap junction channels in connexin-transfected HeLa cells. The Journal of cell biology. 1995;129:805-17.

[166] Veenstra RD, Wang HZ, Beblo DA, Chilton MG, Harris AL, Beyer EC, et al. Selectivity of connexin-specific gap junctions does not correlate with channel conductance. Circulation research. 1995;77:1156-65.

[167] Kanaporis G, Mese G, Valiuniene L, White TW, Brink PR, Valiunas V. Gap junction channels exhibit connexin-specific permeability to cyclic nucleotides. J Gen Physiol. 2008;131:293-305.

[168] Kanaporis G, Brink PR, Valiunas V. Gap junction permeability: selectivity for anionic and cationic probes. Am J Physiol Cell Physiol. 2011;300:C600-9.

[169] Heyman NS, Kurjiaka DT, Ek Vitorin JF, Burt JM. Regulation of gap junctional charge selectivity in cells coexpressing connexin 40 and connexin 43. American journal of physiology. 2009;297:H450-9.

[170] Weber PA, Chang HC, Spaeth KE, Nitsche JM, Nicholson BJ. The permeability of gap junction channels to probes of different size is dependent on connexin composition and permeant-pore affinities. Biophys J. 2004;87:958-73.

[171] Rackauskas M, Verselis VK, Bukauskas FF. Permeability of homotypic and heterotypic gap junction channels formed of cardiac connexins mCx30.2, Cx40, Cx43, and Cx45. American journal of physiology. 2007;293:H1729-36.

[172] Koval M, Geist ST, Westphale EM, Kemendy AE, Civitelli R, Beyer EC, et al. Transfected connexin45 alters gap junction permeability in cells expressing endogenous connexin43. The Journal of cell biology. 1995;130:987-95.

[173] Beblo DA, Veenstra RD. Monovalent cation permeation through the connexin40 gap junction channel. Cs, Rb, K, Na, Li, TEA, TMA, TBA, and effects of anions Br, Cl, F, acetate, aspartate, glutamate, and NO3. J Gen Physiol. 1997;109:509-22.

[174] Moore LK, Beyer EC, Burt JM. Characterization of gap junction channels in A7r5 vascular smooth muscle cells. The American journal of physiology. 1991;260:C975-81.

[175] He DS, Burt JM. Mechanism and selectivity of the effects of halothane on gap junction channel function. Circulation research. 2000;86:E104-9.

[176] Rozental R, Srinivas M, Spray DC. How to close a gap junction channel. Efficacies and potencies of uncoupling agents. Methods in molecular biology (Clifton, NJ. 2001;154:447-76.

[177] Moreno AP, Eghbali B, Spray DC. Connexin32 gap junction channels in stably transfected cells: unitary conductance. Biophys J. 1991;60:1254-66.

[178] Campos-de-Carvalho AC, Eiras LA, Waltzman M, Hertzberg EL, Spray DC. Properties of channels from rat liver gap junction membrane fractions incorporated into planar lipid bilayers. Braz J Med Biol Res. 1992;25:81-92.

[179] Reynhout JK, Lampe PD, Johnson RG. An activator of protein kinase C inhibits gap junction communication between cultured bovine lens cells. Exp Cell Res. 1992;198:337-42.

[180] Rami A, Volkmann T, Winckler J. Effective reduction of neuronal death by inhibiting gap junctional intercellular communication in a rodent model of global transient cerebral ischemia. Experimental neurology. 2001;170:297-304.

[181] Hirschi KK, Minnich BN, Moore LK, Burt JM. Oleic acid differentially affects gap junction-mediated communication in heart and vascular smooth muscle cells. The American journal of physiology. 1993;265:C1517-26.

[182] Huang YS, Tseng YZ, Wu JC, Wang SM. Mechanism of oleic acid-induced gap junctional disassembly in rat cardiomyocytes. J Mol Cell Cardiol. 2004;37:755-66.

[183] Moreno AP, Rook MB, Fishman GI, Spray DC. Gap junction channels: distinct voltage-sensitive and -insensitive conductance states. Biophys J. 1994;67:113-9.

[184] Turner LA, Vodanovic S, Bosnjak ZJ. Interaction of anesthetics and catecholamines on conduction in the canine His-Purkinje system. Adv Pharmacol. 1994;31:167-84.

[185] O'Carroll SJ, Alkadhi M, Nicholson LF, Green CR. Connexin 43 mimetic peptides reduce swelling, astrogliosis, and neuronal cell death after spinal cord injury. Cell Commun Adhes. 2008;15:27-42.

[186] Chaytor AT, Bakker LM, Edwards DH, Griffith TM. Connexin-mimetic peptides dissociate electrotonic EDHF-type signalling via myoendothelial and smooth muscle gap junctions in the rabbit iliac artery. British journal of pharmacology. 2005;144:108-14.

[187] Kwak BR, Jongsma HJ. Selective inhibition of gap junction channel activity by synthetic peptides. The Journal of physiology. 1999;516 (Pt 3):679-85.

[188] Chaytor AT, Evans WH, Griffith TM. Peptides homologous to extracellular loop motifs of connexin 43 reversibly abolish rhythmic contractile activity in rabbit arteries. The Journal of physiology. 1997;503 (Pt 1):99-110.

[189] Aonuma S, Kohama Y, Akai K, Iwasaki S. Studies on heart. II. Further effects of bovine ventricle protein (BVP) and antiarrhythmic peptide (AAP) on myocardial cells in culture. Chem Pharm Bull (Tokyo). 1980;28:3340-6.

[190] Aonuma S, Kohama Y, Makino T, Hattori K. [Studies on the heart (22). Inhibitory effect of an atrial peptide (AAP) on drug-induced arrhythmia]. Yakugaku Zasshi. 1983;103:662-6.

[191] Aonuma S, Kohama Y, Makino T, Fujisawa Y. Studies of heart. XXI. Amino acid sequence of antiarrhythmic peptide (AAP) isolated from atria. J Pharmacobiodyn. 1982;5:40-8.

[192] Muller A, Gottwald M, Tudyka T, Linke W, Klaus W, Dhein S. Increase in gap junction conductance by an antiarrhythmic peptide. European journal of pharmacology. 1997;327:65-72.

[193] Dhein S, Tudyka T. Therapeutic potential of antiarrhythmic peptides. Cellular coupling as a new antiarrhythmic target. Drugs. 1995;49:851-5.

[194] Dhein S, Manicone N, Muller A, Gerwin R, Ziskoven U, Irankhahi A, et al. A new synthetic antiarrhythmic peptide reduces dispersion of epicardial activation recovery interval and

diminishes alterations of epicardial activation patterns induced by regional ischemia. A mapping study. Naunyn Schmiedebergs ArchPharmacol. 1994;350:174-84.

[195] Xing D, Kjolbye AL, Nielsen MS, Petersen JS, Harlow KW, Holstein-Rathlou NH, et al. ZP123 increases gap junctional conductance and prevents reentrant ventricular tachycardia during myocardial ischemia in open chest dogs. Journal of cardiovascular electrophysiology. 2003;14:510-20.

[196] Boitano S, Evans WH. Connexin mimetic peptides reversibly inhibit Ca(2+) signaling through gap junctions in airway cells. American journal of physiology Lung cellular and molecular physiology. 2000;279:L623-30.

[197] Spray DC, Rozental R, Srinivas M. Prospects for rational development of pharmacological gap junction channel blockers. Curr Drug Targets. 2002;3:455-64.

[198] De Vriese AS, Van dV, Lameire NH. Effects of connexin-mimetic peptides on nitric oxide synthase- and cyclooxygenase-independent renal vasodilation. Kidney Int. 2002;61:177-85.

[199] Kjolbye AL, Knudsen CB, Jepsen T, Larsen BD, Petersen JS. Pharmacological characterization of the new stable antiarrhythmic peptide analog Ac-D-Tyr-D-Pro-D-Hyp-Gly-D-Ala-Gly-NH2 (ZP123): in vivo and in vitro studies. J Pharmacol Exp Ther. 2003;306:1191-9.

[200] Erichsen JE. Oxygen Lack: Ischemia and Angina. In: Opie LH, editor. Philadelphia: Lippincott - Raven; 1998. p. 515-41.

[201] Contreras JE, Sanchez HA, Eugenin EA, Speidel D, Theis M, Willecke K, et al. Metabolic inhibition induces opening of unapposed connexin 43 gap junction hemichannels and reduces gap junctional communication in cortical astrocytes in culture. Proceedings of the National Academy of Sciences of the United States of America. 2002;99:495-500.

[202] Weiss JN, Lamp ST. Glycolysis preferentially inhibits ATP-sensitive K+ channels in isolated guinea pig cardiac myocytes. Science. 1987;238:67-9.

[203] Beyer EC, Steinberg TH. Evidence that the gap junction protein connexin-43 is the ATP-induced pore of mouse macrophages. J Biol Chem. 1991;266:7971-4.

[204] Clarke TC, Williams OJ, Martin PE, Evans WH. ATP release by cardiac myocytes in a simulated ischaemia model Inhibition by a connexin mimetic and enhancement by an antiarrhythmic peptide. European journal of pharmacology. 2008.

[205] Faigle M, Seessle J, Zug S, El Kasmi KC, Eltzschig HK. ATP release from vascular endothelia occurs across Cx43 hemichannels and is attenuated during hypoxia. PLoS ONE. 2008;3:e2801.

[206] Hendrickson SC, St.Louis JD, Lowe JE, Abdel-Aleem S. Free fatty acid metabolism during myocardial ischemia and reperfusion. MolCell Biochem. 1997;166:85-94.

[207] Yamada KA, McHowat J, Yan GX, Donahue K, Peirick J, Kleber AG, et al. Cellular uncoupling induced by accumulation of long-chain acylcarnitine during ischemia. Circulation research. 1994;74:83-95.

[208] Barger PM, Kelly DP. Fatty acid utilization in the hypertrophied and failing heart: molecular regulatory mechanisms. AmJMedSci. 1999;318:36-42.

[209] Tian R, Musi N, D'Agostino J, Hirshman MF, Goodyear LJ. Increased adenosine monophosphate-activated protein kinase activity in rat hearts with pressure-overload hypertrophy. Circulation. 2001;104:1664-9.

[210] Pogwizd SM, Corr PB. Biochemical and electrophysiological alterations underlying ventricular arrhythmias in the failing heart. EurHeart J. 1994;15 Suppl D:145-54.

[211] Kudo N, Gillespie JG, Kung L, Witters LA, Schulz R, Clanachan AS, et al. Characterization of 5'AMP-activated protein kinase activity in the heart and its role in inhibiting acetyl-CoA carboxylase during reperfusion following ischemia. Biochim Biophys Acta. 1996;1301:67-75.

[212] Atkinson DE. The energy charge of the adenylate pool as a regulatory parameter. Interaction with feedback modifiers. Biochemistry. 1968;7:4030-4.

[213] Hardie DG, Carling D. The AMP-activated protein kinase--fuel gauge of the mammalian cell? European journal of biochemistry / FEBS. 1997;246:259-73.

[214] O'Neill HM, Holloway GP, Steinberg GR. AMPK regulation of fatty acid metabolism and mitochondrial biogenesis: implications for obesity. Mol Cell Endocrinol. 2013;366:135-51.

[215] Oakhill JS, Scott JW, Kemp BE. AMPK functions as an adenylate charge-regulated protein kinase. Trends in endocrinology and metabolism: TEM. 2012;23:125-32.

[216] Xiao B, Sanders MJ, Underwood E, Heath R, Mayer FV, Carmena D, et al. Structure of mammalian AMPK and its regulation by ADP. Nature. 2011;472:230-3.

[217] Li X, Wang L, Zhou XE, Ke J, de Waal PW, Gu X, et al. Structural basis of AMPK regulation by adenine nucleotides and glycogen. Cell Res. 2015;25:398.

[218] Li X, Wang L, Zhou XE, Ke J, de Waal PW, Gu X, et al. Structural basis of AMPK regulation by adenine nucleotides and glycogen. Cell Res. 2015;25:50-66.

[219] Xiao B, Sanders MJ, Carmena D, Bright NJ, Haire LF, Underwood E, et al. Structural basis of AMPK regulation by small molecule activators. Nature communications. 2013;4:3017.

[220] Oakhill JS, Chen ZP, Scott JW, Steel R, Castelli LA, Ling N, et al. beta-Subunit myristoylation is the gatekeeper for initiating metabolic stress sensing by AMP-activated protein kinase (AMPK). Proceedings of the National Academy of Sciences of the United States of America. 2010;107:19237-41.

[221] Oakhill JS, Steel R, Chen ZP, Scott JW, Ling N, Tam S, et al. AMPK is a direct adenylate charge-regulated protein kinase. Science. 2011;332:1433-5.

[222] Zhang YL, Guo H, Zhang CS, Lin SY, Yin Z, Peng Y, et al. AMP as a low-energy charge signal autonomously initiates assembly of AXIN-AMPK-LKB1 complex for AMPK activation. Cell Metab. 2013;18:546-55.

[223] Wu Y, Song P, Xu J, Zhang M, Zou MH. Activation of protein phosphatase 2A by palmitate inhibits AMP-activated protein kinase. J Biol Chem. 2007;282:9777-88.

[224] Sanders MJ, Grondin PO, Hegarty BD, Snowden MA, Carling D. Investigating the mechanism for AMP activation of the AMP-activated protein kinase cascade. Biochem J. 2007;403:139-48.

[225] Wang MY, Unger RH. Role of PP2C in cardiac lipid accumulation in obese rodents and its prevention by troglitazone. Am J Physiol Endocrinol Metab. 2005;288:E216-21.

[226] Gowans GJ, Hardie DG. AMPK: a cellular energy sensor primarily regulated by AMP. Biochem Soc Trans. 2014;42:71-5.

[227] Gowans GJ, Hawley SA, Ross FA, Hardie DG. AMP is a true physiological regulator of AMP-activated protein kinase by both allosteric activation and enhancing net phosphorylation. Cell Metab. 2013;18:556-66.

[228] Lin YY, Kiihl S, Suhail Y, Liu SY, Chou YH, Kuang Z, et al. Functional dissection of lysine deacetylases reveals that HDAC1 and p300 regulate AMPK. Nature. 2012;482:251-5.

[229] Kovacic S, Soltys CL, Barr AJ, Shiojima I, Walsh K, Dyck JR. Akt activity negatively regulates phosphorylation of AMP-activated protein kinase in the heart. J Biol Chem. 2003;278:39422-7.

[230] Pulinilkunnil T, He H, Kong D, Asakura K, Peroni OD, Lee A, et al. Adrenergic regulation of AMP-activated protein kinase in brown adipose tissue in vivo. J Biol Chem. 2011;286:8798-809.

[231] Hawley SA, Ross FA, Gowans GJ, Tibarewal P, Leslie NR, Hardie DG. Phosphorylation by Akt within the ST loop of AMPK-alpha1 down-regulates its activation in tumour cells. Biochem J. 2014;459:275-87.

[232] Soltys CL, Kovacic S, Dyck JR. Activation of cardiac AMP-activated protein kinase by LKB1 expression or chemical hypoxia is blunted by increased Akt activity. American journal of physiology. 2006;290:H2472-9.

[233] Djouder N, Tuerk RD, Suter M, Salvioni P, Thali RF, Scholz R, et al. PKA phosphorylates and inactivates AMPKalpha to promote efficient lipolysis. EMBO J. 2010;29:469-81.

[234] Fogarty S, Hawley SA, Green KA, Saner N, Mustard KJ, Hardie DG. Calmodulin-dependent protein kinase kinase-beta activates AMPK without forming a stable complex: synergistic effects of Ca2+ and AMP. Biochem J. 2010;426:109-18.

[235] Anderson KA, Ribar TJ, Lin F, Noeldner PK, Green MF, Muehlbauer MJ, et al. Hypothalamic CaMKK2 contributes to the regulation of energy balance. Cell Metab. 2008;7:377-88.

[236] Hurley RL, Anderson KA, Franzone JM, Kemp BE, Means AR, Witters LA. The Ca2+/calmodulin-dependent protein kinase kinases are AMP-activated protein kinase kinases. J Biol Chem. 2005;280:29060-6.

[237] Woods A, Dickerson K, Heath R, Hong SP, Momcilovic M, Johnstone SR, et al. Ca2+/calmodulin-dependent protein kinase kinase-beta acts upstream of AMP-activated protein kinase in mammalian cells. Cell Metab. 2005;2:21-33.

[238] Sanli T, Steinberg GR, Singh G, Tsakiridis T. AMP-activated protein kinase (AMPK) beyond metabolism: A novel genomic stress sensor participating in the DNA damage response pathway. Cancer biology & therapy. 2014;15:156-69.

[239] Zaha VG, Young LH. AMP-activated protein kinase regulation and biological actions in the heart. Circulation research. 2012;111:800-14.

[240] Hardie DG, Ross FA, Hawley SA. AMPK: a nutrient and energy sensor that maintains energy homeostasis. Nat Rev Mol Cell Biol. 2012;13:251-62.

[241] Ducommun S, Deak M, Sumpton D, Ford RJ, Nunez Galindo A, Kussmann M, et al. Motif affinity and mass spectrometry proteomic approach for the discovery of cellular AMPK targets: Identification of mitochondrial fission factor as a new AMPK substrate. Cell Signal. 2015.

[242] Ruderman NB, Saha AK, Kraegen EW. Minireview: malonyl CoA, AMP-activated protein kinase, and adiposity. Endocrinology. 2003;144:5166-71.

[243] Unger RH. The hyperleptinemia of obesity-regulator of caloric surpluses. Cell. 2004;117:145-6.

[244] Folmes CD, Lopaschuk GD. Role of malonyl-CoA in heart disease and the hypothalamic control of obesity. Cardiovascular research. 2007;73:278-87.

[245] Lane MD, Wolfgang M, Cha SH, Dai Y. Regulation of food intake and energy expenditure by hypothalamic malonyl-CoA. Int J Obes (Lond). 2008;32 Suppl 4:S49-54.

[246] Minokoshi Y, Shiuchi T, Lee S, Suzuki A, Okamoto S. Role of hypothalamic AMP-kinase in food intake regulation. Nutrition (Burbank, Los Angeles County, Calif. 2008;24:786-90.

[247] Kubli DA, Gustafsson AB. Cardiomyocyte health: adapting to metabolic changes through autophagy. Trends in endocrinology and metabolism: TEM. 2014;25:156-64.

[248] Ju TC, Chen HM, Lin JT, Chang CP, Chang WC, Kang JJ, et al. Nuclear translocation of AMPK-alpha1 potentiates striatal neurodegeneration in Huntington's disease. The Journal of cell biology. 2011;194:209-27.

[249] McGee SL, Hargreaves M. AMPK-mediated regulation of transcription in skeletal muscle. Clin Sci (Lond). 2010;118:507-18.

[250] Marcinko K, Steinberg GR. The role of AMPK in controlling metabolism and mitochondrial biogenesis during exercise. Exp Physiol. 2014;99:1581-5.

[251] Funk JA, Odejinmi S, Schnellmann RG. SRT1720 induces mitochondrial biogenesis and rescues mitochondrial function after oxidant injury in renal proximal tubule cells. J Pharmacol Exp Ther. 2010;333:593-601.

[252] Jornayvaz FR, Shulman GI. Regulation of mitochondrial biogenesis. Essays in biochemistry. 2010;47:69-84.

[253] Li L, Pan R, Li R, Niemann B, Aurich AC, Chen Y, et al. Mitochondrial biogenesis and peroxisome proliferator-activated receptor-gamma coactivator-1alpha (PGC-1alpha) deacetylation by physical activity: intact adipocytokine signaling is required. Diabetes. 2011;60:157-67.

[254] Li L, Muhlfeld C, Niemann B, Pan R, Li R, Hilfiker-Kleiner D, et al. Mitochondrial biogenesis and PGC-1alpha deacetylation by chronic treadmill exercise: differential response in cardiac and skeletal muscle. Basic research in cardiology. 2011;106:1221-34.

[255] Marsin AS, Bouzin C, Bertrand L, Hue L. The stimulation of glycolysis by hypoxia in activated monocytes is mediated by AMP-activated protein kinase and inducible 6-phosphofructo-2-kinase. J Biol Chem. 2002;277:30778-83.

[256] Nagendran J, Waller TJ, Dyck JR. AMPK signalling and the control of substrate use in the heart. Mol Cell Endocrinol. 2013;366:180-93.

[257] Solskov L, Lofgren B, Kristiansen SB, Jessen N, Pold R, Nielsen TT, et al. Metformin induces cardioprotection against ischaemia/reperfusion injury in the rat heart 24 hours after administration. Basic & clinical pharmacology & toxicology. 2008;103:82-7.

[258] Hauton D. Does long-term metformin treatment increase cardiac lipoprotein lipase? Metabolism. 2011;60:32-42.

[259] Pulinilkunnil T, Puthanveetil P, Kim MS, Wang F, Schmitt V, Rodrigues B. Ischemia-reperfusion alters cardiac lipoprotein lipase. Biochim Biophys Acta. 2010;1801:171-5.

[260] Chabowski A, Coort SL, Calles-Escandon J, Tandon NN, Glatz JF, Luiken JJ, et al. The subcellular compartmentation of fatty acid transporters is regulated differently by insulin and by AICAR. FEBS Lett. 2005;579:2428-32.

[261] Luiken JJ, Coort SL, Koonen DP, Bonen A, Glatz JF. Signalling components involved in contraction-inducible substrate uptake into cardiac myocytes. The Proceedings of the Nutrition Society. 2004;63:251-8.

[262] Habets DD, Coumans WA, El Hasnaoui M, Zarrinpashneh E, Bertrand L, Viollet B, et al. Crucial role for LKB1 to AMPKalpha2 axis in the regulation of CD36-mediated long-chain fatty acid uptake into cardiomyocytes. Biochim Biophys Acta. 2009;1791:212-9.

[263] Munday MR, Campbell DG, Carling D, Hardie DG. Identification by amino acid sequencing of three major regulatory phosphorylation sites on rat acetyl-CoA carboxylase. European journal of biochemistry / FEBS. 1988;175:331-8.

[264] Munday MR, Carling D, Hardie DG. Negative interactions between phosphorylation of acetyl-CoA carboxylase by the cyclic AMP-dependent and AMP-activated protein kinases. FEBS Lett. 1988;235:144-8.

[265] McGarry JD, Leatherman GF, Foster DW. Carnitine palmitoyltransferase I. The site of inhibition of hepatic fatty acid oxidation by malonyl-CoA. J Biol Chem. 1978;253:4128-36.

[266] McGarry JD, Brown NF. The mitochondrial carnitine palmitoyltransferase system. From concept to molecular analysis. European journal of biochemistry / FEBS. 1997;244:1-14.

[267] Dyck JR, Kudo N, Barr AJ, Davies SP, Hardie DG, Lopaschuk GD. Phosphorylation control of cardiac acetyl-CoA carboxylase by cAMP-dependent protein kinase and 5'-AMP activated protein kinase. European journal of biochemistry / FEBS. 1999;262:184-90.

[268] Olson DP, Pulinilkunnil T, Cline GW, Shulman GI, Lowell BB. Gene knockout of Acc2 has little effect on body weight, fat mass, or food intake. Proceedings of the National Academy of Sciences of the United States of America. 2010;107:7598-603.

[269] Dyck JR, Barr AJ, Barr RL, Kolattukudy PE, Lopaschuk GD. Characterization of cardiac malonyl-CoA decarboxylase and its putative role in regulating fatty acid oxidation. The American journal of physiology. 1998;275:H2122-9.

[270] Saha AK, Schwarsin AJ, Roduit R, Masse F, Kaushik V, Tornheim K, et al. Activation of malonyl-CoA decarboxylase in rat skeletal muscle by contraction and the AMP-activated protein kinase activator 5-aminoimidazole-4-carboxamide-1-beta -D-ribofuranoside. J Biol Chem. 2000;275:24279-83.

[271] Thomson DM, Brown JD, Fillmore N, Condon BM, Kim HJ, Barrow JR, et al. LKB1 and the regulation of malonyl-CoA and fatty acid oxidation in muscle. Am J Physiol Endocrinol Metab. 2007;293:E1572-9.

[272] Dzamko NL, Schertzer JD, Ryall J, Steel R, Macaulay SL, Wee S, et al. AMPK independent pathways regulate skeletal muscle fatty acid oxidation. The Journal of physiology. 2008.

[273] Smith BK, Jain SS, Rimbaud S, Dam A, Quadrilatero J, Ventura-Clapier R, et al. FAT/CD36 is located on the outer mitochondrial membrane, upstream of long-chain acyl-CoA synthetase, and regulates palmitate oxidation. Biochem J. 2011;437:125-34.

[274] Omar MA, Fraser H, Clanachan AS. Ischemia-induced activation of AMPK does not increase glucose uptake in glycogen-replete isolated working rat hearts. American journal of physiology. 2008;294:H1266-73.

[275] Jing M, Cheruvu VK, Ismail-Beigi F. Stimulation of glucose transport in response to activation of distinct AMPK signaling pathways. Am J Physiol Cell Physiol. 2008;295:C1071-82.

[276] Barnes K, Ingram JC, Porras OH, Barros LF, Hudson ER, Fryer LG, et al. Activation of GLUT1 by metabolic and osmotic stress: potential involvement of AMP-activated protein kinase (AMPK). Journal of cell science. 2002;115:2433-42.

[277] O'Neill HM, Maarbjerg SJ, Crane JD, Jeppesen J, Jorgensen SB, Schertzer JD, et al. AMP-activated protein kinase (AMPK) beta1beta2 muscle null mice reveal an essential role for AMPK in maintaining mitochondrial content and glucose uptake during exercise. Proceedings of the National Academy of Sciences of the United States of America. 2011;108:16092-7.

[278] Russell RR, 3rd, Li J, Coven DL, Pypaert M, Zechner C, Palmeri M, et al. AMP-activated protein kinase mediates ischemic glucose uptake and prevents postischemic cardiac dysfunction, apoptosis, and injury. The Journal of clinical investigation. 2004;114:495-503.

[279] Russell RR, 3rd, Bergeron R, Shulman GI, Young LH. Translocation of myocardial GLUT-4 and increased glucose uptake through activation of AMPK by AICAR. The American journal of physiology. 1999;277:H643-9.

[280] Corton JM, Gillespie JG, Hawley SA, Hardie DG. 5-aminoimidazole-4-carboxamide ribonucleoside. A specific method for activating AMP-activated protein kinase in intact cells? European journal of biochemistry / FEBS. 1995;229:558-65.

[281] Coven DL, Hu X, Cong L, Bergeron R, Shulman GI, Hardie DG, et al. Physiological role of AMP-activated protein kinase in the heart: graded activation during exercise. Am J Physiol Endocrinol Metab. 2003;285:E629-36.

[282] Till M, Ouwens DM, Kessler A, Eckel J. Molecular mechanisms of contraction-regulated cardiac glucose transport. Biochem J. 2000;346 Pt 3:841-7.

[283] Ducommun S, Wang HY, Sakamoto K, MacKintosh C, Chen S. Thr649Ala-AS160 knock-in mutation does not impair contraction/AICAR-induced glucose transport in mouse muscle. Am J Physiol Endocrinol Metab. 2012;302:E1036-43.

[284] Chen S, Wasserman DH, MacKintosh C, Sakamoto K. Mice with AS160/TBC1D4-Thr649Ala knockin mutation are glucose intolerant with reduced insulin sensitivity and altered GLUT4 trafficking. Cell Metab. 2011;13:68-79.

[285] Sakamoto K, Holman GD. Emerging role for AS160/TBC1D4 and TBC1D1 in the regulation of GLUT4 traffic. Am J Physiol Endocrinol Metab. 2008;295:E29-37.

[286] Gaidhu MP, Perry RL, Noor F, Ceddia RB. Disruption of AMPKalpha1 signaling prevents AICAR-induced inhibition of AS160/TBC1D4 phosphorylation and glucose uptake in primary rat adipocytes. Mol Endocrinol. 2010;24:1434-40.

[287] Treebak JT, Glund S, Deshmukh A, Klein DK, Long YC, Jensen TE, et al. AMPK-mediated AS160 phosphorylation in skeletal muscle is dependent on AMPK catalytic and regulatory subunits. Diabetes. 2006;55:2051-8.

[288] Hunter RW, Treebak JT, Wojtaszewski JF, Sakamoto K. Molecular mechanism by which AMP-activated protein kinase activation promotes glycogen accumulation in muscle. Diabetes. 2011;60:766-74.

[289] Bouskila M, Hunter RW, Ibrahim AF, Delattre L, Peggie M, van Diepen JA, et al. Allosteric regulation of glycogen synthase controls glycogen synthesis in muscle. Cell Metab. 2010;12:456-66.

[290] Carling D, Hardie DG. The substrate and sequence specificity of the AMP-activated protein kinase. Phosphorylation of glycogen synthase and phosphorylase kinase. Biochim Biophys Acta. 1989;1012:81-6.

[291] Jorgensen SB, Nielsen JN, Birk JB, Olsen GS, Viollet B, Andreelli F, et al. The alpha2-5'AMP-activated protein kinase is a site 2 glycogen synthase kinase in skeletal muscle and is responsive to glucose loading. Diabetes. 2004;53:3074-81.

[292] Longnus SL, Wambolt RB, Parsons HL, Brownsey RW, Allard MF. 5-Aminoimidazole-4-carboxamide 1-beta -D-ribofuranoside (AICAR) stimulates myocardial glycogenolysis by allosteric mechanisms. Am J Physiol Regul Integr Comp Physiol. 2003;284:R936-44.

[293] Ercan-Fang N, Gannon MC, Rath VL, Treadway JL, Taylor MR, Nuttall FQ. Integrated effects of multiple modulators on human liver glycogen phosphorylase a. Am J Physiol Endocrinol Metab. 2002;283:E29-37.

[294] Marsin AS, Bertrand L, Rider MH, Deprez J, Beauloye C, Vincent MF, et al. Phosphorylation and activation of heart PFK-2 by AMPK has a role in the stimulation of glycolysis during ischaemia. CurrBiol. 2000;10:1247-55.

[295] Hue L, Beauloye C, Marsin AS, Bertrand L, Horman S, Rider MH. Insulin and ischemia stimulate glycolysis by acting on the same targets through different and opposing signaling pathways. J Mol Cell Cardiol. 2002;34:1091-7.

[296] Liu Q, Docherty JC, Rendell JC, Clanachan AS, Lopaschuk GD. High levels of fatty acids delay the recovery of intracellular pH and cardiac efficiency in post-ischemic hearts by inhibiting glucose oxidation. J Am Coll Cardiol. 2002;39:718-25.

[297] Itoi T, Huang L, Lopaschuk GD. Glucose use in neonatal rabbit hearts reperfused after global ischemia. The American journal of physiology. 1993;265:H427-33.

[298] Lopaschuk GD. AMP-activated protein kinase control of energy metabolism in the ischemic heart. Int J Obes (Lond). 2008;32 Suppl 4:S29-35.

[299] Lopaschuk GD, Stanley WC. Malonyl-CoA decarboxylase inhibition as a novel approach to treat ischemic heart disease. Cardiovascular drugs and therapy / sponsored by the International Society of Cardiovascular Pharmacotherapy. 2006;20:433-9.

[300] Lopaschuk GD, Barr R, Thomas PD, Dyck JR. Beneficial effects of trimetazidine in ex vivo working ischemic hearts are due to a stimulation of glucose oxidation secondary to inhibition of long-chain 3-ketoacyl coenzyme a thiolase. Circulation research. 2003;93:e33-7.

[301] Hopkins TA, Dyck JR, Lopaschuk GD. AMP-activated protein kinase regulation of fatty acid oxidation in the ischaemic heart. Biochem Soc Trans. 2003;31:207-12.

[302] Dyck JR, Lopaschuk GD. Malonyl CoA control of fatty acid oxidation in the ischemic heart. J Mol Cell Cardiol. 2002;34:1099-109.

[303] Kantor PF, Dyck JR, Lopaschuk GD. Fatty acid oxidation in the reperfused ischemic heart. The American journal of the medical sciences. 1999;318:3-14.

[304] Liu B, Clanachan AS, Schulz R, Lopaschuk GD. Cardiac efficiency is improved after ischemia by altering both the source and fate of protons. Circulation research. 1996;79:940-8.

[305] Hu X, Xu X, Lu Z, Zhang P, Fassett J, Zhang Y, et al. AMP activated protein kinase-alpha2 regulates expression of estrogen-related receptor-alpha, a metabolic transcription factor related to heart failure development. Hypertension. 2011;58:696-703.

[306] Zhu L, Wang Q, Zhang L, Fang Z, Zhao F, Lv Z, et al. Hypoxia induces PGC-1alpha expression and mitochondrial biogenesis in the myocardium of TOF patients. Cell Res. 2010;20:676-87.

[307] Wang W, Fan J, Yang X, Furer-Galban S, Lopez de Silanes I, von Kobbe C, et al. AMP-activated kinase regulates cytoplasmic HuR. Mol Cell Biol. 2002;22:3425-36.

[308] Hoppe S, Bierhoff H, Cado I, Weber A, Tiebe M, Grummt I, et al. AMP-activated protein kinase adapts rRNA synthesis to cellular energy supply. Proceedings of the National Academy of Sciences of the United States of America. 2009;106:17781-6.

[309] Cheng SW, Fryer LG, Carling D, Shepherd PR. Thr2446 is a novel mammalian target of rapamycin (mTOR) phosphorylation site regulated by nutrient status. J Biol Chem. 2004;279:15719-22.

[310] Hardie DG, Ashford ML. AMPK: regulating energy balance at the cellular and whole body levels. Physiology (Bethesda, Md. 2014;29:99-107.

[311] Inoki K, Li Y, Zhu T, Wu J, Guan KL. TSC2 is phosphorylated and inhibited by Akt and suppresses mTOR signalling. Nature cell biology. 2002;4:648-57.

[312] Gwinn DM, Shackelford DB, Egan DF, Mihaylova MM, Mery A, Vasquez DS, et al. AMPK phosphorylation of raptor mediates a metabolic checkpoint. Mol Cell. 2008;30:214-26.

[313] Hardie DG. AMPK and Raptor: matching cell growth to energy supply. Mol Cell. 2008;30:263-5.

[314] Horman S, Browne G, Krause U, Patel J, Vertommen D, Bertrand L, et al. Activation of AMP-activated protein kinase leads to the phosphorylation of elongation factor 2 and an inhibition of protein synthesis. Curr Biol. 2002;12:1419-23.

[315] Browne GJ, Finn SG, Proud CG. Stimulation of the AMP-activated protein kinase leads to activation of eukaryotic elongation factor 2 kinase and to its phosphorylation at a novel site, serine 398. J Biol Chem. 2004;279:12220-31.

[316] Inoki K, Zhu T, Guan KL. TSC2 mediates cellular energy response to control cell growth and survival. Cell. 2003;115:577-90.

[317] Horman S, Beauloye C, Vertommen D, Vanoverschelde JL, Hue L, Rider MH. Myocardial ischemia and increased heart work modulate the phosphorylation state of eukaryotic elongation factor-2. J Biol Chem. 2003;278:41970-6.

[318] Nakai A, Yamaguchi O, Takeda T, Higuchi Y, Hikoso S, Taniike M, et al. The role of autophagy in cardiomyocytes in the basal state and in response to hemodynamic stress. Nature medicine. 2007;13:619-24.

[319] Fong JT, Kells RM, Gumpert AM, Marzillier JY, Davidson MW, Falk MM. Internalized gap junctions are degraded by autophagy. Autophagy. 2012;8:794-811.

[320] Garcia L, Verdejo HE, Kuzmicic J, Zalaquett R, Gonzalez S, Lavandero S, et al. Impaired cardiac autophagy in patients developing postoperative atrial fibrillation. J Thorac Cardiovasc Surg. 2012;143:451-9.

[321] Yan L, Vatner DE, Kim SJ, Ge H, Masurekar M, Massover WH, et al. Autophagy in chronically ischemic myocardium. Proceedings of the National Academy of Sciences of the United States of America. 2005;102:13807-12.

[322] Yuan Y, Zhao J, Yan S, Wang D, Zhang S, Yun F, et al. Autophagy: A potential novel mechanistic contributor to atrial fibrillation. International journal of cardiology. 2014;172:492-4.

[323] Sinnett SE, Brenman JE. Past strategies and future directions for identifying AMP-activated protein kinase (AMPK) modulators. Pharmacology & therapeutics. 2014.

[324] Hinke SA, Martens GA, Cai Y, Finsi J, Heimberg H, Pipeleers D, et al. Methyl succinate antagonises biguanide-induced AMPK-activation and death of pancreatic beta-cells through restoration of mitochondrial electron transfer. British journal of pharmacology. 2007;150:1031-43.

[325] Sakamoto K, Goransson O, Hardie DG, Alessi DR. Activity of LKB1 and AMPK-related kinases in skeletal muscle: effects of contraction, phenformin, and AICAR. Am J Physiol Endocrinol Metab. 2004;287:E310-7.

[326] Zhang L, He H, Balschi JA. Metformin and phenformin activate AMP-activated protein kinase in the heart by increasing cytosolic AMP concentration. American journal of physiology. 2007;293:H457-66.

[327] Cool B, Zinker B, Chiou W, Kifle L, Cao N, Perham M, et al. Identification and characterization of a small molecule AMPK activator that treats key components of type 2 diabetes and the metabolic syndrome. Cell Metab. 2006;3:403-16.

[328] Goransson O, McBride A, Hawley SA, Ross FA, Shpiro N, Foretz M, et al. Mechanism of action of A-769662, a valuable tool for activation of AMP-activated protein kinase. J Biol Chem. 2007.

[329] Pang T, Zhang ZS, Gu M, Qiu BY, Yu LF, Cao PR, et al. Small molecule antagonizes autoinhibition and activates AMP-activated protein kinase in cells. J Biol Chem. 2008;283:16051-60.

[330] Li YY, Yu LF, Zhang LN, Qiu BY, Su MB, Wu F, et al. Novel small-molecule AMPK activator orally exerts beneficial effects on diabetic db/db mice. Toxicology and applied pharmacology. 2013;273:325-34.

[331] Hawley SA, Fullerton MD, Ross FA, Schertzer JD, Chevtzoff C, Walker KJ, et al. The ancient drug salicylate directly activates AMP-activated protein kinase. Science. 2012;336:918-22.

[332] Kim EK, Miller I, Aja S, Landree LE, Pinn M, McFadden J, et al. C75, a fatty acid synthase inhibitor, reduces food intake via hypothalamic AMP-activated protein kinase. J Biol Chem. 2004;279:19970-6.

[333] McCullough LD, Zeng Z, Li H, Landree LE, McFadden J, Ronnett GV. Pharmacological inhibition of AMP-activated protein kinase provides neuroprotection in stroke. J Biol Chem. 2005;280:20493-502.

[334] Zhou G, Myers R, Li Y, Chen Y, Shen X, Fenyk-Melody J, et al. Role of AMP-activated protein kinase in mechanism of metformin action. The Journal of clinical investigation. 2001;108:1167-74.

[335] Machrouhi F, Ouhamou N, Laderoute K, Calaoagan J, Bukhtiyarova M, Ehrlich PJ, et al. The rational design of a novel potent analogue of the 5'-AMP-activated protein kinase inhibitor compound C with improved selectivity and cellular activity. Bioorganic & medicinal chemistry letters. 2010;20:6394-9.

[336] Chu TF, Rupnick MA, Kerkela R, Dallabrida SM, Zurakowski D, Nguyen L, et al. Cardiotoxicity associated with tyrosine kinase inhibitor sunitinib. Lancet. 2007;370:2011-9.

[337] Kerkela R, Woulfe KC, Durand JB, Vagnozzi R, Kramer D, Chu TF, et al. Sunitinib-induced cardiotoxicity is mediated by off-target inhibition of AMP-activated protein kinase. Clinical and translational science. 2009;2:15-25.

[338] Altarejos JY, Taniguchi M, Clanachan AS, Lopaschuk GD. Myocardial ischemia differentially regulates LKB1 and an alternate 5'-AMP-activated protein kinase kinase. J Biol Chem. 2005;280:183-90.

[339] Hawley SA, Boudeau J, Reid JL, Mustard KJ, Udd L, Makela TP, et al. Complexes between the LKB1 tumor suppressor, STRAD alpha/beta and MO25 alpha/beta are upstream kinases in the AMP-activated protein kinase cascade. Journal of biology. 2003;2:28.

[340] Hawley SA, Selbert MA, Goldstein EG, Edelman AM, Carling D, Hardie DG. 5'-AMP activates the AMP-activated protein kinase cascade, and Ca2+/calmodulin activates the calmodulin-dependent protein kinase I cascade, via three independent mechanisms. J Biol Chem. 1995;270:27186-91.

[341] Shaw RJ, Kosmatka M, Bardeesy N, Hurley RL, Witters LA, DePinho RA, et al. The tumor suppressor LKB1 kinase directly activates AMP-activated kinase and regulates apoptosis in response to energy stress. Proceedings of the National Academy of Sciences of the United States of America. 2004;101:3329-35.

[342] Suzuki A, Kusakai G, Kishimoto A, Shimojo Y, Ogura T, Lavin MF, et al. IGF-1 phosphorylates AMPK-alpha subunit in ATM-dependent and LKB1-independent manner. Biochem Biophys Res Commun. 2004;324:986-92.

[343] Ussher JR, Jaswal JS, Wagg CS, Armstrong HE, Lopaschuk DG, Keung W, et al. Role of the atypical protein kinase Czeta in regulation of 5'-AMP-activated protein kinase in cardiac and skeletal muscle. Am J Physiol Endocrinol Metab. 2009;297:E349-57.

[344] Xie M, Zhang D, Dyck JR, Li Y, Zhang H, Morishima M, et al. A pivotal role for endogenous TGF-beta-activated kinase-1 in the LKB1/AMP-activated protein kinase energy-sensor pathway. Proceedings of the National Academy of Sciences of the United States of America. 2006;103:17378-83.

[345] Xie Z, Dong Y, Zhang M, Cui MZ, Cohen RA, Riek U, et al. Activation of protein kinase C zeta by peroxynitrite regulates LKB1-dependent AMP-activated protein kinase in cultured endothelial cells. J Biol Chem. 2006;281:6366-75.

[346] Hurley RL, Barre LK, Wood SD, Anderson KA, Kemp BE, Means AR, et al. Regulation of AMP-activated protein kinase by multisite phosphorylation in response to agents that elevate cellular cAMP. J Biol Chem. 2006;281:36662-72.

[347] Saez JC, Martinez AD, Branes MC, Gonzalez HE. Regulation of gap junctions by protein phosphorylation. Braz J Med Biol Res. 1998;31:593-600.

[348] Lowenstein WR. Regulation of cell-to-cell communication by phosphorylation. Biochemical Society symposium. 1985;50:43-58.

[349] Thevenin AF, Kowal TJ, Fong JT, Kells RM, Fisher CG, Falk MM. Proteins and mechanisms regulating gap-junction assembly, internalization, and degradation. Physiology (Bethesda, Md. 2013;28:93-116.

[350] Chen VC, Gouw JW, Naus CC, Foster LJ. Connexin multi-site phosphorylation: mass spectrometry-based proteomics fills the gap. Biochim Biophys Acta. 2013;1828:23-34.

[351] Marquez-Rosado L, Solan JL, Dunn CA, Norris RP, Lampe PD. Connexin43 phosphorylation in brain, cardiac, endothelial and epithelial tissues. Biochim Biophys Acta. 2012;1818:1985-92.

[352] Solan JL, Lampe PD. Connexin43 phosphorylation: structural changes and biological effects. Biochem J. 2009;419:261-72.

[353] Lampe PD, Lau AF. The effects of connexin phosphorylation on gap junctional communication. The international journal of biochemistry & cell biology. 2004;36:1171-86.

[354] Cooper CD, Solan JL, Dolejsi MK, Lampe PD. Analysis of connexin phosphorylation sites. Methods. 2000;20:196-204.

[355] Lampe PD, Lau AF. Regulation of gap junctions by phosphorylation of connexins. Archives of biochemistry and biophysics. 2000;384:205-15.

[356] Solan JL, Lampe PD. Key Connexin 43 Phosphorylation Events Regulate the Gap Junction Life Cycle. J Membr Biol. 2007.

[357] Swenson KI, Piwnica-Worms H, McNamee H, Paul DL. Tyrosine phosphorylation of the gap junction protein connexin43 is required for the pp60v-src-induced inhibition of communication. Cell regulation. 1990;1:989-1002.

[358] Crow DS, Beyer EC, Paul DL, Kobe SS, Lau AF. Phosphorylation of connexin43 gap junction protein in uninfected and Rous sarcoma virus-transformed mammalian fibroblasts. Mol Cell Biol. 1990;10:1754-63.

[359] Laird DW, Castillo M, Kasprzak L. Gap junction turnover, intracellular trafficking, and phosphorylation of connexin43 in brefeldin A-treated rat mammary tumor cells. The Journal of cell biology. 1995;131:1193-203.

[360] Musil LS, Cunningham BA, Edelman GM, Goodenough DA. Differential phosphorylation of the gap junction protein connexin43 in junctional communication-competent and -deficient cell lines. The Journal of cell biology. 1990;111:2077-88.

[361] Kadle R, Zhang JT, Nicholson BJ. Tissue-specific distribution of differentially phosphorylated forms of Cx43. Mol Cell Biol. 1991;11:363-9.

[362] Solan JL, Fry MD, TenBroek EM, Lampe PD. Connexin43 phosphorylation at S368 is acute during S and G2/M and in response to protein kinase C activation. Journal of cell science. 2003;116:2203-11.

[363] Dunn CA, Lampe PD. Injury-triggered Akt phosphorylation of Cx43: a ZO-1-driven molecular switch that regulates gap junction size. Journal of cell science. 2014;127:455-64.

[364] Musil LS, Goodenough DA. Biochemical analysis of connexin43 intracellular transport, phosphorylation, and assembly into gap junctional plaques. The Journal of cell biology. 1991;115:1357-74.

[365] Park DJ, Wallick CJ, Martyn KD, Lau AF, Jin C, Warn-Cramer BJ. Akt phosphorylates Connexin43 on Ser373, a "mode-1" binding site for 14-3-3. Cell Commun Adhes. 2007;14:211-26.

[366] Cooper CD, Lampe PD. Casein kinase 1 regulates connexin-43 gap junction assembly. J Biol Chem. 2002;277:44962-8.

[367] Lau AF, Kanemitsu MY, Kurata WE, Danesh S, Boynton AL. Epidermal growth factor disrupts gap-junctional communication and induces phosphorylation of connexin43 on serine. Molecular biology of the cell. 1992;3:865-74.

[368] Kanemitsu MY, Lau AF. Epidermal growth factor stimulates the disruption of gap junctional communication and connexin43 phosphorylation independent of 12-0-tetradecanoylphorbol 13-acetate-sensitive protein kinase C: the possible involvement of mitogen-activated protein kinase. Molecular biology of the cell. 1993;4:837-48.

[369] Warn-Cramer BJ, Cottrell GT, Burt JM, Lau AF. Regulation of connexin-43 gap junctional intercellular communication by mitogen-activated protein kinase. J Biol Chem. 1998;273:9188-96.

[370] Polontchouk L, Ebelt B, Jackels M, Dhein S. Chronic effects of endothelin 1 and angiotensin II on gap junctions and intercellular communication in cardiac cells. Faseb J. 2002;16:87-9.

[371] Petrich BG, Gong X, Lerner DL, Wang X, Brown JH, Saffitz JE, et al. c-Jun N-terminal kinase activation mediates downregulation of connexin43 in cardiomyocytes. Circulation research. 2002;91:640-7.

[372] Cameron SJ, Malik S, Akaike M, Lerner-Marmarosh N, Yan C, Lee JD, et al. Regulation of epidermal growth factor-induced connexin 43 gap junction communication by big mitogen-activated protein kinase1/ERK5 but not ERK1/2 kinase activation. J Biol Chem. 2003;278:18682-8.

[373] Brissette JL, Kumar NM, Gilula NB, Dotto GP. The tumor promoter 12-O-tetradecanoylphorbol-13-acetate and the ras oncogene modulate expression and phosphorylation of gap junction proteins. Mol Cell Biol. 1991;11:5364-71.

[374] Berthoud VM, Rook MB, Traub O, Hertzberg EL, Saez JC. On the mechanisms of cell uncoupling induced by a tumor promoter phorbol ester in clone 9 cells, a rat liver epithelial cell line. Eur J Cell Biol. 1993;62:384-96.

[375] Berthoud VM, Ledbetter ML, Hertzberg EL, Saez JC. Connexin43 in MDCK cells: regulation by a tumor-promoting phorbol ester and Ca2+. Eur J Cell Biol. 1992;57:40-50.

[376] Lampe PD. Analyzing phorbol ester effects on gap junctional communication: a dramatic inhibition of assembly. The Journal of cell biology. 1994;127:1895-905.

[377] Saez JC, Nairn AC, Czernik AJ, Fishman GI, Spray DC, Hertzberg EL. Phosphorylation of connexin43 and the regulation of neonatal rat cardiac myocyte gap junctions. J Mol Cell Cardiol. 1997;29:2131-45.

[378] Kanemitsu MY, Jiang W, Eckhart W. Cdc2-mediated phosphorylation of the gap junction protein, connexin43, during mitosis. Cell Growth Differ. 1998;9:13-21.

[379] Lampe PD, Kurata WE, Warn-Cramer BJ, Lau AF. Formation of a distinct connexin43 phosphoisoform in mitotic cells is dependent upon p34cdc2 kinase. Journal of cell science. 1998;111 (Pt 6):833-41.

[380] Xie H, Laird DW, Chang TH, Hu VW. A mitosis-specific phosphorylation of the gap junction protein connexin43 in human vascular cells: biochemical characterization and localization. The Journal of cell biology. 1997;137:203-10.

[381] Atkinson MM, Lampe PD, Lin HH, Kollander R, Li XR, Kiang DT. Cyclic AMP modifies the cellular distribution of connexin43 and induces a persistent increase in the junctional permeability of mouse mammary tumor cells. Journal of cell science. 1995;108 (Pt 9):3079-90.

[382] Burghardt RC, Barhoumi R, Sewall TC, Bowen JA. Cyclic AMP induces rapid increases in gap junction permeability and changes in the cellular distribution of connexin43. J Membr Biol. 1995;148:243-53.

[383] Paulson AF, Lampe PD, Meyer RA, TenBroek E, Atkinson MM, Walseth TF, et al. Cyclic AMP and LDL trigger a rapid enhancement in gap junction assembly through a stimulation of connexin trafficking. Journal of cell science. 2000;113 (Pt 17):3037-49.

[384] Yogo K, Ogawa T, Akiyama M, Ishida-Kitagawa N, Sasada H, Sato E, et al. PKA implicated in the phosphorylation of Cx43 induced by stimulation with FSH in rat granulosa cells. J Reprod Dev. 2006;52:321-8.

[385] Shah MM, Martinez AM, Fletcher WH. The connexin43 gap junction protein is phosphorylated by protein kinase A and protein kinase C: in vivo and in vitro studies. Mol Cell Biochem. 2002;238:57-68.

[386] Axelsen LN, Stahlhut M, Mohammed S, Larsen BD, Nielsen MS, Holstein-Rathlou NH, et al. Identification of ischemia-regulated phosphorylation sites in connexin43: A possible target for the antiarrhythmic peptide analogue rotigaptide (ZP123). J Mol Cell Cardiol. 2006;40:790-8.

[387] TenBroek EM, Lampe PD, Solan JL, Reynhout JK, Johnson RG. Ser364 of connexin43 and the upregulation of gap junction assembly by cAMP. The Journal of cell biology. 2001;155:1307-18.

[388] Solan JL, Lampe PD. Connexin 43 in LA-25 cells with active v-src is phosphorylated on Y247, Y265, S262, S279/282, and S368 via multiple signaling pathways. Cell Commun Adhes. 2008;15:75-84.

[389] Kanemitsu MY, Loo LW, Simon S, Lau AF, Eckhart W. Tyrosine phosphorylation of connexin 43 by v-Src is mediated by SH2 and SH3 domain interactions. J Biol Chem. 1997;272:22824-31.

[390] Lin R, Warn-Cramer BJ, Kurata WE, Lau AF. v-Src phosphorylation of connexin 43 on Tyr247 and Tyr265 disrupts gap junctional communication. The Journal of cell biology. 2001;154:815-27.

[391] Lin R, Martyn KD, Guyette CV, Lau AF, Warn-Cramer BJ. v-Src tyrosine phosphorylation of connexin43: regulation of gap junction communication and effects on cell transformation. Cell Commun Adhes. 2006;13:199-216.

[392] Huang RY, Laing JG, Kanter EM, Berthoud VM, Bao M, Rohrs HW, et al. Identification of CaMKII phosphorylation sites in Connexin43 by high-resolution mass spectrometry. Journal of proteome research. 2011;10:1098-109.

[393] Wisniewski JR, Nagaraj N, Zougman A, Gnad F, Mann M. Brain phosphoproteome obtained by a FASP-based method reveals plasma membrane protein topology. Journal of proteome research. 2010;9:3280-9.

[394] Yogo K, Ogawa T, Akiyama M, Ishida N, Takeya T. Identification and functional analysis of novel phosphorylation sites in Cx43 in rat primary granulosa cells. FEBS Lett. 2002;531:132-6.

[395] Bonnette PC, Robinson BS, Silva JC, Stokes MP, Brosius AD, Baumann A, et al. Phosphoproteomic characterization of PYK2 signaling pathways involved in osteogenesis. Journal of proteomics. 2010;73:1306-20.

[396] Li H, Liu TF, Lazrak A, Peracchia C, Goldberg GS, Lampe PD, et al. Properties and regulation of gap junctional hemichannels in the plasma membranes of cultured cells. The Journal of cell biology. 1996;134:1019-30.

[397] Lampe PD, Qiu Q, Meyer RA, TenBroek EM, Walseth TF, Starich TA, et al. Gap junction assembly: PTX-sensitive G proteins regulate the distribution of connexin43 within cells. Am J Physiol Cell Physiol. 2001;281:C1211-22.

[398] Sosinsky GE, Solan JL, Gaietta GM, Ngan L, Lee GJ, Mackey MR, et al. The C-terminus of connexin43 adopts different conformations in the Golgi and gap junction as detected with structure-specific antibodies. Biochem J. 2007;408:375-85.

[399] Richards TS, Dunn CA, Carter WG, Usui ML, Olerud JE, Lampe PD. Protein kinase C spatially and temporally regulates gap junctional communication during human wound repair via phosphorylation of connexin43 on serine368. The Journal of cell biology. 2004;167:555-62.

[400] Hund TJ, Lerner DL, Yamada KA, Schuessler RB, Saffitz JE. Protein kinase Cepsilon mediates salutary effects on electrical coupling induced by ischemic preconditioning. Heart Rhythm. 2007;4:1183-93.

[401] Hunter AW, Barker RJ, Zhu C, Gourdie RG. Zonula occludens-1 alters connexin43 gap junction size and organization by influencing channel accretion. Molecular biology of the cell. 2005;16:5686-98.

[402] Cottrell GT, Lin R, Warn-Cramer BJ, Lau AF, Burt JM. Mechanism of v-Src- and mitogen-activated protein kinase-induced reduction of gap junction communication. Am J Physiol Cell Physiol. 2003;284:C511-20.

[403] Brautigan DL. Protein Ser/Thr phosphatases--the ugly ducklings of cell signalling. The FEBS journal. 2013;280:324-45.

[404] Ai X, Pogwizd SM. Connexin 43 downregulation and dephosphorylation in nonischemic heart failure is associated with enhanced colocalized protein phosphatase type 2A. Circulation research. 2005;96:54-63.

[405] Moreno AP, Fishman GI, Spray DC. Phosphorylation shifts unitary conductance and modifies voltage dependent kinetics of human connexin43 gap junction channels. Biophys J. 1992;62:51-3.

[406] Duthe F, Plaisance I, Sarrouilhe D, Herve JC. Endogenous protein phosphatase 1 runs down gap junctional communication of rat ventricular myocytes. Am J Physiol Cell Physiol. 2001;281:C1648-56.

[407] Duthe F, Dupont E, Verrecchia F, Plaisance I, Severs NJ, Sarrouilhe D, et al. Dephosphorylation agents depress gap junctional communication between rat cardiac cells without modifying the Connexin43 phosphorylation degree. General physiology and biophysics. 2000;19:441-9.

[408] Jeyaraman M, Tanguy S, Fandrich RR, Lukas A, Kardami E. Ischemia-induced dephosphorylation of cardiomyocyte connexin-43 is reduced by okadaic acid and calyculin A but not fostriecin. Mol Cell Biochem. 2003;242:129-34.

[409] Singh D, Lampe PD. Identification of connexin-43 interacting proteins. Cell Commun Adhes. 2003;10:215-20.

[410] Giepmans BN, Feiken E, Gebbink MF, Moolenaar WH. Association of connexin43 with a receptor protein tyrosine phosphatase. Cell Commun Adhes. 2003;10:201-5.

[411] Morioka M, Hamada J, Ushio Y, Miyamoto E. Potential role of calcineurin for brain ischemia and traumatic injury. Progress in neurobiology. 1999;58:1-30.

[412] Li WE, Nagy JI. Connexin43 phosphorylation state and intercellular communication in cultured astrocytes following hypoxia and protein phosphatase inhibition. Eur J Neurosci. 2000;12:2644-50.

[413] Turner MS, Haywood GA, Andreka P, You L, Martin PE, Evans WH, et al. Reversible connexin 43 dephosphorylation during hypoxia and reoxygenation is linked to cellular ATP levels. Circulation research. 2004;95:726-33.

[414] Toyofuku T, Akamatsu Y, Zhang H, Kuzuya T, Tada M, Hori M. c-Src regulates the interaction between connexin-43 and ZO-1 in cardiac myocytes. J Biol Chem. 2001;276:1780-8.

[415] Traub O, Eckert R, Lichtenberg-Frate H, Elfgang C, Bastide B, Scheidtmann KH, et al. Immunochemical and electrophysiological characterization of murine connexin40 and -43 in mouse tissues and transfected human cells. Eur J Cell Biol. 1994;64:101-12.

[416] van Rijen HV, van Veen TA, Hermans MM, Jongsma HJ. Human connexin40 gap junction channels are modulated by cAMP. Cardiovascular research. 2000;45:941-51.

[417] Hoffmann A, Gloe T, Pohl U, Zahler S. Nitric oxide enhances de novo formation of endothelial gap junctions. Cardiovascular research. 2003;60:421-30.

[418] Dhein S, Polontchouk L, Salameh A, Haefliger JA. Pharmacological modulation and differential regulation of the cardiac gap junction proteins connexin 43 and connexin 40. Biology of the cell / under the auspices of the European Cell Biology Organization. 2002;94:409-22.

[419] Haussig S, Schubert A, Mohr FW, Dhein S. Sub-chronic nicotine exposure induces intercellular communication failure and differential down-regulation of connexins in cultured human endothelial cells. Atherosclerosis. 2007.

[420] Butterweck A, Gergs U, Elfgang C, Willecke K, Traub O. Immunochemical characterization of the gap junction protein connexin45 in mouse kidney and transfected human HeLa cells. J Membr Biol. 1994;141:247-56.

[421] Darrow BJ, Laing JG, Lampe PD, Saffitz JE, Beyer EC. Expression of multiple connexins in cultured neonatal rat ventricular myocytes. Circulation research. 1995;76:381-7.

[422] Hertlein B, Butterweck A, Haubrich S, Willecke K, Traub O. Phosphorylated carboxy terminal serine residues stabilize the mouse gap junction protein connexin45 against degradation. J Membr Biol. 1998;162:247-57.

[423] Hardie DG, Carling D, Carlson M. The AMP-activated/SNF1 protein kinase subfamily: metabolic sensors of the eukaryotic cell? Annual review of biochemistry. 1998;67:821-55.

[424] Scott JW, Norman DG, Hawley SA, Kontogiannis L, Hardie DG. Protein kinase substrate recognition studied using the recombinant catalytic domain of AMP-activated protein kinase and a model substrate. Journal of molecular biology. 2002;317:309-23.

[425] Csepe TA, Kalyanasundaram A, Hansen BJ, Zhao J, Fedorov VV. Fibrosis: a structural modulator of sinoatrial node physiology and dysfunction. Frontiers in physiology. 2015;6:37.

[426] Anumonwo JM, Pandit SV. Ionic mechanisms of arrhythmogenesis. Trends in cardiovascular medicine. 2015.

[427] Jalife J, Kaur K. Atrial remodeling, fibrosis, and atrial fibrillation. Trends in cardiovascular medicine. 2014.

[428] Hong K, Xiong Q. Genetic basis of atrial fibrillation. Current opinion in cardiology. 2014.

[429] Fedorov VV, Glukhov AV, Chang R. Conduction barriers and pathways of the sinoatrial pacemaker complex: their role in normal rhythm and atrial arrhythmias. American journal of physiology. 2012;302:H1773-83.

[430] Temple IP, Inada S, Dobrzynski H, Boyett MR. Connexins and the atrioventricular node. Heart Rhythm. 2013;10:297-304.

[431] Jansen JA, van Veen TA, de Bakker JM, van Rijen HV. Cardiac connexins and impulse propagation. J Mol Cell Cardiol. 2010;48:76-82.

[432] Terentyev D, Rees CM, Li W, Cooper LL, Jindal HK, Peng X, et al. Hyperphosphorylation of RyRs underlies triggered activity in transgenic rabbit model of LQT2 syndrome. Circulation research. 2014;115:919-28.

[433] Zhou Q, Xiao J, Jiang D, Wang R, Vembaiyan K, Wang A, et al. Carvedilol and its new analogs suppress arrhythmogenic store overload-induced Ca2+ release. Nature medicine. 2011;17:1003-9.

[434] Andersen MN, Rasmussen HB. AMPK: A regulator of ion channels. Commun Integr Biol. 2012;5:480-4.

[435] Light PE, Wallace CH, Dyck JR. Constitutively active adenosine monophosphate-activated protein kinase regulates voltage-gated sodium channels in ventricular myocytes. Circulation. 2003;107:1962-5.

[436] Duan D. Phenomics of cardiac chloride channels: the systematic study of chloride channel function in the heart. The Journal of physiology. 2009;587:2163-77.

[437] Hegedus T, Aleksandrov A, Mengos A, Cui L, Jensen TJ, Riordan JR. Role of individual R domain phosphorylation sites in CFTR regulation by protein kinase A. Biochim Biophys Acta. 2009;1788:1341-9.

[438] Hwang TC, Kirk KL. The CFTR ion channel: gating, regulation, and anion permeation. Cold Spring Harbor perspectives in medicine. 2013;3:a009498.

[439] Alzamora R, King JD, Jr., Hallows KR. CFTR regulation by phosphorylation. Methods in molecular biology (Clifton, NJ. 2011;741:471-88.

[440] Siwiak M, Edelman A, Zielenkiewicz P. Structural models of CFTR-AMPK and CFTR-PKA interactions: R-domain flexibility is a key factor in CFTR regulation. Journal of molecular modeling. 2012;18:83-90.

[441] Hallows KR, Raghuram V, Kemp BE, Witters LA, Foskett JK. Inhibition of cystic fibrosis transmembrane conductance regulator by novel interaction with the metabolic sensor AMP-activated protein kinase. The Journal of clinical investigation. 2000;105:1711-21.

[442] Hallows KR, McCane JE, Kemp BE, Witters LA, Foskett JK. Regulation of channel gating by AMP-activated protein kinase modulates cystic fibrosis transmembrane conductance regulator activity in lung submucosal cells. J Biol Chem. 2003;278:998-1004.

[443] Hallows KR. Emerging role of AMP-activated protein kinase in coupling membrane transport to cellular metabolism. Current opinion in nephrology and hypertension. 2005;14:464-71.

[444] King JD, Jr., Fitch AC, Lee JK, McCane JE, Mak DO, Foskett JK, et al. AMP-activated protein kinase phosphorylation of the R domain inhibits PKA stimulation of CFTR. Am J Physiol Cell Physiol. 2009;297:C94-101.

[445] Kongsuphol P, Cassidy D, Hieke B, Treharne KJ, Schreiber R, Mehta A, et al. Mechanistic insight into control of CFTR by AMPK. J Biol Chem. 2009;284:5645-53.

[446] King JD, Jr., Lee J, Riemen CE, Neumann D, Xiong S, Foskett JK, et al. Role of binding and nucleoside diphosphate kinase A in the regulation of the cystic fibrosis transmembrane conductance regulator by AMP-activated protein kinase. J Biol Chem. 2012;287:33389-400.

[447] Ikematsu N, Dallas ML, Ross FA, Lewis RW, Rafferty JN, David JA, et al. Phosphorylation of the voltage-gated potassium channel Kv2.1 by AMP-activated protein kinase regulates membrane excitability. Proceedings of the National Academy of Sciences of the United States of America. 2011;108:18132-7.

[448] Wang CZ, Wang Y, Di A, Magnuson MA, Ye H, Roe MW, et al. 5-amino-imidazole carboxamide riboside acutely potentiates glucose-stimulated insulin secretion from mouse pancreatic islets by KATP channel-dependent and -independent pathways. Biochem Biophys Res Commun. 2005;330:1073-9.

[449] Chang TJ, Chen WP, Yang C, Lu PH, Liang YC, Su MJ, et al. Serine-385 phosphorylation of inwardly rectifying K+ channel subunit (Kir6.2) by AMP-dependent protein kinase plays a key role in rosiglitazone-induced closure of the K(ATP) channel and insulin secretion in rats. Diabetologia. 2009;52:1112-21.

[450] Gollob MH. Glycogen storage disease as a unifying mechanism of disease in the PRKAG2 cardiac syndrome. Biochem Soc Trans. 2003;31:228-31.

[451] Gollob MH, Green MS, Tang AS, Gollob T, Karibe A, Hassan AS, et al. Identification of a gene responsible for familial Wolff-Parkinson-White syndrome. NEnglJMed. 2001;344:1823-31.

[452] Gollob MH, Seger JJ, Gollob TN, Tapscott T, Gonzales O, Bachinski L, et al. Novel PRKAG2 mutation responsible for the genetic syndrome of ventricular preexcitation and conduction system disease with childhood onset and absence of cardiac hypertrophy. Circulation. 2001;104:3030-3.

[453] Folmes KD, Chan AY, Koonen DP, Pulinilkunnil TC, Baczko I, Hunter BE, et al. Distinct early signaling events resulting from the expression of the PRKAG2 R302Q mutant of AMPK contribute to increased myocardial glycogen. Circulation Cardiovascular genetics. 2009;2:457-66.

[454] Gollob MH, Seger JJ, Gollob TN, Tapscott T, Gonzales O, Bachinski L, et al. Novel PRKAG2 mutation responsible for the genetic syndrome of ventricular preexcitation and conduction system disease with childhood onset and absence of cardiac hypertrophy. Circulation. 2001;104:3030-3.

[455] Sakamoto J, Barr RL, Kavanagh KM, Lopaschuk GD. Contribution of malonyl-CoA decarboxylase to the high fatty acid oxidation rates seen in the diabetic heart. American journal of physiology. 2000;278:H1196-204.

[456] Laemmli UK. Cleavage of structural proteins during the assembly of the head of bacteriophage T4. Nature. 1970;227:680-5.

[457] Li R, Shen Y. An old method facing a new challenge: re-visiting housekeeping proteins as internal reference control for neuroscience research. Life sciences. 2013;92:747-51.

[458] Romero-Calvo I, Ocon B, Martinez-Moya P, Suarez MD, Zarzuelo A, Martinez-Augustin O, et al. Reversible Ponceau staining as a loading control alternative to actin in Western blots. Analytical biochemistry. 2010;401:318-20.

[459] Dang X, Jeyaraman M, Kardami E. Regulation of connexin-43-mediated growth inhibition by a phosphorylatable amino-acid is independent of gap junction-forming ability. Mol Cell Biochem. 2006;289:201-7.

[460] Gemel J, Lin X, Veenstra RD, Beyer EC. N-terminal residues in Cx43 and Cx40 determine physiological properties of gap junction channels, but do not influence heteromeric assembly with each other or with Cx26. Journal of cell science. 2006;119:2258-68.

[461] Lin X, Gemel J, Beyer EC, Veenstra RD. Dynamic model for ventricular junctional conductance during the cardiac action potential. American journal of physiology. 2005;288:H1113-23.

[462] Blom N, Gammeltoft S, Brunak S. Sequence and structure-based prediction of eukaryotic protein phosphorylation sites. Journal of molecular biology. 1999;294:1351-62.

[463] Blom N, Sicheritz-Ponten T, Gupta R, Gammeltoft S, Brunak S. Prediction of post-translational glycosylation and phosphorylation of proteins from the amino acid sequence. Proteomics. 2004;4:1633-49.

[464] Huang HD, Lee TY, Tzeng SW, Horng JT. KinasePhos: a web tool for identifying protein kinase-specific phosphorylation sites. Nucleic acids research. 2005;33:W226-9.

[465] Kavanagh KM, Guerrero PA, Jugdutt BI, Witkowski FX, Saffitz JE. Electrophysiologic properties and ventricular fibrillation in normal and myopathic hearts. Canadian journal of physiology and pharmacology. 1999;77:510-9.

[466] Balaji S, Hewett KW, Krombach RS, Clair MJ, Ye X, Spinale FG. Inducible lethal ventricular arrhythmias in swine with pacing-induced heart failure. Basic Res Cardiol. 1999;94:496-503.

[467] McElmurray JH, Mukherjee R, Patterson TM, Goldberg A, King MK, Hendrick JW, et al. Comparison of amlodipine or nifedipine treatment with developing congestive heart failure: effects on myocyte contractility. JCard Fail. 2001;7:158-64.

[468] Stephens TJ, Chen ZP, Canny BJ, Michell BJ, Kemp BE, McConell GK. Progressive increase in human skeletal muscle AMPKalpha2 activity and ACC phosphorylation during exercise. Am J Physiol Endocrinol Metab. 2002;282:E688-94.

[469] Saffitz JE, Laing JG, Yamada KA. Connexin expression and turnover : implications for cardiac excitability. Circulation research. 2000;86:723-8.

[470] Salameh A. Life cycle of connexins: regulation of connexin synthesis and degradation. Advances in cardiology. 2006;42:57-70.

[471] Witkowski FX, Kavanagh KM, Penkoske PA, Plonsey R. In vivo estimation of cardiac transmembrane current. CircRes. 1993;72:424-39.

[472] Witkowski FX, Plonsey R, Penkoske PA, Kavanagh KM. Significance of inwardly directed transmembrane current in determination of local myocardial electrical activation during ventricular fibrillation. CircRes. 1994;74:507-24.

[473] Levine JH, Moore EN, Weisman HF, Kadish AH, Becker LC, Spear JF. Depression of action potential characteristics and a decreased space constant are present in postischemic, reperfused myocardium. JClin Invest. 1987;79:107-16.

[474] Bonke FI. Passive electrical properties of atrial fibers of the rabbit heart. Pflugers Arch. 1973;339:1-15.

[475] Steendijk P, Mur G, van der Velde ET, Baan J. The four-electrode resistivity technique in anisotropic media: theoretical analysis and application on myocardial tissue in vivo. IEEE TransBiomedEng. 1993;40:1138-48.

[476] Padilla F, Garcia-Dorado D, Rodriguez-Sinovas A, Ruiz-Meana M, Inserte J, Soler-Soler J. Protection afforded by ischemic preconditioning is not mediated by effects on cell-to-cell electrical coupling during myocardial ischemia-reperfusion. American journal of physiology. 2003;285:H1909-16.

[477] Baynham TC, Knisley SB. Effective epicardial resistance of rabbit ventricles. AnnBiomedEng. 1999;27:96-102.

[478] Guzman RJ, Lemarchand P, Crystal RG, Epstein SE, Finkel T. Efficient gene transfer into myocardium by direct injection of adenovirus vectors. Circulation research. 1993;73:1202-7.

[479] Hajjar RJ, Schmidt U, Matsui T, Guerrero JL, Lee KH, Gwathmey JK, et al. Modulation of ventricular function through gene transfer in vivo. Proceedings of the National Academy of Sciences of the United States of America. 1998;95:5251-6.

[480] Nygren A, Clark RB, Belke DD, Kondo C, Giles WR, Witkowski FX. Voltage-sensitive dye mapping of activation and conduction in adult mouse hearts. AnnBiomedEng. 2000;28:958-67.

[481] Witkowski FX, Leon LJ, Penkoske PA, Giles WR, Spano ML, Ditto WL, et al. Spatiotemporal evolution of ventricular fibrillation. Nature. 1998;392:78-82.

[482] Witkowski FX, Clark RB, Larsen TS, Melnikov A, Giles WR. Voltage-sensitive dye recordings of electrophysiological activation in a Langendorff-perfused mouse heart. CanJCardiol. 1997;13:1077-82.

[483] Nygren A, Kondo C, Clark RB, Giles WR. Voltage-sensitive dye mapping in Langendorff-perfused rat hearts. American journal of physiology. 2003;284:H892-902.

[484] Guo Q, Mandal MK, Liu G, Kavanagh KM. Cardiac video analysis using Hodge-Helmholtz field decomposition. Computers in biology and medicine. 2006;36:1-20.

[485] Xin L, Gong XQ, Bai D. The role of amino terminus of mouse Cx50 in determining transjunctional voltage-dependent gating and unitary conductance. Biophys J. 2010;99:2077-86.

[486] Woods A, Azzout-Marniche D, Foretz M, Stein SC, Lemarchand P, Ferre P, et al. Characterization of the role of AMP-activated protein kinase in the regulation of glucose-activated gene expression using constitutively active and dominant negative forms of the kinase. Mol Cell Biol. 2000;20:6704-11.

[487] Woollhead AM, Scott JW, Hardie DG, Baines DL. Phenformin and 5-aminoimidazole-4-carboxamide-1-beta-D-ribofuranoside (AICAR) activation of AMP-activated protein kinase inhibits transepithelial Na+ transport across H441 lung cells. The Journal of physiology. 2005;566:781-92.

[488] Ropelle ER, Pauli JR, Fernandes MF, Rocco SA, Marin RM, Morari J, et al. A central role for neuronal AMP-activated protein kinase (AMPK) and mammalian target of rapamycin (mTOR) in high-protein diet-induced weight loss. Diabetes. 2008;57:594-605.

[489] Brugarolas J, Lei K, Hurley RL, Manning BD, Reiling JH, Hafen E, et al. Regulation of mTOR function in response to hypoxia by REDD1 and the TSC1/TSC2 tumor suppressor complex. Genes & development. 2004;18:2893-904.

[490] Hahn-Windgassen A, Nogueira V, Chen CC, Skeen JE, Sonenberg N, Hay N. Akt activates the mammalian target of rapamycin by regulating cellular ATP level and AMPK activity. J Biol Chem. 2005;280:32081-9.

[491] Kimball SR. Interaction between the AMP-activated protein kinase and mTOR signaling pathways. Medicine and science in sports and exercise. 2006;38:1958-64.

[492] Tripp ME. Developmental cardiac metabolism in health and disease. Pediatric cardiology. 1989;10:150-8.

[493] Chen Y, Hu HZ, Wu JW, Peng QY, Yang G, Liao ZG. [Changes of connexin 43 in rabbit with early myocardial ischemia]. Sichuan da xue xue bao Yi xue ban = Journal of Sichuan University. 2004;35:191-3.

[494] Garcia-Dorado D, Rodriguez-Sinovas A, Ruiz-Meana M. Gap junction-mediated spread of cell injury and death during myocardial ischemia-reperfusion. Cardiovascular research. 2004;61:386-401.

[495] Hatanaka K, Kawata H, Toyofuku T, Yoshida K. Down-regulation of connexin43 in early myocardial ischemia and protective effect by ischemic preconditioning in rat hearts in vivo. Japanese heart journal. 2004;45:1007-19.

[496] Plaisance I, Duthe F, Sarrouilhe D, Herve JC. The metabolic inhibitor antimycin A can disrupt cell-to-cell communication by an ATP- and Ca(2+)-independent mechanism. Pflugers Arch. 2003;447:181-94.

[497] Tansey EE, Kwaku KF, Hammer PE, Cowan DB, Federman M, Levitsky S, et al. Reduction and redistribution of gap and adherens junction proteins after ischemia and reperfusion. The Annals of thoracic surgery. 2006;82:1472-9.

[498] Nattel S, Li D, Yue L. Basic mechanisms of atrial fibrillation--very new insights into very old ideas. AnnuRevPhysiol. 2000;62:51-77.

[499] Van Wagoner DR, Nerbonne JM. Molecular basis of electrical remodeling in atrial fibrillation. JMolCell Cardiol. 2000;32:1101-17.

[500] Li D, Fareh S, Leung TK, Nattel S. Promotion of atrial fibrillation by heart failure in dogs: atrial remodeling of a different sort. Circulation. 1999;100:87-95.

[501] Morillo CA, Klein GJ, Jones DL, Guiraudon CM. Chronic rapid atrial pacing. Structural, functional, and electrophysiological characteristics of a new model of sustained atrial fibrillation. Circulation. 1995;91:1588-95.

[502] Wijffels MC, Kirchhof CJ, Dorland R, Allessie MA. Atrial fibrillation begets atrial fibrillation. A study in awake chronically instrumented goats. Circulation. 1995;92:1954-68.

[503] Ausma J, van dV, Lenders MH, van Ankeren EP, Jongsma HJ, Ramaekers FC, et al. Reverse structural and gap-junctional remodeling after prolonged atrial fibrillation in the goat. Circulation. 2003;107:2051-8.

[504] Ohara K, Miyauchi Y, Ohara T, Fishbein MC, Zhou S, Lee MH, et al. Downregulation of immunodetectable atrial connexin40 in a canine model of chronic left ventricular myocardial infarction: implications to atrial fibrillation. Journal of cardiovascular pharmacology and therapeutics. 2002;7:89-94.

[505] Takeuchi S, Akita T, Takagishi Y, Watanabe E, Sasano C, Honjo H, et al. Disorganization of gap junction distribution in dilated atria of patients with chronic atrial fibrillation. Circ J. 2006;70:575-82.

[506] Wilhelm M, Kirste W, Kuly S, Amann K, Neuhuber W, Weyand M, et al. Atrial distribution of connexin 40 and 43 in patients with intermittent, persistent, and postoperative atrial fibrillation. Heart, lung & circulation. 2006;15:30-7.

[507] Gollob MH. Cardiac connexins as candidate genes for idiopathic atrial fibrillation. Current opinion in cardiology. 2006;21:155-8.

[508] Fialova M, Dlugosova K, Okruhlicova L, Kristek F, Manoach M, Tribulova N. Adaptation of the heart to hypertension is associated with maladaptive gap junction connexin-43 remodelling. Physiol Res. 2007.

[509] Sasano C, Honjo H, Takagishi Y, Uzzaman M, Emdad L, Shimizu A, et al. Internalization and dephosphorylation of connexin43 in hypertrophied right ventricles of rats with pulmonary hypertension. Circ J. 2007;71:382-9.

[510] Kostin S, Dammer S, Hein S, Klovekorn WP, Bauer EP, Schaper J. Connexin 43 expression and distribution in compensated and decompensated cardiac hypertrophy in patients with aortic stenosis. Cardiovascular research. 2004;62:426-36.

[511] Saffitz JE, Kleber AG. Effects of mechanical forces and mediators of hypertrophy on remodeling of gap junctions in the heart. Circulation research. 2004;94:585-91.

[512] Teunissen BE, Jongsma HJ, Bierhuizen MF. Regulation of myocardial connexins during hypertrophic remodelling. European heart journal. 2004;25:1979-89.

[513] Gutstein DE, Morley GE, Vaidya D, Liu F, Chen FL, Stuhlmann H, et al. Heterogeneous expression of Gap junction channels in the heart leads to conduction defects and ventricular dysfunction. Circulation. 2001;104:1194-9.

[514] Spach MS, Heidlage JF, Dolber PC, Barr RC. Changes in anisotropic conduction caused by remodeling cell size and the cellular distribution of gap junctions and Na(+) channels. Journal of electrocardiology. 2001;34 Suppl:69-76.

[515] Peters NS, Green CR, Poole-Wilson PA, Severs NJ. Reduced content of connexin43 gap junctions in ventricular myocardium from hypertrophied and ischemic human hearts. Circulation. 1993;88:864-75.

[516] Lauf U, Giepmans BN, Lopez P, Braconnot S, Chen SC, Falk MM. Dynamic trafficking and delivery of connexons to the plasma membrane and accretion to gap junctions in living cells. Proceedings of the National Academy of Sciences of the United States of America. 2002;99:10446-51.

[517] Beauchamp P, Yamada KA, Baertschi AJ, Green K, Kanter EM, Saffitz JE, et al. Relative contributions of connexins 40 and 43 to atrial impulse propagation in synthetic strands of neonatal and fetal murine cardiomyocytes. Circulation research. 2006;99:1216-24.

[518] Pumir A, Plaza F, Krinsky VI. Effect of an externally applied electric field on excitation propagation in the cardiac muscle. Chaos (Woodbury, NY. 1994;4:547-55.

[519] Akar FG, Roth BJ, Rosenbaum DS. Optical measurement of cell-to-cell coupling in intact heart using subthreshold electrical stimulation. American journal of physiology. 2001;281:H533-42.

[520] Lopaschuk GD. Regulation of carbohydrate metabolism in ischemia and reperfusion. American Heart Journal2000.

[521] Lopaschuk GD. Optimizing cardiac energy metabolism: how can fatty acid and carbohydrate metabolism be manipulated? Coronary artery disease. 2001;12 Suppl 1:S8-11.

[522] Vorperian VR, Wisialowski TA, Deegan R, Roden DM. Effect of hypercapnic acidemia on anisotropic propagation in the canine ventricle. Circulation. 1994;90:456-61.

[523] Apstein CS. Glucose-insulin-potassium for acute myocardial infarction: remarkable results from a new prospective, randomized trial. Circulation. 1998;98:2223-6.

[524] Avitall B, Hare J, Zander G, Lessila C, Dhala A, Deshpande S, et al. Cardioversion, defibrillation, and overdrive pacing of ventricular arrhythmias: the effect of moricizine in dogs with sustained monomorphic ventricular tachycardia. Pacing ClinElectrophysiol. 1993;16:2092-7.

[525] Bonnet D, Martin D, Pascale DL, Villain E, Jouvet P, Rabier D, et al. Arrhythmias and conduction defects as presenting symptoms of fatty acid oxidation disorders in children. Circulation. 1999;100:2248-53.

[526] Schmilinsky-Fluri G, Valiunas V, Willi M, Weingart R. Modulation of cardiac gap junctions: the mode of action of arachidonic acid. J Mol Cell Cardiol. 1997;29:1703-13.

[527] Camors E, Valdivia HH. CaMKII regulation of cardiac ryanodine receptors and inositol triphosphate receptors. Frontiers in pharmacology. 2014;5:101.

[528] Zhang H, Makarewich CA, Kubo H, Wang W, Duran JM, Li Y, et al. Hyperphosphorylation of the cardiac ryanodine receptor at serine 2808 is not involved in cardiac dysfunction after myocardial infarction. Circulation research. 2012;110:831-40.

[529] Ke J, Xiao X, Chen F, He L, Dai MS, Wang XP, et al. Function of the CaMKII-ryanodine receptor signaling pathway in rabbits with left ventricular hypertrophy and triggered ventricular arrhythmia. World journal of emergency medicine. 2012;3:65-70.

[530] Lokuta AJ, Rogers TB, Lederer WJ, Valdivia HH. Modulation of cardiac ryanodine receptors of swine and rabbit by a phosphorylation-dephosphorylation mechanism. The Journal of physiology. 1995;487 (Pt 3):609-22.

[531] Burt JM, Steele TD. Selective effect of PDGF on connexin43 versus connexin40 comprised gap junction channels. Cell Commun Adhes. 2003;10:287-91.

[532] Cottrell GT, Wu Y, Burt JM. Cx40 and Cx43 expression ratio influences heteromeric/ heterotypic gap junction channel properties. Am J Physiol Cell Physiol. 2002;282:C1469-82.

[533] Haefliger JA, Demotz S, Braissant O, Suter E, Waeber B, Nicod P, et al. Connexins 40 and 43 are differentially regulated within the kidneys of rats with renovascular hypertension. Kidney Int. 2001;60:190-201.

[534] Oyamada Y, Komatsu K, Kimura H, Mori M, Oyamada M. Differential regulation of gap junction protein (connexin) genes during cardiomyocytic differentiation of mouse embryonic stem cells in vitro. Exp Cell Res. 1996;229:318-26.

[535] Johnson TL, Nerem RM. Endothelial connexin 37, connexin 40, and connexin 43 respond uniquely to substrate and shear stress. Endothelium. 2007;14:215-26.

[536] Salameh A, Frenzel C, Boldt A, Rassler B, Glawe I, Schulte J, et al. Subchronic alpha- and beta-adrenergic regulation of cardiac gap junction protein expression. Faseb J. 2006;20:365-7.

[537] Rossi S, Baruffi S, Bertuzzi A, Miragoli M, Corradi D, Maestri R, et al. Ventricular activation is impaired in aged rat hearts. American journal of physiology. 2008;295:H2336-47.

[538] Simonotto JD, Myers SM, Furman MD, Norman WM, Liu Z, DeMarse TB, et al. Coherence analysis over the latent period of epileptogenesis reveal that high-frequency communication is increased across hemispheres in an animal model of limbic epilepsy. Conf Proc IEEE Eng Med Biol Soc. 2006;1:1154-6.

[539] Furman MD, Simonotto JD, Beaver TM, Spano ML, Ditto WL. Using recurrence quantification analysis determinism for noise removal in cardiac optical mapping. IEEE transactions on bio-medical engineering. 2006;53:767-70.

[540] Nygren A, Olson ML, Chen KY, Emmett T, Kargacin G, Shimoni Y. Propagation of the cardiac impulse in the diabetic rat heart: reduced conduction reserve. The Journal of physiology. 2007;580:543-60.

[541] Veenstra RD, Wang HZ, Westphale EM, Beyer EC. Multiple connexins confer distinct regulatory and conductance properties of gap junctions in developing heart. Circulation research. 1992;71:1277-83.

[542] van Rijen HV, van Kempen MJ, Postma S, Jongsma HJ. Tumour necrosis factor alpha alters the expression of connexin43, connexin40, and connexin37 in human umbilical vein endothelial cells. Cytokine. 1998;10:258-64.

[543] Veenstra RD, DeHaan RL. Cardiac gap junction channel activity in embryonic chick ventricle cells. The American journal of physiology. 1988;254:H170-80.

[544] Burt JM, Spray DC. Volatile anesthetics block intercellular communication between neonatal rat myocardial cells. Circulation research. 1989;65:829-37.

[545] Zhong G, Mantel PL, Jiang X, Jarry-Guichard T, Gros D, Labarrere C, et al. LacSwitch II regulation of connexin43 cDNA expression enables gap-junction single-channel analysis. BioTechniques. 2003;34:1034-9, 41-4, 46.

[546] Beblo DA, Wang HZ, Beyer EC, Westphale EM, Veenstra RD. Unique conductance, gating, and selective permeability properties of gap junction channels formed by connexin40. Circulation research. 1995;77:813-22.

[547] Srinivas M, Costa M, Gao Y, Fort A, Fishman GI, Spray DC. Voltage dependence of macroscopic and unitary currents of gap junction channels formed by mouse connexin50 expressed in rat neuroblastoma cells. The Journal of physiology. 1999;517 (Pt 3):673-89.

[548] Valiunas V, Beyer EC, Brink PR. Cardiac gap junction channels show quantitative differences in selectivity. Circulation research. 2002;91:104-11.

[549] Ponsioen B, van Zeijl L, Moolenaar WH, Jalink K. Direct measurement of cyclic AMP diffusion and signaling through connexin43 gap junctional channels. Exp Cell Res. 2007;313:415-23.

[550] Brink PR, Ramanan SV. A model for the diffusion of fluorescent probes in the septate giant axon of earthworm. Axoplasmic diffusion and junctional membrane permeability. Biophys J. 1985;48:299-309.

[551] Moreno AP, Lau AF. Gap junction channel gating modulated through protein phosphorylation. Progress in biophysics and molecular biology. 2007;94:107-19.

[552] Herve JC, Dhein S. Pharmacology of cardiovascular gap junctions. Advances in cardiology. 2006;42:107-31.

[553] King TJ, Lampe PD. Temporal regulation of connexin phosphorylation in embryonic and adult tissues. Biochim Biophys Acta. 2005;1719:24-35.

[554] Laird DW. Connexin phosphorylation as a regulatory event linked to gap junction internalization and degradation. Biochim Biophys Acta. 2005;1711:172-82.

[555] Moreno AP. Connexin phosphorylation as a regulatory event linked to channel gating. Biochim Biophys Acta. 2005;1711:164-71.

[556] Solan JL, Lampe PD. Connexin phosphorylation as a regulatory event linked to gap junction channel assembly. Biochim Biophys Acta. 2005;1711:154-63.

[557] Alesutan I, Sopjani M, Munoz C, Fraser S, Kemp BE, Foller M, et al. Inhibition of connexin 26 by the AMP-activated protein kinase. J Membr Biol. 2011;240:151-8.

[558] Sarma JD, Wang F, Koval M. Targeted gap junction protein constructs reveal connexin-specific differences in oligomerization. J Biol Chem. 2002;277:20911-8.

[559] Musil LS, Goodenough DA. Multisubunit assembly of an integral plasma membrane channel protein, gap junction connexin43, occurs after exit from the ER. Cell. 1993;74:1065-77.

[560] An Z, Wang H, Song P, Zhang M, Geng X, Zou MH. Nicotine-induced Activation of AMP-activated Protein Kinase Inhibits Fatty Acid Synthase in 3T3L1 Adipocytes: A ROLE FOR OXIDANT STRESS. J Biol Chem. 2007;282:26793-801.

[561] Wang W, Yang X, Lopez dSI, Carling D, Gorospe M. Increased AMP:ATP ratio and AMP-activated protein kinase activity during cellular senescence linked to reduced HuR function. JBiolChem. 2003;278:27016-23.

[562] Sambandam N, Steinmetz M, Chu A, Altarejos JY, Dyck JR, Lopaschuk GD. Malonyl-CoA decarboxylase (MCD) is differentially regulated in subcellular compartments by 5'AMP-activated protein kinase (AMPK). Studies using H9c2 cells overexpressing MCD and AMPK by adenoviral gene transfer technique. European journal of biochemistry / FEBS. 2004;271:2831-40.

[563] Eugenin EA. Role of connexin/pannexin containing channels in infectious diseases. FEBS Lett. 2014;588:1389-95.

[564] Dykens JA, Jamieson J, Marroquin L, Nadanaciva S, Billis PA, Will Y. Biguanide-induced mitochondrial dysfunction yields increased lactate production and cytotoxicity of aerobically-poised HepG2 cells and human hepatocytes in vitro. Toxicology and applied pharmacology. 2008.

[565] Wang DS, Kusuhara H, Kato Y, Jonker JW, Schinkel AH, Sugiyama Y. Involvement of organic cation transporter 1 in the lactic acidosis caused by metformin. Molecular pharmacology. 2003;63:844-8.

[566] Davidoff F. Effects of guanidine derivatives on mitochondrial function. 3. The mechanism of phenethylbiguanide accumulation and its relationship to in vitro respiratory inhibition. J Biol Chem. 1971;246:4017-27.

[567] Owen MR, Doran E, Halestrap AP. Evidence that metformin exerts its anti-diabetic effects through inhibition of complex 1 of the mitochondrial respiratory chain. Biochem J. 2000;348 Pt 3:607-14.

[568] Kane DA. Lactate oxidation at the mitochondria: a lactate-malate-aspartate shuttle at work. Frontiers in neuroscience. 2014;8:366.

[569] Rogatzki MJ, Ferguson BS, Goodwin ML, Gladden LB. Lactate is always the end product of glycolysis. Frontiers in neuroscience. 2015;9:22.

[570] Peracchia C. Chemical gating of gap junction channels; roles of calcium, pH and calmodulin. Biochim Biophys Acta. 2004;1662:61-80.

[571] Bevans CG, Harris AL. Regulation of connexin channels by pH. Direct action of the protonated form of taurine and other aminosulfonates. J Biol Chem. 1999;274:3711-9.

[572] Abudara V, Jiang RG, Eyzaguirre C. Acidic regulation of junction channels between glomus cells in the rat carotid body. Possible role of [Ca(2+)](i). Brain research. 2001;916:50-60.

[573] Ek JF, Delmar M, Perzova R, Taffet SM. Role of histidine 95 on pH gating of the cardiac gap junction protein connexin43. Circulation research. 1994;74:1058-64.

[574] Ek-Vitorin JF, Calero G, Morley GE, Coombs W, Taffet SM, Delmar M. PH regulation of connexin43: molecular analysis of the gating particle. Biophys J. 1996;71:1273-84.

[575] Gu H, Ek-Vitorin JF, Taffet SM, Delmar M. UltraRapid communication : coexpression of connexins 40 and 43 enhances the pH sensitivityof gap junctions: A model for synergistic interactions among connexins. Circulation research. 2000;86:1100.

[576] Morley GE, Ek-Vitorin JF, Taffet SM, Delmar M. Structure of connexin43 and its regulation by pHi. Journal of cardiovascular electrophysiology. 1997;8:939-51.

[577] Zhou Y, Yang W, Lurtz MM, Ye Y, Huang Y, Lee HW, et al. Identification of the calmodulin binding domain of connexin 43. J Biol Chem. 2007;282:35005-17.

[578] Saez JC, Nairn AC, Czernik AJ, Spray DC, Hertzberg EL, Greengard P, et al. Phosphorylation of connexin 32, a hepatocyte gap-junction protein, by cAMP-dependent protein kinase, protein kinase C and Ca2+/calmodulin-dependent protein kinase II. European journal of biochemistry / FEBS. 1990;192:263-73.

[579] Beauloye C, Marsin AS, Bertrand L, Krause U, Hardie DG, Vanoverschelde JL, et al. Insulin antagonizes AMP-activated protein kinase activation by ischemia or anoxia in rat hearts, without affecting total adenine nucleotides. FEBS Lett. 2001;505:348-52.

[580] Fryer LG, Parbu-Patel A, Carling D. The Anti-diabetic drugs rosiglitazone and metformin stimulate AMP-activated protein kinase through distinct signaling pathways. J Biol Chem. 2002;277:25226-32.

[581] Hawley SA, Gadalla AE, Olsen GS, Hardie DG. The antidiabetic drug metformin activates the AMP-activated protein kinase cascade via an adenine nucleotide-independent mechanism. Diabetes. 2002;51:2420-5.

[582] Itani SI, Saha AK, Kurowski TG, Coffin HR, Tornheim K, Ruderman NB. Glucose autoregulates its uptake in skeletal muscle: involvement of AMP-activated protein kinase. Diabetes. 2003;52:1635-40.

[583] Carling D, Sanders MJ, Woods A. The regulation of AMP-activated protein kinase by upstream kinases. Int J Obes (Lond). 2008;32 Suppl 4:S55-9.

[584] Jaswal JS, Gandhi M, Finegan BA, Dyck JR, Clanachan AS. p38 mitogen-activated protein kinase mediates adenosine-induced alterations in myocardial glucose utilization via 5'-AMP-activated protein kinase. American journal of physiology. 2007;292:H1978-85.

[585] Momcilovic M, Hong SP, Carlson M. Mammalian TAK1 activates Snf1 protein kinase in yeast and phosphorylates AMP-activated protein kinase in vitro. J Biol Chem. 2006;281:25336-43.

[586] Huang X, Wullschleger S, Shpiro N, McGuire VA, Sakamoto K, Woods YL, et al. Important role of the LKB1-AMPK pathway in suppressing tumorigenesis in PTEN-deficient mice. Biochem J. 2008;412:211-21.

[587] Sakamoto K, McCarthy A, Smith D, Green KA, Grahame HD, Ashworth A, et al. Deficiency of LKB1 in skeletal muscle prevents AMPK activation and glucose uptake during contraction. EMBO J. 2005;24:1810-20.

[588] Sun Y, Connors KE, Yang DQ. AICAR induces phosphorylation of AMPK in an ATM-dependent, LKB1-independent manner. Mol Cell Biochem. 2007.

[589] Dokladda K, Green KA, Pan DA, Hardie DG. PD98059 and U0126 activate AMP-activated protein kinase by increasing the cellular AMP:ATP ratio and not via inhibition of the MAP kinase pathway. FEBS Lett. 2005;579:236-40.

[590] Hezel AF, Bardeesy N. LKB1; linking cell structure and tumor suppression. Oncogene. 2008;27:6908-19.

[591] Geraghty KM, Chen S, Harthill JE, Ibrahim AF, Toth R, Morrice NA, et al. Regulation of multisite phosphorylation and 14-3-3 binding of AS160 in response to IGF-1, EGF, PMA and AICAR. Biochem J. 2007;407:231-41.

[592] Chen S, Murphy J, Toth R, Campbell DG, Morrice NA, Mackintosh C. Complementary regulation of TBC1D1 and AS160 by growth factors, insulin and AMPK activators. Biochem J. 2008;409:449-59.

[593] Tamas P, Hawley SA, Clarke RG, Mustard KJ, Green K, Hardie DG, et al. Regulation of the energy sensor AMP-activated protein kinase by antigen receptor and Ca2+ in T lymphocytes. The Journal of experimental medicine. 2006;203:1665-70.

[594] Pina-Benabou MH, Srinivas M, Spray DC, Scemes E. Calmodulin kinase pathway mediates the K+-induced increase in Gap junctional communication between mouse spinal cord astrocytes. JNeurosci. 2001;21:6635-43.

[595] Del Corsso C, Iglesias R, Zoidl G, Dermietzel R, Spray DC. Calmodulin dependent protein kinase increases conductance at gap junctions formed by the neuronal gap junction protein connexin36. Brain research. 2012;1487:69-77.

[596] Saeedi R, Parsons HL, Wambolt RB, Paulson K, Sharma V, Dyck JR, et al. Metabolic actions of metformin in the heart can occur by AMPK-independent mechanisms. American journal of physiology. 2008;294:H2497-506.

[597] Leykauf K, Durst M, Alonso A. Phosphorylation and subcellular distribution of connexin43 in normal and stressed cells. Cell Tissue Res. 2003;311:23-30.

[598] Ogawa T, Hayashi T, Kyoizumi S, Kusunoki Y, Nakachi K, MacPhee DG, et al. Anisomycin downregulates gap-junctional intercellular communication via the p38 MAP-kinase pathway. Journal of cell science. 2004;117:2087-96.

[599] Louden E, Chi MM, Moley KH. Crosstalk between the AMP-activated kinase and insulin signaling pathways rescues murine blastocyst cells from insulin resistance. Reproduction. 2008;136:335-44.

[600] Gerner L, Youssef G, O'Shaughnessy RF. The protein phosphatase 2A regulatory subunit Ppp2r2a is required for Connexin-43 dephosphorlyation during epidermal barrier acquisition. Exp Dermatol. 2013;22:754-6.

[601] Lampe PD, Lau AF. The effects of connexin phosphorylation on gap junctional communication. IntJBiochemCell Biol. 2004;36:1171-86.

[602] Gu H, Smith FC, Taffet SM, Delmar M. High incidence of cardiac malformations in connexin40-deficient mice. CircRes. 2003;93:201-6.

[603] Simon AM, McWhorter AR. Vascular abnormalities in mice lacking the endothelial gap junction proteins connexin37 and connexin40. DevBiol. 2002;251:206-20.

[604] Kirchhoff S, Nelles E, Hagendorff A, Kruger O, Traub O, Willecke K. Reduced cardiac conduction velocity and predisposition to arrhythmias in connexin40-deficient mice. Curr Biol. 1998;8:299-302.

[605] Verheule S, van Batenburg CA, Coenjaerts FE, Kirchhoff S, Willecke K, Jongsma HJ. Cardiac conduction abnormalities in mice lacking the gap junction protein connexin40. JCardiovascElectrophysiol. 1999;10:1380-9.

[606] Tamaddon HS, Vaidya D, Simon AM, Paul DL, Jalife J, Morley GE. High-resolution optical mapping of the right bundle branch in connexin40 knockout mice reveals slow conduction in the specialized conduction system. CircRes. 2000;87:929-36.

[607] van Rijen HV, van Veen TA, van Kempen MJ, Wilms-Schopman FJ, Potse M, Krueger O, et al. Impaired conduction in the bundle branches of mouse hearts lacking the gap junction protein connexin40. Circulation. 2001;103:1591-8.

[608] Gollob MH, Jones DL, Krahn AD, Danis L, Gong XQ, Shao Q, et al. Somatic mutations in the connexin 40 gene (GJA5) in atrial fibrillation. The New England journal of medicine. 2006;354:2677-88.

[609] Groenewegen WA, Firouzi M, Bezzina CR, Vliex S, van Langen IM, Sandkuijl L, et al. A cardiac sodium channel mutation cosegregates with a rare connexin40 genotype in familial atrial standstill. Circulation research. 2003;92:14-22.

[610] Firouzi M, Ramanna H, Kok B, Jongsma HJ, Koeleman BP, Doevendans PA, et al. Association of human connexin40 gene polymorphisms with atrial vulnerability as a risk factor for idiopathic atrial fibrillation. Circulation research. 2004;95:e29-33.

[611] Firouzi M, Bierhuizen MF, Kok B, Teunissen BE, Jansen AT, Jongsma HJ, et al. The human Cx40 promoter polymorphism -44G-->A differentially affects transcriptional regulation by Sp1 and GATA4. Biochim Biophys Acta. 2006;1759:491-6.

[612] Hauer RN, Groenewegen WA, Firouzi M, Ramanna H, Jongsma HJ. Cx40 polymorphism in human atrial fibrillation. Advances in cardiology. 2006;42:284-91.

[613] Juang JM, Chern YR, Tsai CT, Chiang FT, Lin JL, Hwang JJ, et al. The association of human connexin 40 genetic polymorphisms with atrial fibrillation. International journal of cardiology. 2007;116:107-12.

[614] Nao T, Ohkusa T, Hisamatsu Y, Inoue N, Matsumoto T, Yamada J, et al. Comparison of expression of connexin in right atrial myocardium in patients with chronic atrial fibrillation versus those in sinus rhythm. Am J Cardiol. 2003;91:678-83.

[615] van Rijen HV, van Veen TA, Hermans MM, Jongsma HJ. Human connexin40 gap junction channels are modulated by cAMP. CardiovascRes. 2000;45:941-51.

[616] Hoffmann A, Gloe T, Pohl U, Zahler S. Nitric oxide enhances de novo formation of endothelial gap junctions. CardiovascRes. 2003;60:421-30.

[617] Doble BW, Dang X, Ping P, Fandrich RR, Nickel BE, Jin Y, et al. Phosphorylation of serine 262 in the gap junction protein connexin-43 regulates DNA synthesis in cell-cell contact forming cardiomyocytes. Journal of cell science. 2004;117:507-14.

[618] Patel LS, Mitchell CK, Dubinsky WP, O'Brien J. Regulation of gap junction coupling through the neuronal connexin Cx35 by nitric oxide and cGMP. Cell Commun Adhes. 2006;13:41-54.

[619] Xue Y, Li A, Wang L, Feng H, Yao X. PPSP: prediction of PK-specific phosphorylation site with Bayesian decision theory. BMC bioinformatics. 2006;7:163.

[620] Bordoli L, Kiefer F, Arnold K, Benkert P, Battey J, Schwede T. Protein structure homology modeling using SWISS-MODEL workspace. Nat Protoc. 2009;4:1-13.

[621] Biasini M, Bienert S, Waterhouse A, Arnold K, Studer G, Schmidt T, et al. SWISS-MODEL: modelling protein tertiary and quaternary structure using evolutionary information. Nucleic acids research. 2014;42:W252-8.

[622] Baker NA, Sept D, Joseph S, Holst MJ, McCammon JA. Electrostatics of nanosystems: Application to microtubules and the ribosome. Proceedings of the National Academy of Sciences. 2001;98:10037-41.

[623] Dolinsky TJ, Nielsen JE, McCammon JA, Baker NA. PDB2PQR: an automated pipeline for the setup of Poisson–Boltzmann electrostatics calculations. Nucleic acids research. 2004;32:W665-W7.

[624] Pellegrini-Calace M, Maiwald T, Thornton JM. PoreWalker: A Novel Tool for the Identification and Characterization of Channels in Transmembrane Proteins from Their Three-Dimensional Structure. PLoS computational biology. 2009;5:e1000440.

[625] Shearer D, Ens W, Standing K, Valdimarsson G. Posttranslational modifications in lens fiber connexins identified by off-line-HPLC MALDI-quadrupole time-of-flight mass spectrometry. Investigative ophthalmology & visual science. 2008;49:1553-62.

[626] Kwon T, Harris AL, Rossi A, Bargiello TA. Molecular dynamics simulations of the Cx26 hemichannel: evaluation of structural models with Brownian dynamics. J Gen Physiol. 2011;138:475-93.

[627] Matesic D, Tillen T, Sitaramayya A. Connexin 40 expression in bovine and rat retinas. Cell Biol Int. 2003;27:89-99.

[628] Berthoud VM, Beyer EC, Kurata WE, Lau AF, Lampe PD. The gap-junction protein connexin 56 is phosphorylated in the intracellular loop and the carboxy-terminal region. European journal of biochemistry / FEBS. 1997;244:89-97.

[629] Liu J, Ek Vitorin JF, Weintraub ST, Gu S, Shi Q, Burt JM, et al. Phosphorylation of connexin 50 by protein kinase A enhances gap junction and hemichannel function. J Biol Chem. 2011;286:16914-28.

[630] Seki A, Duffy HS, Coombs W, Spray DC, Taffet SM, Delmar M. Modifications in the biophysical properties of connexin43 channels by a peptide of the cytoplasmic loop region. Circulation research. 2004;95:e22-8.

[631] Manthey D, Banach K, Desplantez T, Lee CG, Kozak CA, Traub O, et al. Intracellular domains of mouse connexin26 and -30 affect diffusional and electrical properties of gap junction channels. J Membr Biol. 2001;181:137-48.

[632] Xue J, Zhang H, Liu W, Liu M, Shi M, Wen Z, et al. Metformin inhibits growth of eutopic stromal cells from adenomyotic endometrium via AMPK activation and subsequent inhibition of AKT phosphorylation: a possible role in the treatment of adenomyosis. Reproduction. 2013;146:397-406.

[633] Kristensen JM, Treebak JT, Schjerling P, Goodyear L, Wojtaszewski JF. Two weeks of metformin treatment induces AMPK dependent enhancement of insulin-stimulated glucose uptake in mouse soleus muscle. Am J Physiol Endocrinol Metab. 2014.

[634] Zhang Y, Han X, Hu N, Huff AF, Gao F, Ren J. Akt2 knockout alleviates prolonged caloric restriction-induced change in cardiac contractile function through regulation of autophagy. J Mol Cell Cardiol. 2013.

[635] Hawley SA, Ross FA, Gowans GJ, Tibarewal P, Leslie NR, Hardie DG. Phosphorylation by Akt within the ST loop of AMPK-alpha1 down-regulates its activation in tumour cells. Biochem J. 2014.

[636] Laughner JI, Marrus SB, Zellmer ER, Weinheimer CJ, MacEwan MR, Cui SX, et al. A fully implantable pacemaker for the mouse: from battery to wireless power. PLoS ONE. 2013;8:e76291.

[637] Mitra SS, Xu J, Nicholson BJ. Coregulation of multiple signaling mechanisms in pp60v-Src-induced closure of Cx43 gap junction channels. J Membr Biol. 2012;245:495-506.

[638] Muona K, Makinen K, Hedman M, Manninen H, Yla-Herttuala S. 10-year safety follow-up in patients with local VEGF gene transfer to ischemic lower limb. Gene therapy. 2012;19:392-5.

[639] Wirth T, Parker N, Yla-Herttuala S. History of gene therapy. Gene. 2013;525:162-9.

[640] Jordan K, Solan JL, Dominguez M, Sia M, Hand A, Lampe PD, et al. Trafficking, assembly, and function of a connexin43-green fluorescent protein chimera in live mammalian cells. Molecular biology of the cell. 1999;10:2033-50.

[641] Guo YN, Wang JC, Cai GY, Hu X, Cui SY, Lv Y, et al. AMPK-mediated downregulation of connexin43 and premature senescence of mesangial cells under high-glucose conditions. Exp Gerontol. 2014;51:71-81.

[642] Ma Y, Bu J, Dang H, Sha J, Jing Y, Shan-Jiang A, et al. Inhibition of adenosine monophosphate-activated protein kinase reduces glial cell-mediated inflammation and induces the expression of Cx43 in astroglias after cerebral ischemia. Brain research. 2015.

[643] Martins-Marques T, Catarino S, Zuzarte M, Marques C, Matafome P, Pereira P, et al. Ischemia-induced autophagy leads to degradation of gap junction protein Connexin43 in cardiomyocytes. Biochem J. 2015.

[644] Alesutan I, Voelkl J, Stockigt F, Mia S, Feger M, Primessnig U, et al. AMP-activated protein kinase alpha1 regulates cardiac gap junction protein connexin 43 and electrical remodeling following pressure overload. Cell Physiol Biochem. 2015;35:406-18.